The Abdus Salam
International Centre for Theoretical Physics

United Nations
Educational, Scientific and
Cultural Organization

IAEA
International Atomic Energy Agency

2139-22c

School on Synchrotron and Free-Electron-Laser Sources and their Multidisciplinary Applications

26 April - 7 May, 2010

Surface, Interface, and Materials Studies Using Photoelectron Spectroscopy, Diffraction, and Holography (Part 4)

Charles S. Fadley
Lawrence Berkeley National Laboratory
USA

Outline

Surface, interface, and nanoscience—short introduction

Some surface concepts and techniques→photoemission

Synchrotron radiation: experimental aspects

Electronic structure—a brief review

The basic synchrotron radiation techniques:
more experimental and theoretical details

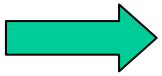

Valence-level photoemission

Core-level photoemission

Photoemission with high ambient pressure
around the sample

Outline

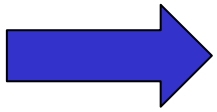

- Valence-band spectra: low-energy UPS limit and high-energy XPS limit
- Core-level chemical shifts: the potential model
- Core-level chemical shifts: equivalent-core (Z+1) and thermochemical energies
- Multiplet splittings
- Spin-orbit splitting, the Fano effect, and spin-polarized outgoing electrons
- Magnetic circular dichroism (MCD) in core-level emission
- Non-magnetic circular dichroism in core-level emission: a.k.a. circular dichroism in angular distributions (CDAD)
- Various other final state effects providing information in core-level spectra

PHOTOELECTRON EMISSION - BASIC MATRIX ELEMENTS & SELECTION RULES:

- **ATOMIC-LIKE (LOCALIZED) STATES ⇒ CORE:**

$$\varphi_i(\vec{r}) = \varphi_{n_i l_i m_i}(r,\theta,\phi) = R_{n_i l_i}(r) Y_{l_i m_i}(\theta,\phi)$$

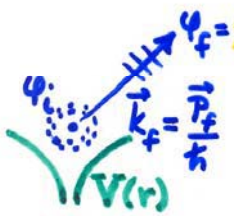

$$\varphi_f(\vec{r},\vec{k}_f) = \varphi_{E_f}(\vec{r},\vec{k}_f)$$

$$= 4\pi \sum_{l_f,m_f} i^{l_f} e^{-i\delta_{l_f}} Y^*_{l_f m_f}(\theta_{k_f},\phi_{k_f}) Y_{l_f m_f}(\theta,\phi) R_{E_f l_f}(r)$$

(δ_{l_f}: PHASE SHIFT OF l_f WAVE IN $V(r)$)

DIPOLE APPROX.: INT. $\propto |\langle\varphi_f|\hat{\varepsilon}\cdot\vec{r}|\varphi_i\rangle|^2 = |\hat{\varepsilon}\cdot\langle\varphi_f|\vec{r}|\varphi_i\rangle|^2 \Rightarrow$

$\Delta l = l_f - l_i = \pm 1$ TWO CHANNELS

$\Delta m = m_f - m_i = 0, \pm 1$ LINEAR POLARIZ.

$\Delta m = \pm 1$, CIRCULAR POLARIZATION

EQUIVALENT WITHIN CONSTANT FACTOR: $\vec{p} \leftrightarrow \vec{\nabla} V(r)$

VALENCE BANDS IN SOLIDS:

- **BLOCH-FUNCTION (DELOCALIZED) STATES ⇒ VALENCE:**

$$\varphi_i(\vec{r}) = u_{\vec{k}_i}(\vec{r}) e^{i\vec{k}_i\cdot\vec{r}}$$

BRILLOUIN ZONE

$$\varphi_f(\vec{r}) = u_{\vec{k}_f}(\vec{r}) e^{i\vec{k}_f\cdot\vec{r}} \; ; \; E_f = \frac{p_f^2}{2m} = \frac{\hbar^2 k_f^2}{2m}$$ (USUALLY NEGLIG.)

$$|\langle\varphi_f|\hat{\varepsilon}\cdot\vec{p}|\varphi_i\rangle|^2 = |\hat{\varepsilon}\cdot\langle\varphi_f|\vec{p}|\varphi_i\rangle|^2 \Rightarrow \Delta\vec{k} = \vec{k}_f - \vec{k}_i - \vec{k}_{hv} + \vec{k}_{PHONON}$$

$$= \vec{g}_{BULK} \text{ (OR } \vec{g}_{SURF})$$

"DIRECT" TRANSITIONS

BUT LATTICE VIBRATIONS ⇒ SUM OVER $\vec{k}_{PHONON}$

⇒ FRACTION DIRECT ≈ DEBYE-WALLER FACTOR

$$\approx \exp[-g^2 \overline{u^2}]$$

NEARLY-FREE ELECTRONS IN A WEAK PERIODIC POTENTIAL—1 DIM.

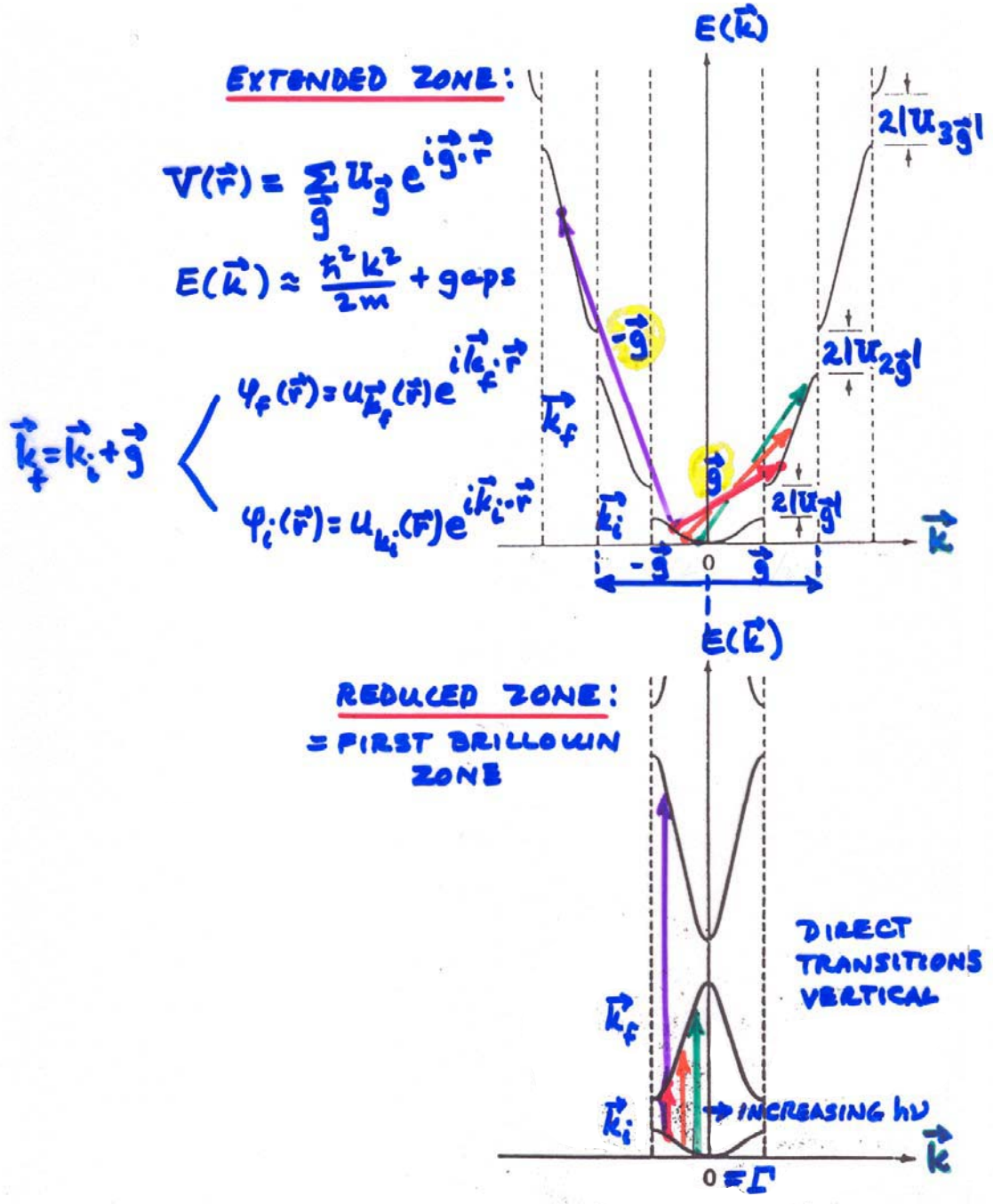

The electronic structure of a nearly free-electron metal—fcc Al

$$\phi(\vec{r}) = u_{\vec{k}}(\vec{r})\, e^{i\vec{k}\cdot\vec{r}}; \quad E(\vec{k}) \approx \frac{\hbar^2 k^2}{2m}$$

(Bloch)

3D Brillouin zone

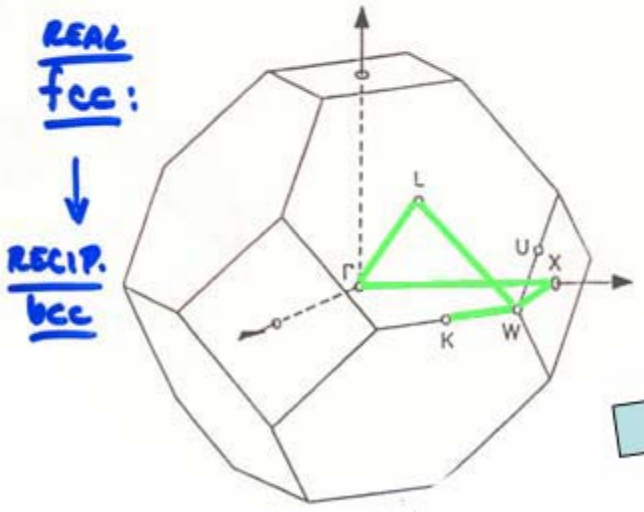

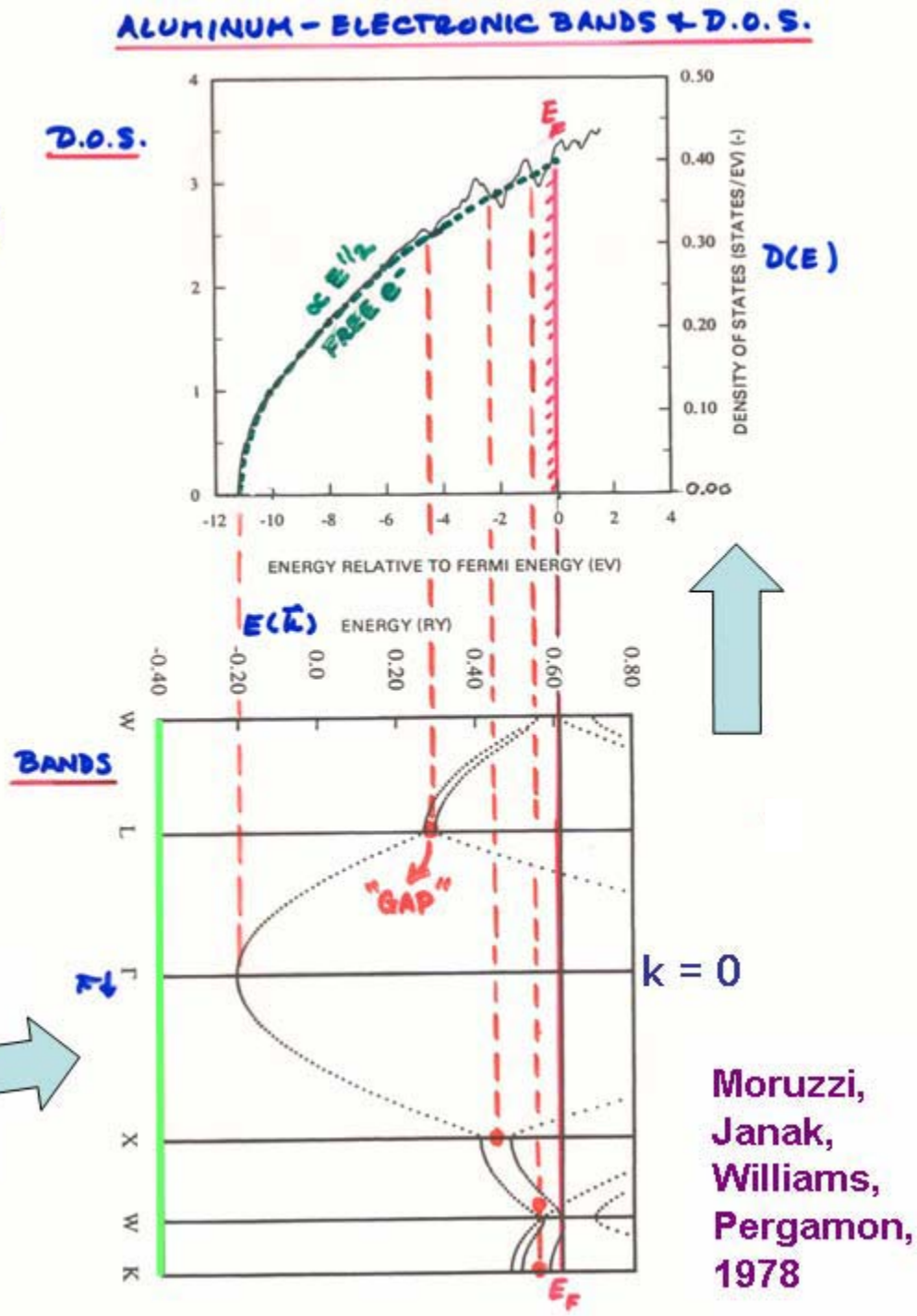

Moruzzi, Janak, Williams, Pergamon, 1978

Valence-band photoemission: Angle-Resolved Photoemission (ARPES)

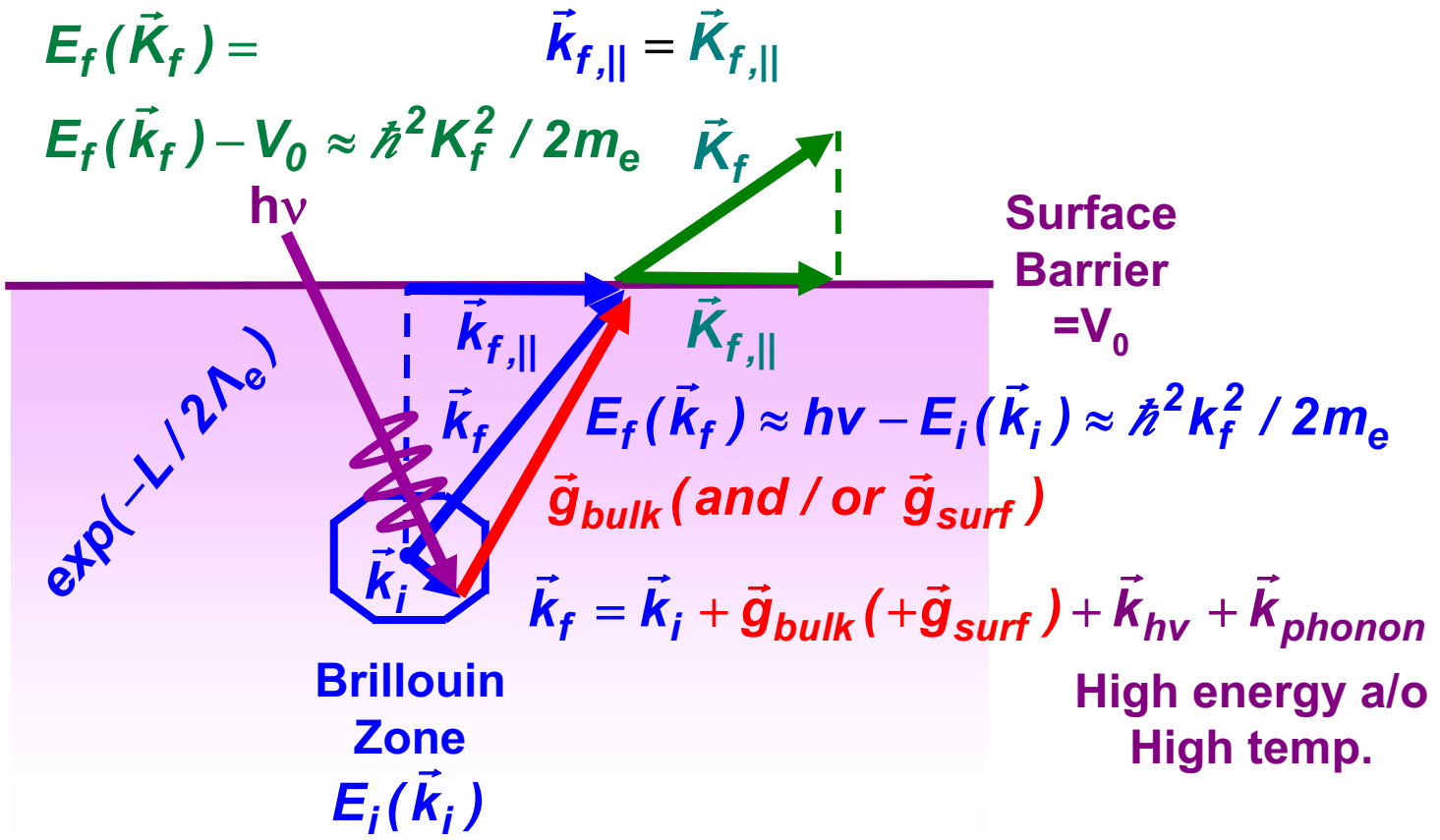

$$I(E_f, \vec{k}_f) \propto \left| \hat{\varepsilon} \bullet \left\langle \varphi_{photoe}(E_f = h\nu + E_i, \vec{k}_f = \vec{k}_i + \vec{g}) \middle| \vec{r} \middle| \varphi(E_i, \vec{k}_i) \right\rangle \right|^2$$

"Direct" or k-conserving transitions

Angle-Resolved Photoemission from ferromagnetic Ni(111)
$h\nu$ = 21.2 eV
Spin-split bands

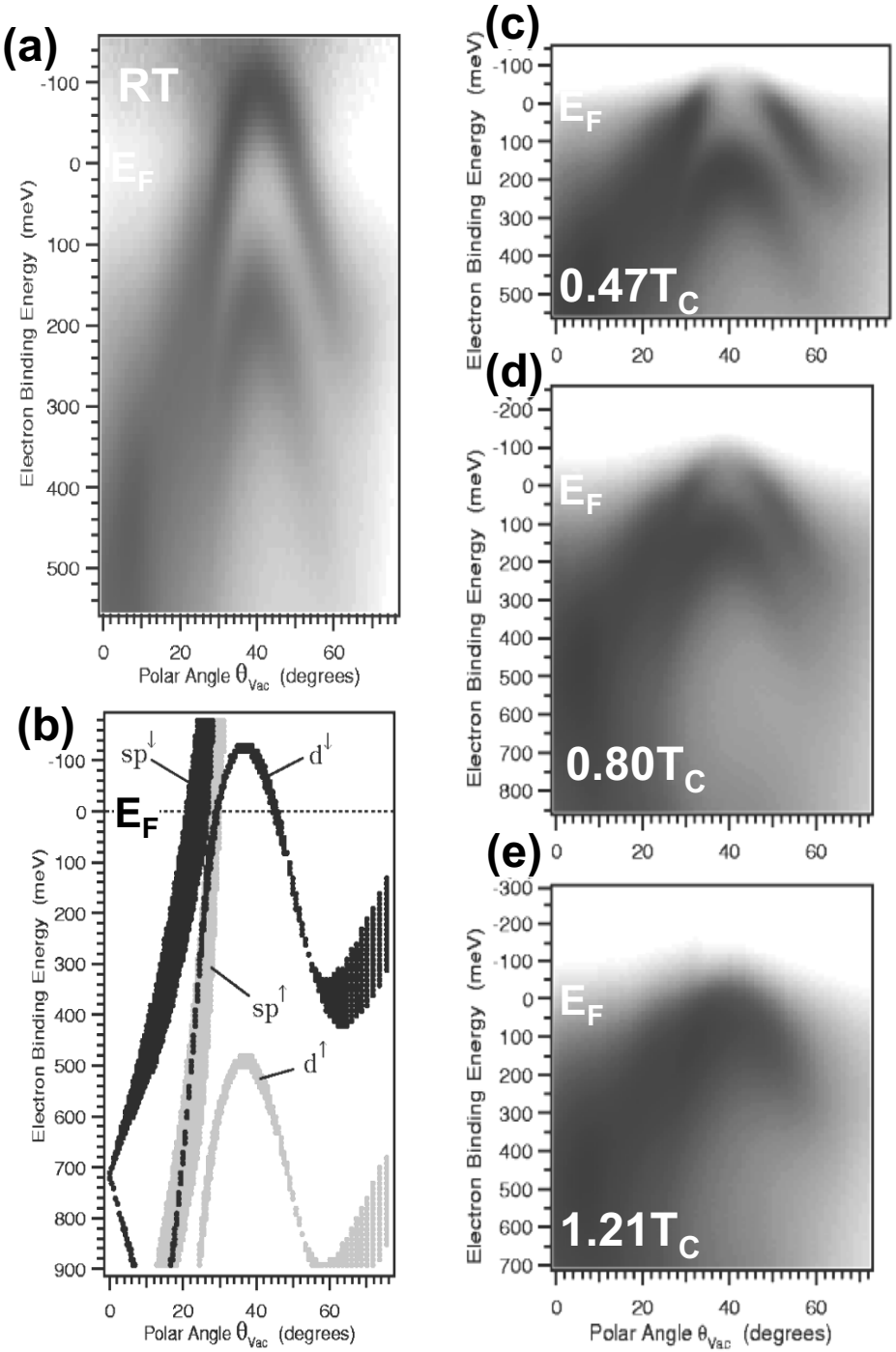

Kreutz et al.,
Phys. Rev. B 58 (1998) 1300

EXAMPLE:
NORMAL-EMISSION UPS FROM Cu(001)

$\Delta p_z \Delta z \approx \hbar/2$
$\Delta k_z \Lambda_e \approx ½$
$\Delta k_z \approx 1/(2\Lambda_e)$
For Cu @ $E_{kin} \approx 80$ eV,
$\Lambda_e \approx 4$ Å, $\Delta k_z \approx 0.12$ Å^{-1}
Compare $2\pi/a = 0.98$ Å^{-1}

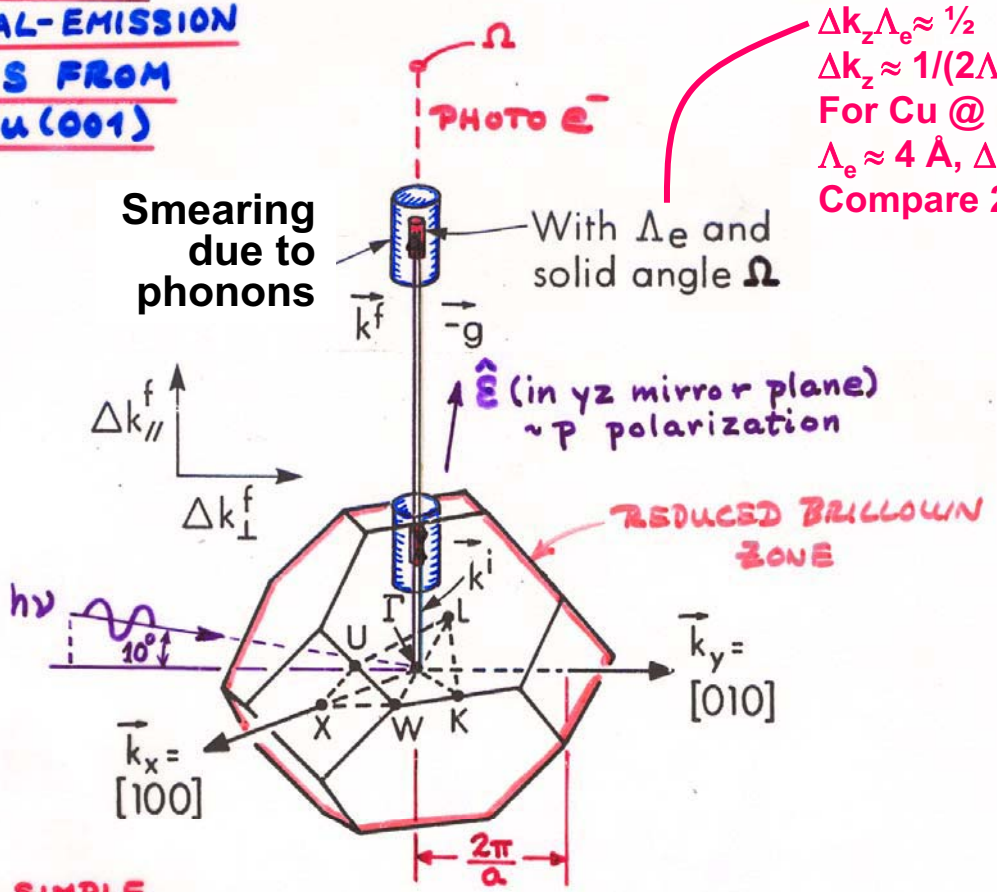

SIMPLE DT MODEL: Direct: $\vec{k}^f = \vec{k}^i + \vec{g} + \cancel{\vec{k}_{h\nu}}$

$E^i(\vec{k}^i)$ = initial band structure

$E^f(\vec{k}^f) \approx \hbar^2 (k^f)^2/2m$

Constant matrix elements

Expectations from simple direct-transition theory + symmetry considerations in matrix elements

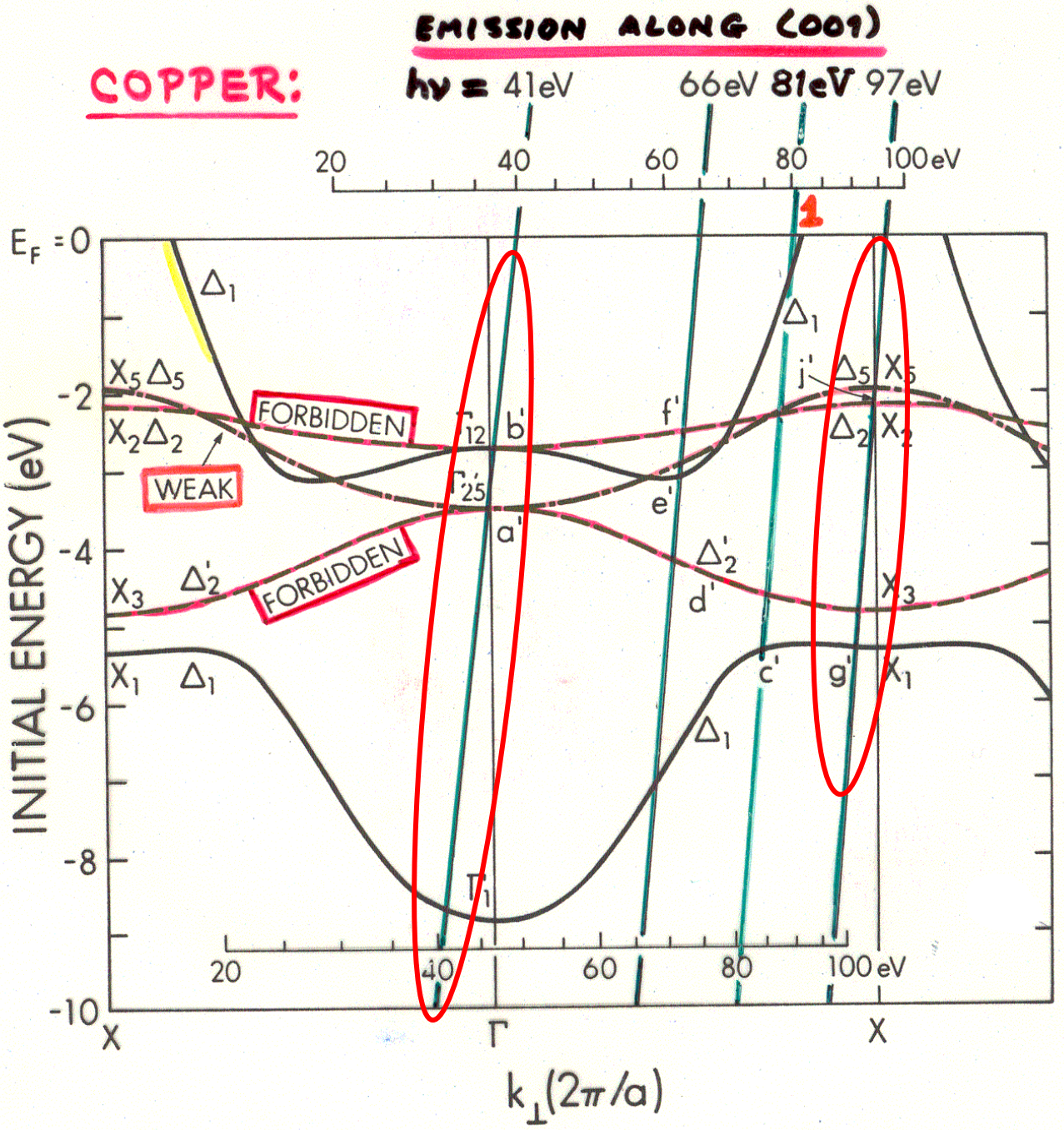

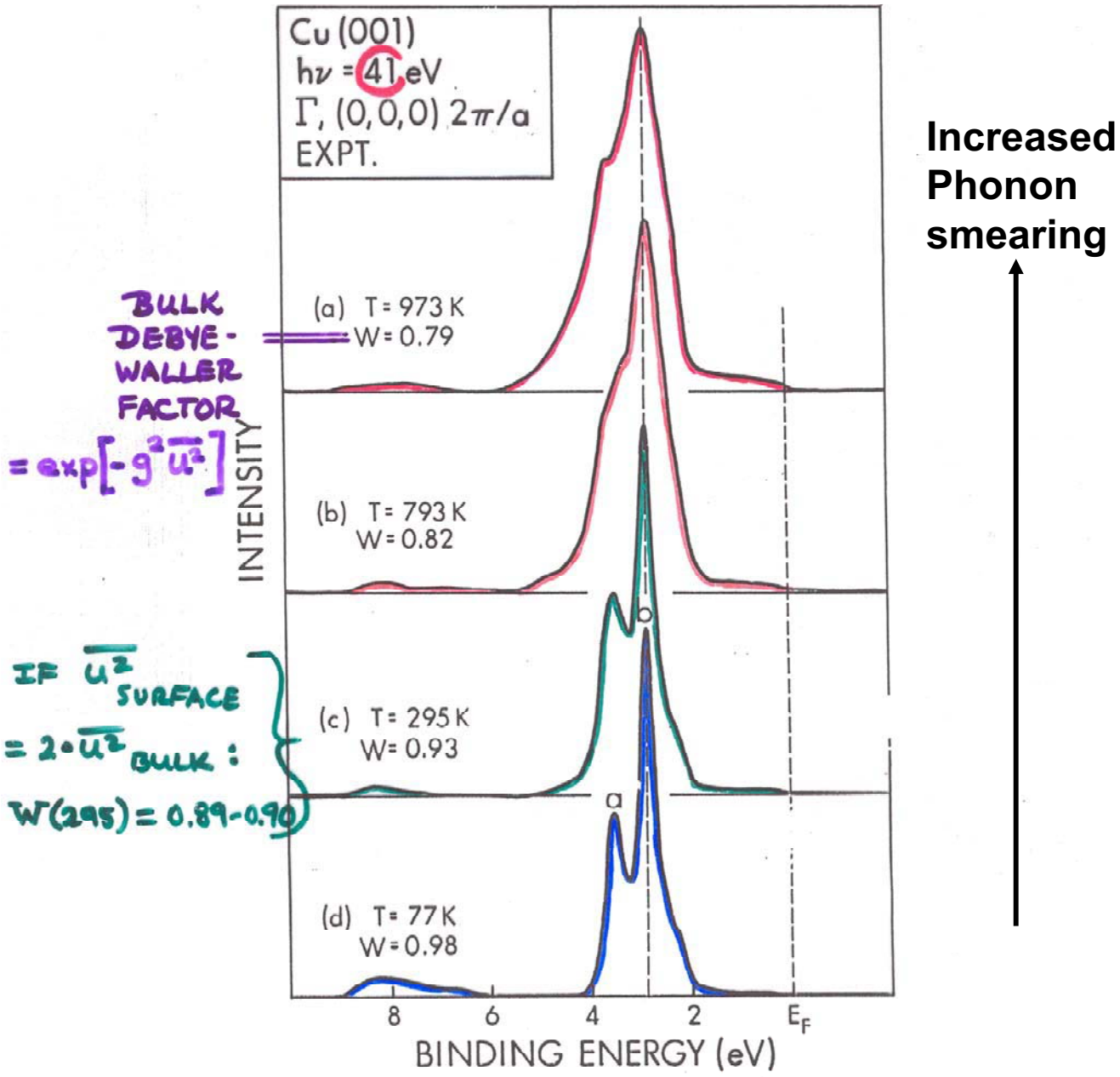

R.C. WHITE ET AL., PHYS. REV. B 35, 1147 (1987)

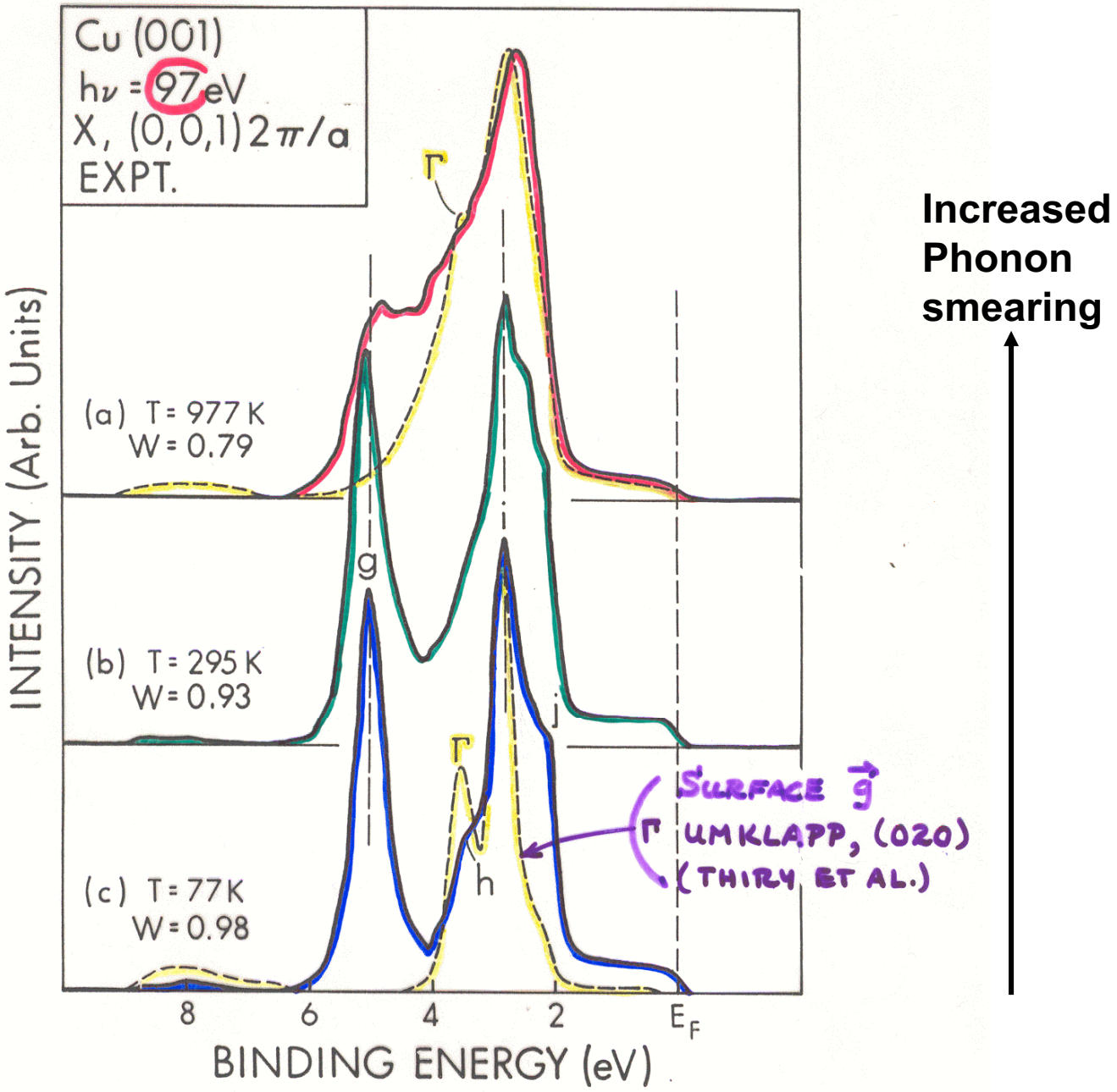
Cu (001)
hν = 97 eV
X, (0,0,1) 2π/a
EXPT.
Γ
(a) T = 977 K
W = 0.79
g
(b) T = 295 K
W = 0.93
Γ
h
(c) T = 77 K
W = 0.98
SURFACE g
Γ UMKLAPP, (020)
(THIRY ET AL.)
INTENSITY (Arb. Units)
8
6
4
2
E_F
BINDING ENERGY (eV)
Increased
Phonon
smearing

Cu: ANGLE-RESOLVED PHOTOEMISSION AND BAND-MAPPING ALONG (001)

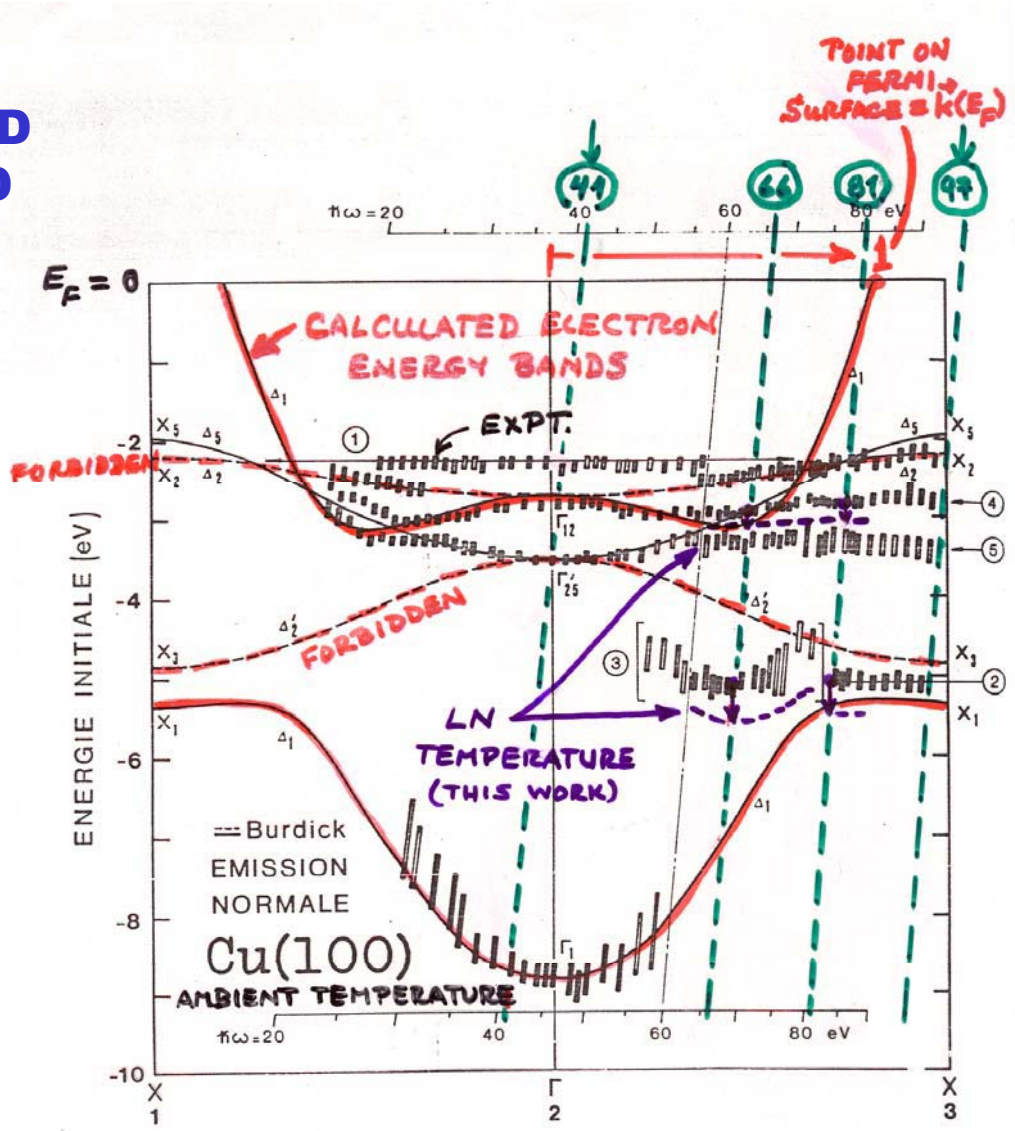

P. THIRY, THESIS, UNIV. OF PARIS (1980)
+ WHITE ET AL. P.R.B 35, 1147 (1987)

FIG.56

Cu: ANGLE-RESOLVED PHOTOEMISSION AND BAND-MAPPING ALONG (110)

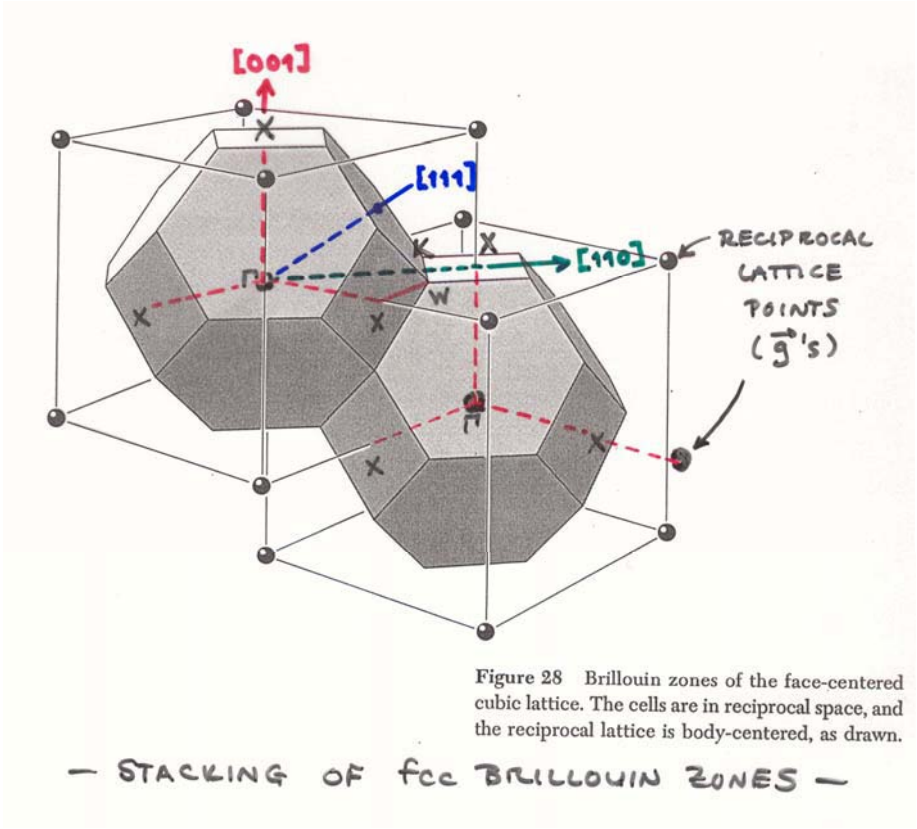

Figure 28 Brillouin zones of the face-centered cubic lattice. The cells are in reciprocal space, and the reciprocal lattice is body-centered, as drawn.

— STACKING OF fcc BRILLOUIN ZONES —

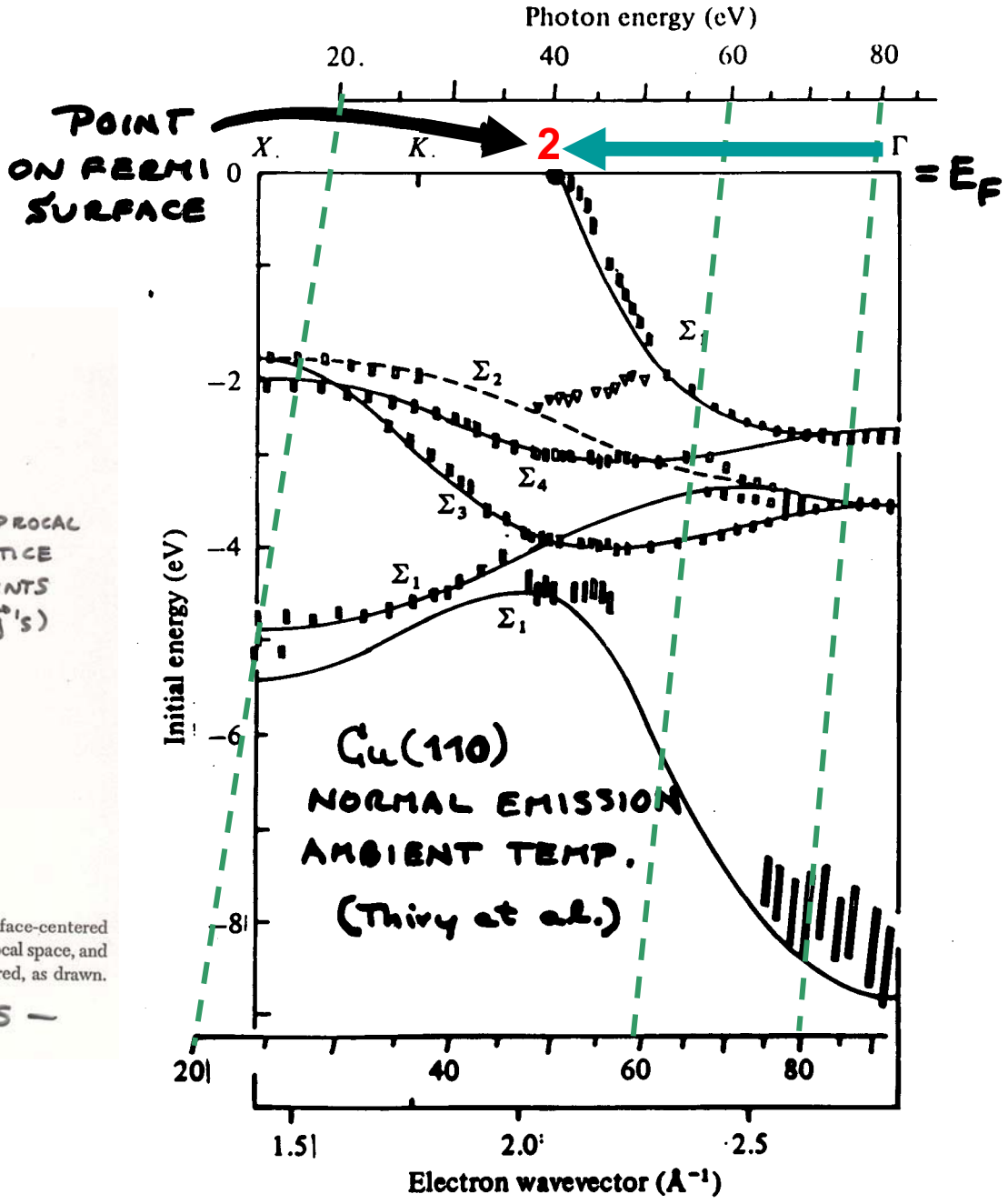

P.Thiry, Ph.D. thesis, Univ. of Paris (1980)

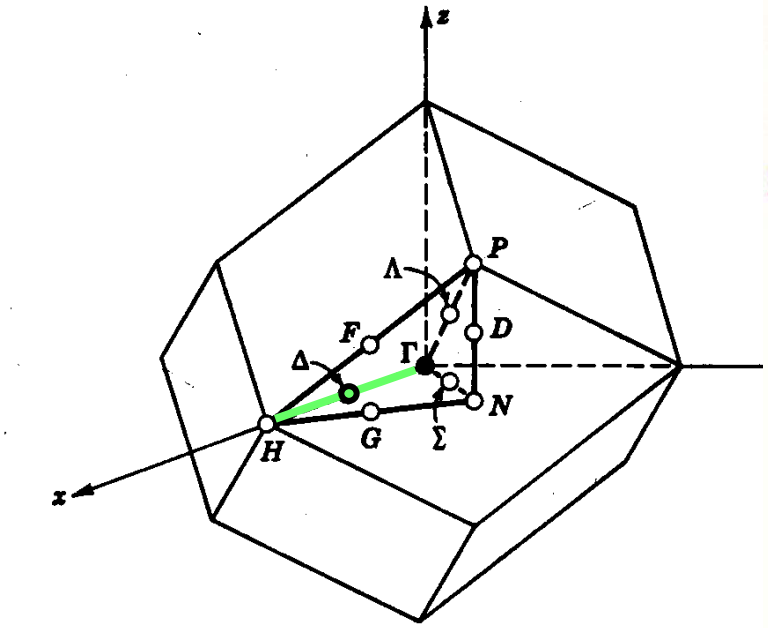

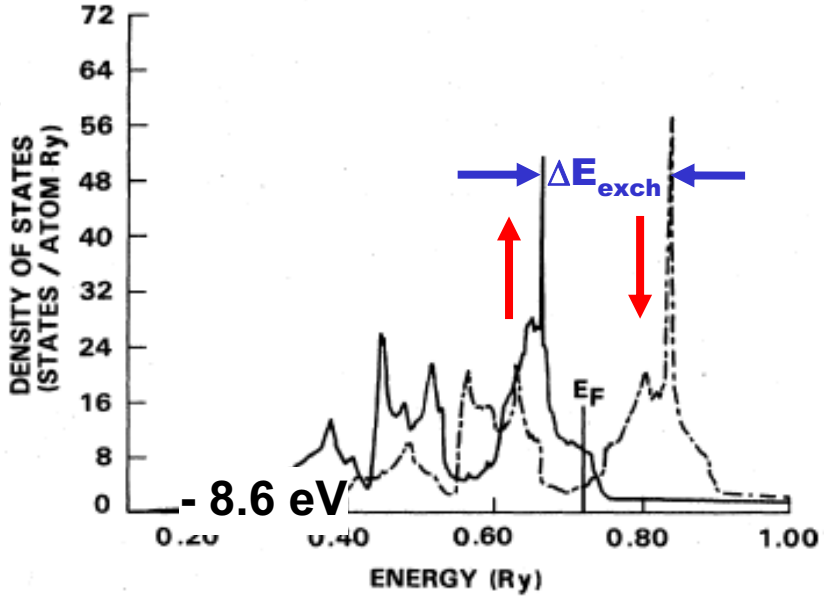

FIG. 4. Density of states at the equilibrium lattice constant of Fe for majority- (solid line) and minority- (broken line) spin states.

Hathaway et al., Phys. Rev. B 31, 7603 ('85)

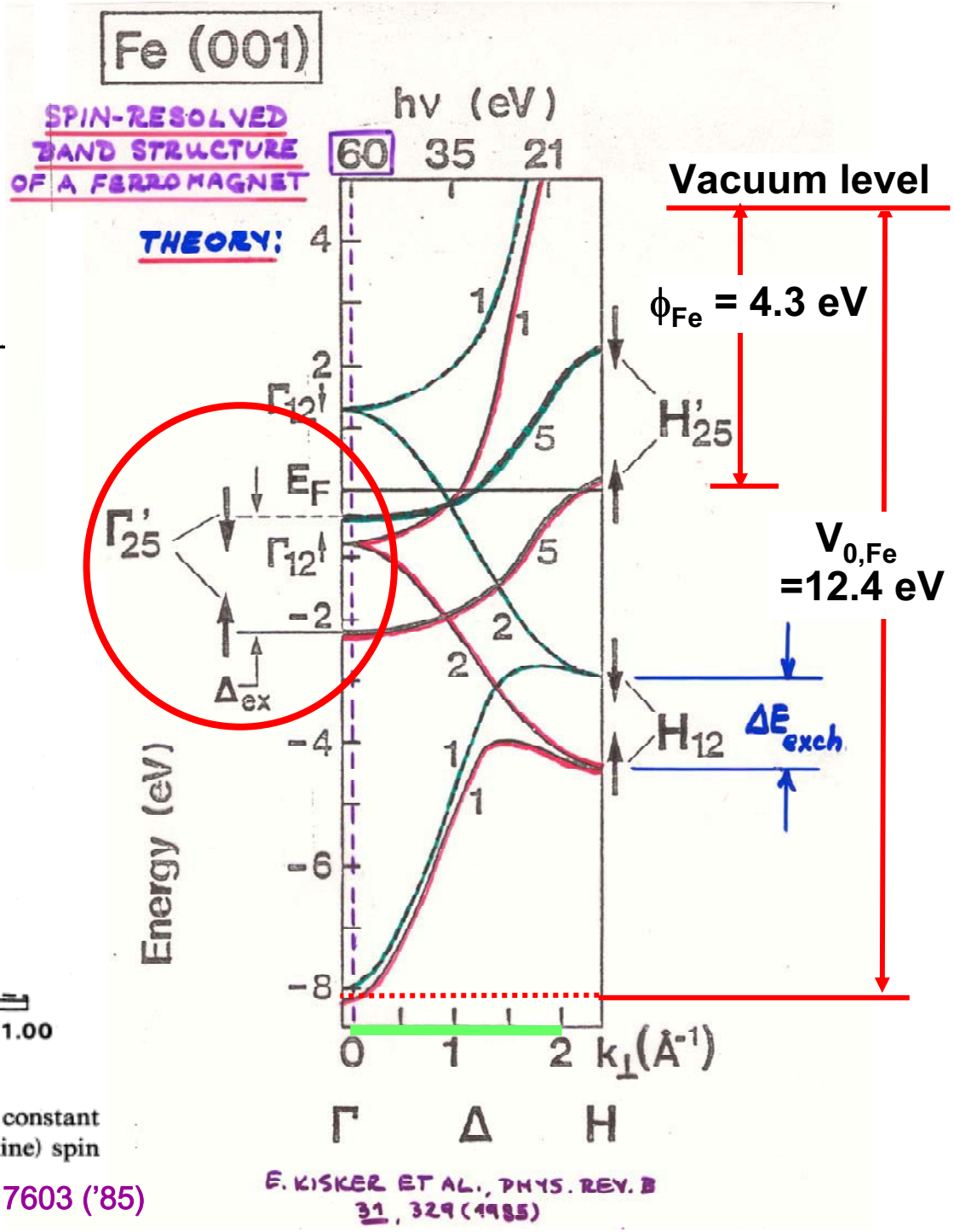

Fe: ANGLE AND SPIN-RESOLVED SPECTRA AT Γ POINT

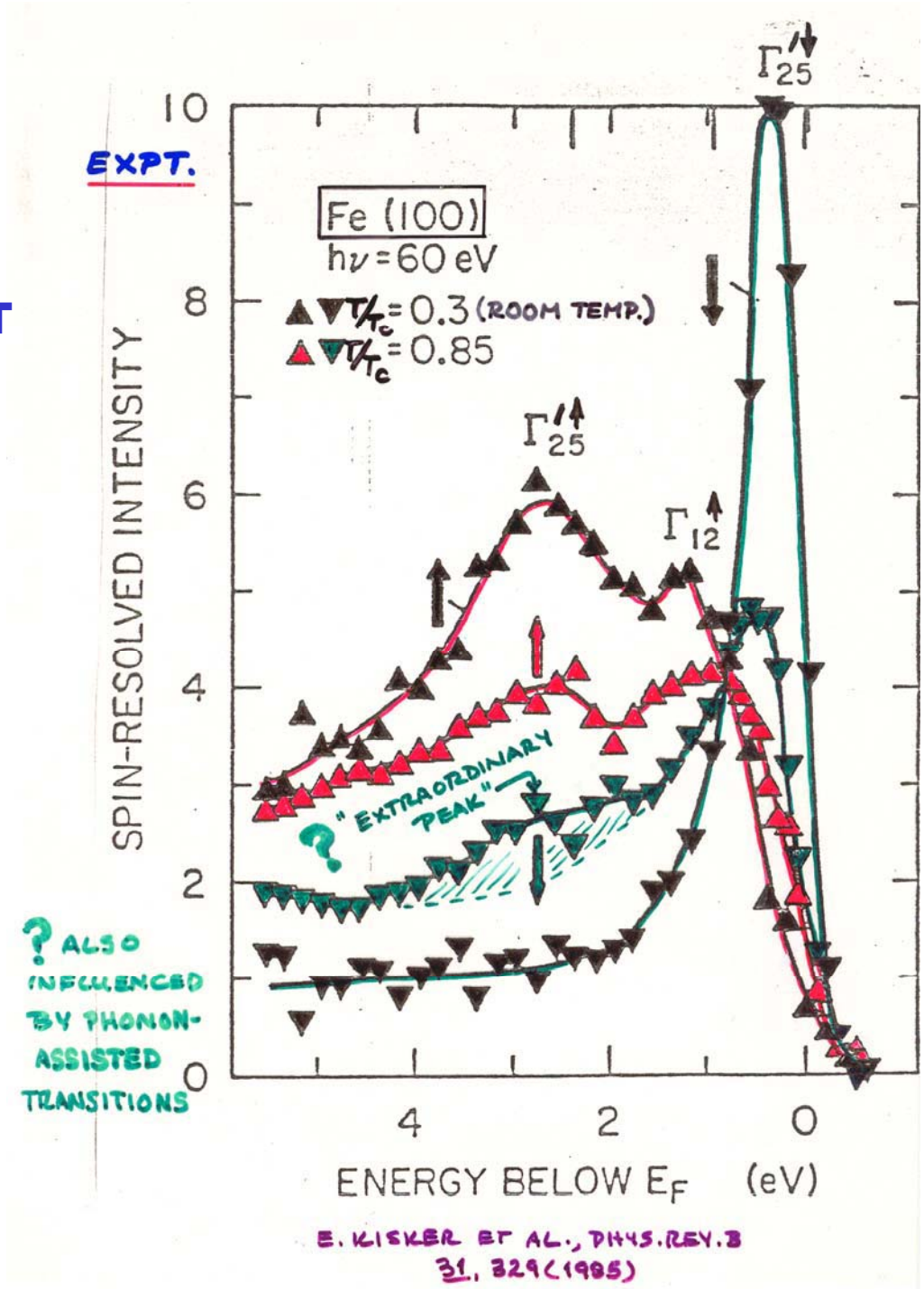

Half-Metallic Ferromagnetism

LDA theory- FM $La_{0.75}Ca_{0.25}MnO_3$

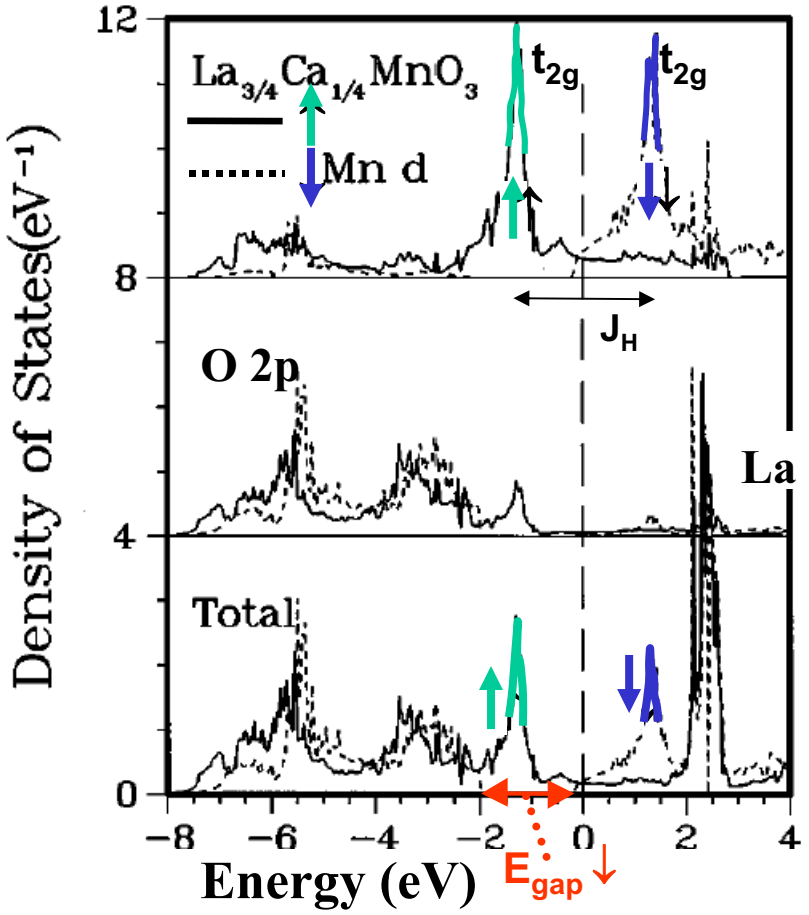

Pickett and Singh, PRB 53, 1146 (1996)

Experiment- spin-resolved PS
$La_{0.70}Sr_{0.30}MnO_3$ as thin film

Park et al., Nature, PRB 392, 794 (1998)

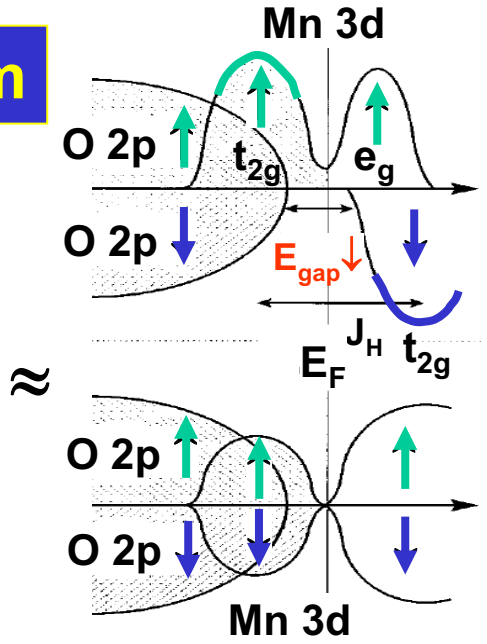

FM : $T \ll T_C$

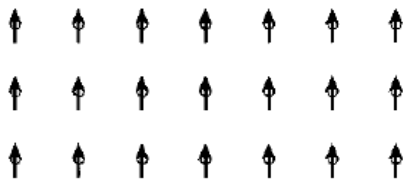

PM : $T > T_C$

$T \ll T_C$

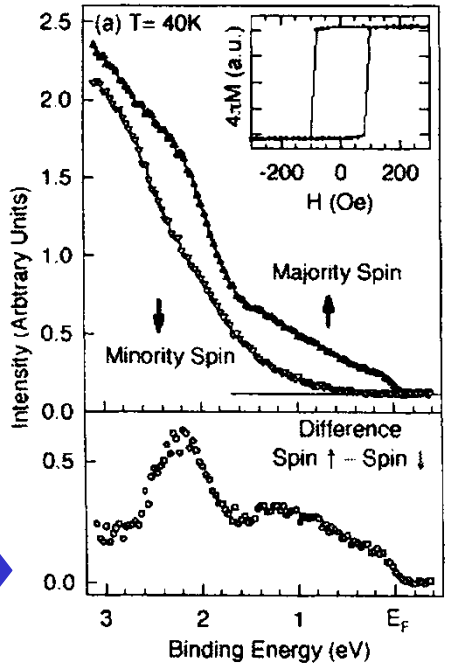

$T > T_C$

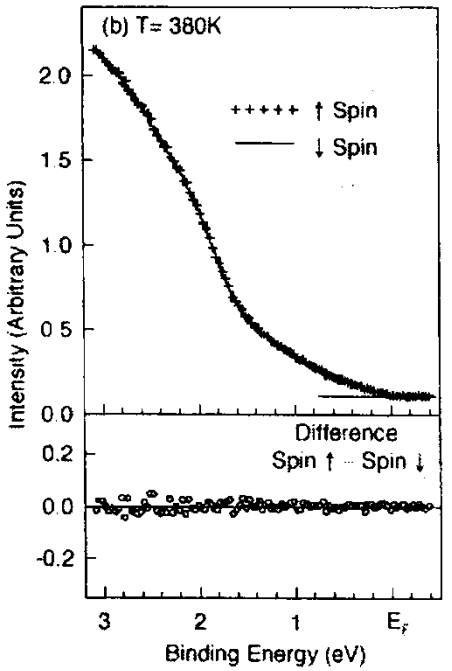

The electronic structure of a transition metal—fcc Cu

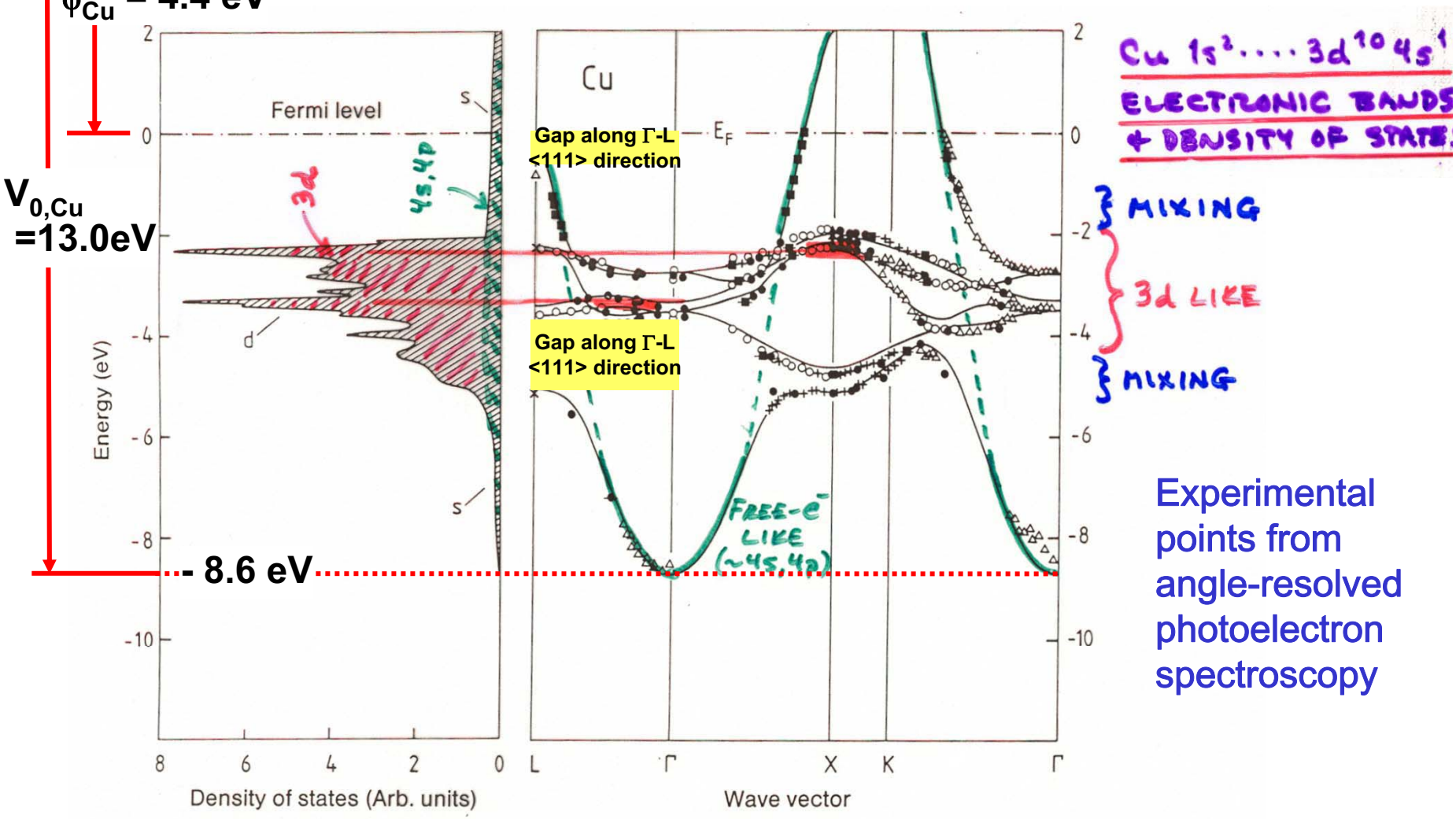

Experimental points from angle-resolved photoelectron spectroscopy

Fig. 7.12. Bandstructure $E(k)$ for copper along directions of high crystal symmetry (*right*). The experimental data were measured by various authors and were presented collectively by Courths and Hüfner [7.4]. The full lines showing the calculated energy bands and the density of states (*left*) are from [7.5]. The experimental data agree very well, not only among themselves, but also with the calculation

Surface states on Cu(111)

Shockley surface state

Tamm surface state

Fig. 4.21. Experimental dispersion of Cu(111) surface states plotted with a projection of the bulk bands: (*a*) Shockley state near the zone center (Kevan, 1983); (*b*) Tamm state near the zone boundary (Heimann, Hermanson, Miosga and Neddermeyer, 1979). Compare with Fig. 4.17.

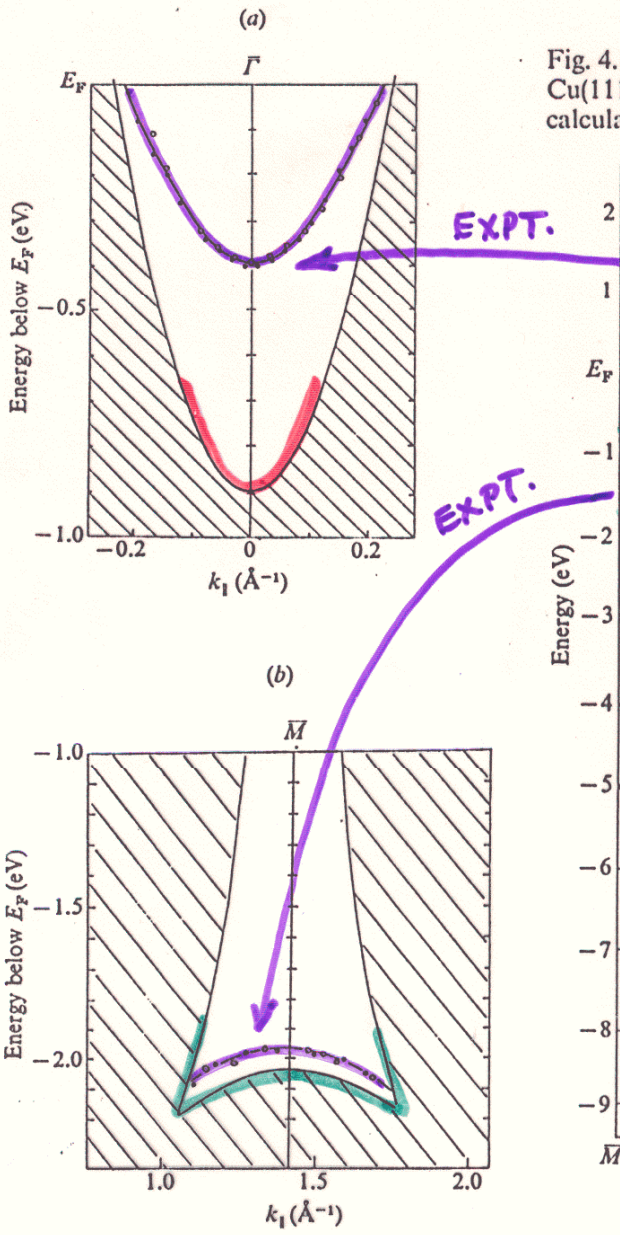

THEORY

Fig. 4.17. Surface states (dashed curves) and bulk projected ban Cu(111) surface according to a six-layer surface band structure calculation (Euceda, Bylander & Kleinman, 1983).

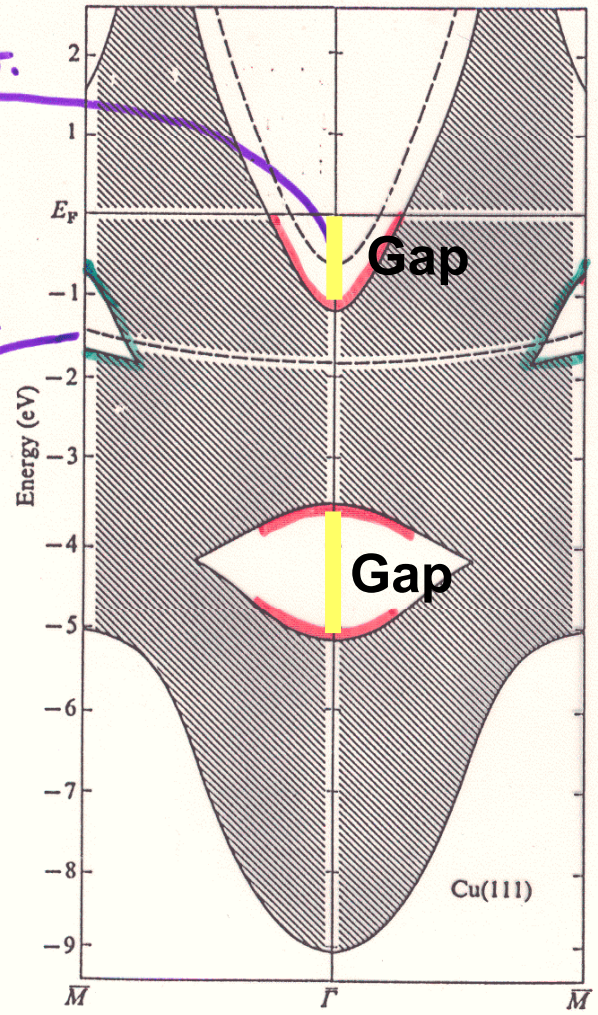

Zangwill, Surface Physics,

Fig. 4.20. Photoemission energy distribution curves from Cu(111) at different collection angles. Equation (4.32) has been used to express the electron kinetic energy in terms of the binding energy of the electron state (Kevan, 1983).

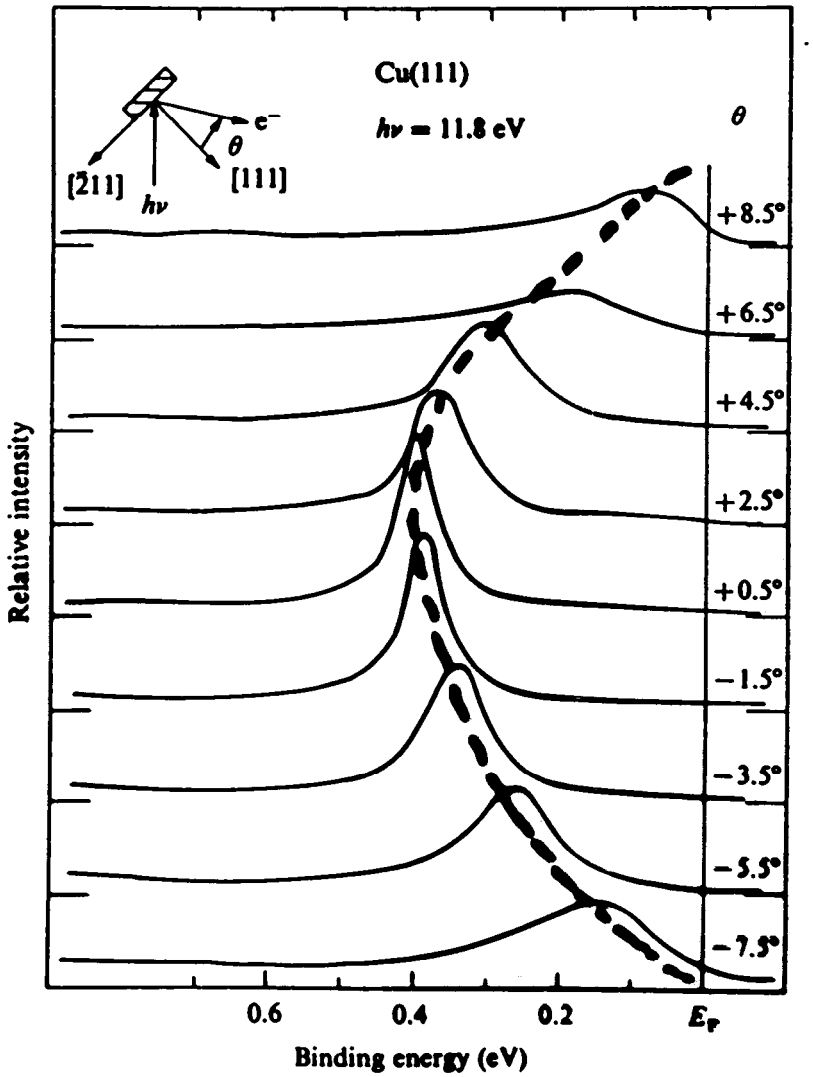

Zangwill,
Surface Physics,

Valence-Band Photoemission at High Energy-- What & Where is the "XPS Limit"?:

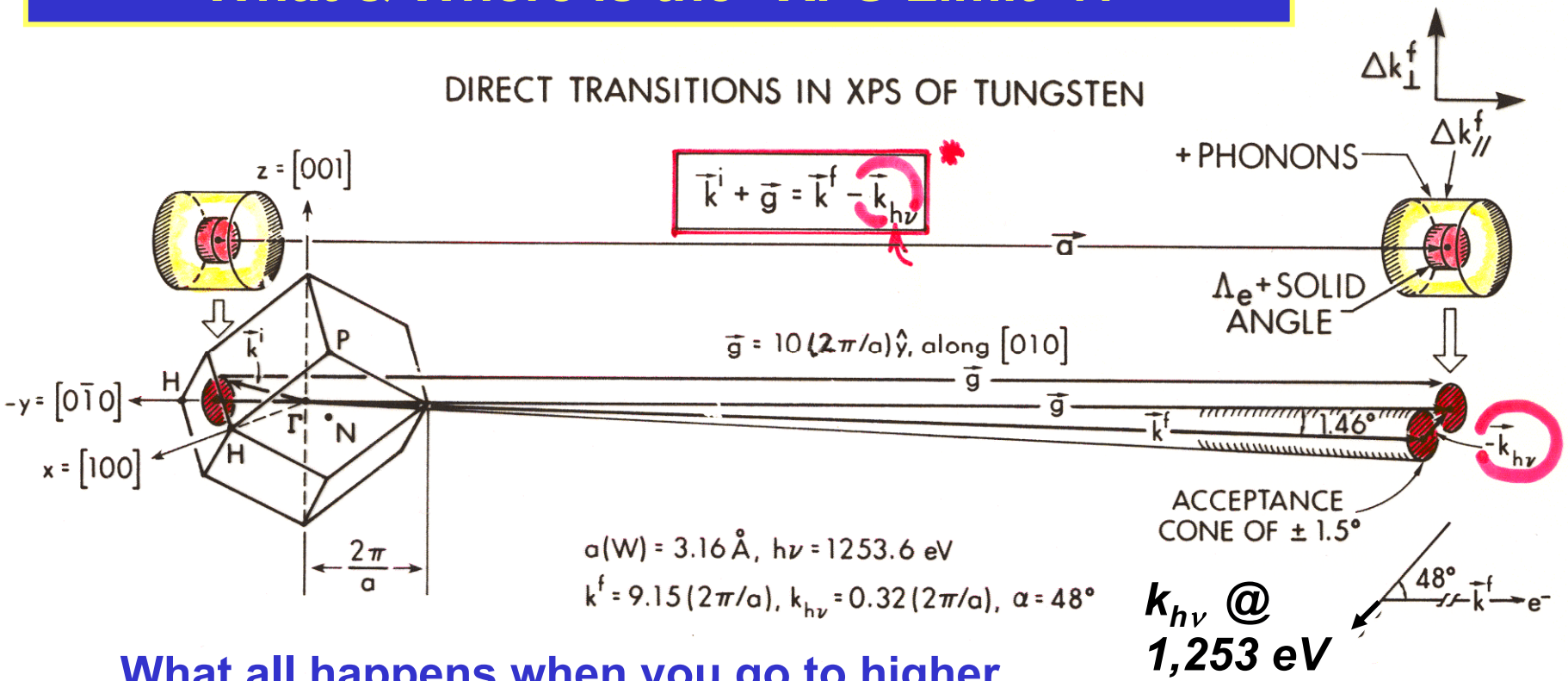

$k_{h\nu}$ @ 1,253 eV

What all happens when you go to higher photon energies?

- **non-dipole effect→the photon momentum**
- **angular acceptance→B.Z. averaging**
- **lattice recoil, phonon creation→more Brillouin Zone averaging**

→The XPS limit of full B.Z. averaging and D.O.S. sensitivity

Hussain et al., Phys. Rev. B 22, 3750 ('80)

Valence-band photoemission—at higher energy

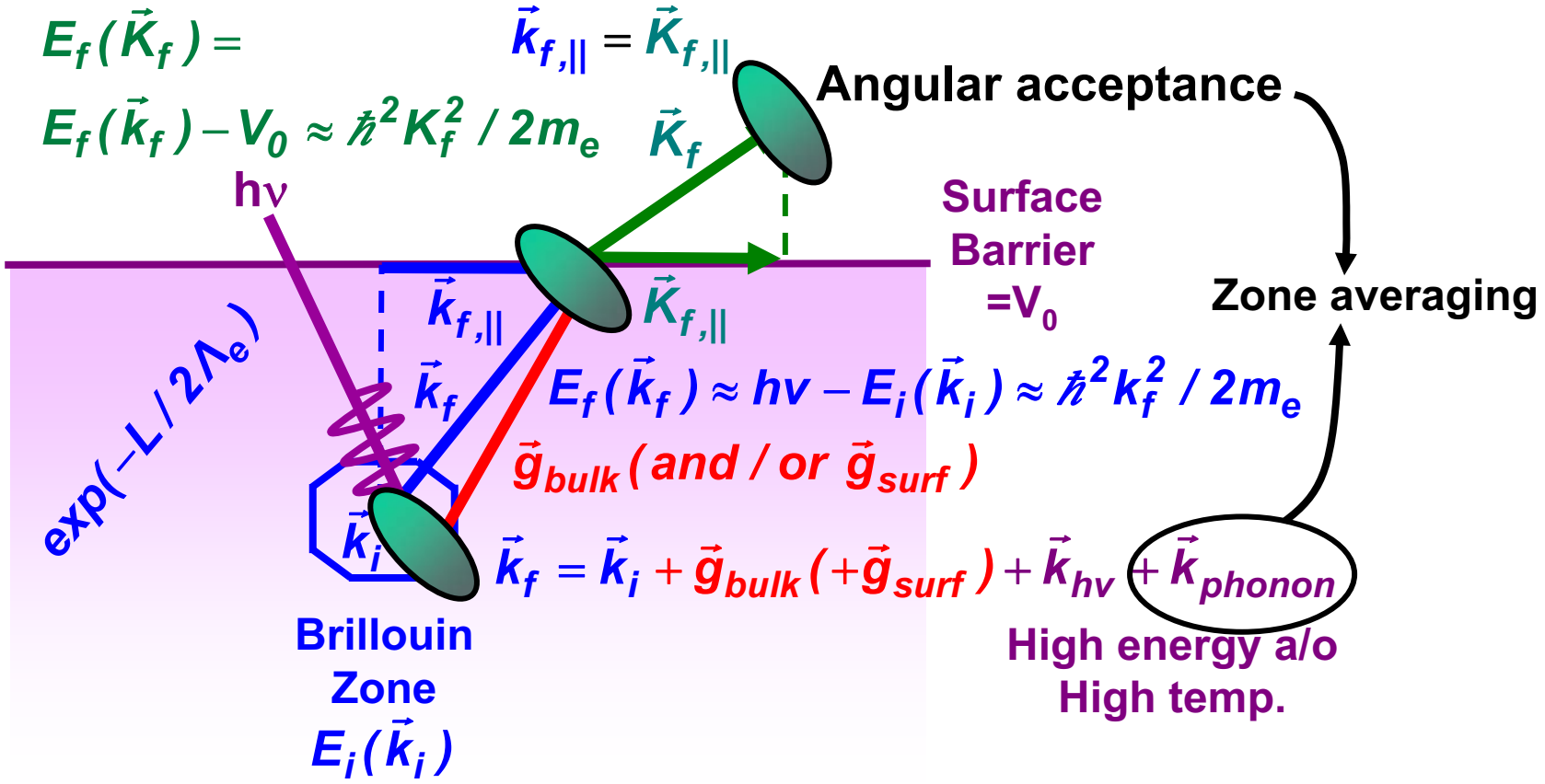

$$I(E_f, \vec{k}_f) \propto \left| \hat{\varepsilon} \bullet \left\langle \varphi_{photoe}(E_f = h\nu + E_i, \vec{k}_f = \vec{k}_i + \vec{g}) \middle| \vec{r} \middle| \varphi(E_i, \vec{k}_i) \right\rangle \right|^2$$

Hussain et al., Phys. Rev. B 34 (1986) 5226.

CORE PHOTOELECTRON INTENSITIES AND COMPOSITION

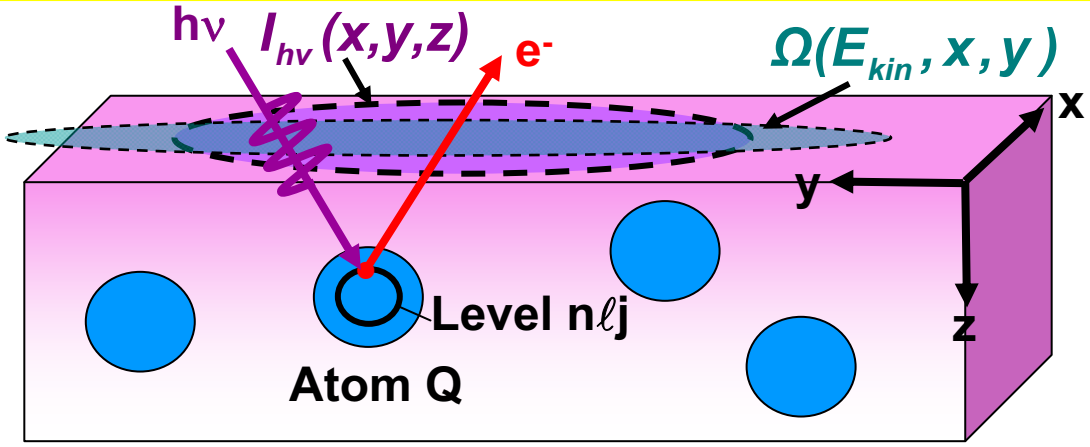

$$I(Qn\ell j) =$$

$$C \int_0^{\infty} I_{hv}(x,y,z)\rho_Q(x,y,z)\frac{d\sigma_{Qn\ell j}(hv)}{d\Omega} exp\left[-\frac{z}{\Lambda_e(E_{kin})\sin\theta}\right]\Omega(E_{kin}, x, y)dxdydz$$

$I_{hv}(x,y,z)$ = x-ray flux

$\rho_Q(x,y,z)$ = density of atoms Q → quantitative analysis

$\frac{d\sigma_{Qn\ell j}(hv)}{d\Omega}$ = energy-dependent differential photoelectric cross section for subshell $Qn\ell j$

$\Lambda_e(E_{kin})$ = energy-dependent inelastic attenuation length

→ Effective Attenuation Length (EAD) → Mean Emission Depth (MED)

$\Omega(E_{kin}, x, y)$ = energy-dependent spectrometer acceptance solid angle

VALENCE-BAND PHOTOELECTRON INTENSITIES AND DENSITIES OF STATES

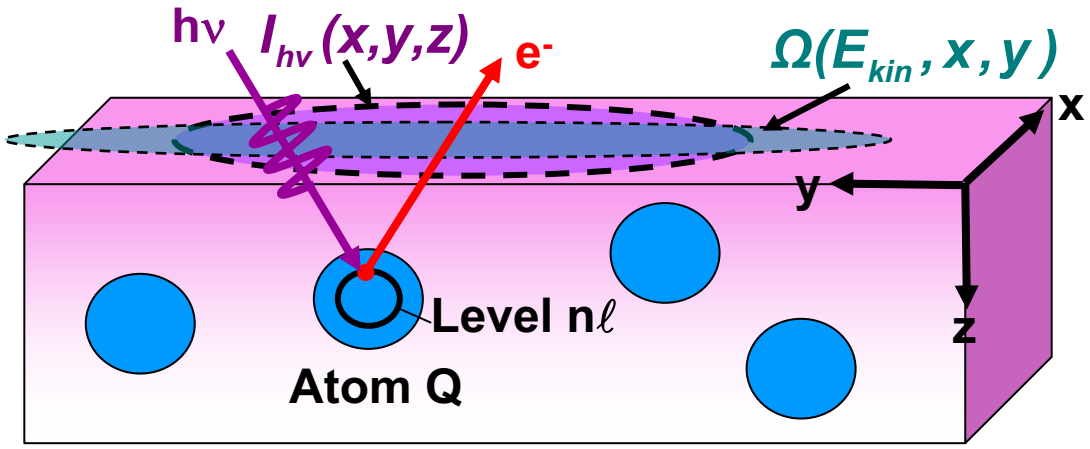

$$I(E_{kin}, Qn\ell) =$$

$$C' \int_0^{\infty} I_{hv}(x,y,z)\rho_{Qn\ell}(E_b,x,y,z)\frac{d\sigma_{Qn\ell}(hv)}{d\Omega}\exp\left[-\frac{z}{\Lambda_e(E_{kin})\sin\theta}\right]\Omega(E_{kin},x,y)dxdydz$$

$I_{hv}(x,y,z)$ = x-ray flux

$\rho_{Qn\ell}(E_b,x,y,z)$ = density of states, projected onto $Qn\ell$ character

$\frac{d\sigma_{Qn\ell}(hv)}{d\Omega}$ = energy-dependent differential photoelectric cross section for subshell $Qn\ell$

$\Lambda_e(E_{kin})$ = energy-dependent inelastic attenuation length

→ Mean Emission Depth

$\Omega(E_{kin}, x, y)$ = energy-dependent spectrometer acceptance solid angle

Estimating phonon effects: 1st approx.

$W(T) = \text{Debye-Waller factor} = \exp\left(-\frac{1}{3}g^2\left\langle U^2(T)\right\rangle\right)$

$I(E,T) = W(T)I_{DT} + [1-W(T)]I_{NDT}$

Shevchik, Phys. Rev. B 20, 3020 ('79); Hussain et al., Phys. Rev. 22, 3750 ('80)

hν = 1487 eV

TABLE I. Tabulation of thermal displacements $\langle U^2\rangle$ and Debye-Waller factors $[W(T)=\exp(-\frac{1}{3}\langle U^2\rangle g^2)]$ in the XPS regime (E_{kin} = 1482 eV) for various elements. The Debye temperatures are taken from Ref. 30. The solid line divides the Debye-Waller factors so as to indicate when $\geq\frac{1}{2}$ of the transitions will be direct. Elements are in order of Z.

Element	Θ_D (K)	A (amu)	T = 4 K $\langle U^2\rangle$ (10^{-18} cm^2)	W	T = 77 K $\langle U^2\rangle$ (10^{-18} cm^2)	W	T = 300 K $\langle U^2\rangle$ (10^{-18} cm^2)	W	T = 1000 K $\langle U^2\rangle$ (10^{-18} cm^2)	W
Be	1440	9.012	0.84	0.34	0.86	0.33	1.07	0.25	2.47	0.04
C	2230	12.001	0.21	0.03	0.41	0.59	0.46	0.53	0.83	0.34
Mg	400	24.312	1.18	0.22	1.46	0.16	2.58	0.01		
Al	428	26.981	0.95	0.29	1.15	0.22	2.79	0.03		
Si	645	28.086	0.60	0.46	0.66	0.42	1.26	0.19	3.07	0.02
Ca	230	40.08	1.19	0.21	1.94	0.08	6.24	0.0		
Ti	420	47.9	0.54	0.49	0.66	0.42	1.63	0.12	5.16	0.0
V	380	50.942	0.56	0.48	0.72	0.39	1.85	0.09	5.93	0.0
Cr	630	51.996	0.33	0.65	0.37	0.62	0.71	0.40	2.15	0.06
Mn	410	54.938	0.48	0.58	0.60	0.46	1.49	0.14	4.72	0.0
Fe	470	55.847	0.42	0.58	0.43	0.53	1.13	0.23	3.58	0.01
Co	445	58.933	0.42	0.58	0.50	0.52	1.19	0.21	3.74	0.0
Ni	450	58.71	0.41	0.58	0.49	0.53	1.17	0.22	3.67	0.01
Cu	343	63.54	0.50	0.52	0.67	0.42	1.82	0.09	5.84	0.0
Zn	327	65.37	0.51	0.51	0.79	0.40	1.82	0.08		
Ge	374	72.59	0.46	0.58	0.51	0.51	1.34	0.17	4.28	0.0
As	282	74.922	0.52	0.51	0.77	0.37	2.25	0.05	7.33	0.0
Zr	291	91.22	0.41	0.59	0.60	0.46	1.74	0.10	5.66	0.0
Nb	275	92.906	0.43	0.57	0.65	0.43	1.90	0.08	6.21	0.0
Mo	450	95.94	0.26	0.72	0.39	0.63	0.71	0.33	2.25	0.05
Ru	600	101.07	0.18	0.38	0.26	0.77	0.40	0.60	1.21	0.21
Rh	480	102.905	0.22	0.75	0.26	0.71	0.59	0.46	1.84	0.09
Pd	274	106.4	0.37	0.61	0.57	0.48	1.68	0.11	5.46	0.0
Ag	225	107.87	0.45	0.56	0.75	0.38	2.44	0.04	8.00	0.0
Cd	209	112.40	0.47	0.53	0.81	0.35	2.70	0.03		
Sn	200	118.69	0.46	0.55	0.83	0.34	2.53	0.04		
Sb	211	121.75	0.49	0.57	0.79	0.36	2.46	0.04		
Hf	252	178.49	0.24	0.73	0.39	0.66	1.18	0.22	3.85	0.01
Ta	240	180.948	0.25	0.72	0.42	0.58	1.28	0.19	4.19	0.0
W	400	183.85	0.13	0.82	0.18	0.79	0.47	0.55	1.48	0.14
Re	430	186.2	0.12	0.86	0.17	0.81	0.40	0.63	1.23	0.19
Os	500	190.2	0.11	0.86	0.13	0.84	0.30	0.68	0.92	0.30
Ir	420	192.2	0.14	0.84	0.17	0.81	0.41	0.59	1.29	0.13
Pt	240	195.09	0.23	0.74	0.29	0.69	1.19	0.21	3.88	0.01
Au	165	196.967	0.34	0.65	0.52	0.35	2.46	0.04	8.14	0.0
Pb	105	207.19	0.51	0.52	1.54	0.13	5.75	0.0		

Greater than 50% direct transitions

Gold Valence Spectrum

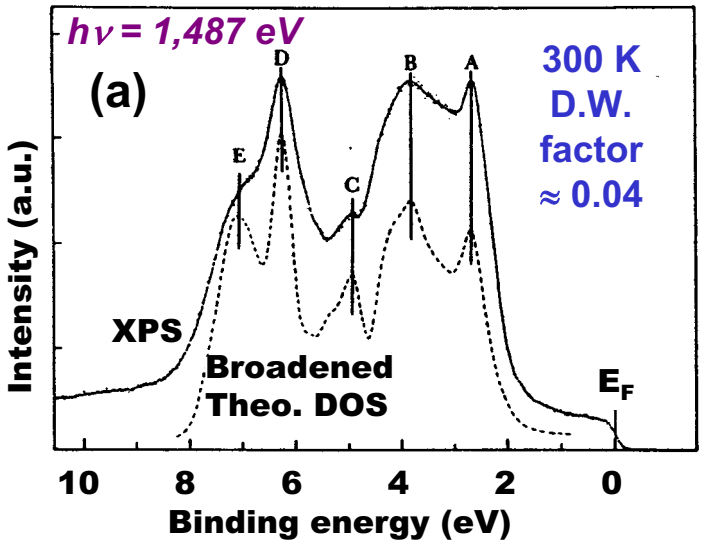

Silver Valence Spectrum

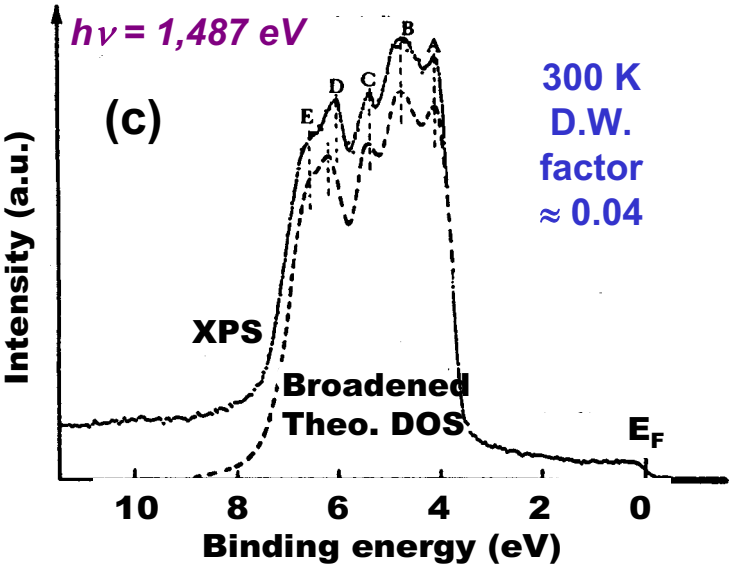

Valence spectra in the XPS Limit

Gold Valence Spectrum

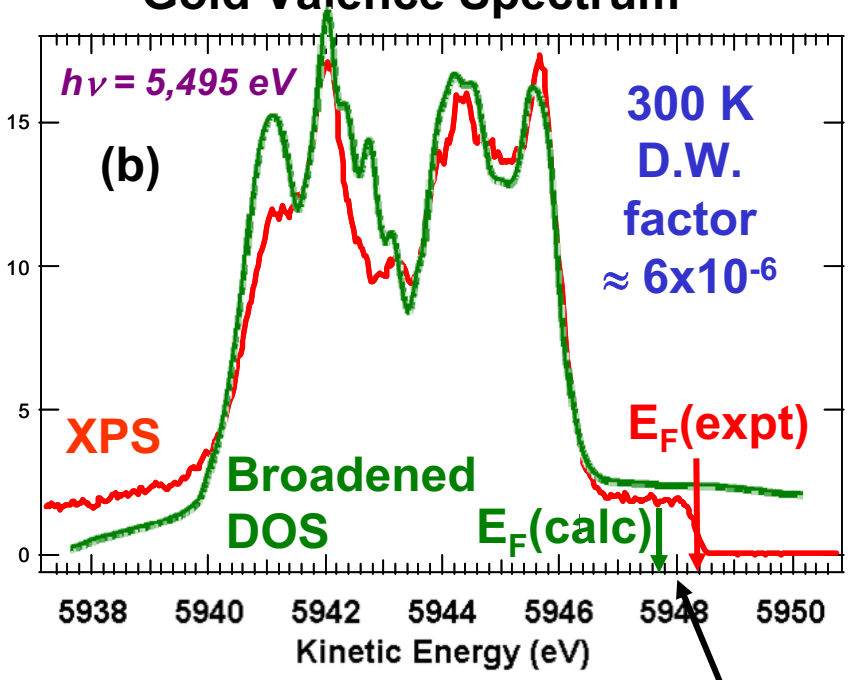

Screening/
self-energy
correction

Some classic cases in the XPS limit:

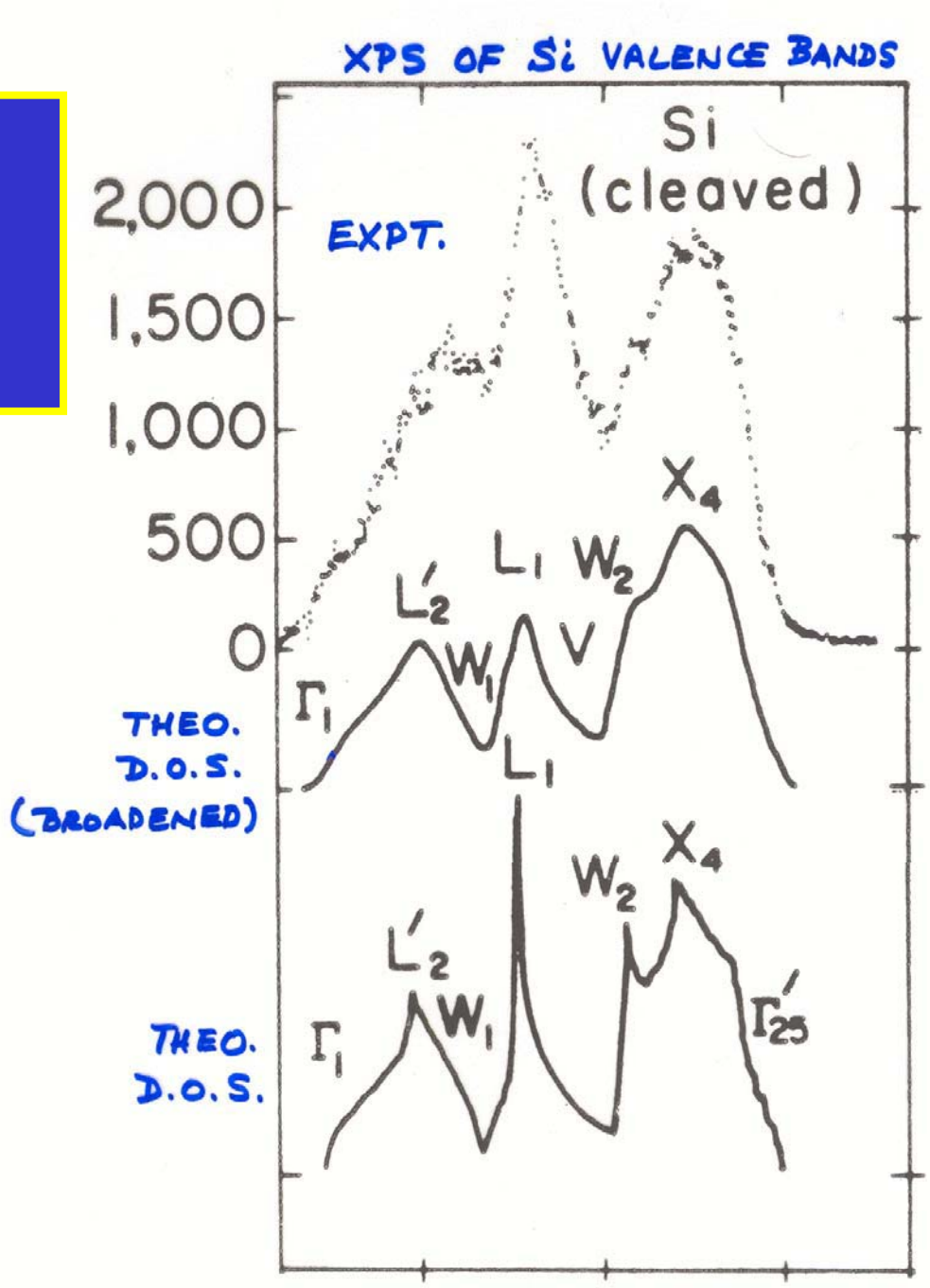

"Basic Concepts of XPS"
Figure 14

XPS and HXPS in k space:

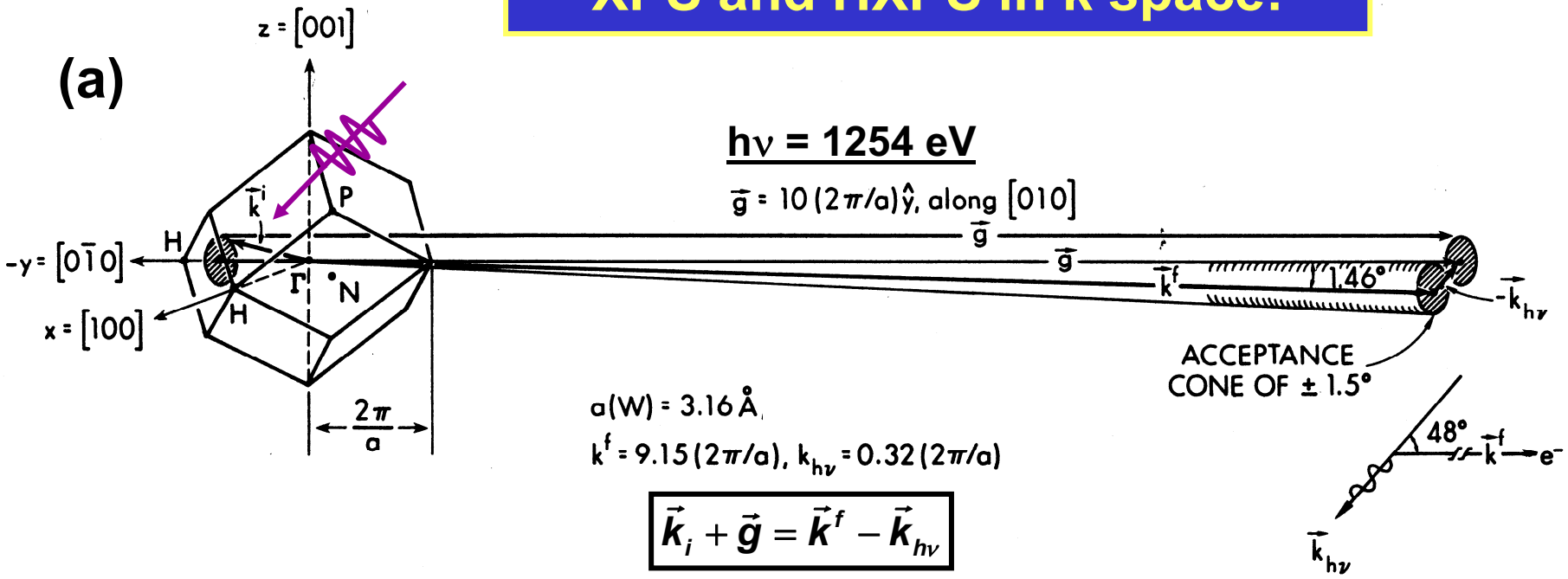

Phonon effects: Approximate fraction of "good" direct transitions

≈ Debye-Waller factor = *W(T) ≈ exp[-g² <u²(T)>]*

= Mean-squared vibrational displacement

Direct-transition effects in XPS: W(110) at 1253.6 eV

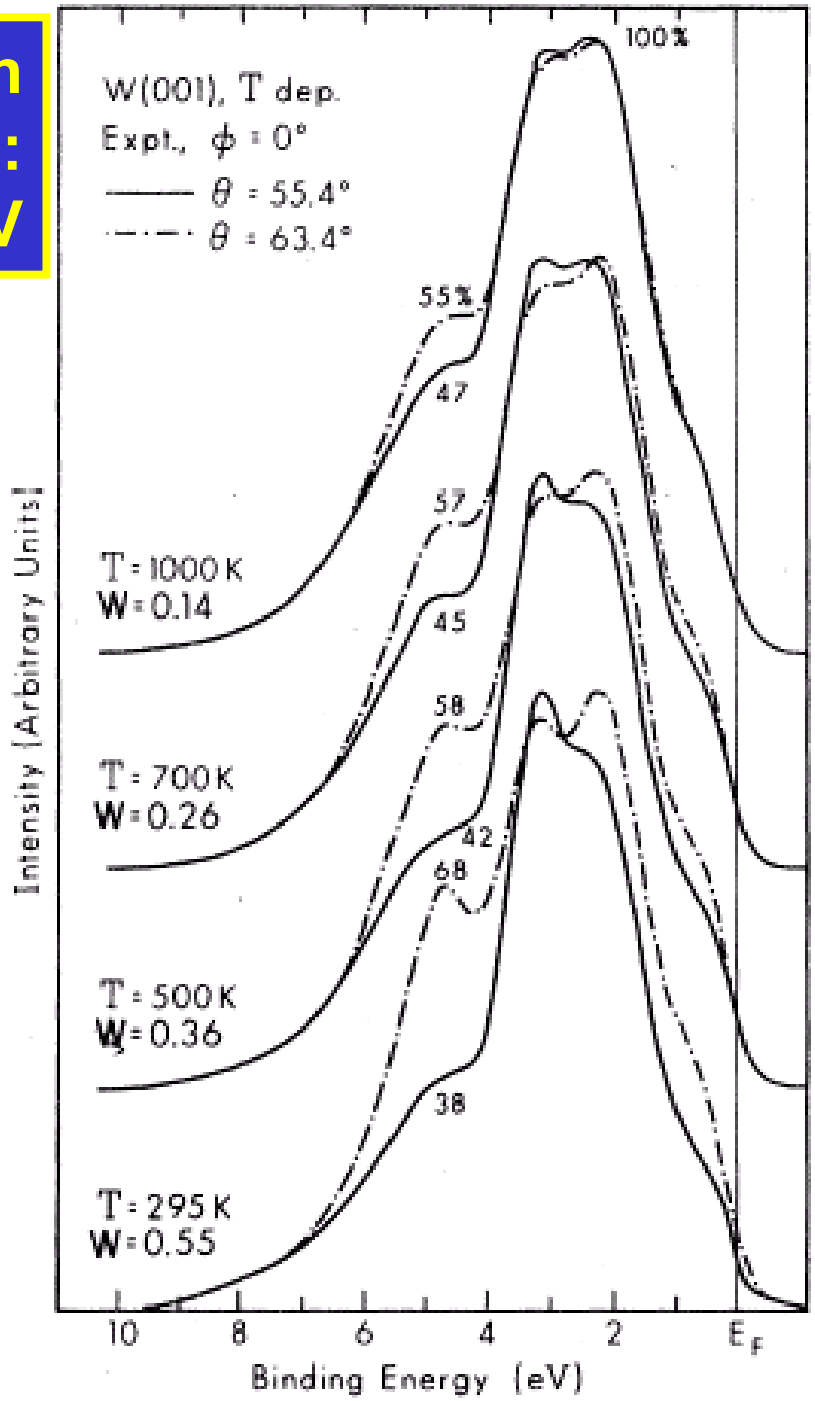

Present if vibrations stiff enough (Debye T high enough), but suppressed as temperature is raised.

Hussain et al., Phys. Rev. 22, 3750 (1980)

Effect of photon momentum on k conservation: W(110) at 1253.6 eV

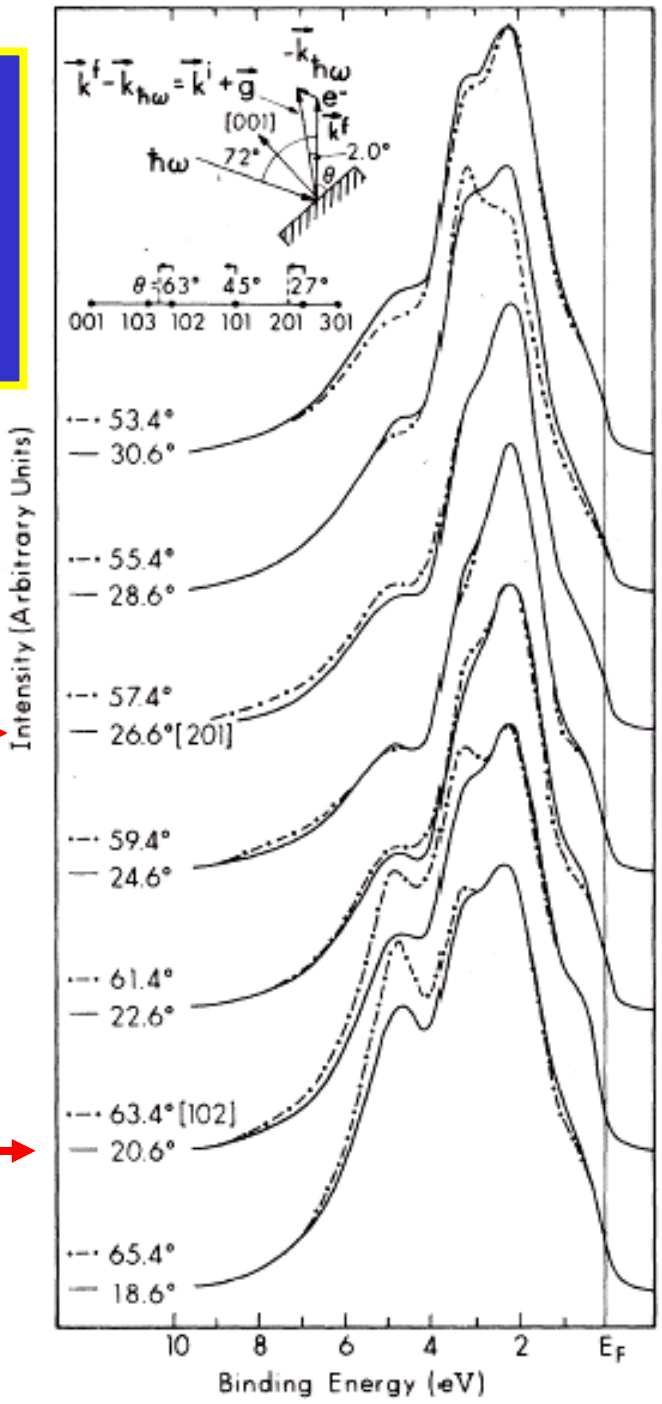

Symmetry-related spectra shifted by 6.0° for best match. Theoretical 4.8° due to $k_{h\nu}$

Hussain et al., Phys. Rev. 22, 3750 (1980)

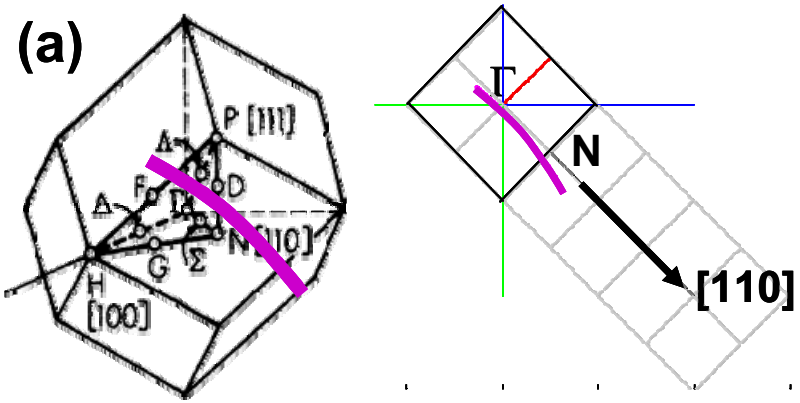

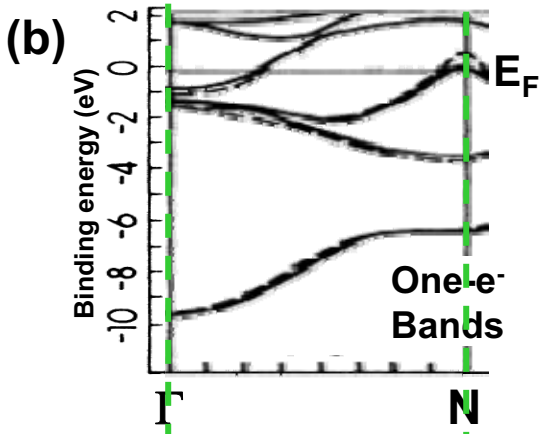

Angle-Resolved Photoemission from W(110)
hν = 260 eV
90° = normal
Θ_{Debye} = 400K

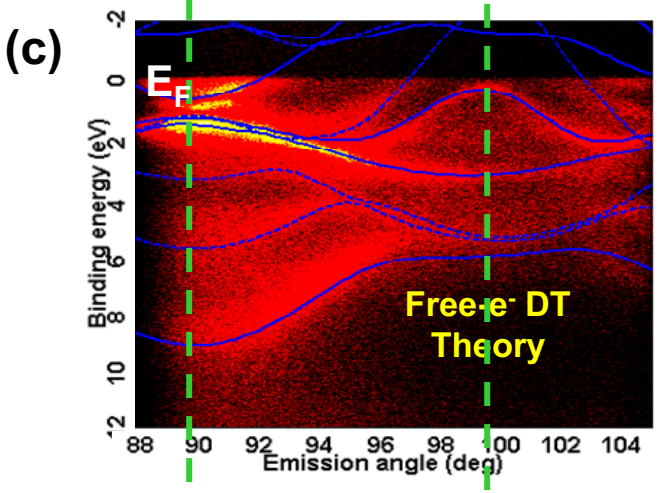

Plucinski

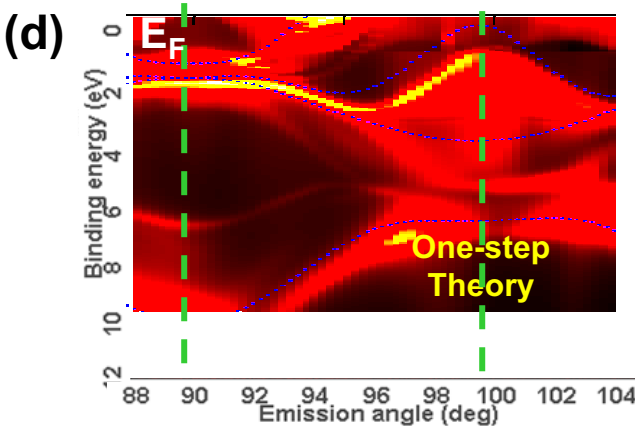

Braun, Minar, Ebert

Plucinski et al., Phys. Rev. B, submitted

ARPES from W(110): Expt, hν = 260 eV, near-normal emission, Θ_{Debye} = 400K

One-electron, free-electron final-state theory

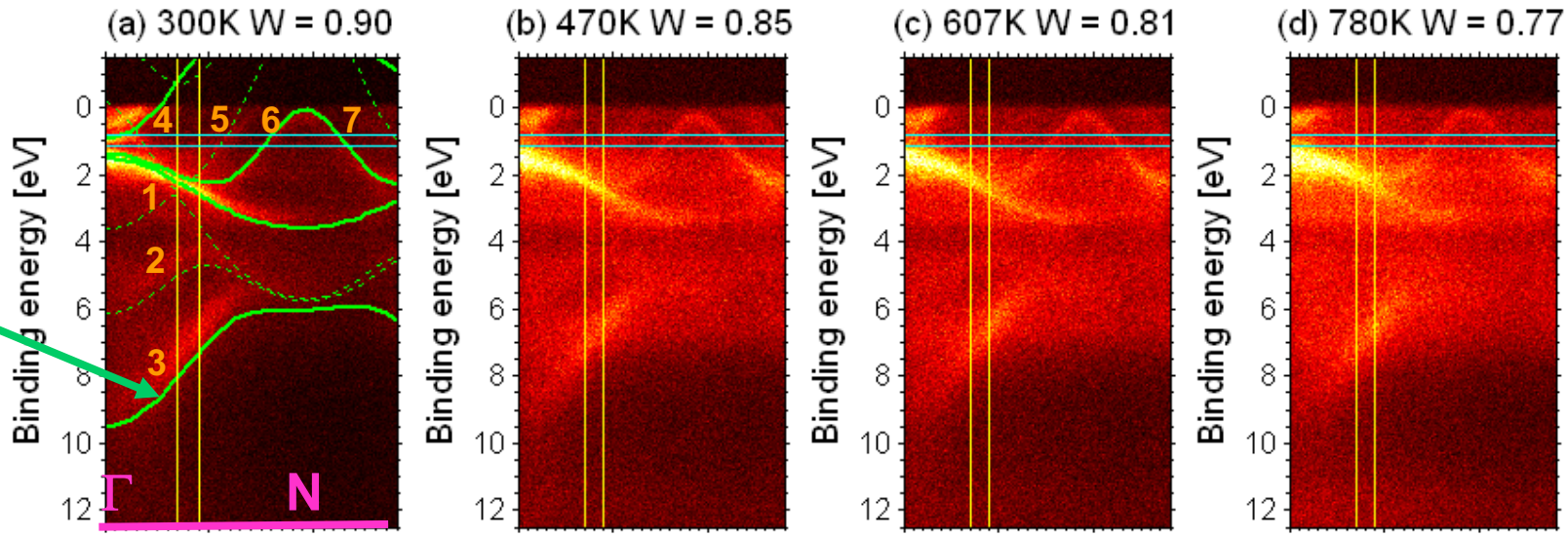

ARPES from W(110): 1-Step Theory, hν = 260 eV, near-normal emission, Θ_{Debye} = 400K

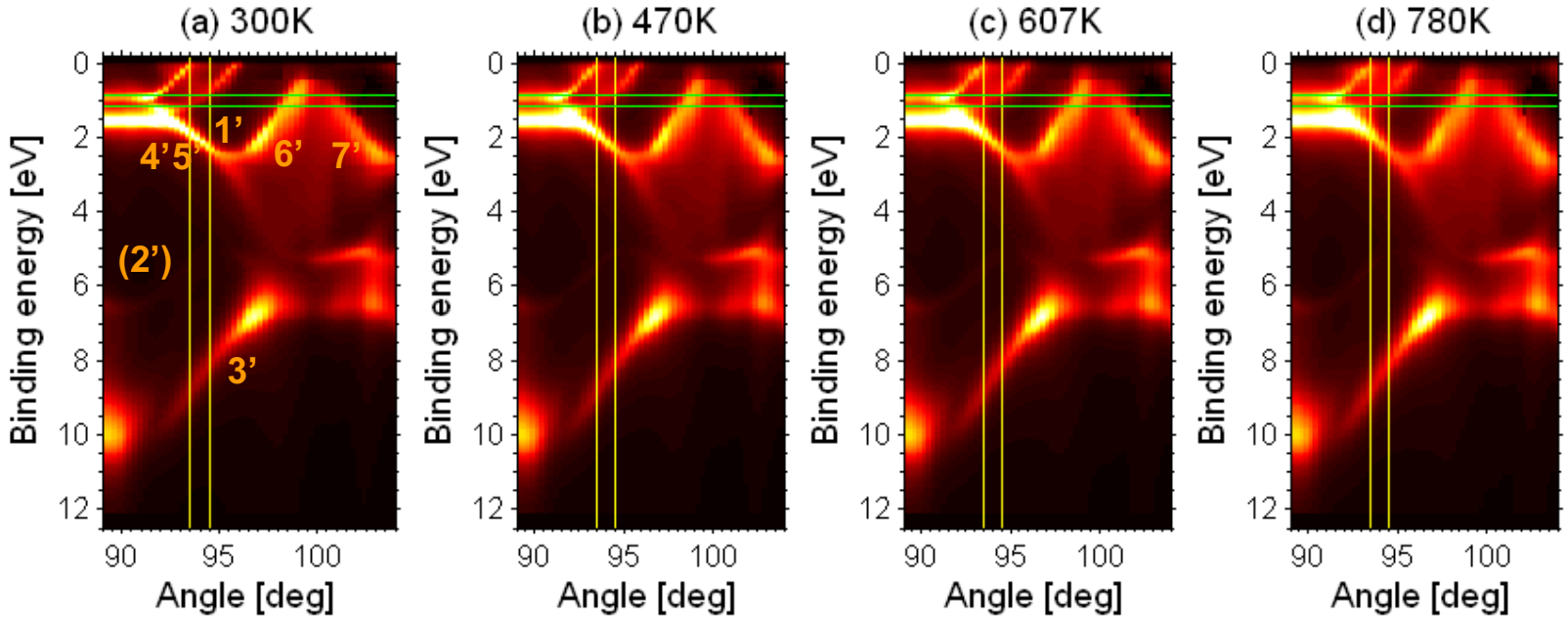

ARPES from W(110): Expt, hν = 860 eV, near-normal emission, Θ_{Debye} = 400K

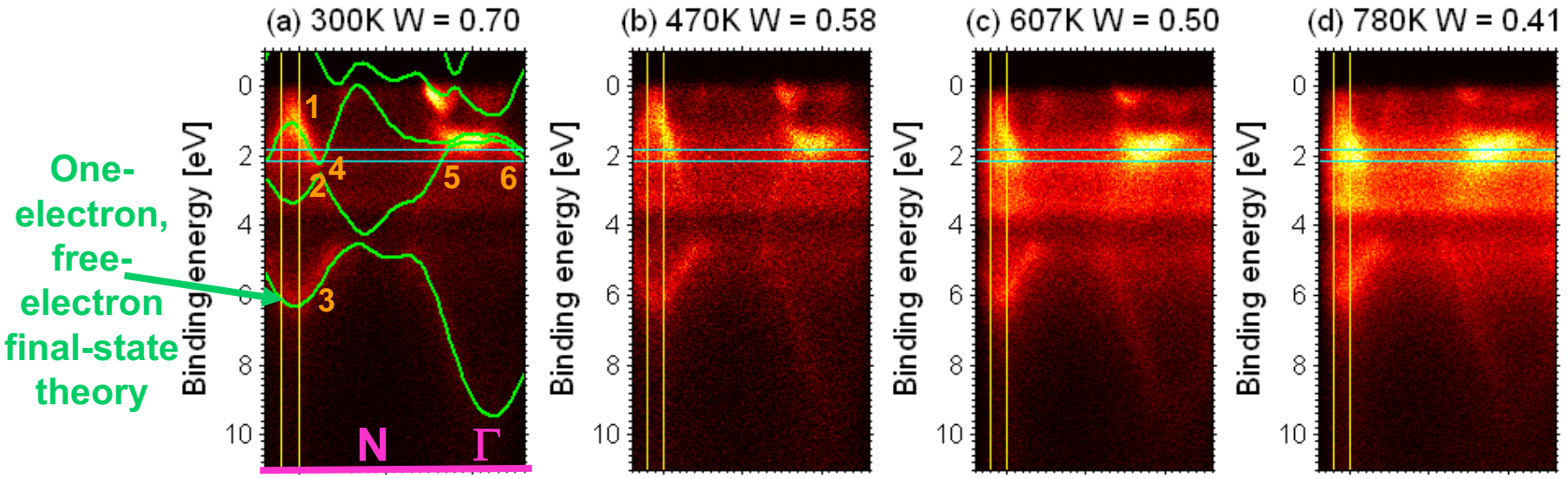

ARPES from W(110): 1-Step Theory, hν = 870 eV, near-normal emission, Θ_{Debye} = 400K

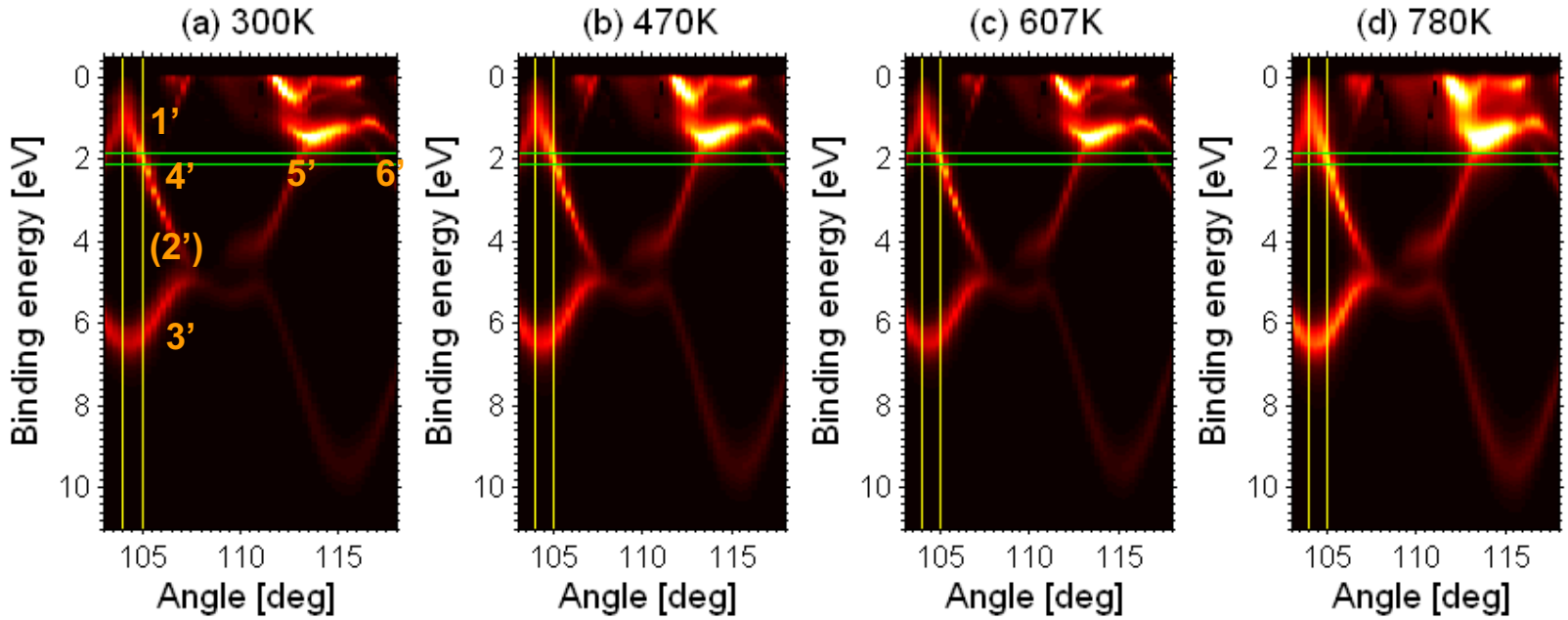

ARPES with a non-monochromatized lab. x-ray source: hν = 1253.6 eV, T = ~77K

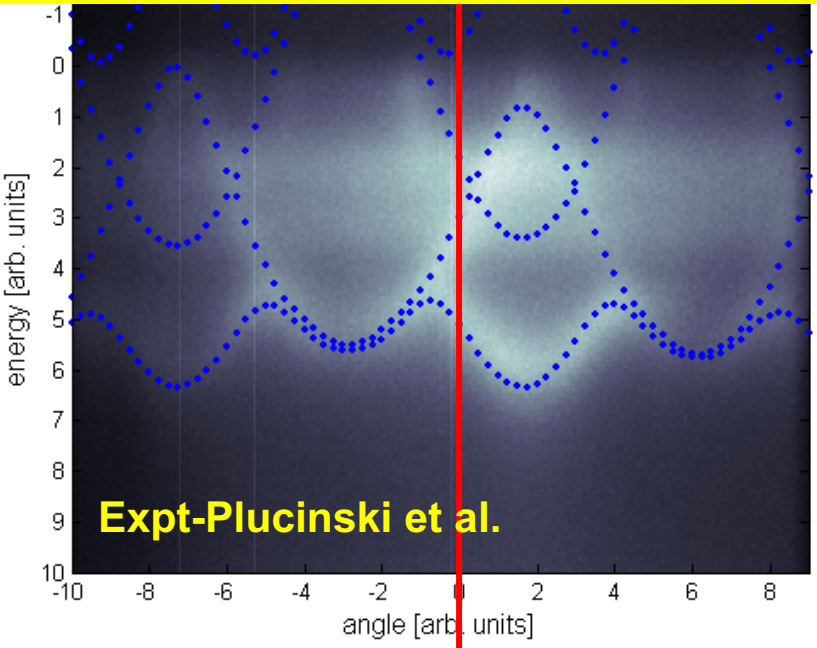

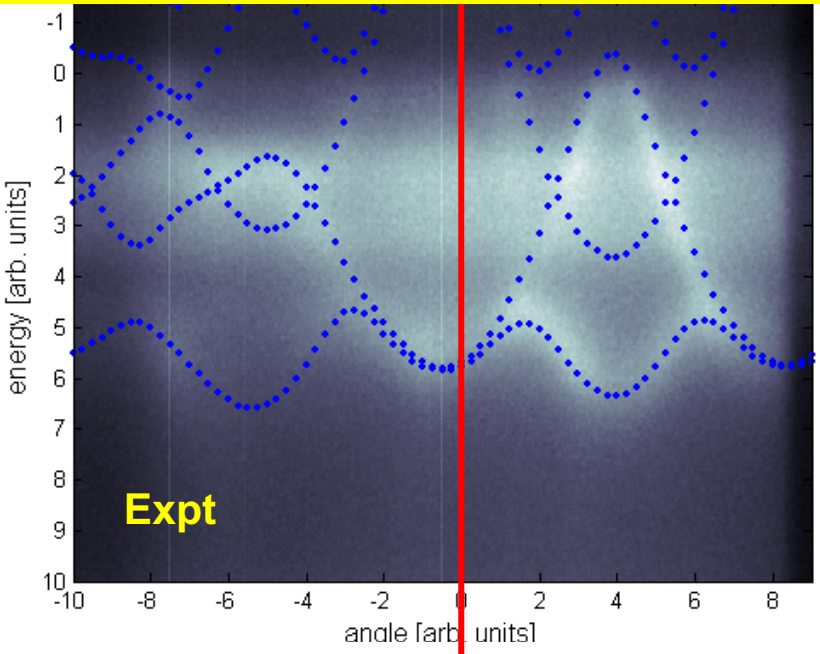

W(110) Normal emission 1283eV

W(110) OFF-Normal emission 1283eV

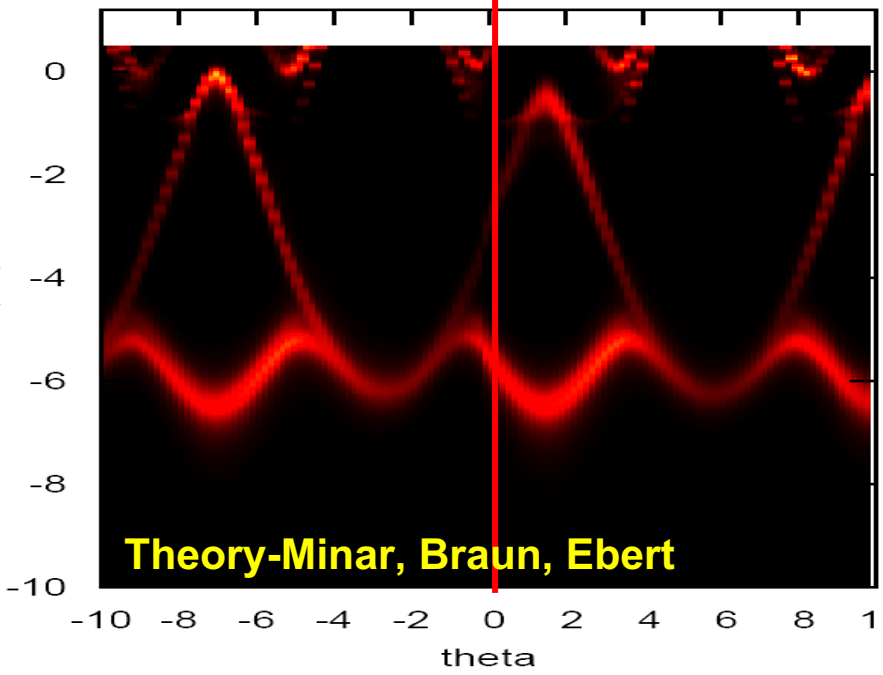

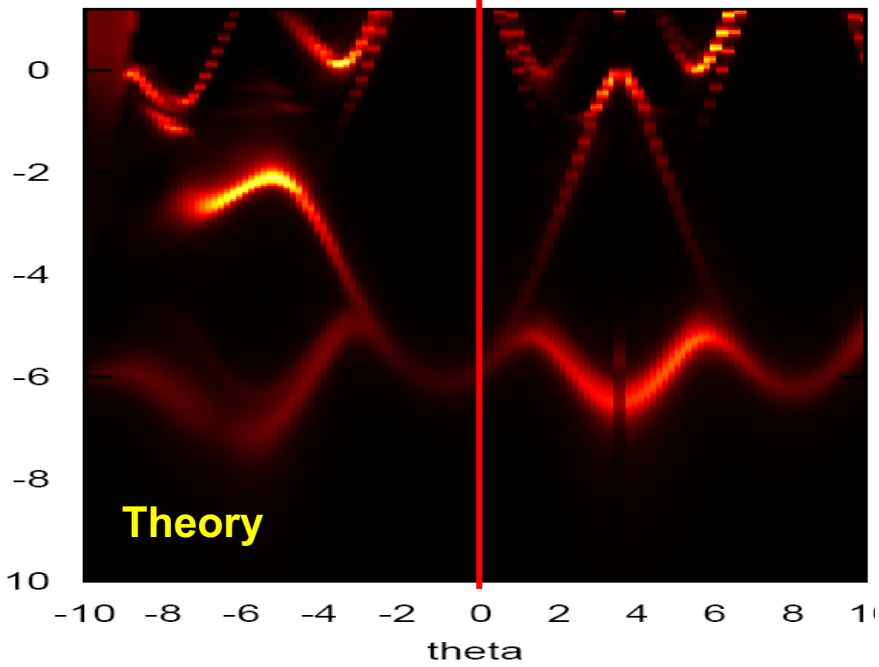

Tour de force ARPES: W(110), hν = 1253.6 eV

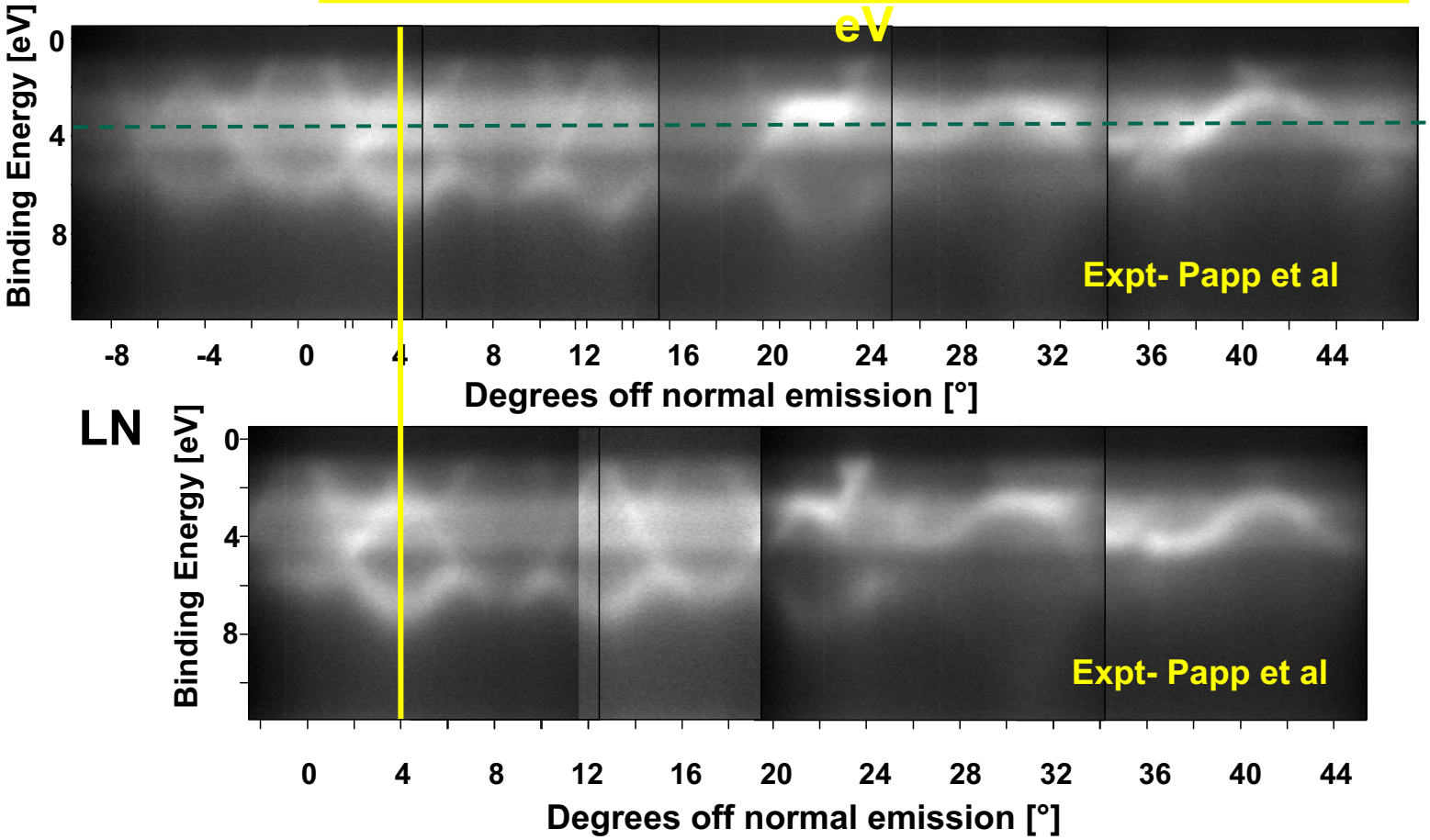

Density of States

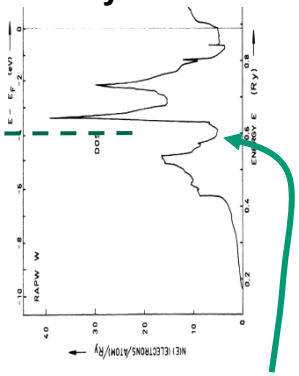

"Pseudo Gap"

Christensen & Feuerbacher, PRB 10, 2349 ('74)

Tour de force ARPES: W(110), hν = 1253.6 eV

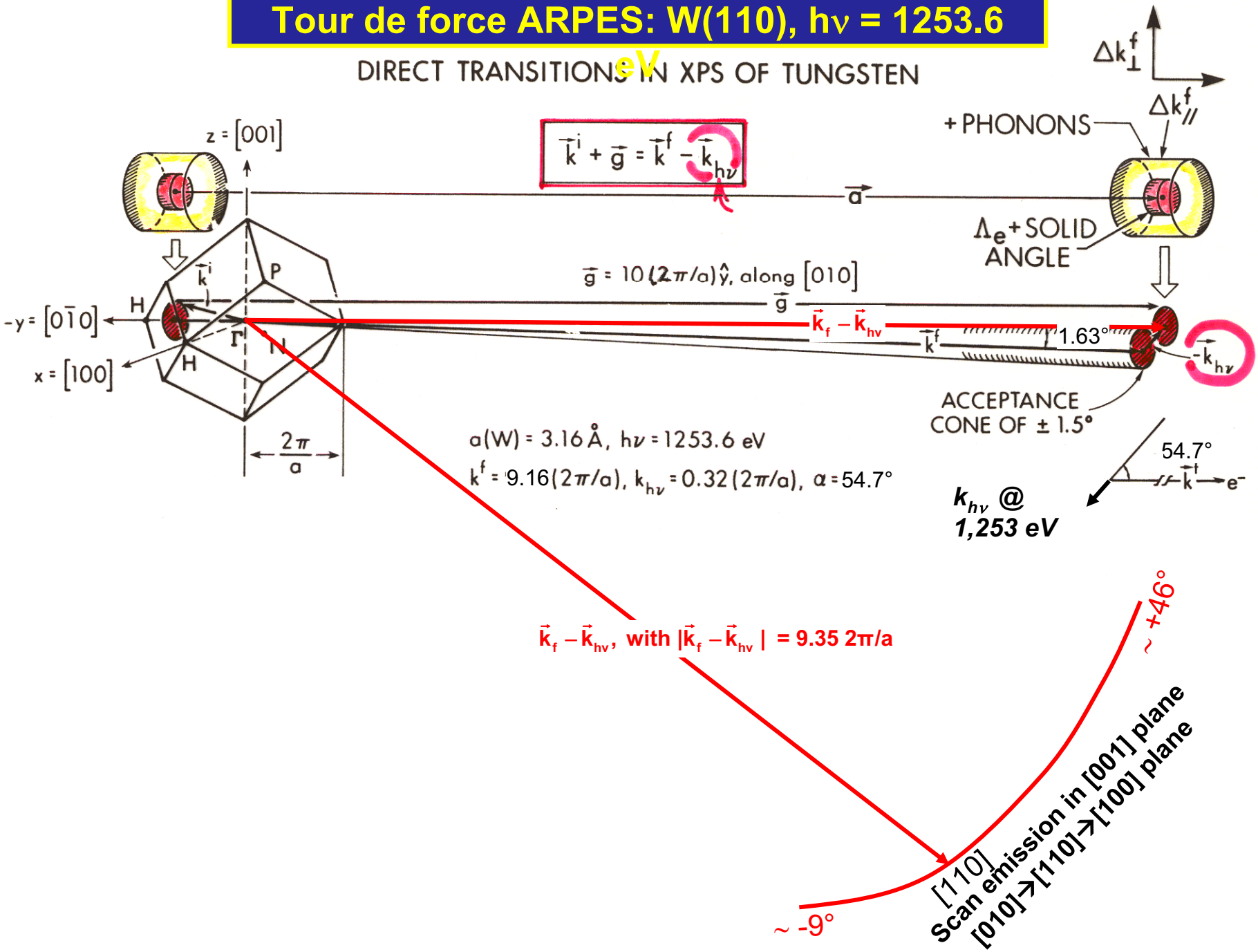

Tour de force ARPES in an extended zone scheme: W(110), [001] plane, hν = 1253.6 eV

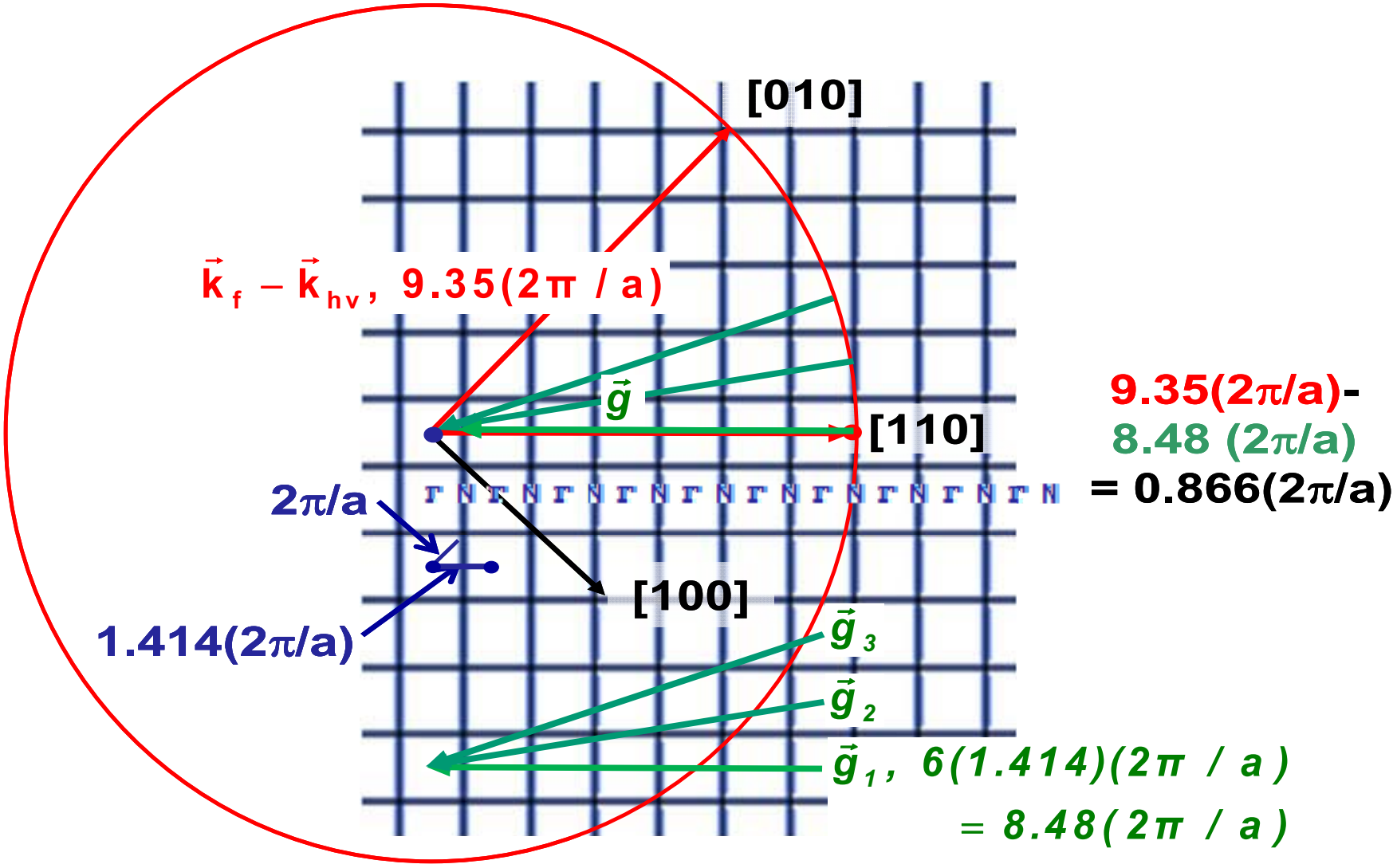

Tour de force ARPES: W(110), hν = 1253.6 eV

RT

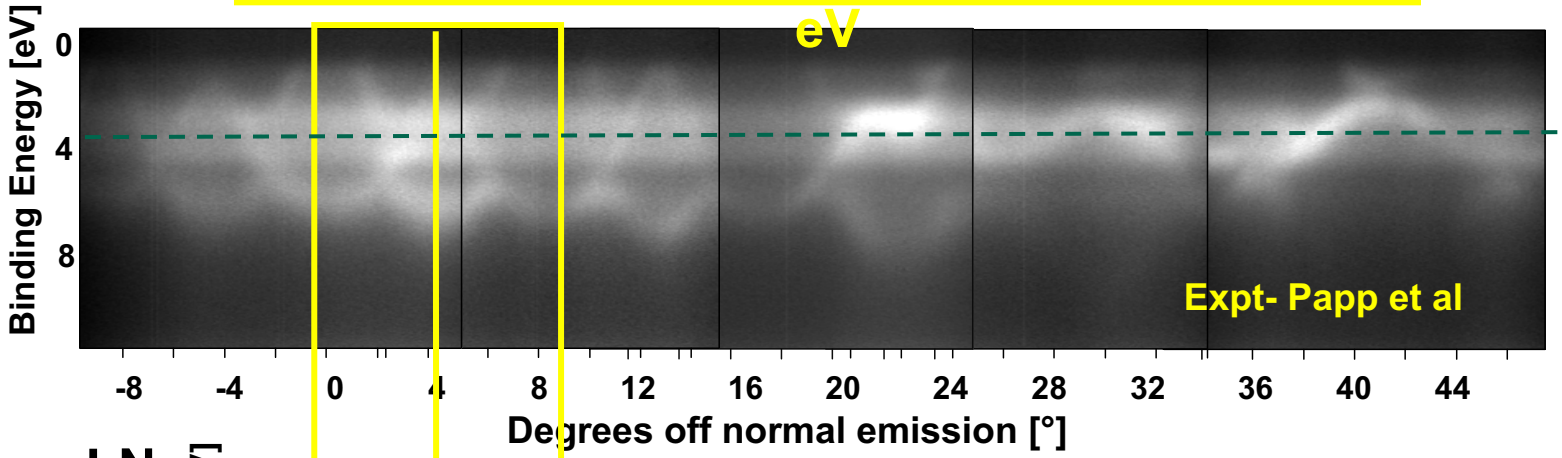

Density of States

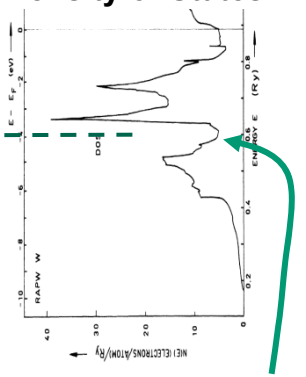

"Pseudo Gap"

Christensen & Feuerbacher, PRB 10, 2349 ('74)

LN

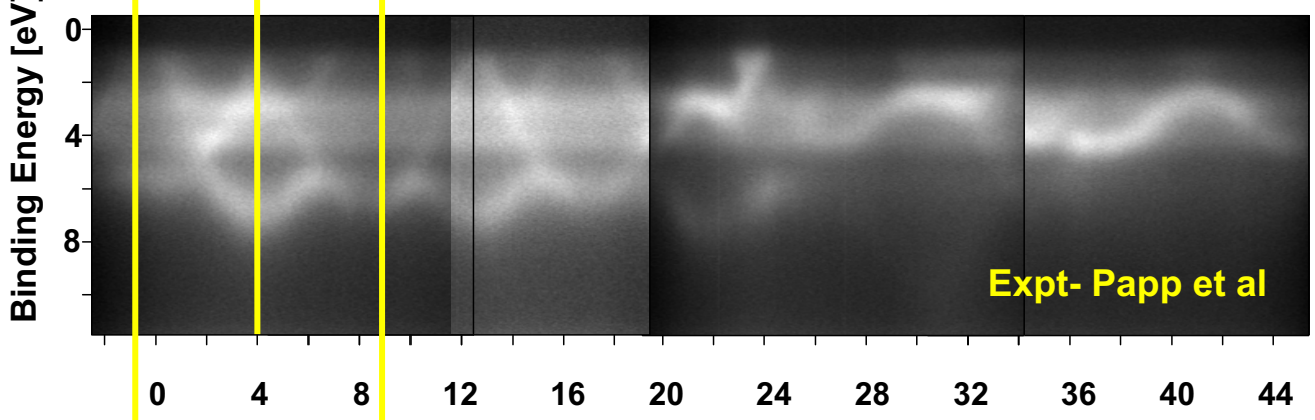

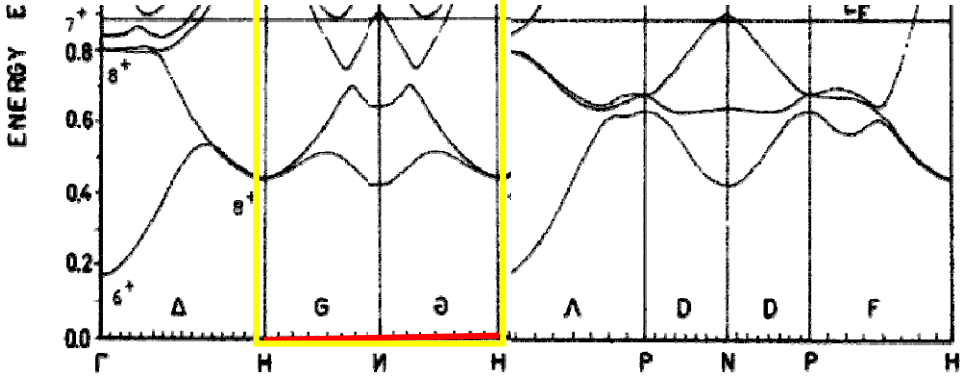

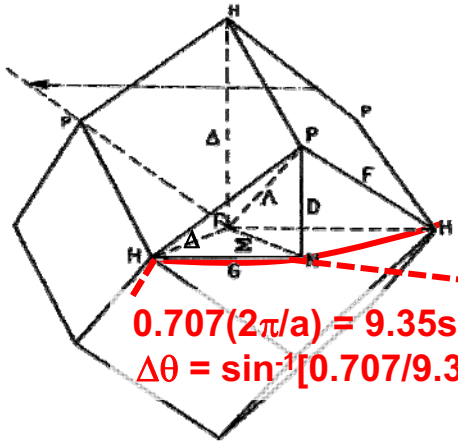

$0.707(2\pi/a) = 9.35\sin\Delta\theta(2\pi/a)$

$\Delta\theta = \sin^{-1}[0.707/9.35] = 4.33°$

And what would happen at 10 keV?:

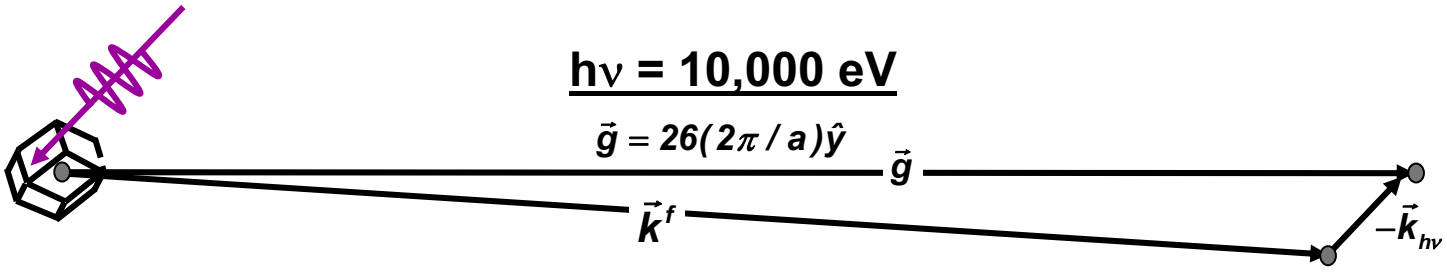

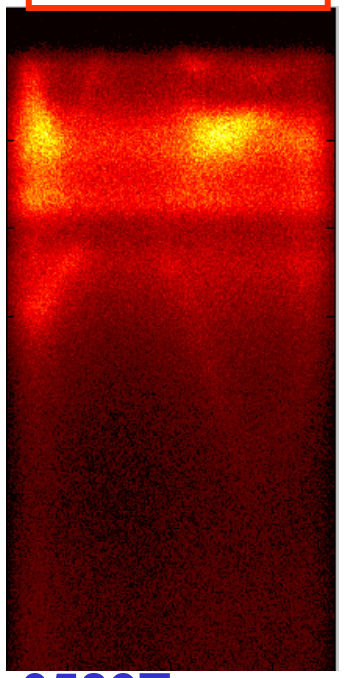

Θ_{Debye} = 310K, $\langle u^2 \rangle$ (10^{-20} cm^2) = 5.34 + 0.0583T $\xrightarrow{High\ T}$ 0.0583T

Debye-Waller Factor = $W(T) \approx exp(-k_e^2 \langle u^2(T) \rangle)$

$= exp(-C_1 E_{kin} \langle u^2(T) \rangle) \xrightarrow{High\ T} exp(-C_2 E_{kin} T)$

W at 4K: W ≈ 0.27, ≈ 27% direct

at 77K: W ≈ 0.20, ≈ 20% direct

at 300K: W ≈ 0.017, ≈ 2% direct

Correlated vibrations and better theory (e.g. Phys. Rev. B 35, 1147 ('87) and 53, 7524 ('96) + 54, 14703 ('96)) may yield different DT percentages, but needs further experimental and theoretical study

For W(110): hν = 5,946 eV: Where are we in the Brillouin Zone?
Calculation of Photon Momentum Effect on *k* Conservation

The free-electron picture:

$(2\pi / a) = 1.988\ A^{-1}$

$h\nu = 5945\ eV$

$|\vec{k}_f| = 0.512E_{kin}^{0.5}(eV) = 39.48\ A^{-1} = 19.85\ (2\pi / a)$

$|\vec{k}_{h\nu}| = 0.000507(h\nu(eV)) = 3.01\ A^{-1} = 1.51\ (2\pi / a)$

$|\vec{k}_f - \vec{k}_{h\nu}| = \left[39.48^2 + 3.01^2\right] = 39.59\ A^{-1} = 19.91\ (2\pi / a) - - > 14.08\ [1.414((2\pi / a)]$

$|\vec{g}_1| = 14.00\ [1.414((2\pi / a)]$

Angular deflection due to $\vec{k}_{h\nu}$ is : $\arctan(3.01 / 39.48) = 4.35°$

Γ – N – Γ is 1.414(2π / a), so angular range of this is $\arctan(1.414/19.19) = 4.21°$

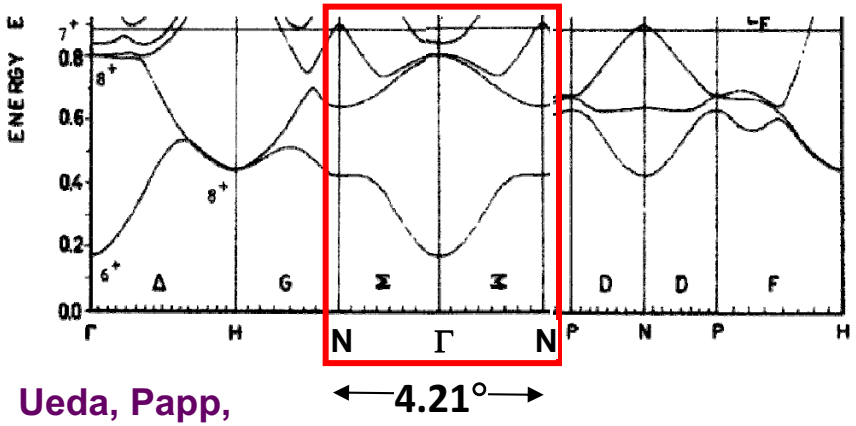

Ueda, Papp, Kobayashi, Minar, et al. to be publ

Experiment in the Extended Brillouin Zone

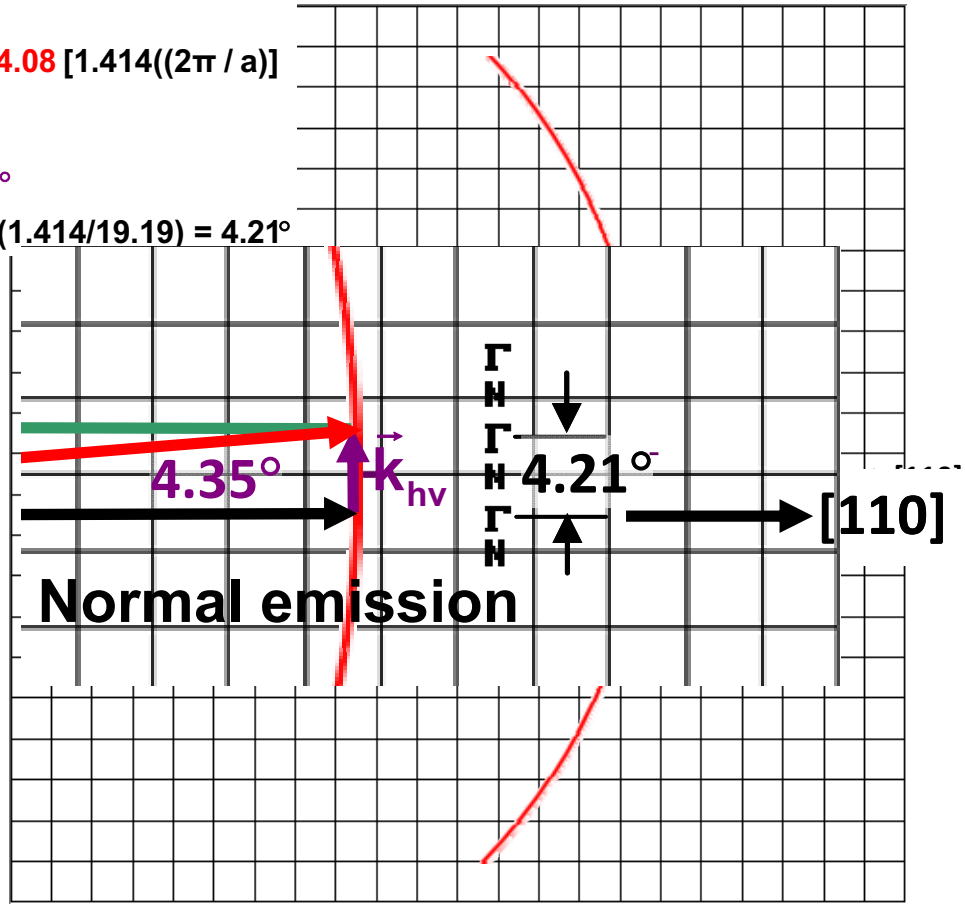

W(110), hν = 5,954 eV, T = 30K: Comparison to one-step theory, matrix elements

W = 0.45

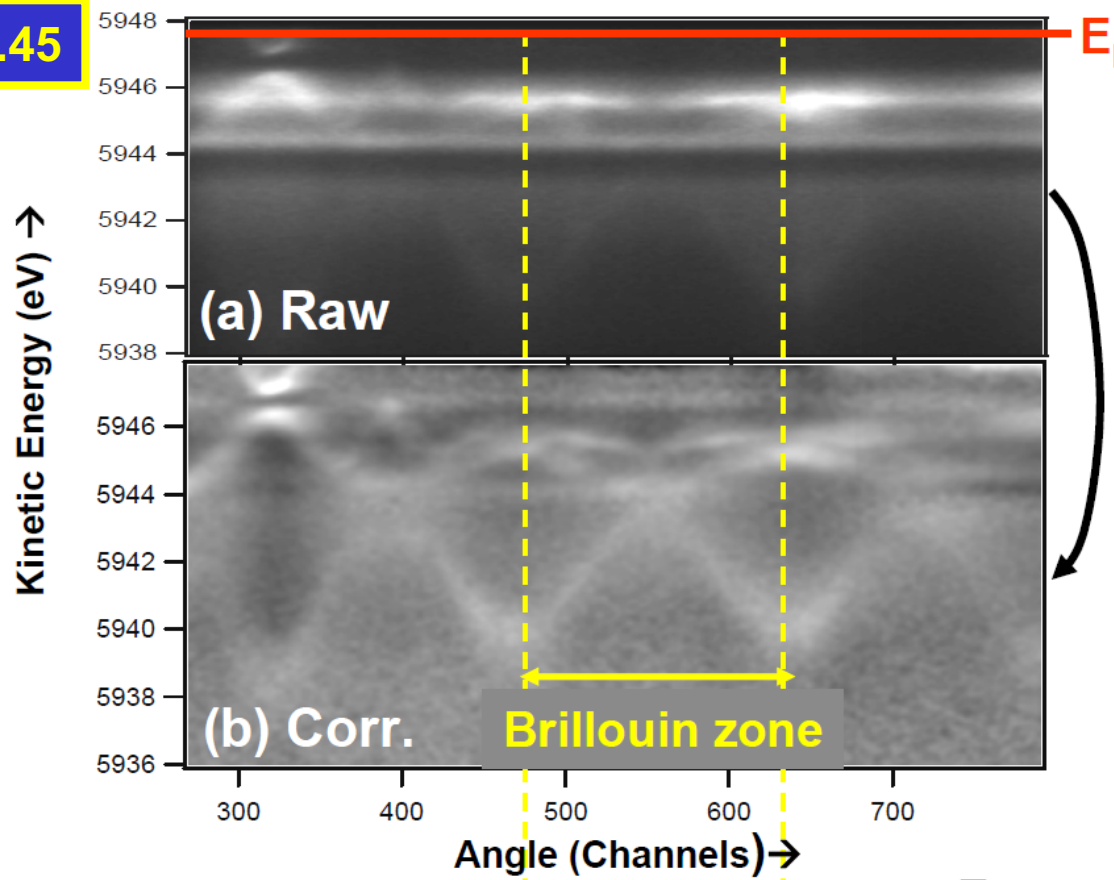

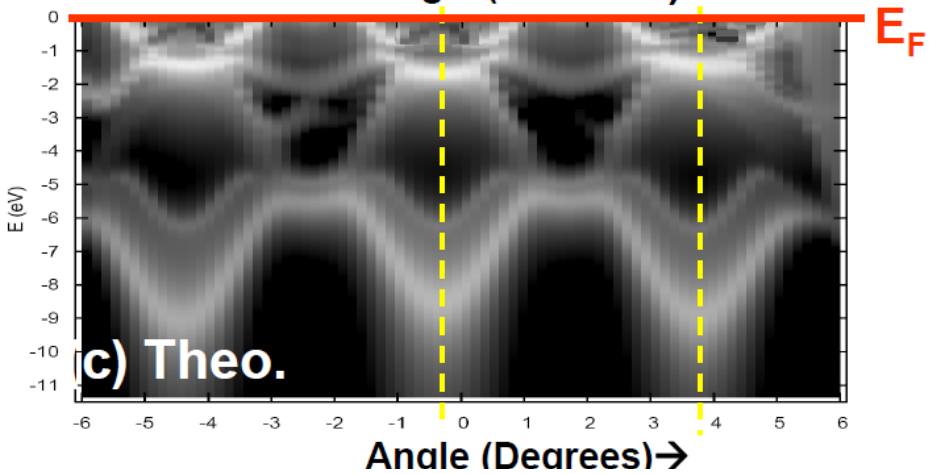

Corrected for phonon-induced density-of-states-like intensity

(Bostwick, Papp)

Expt.-Ueda, Kobayashi, SPring8
Data analysis-Papp, Gray, Plucinski, C.F.
Theory-Minar, Braun, Ebert

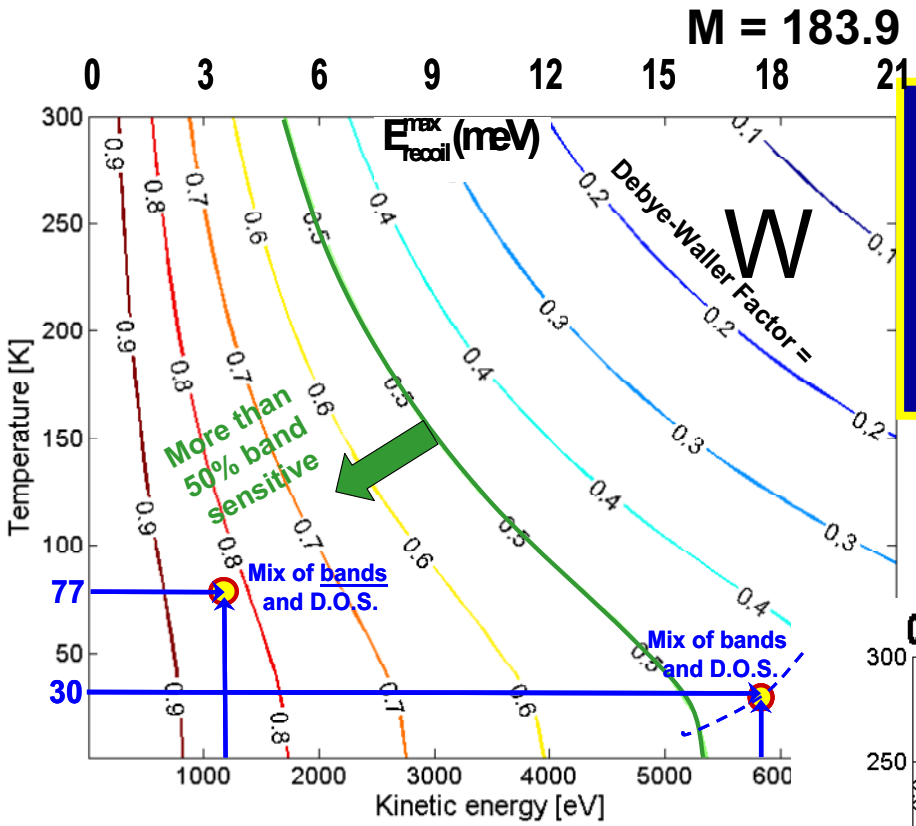

$W(T,E_{kin})$ = Approximate recoil-free fraction→fraction direct transitions

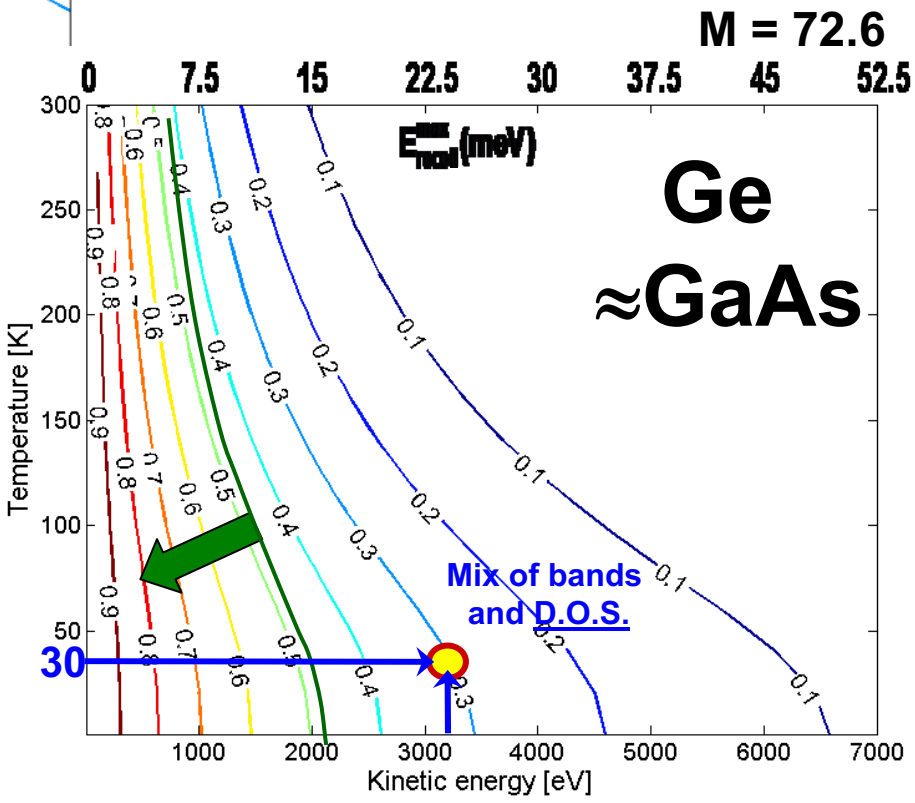

Plucinski

Hard x-ray ARPES from GaAs(001)-3.2 keV, 30 K, W = 0.31

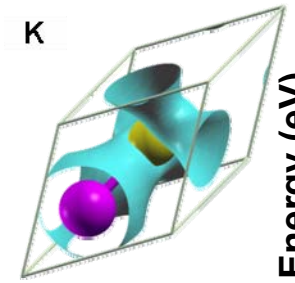

Band-like

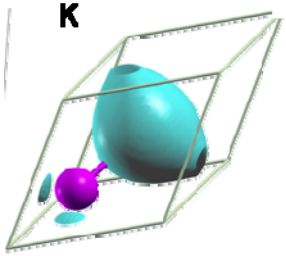

Core-like
As 4s

⇑

Charge densities

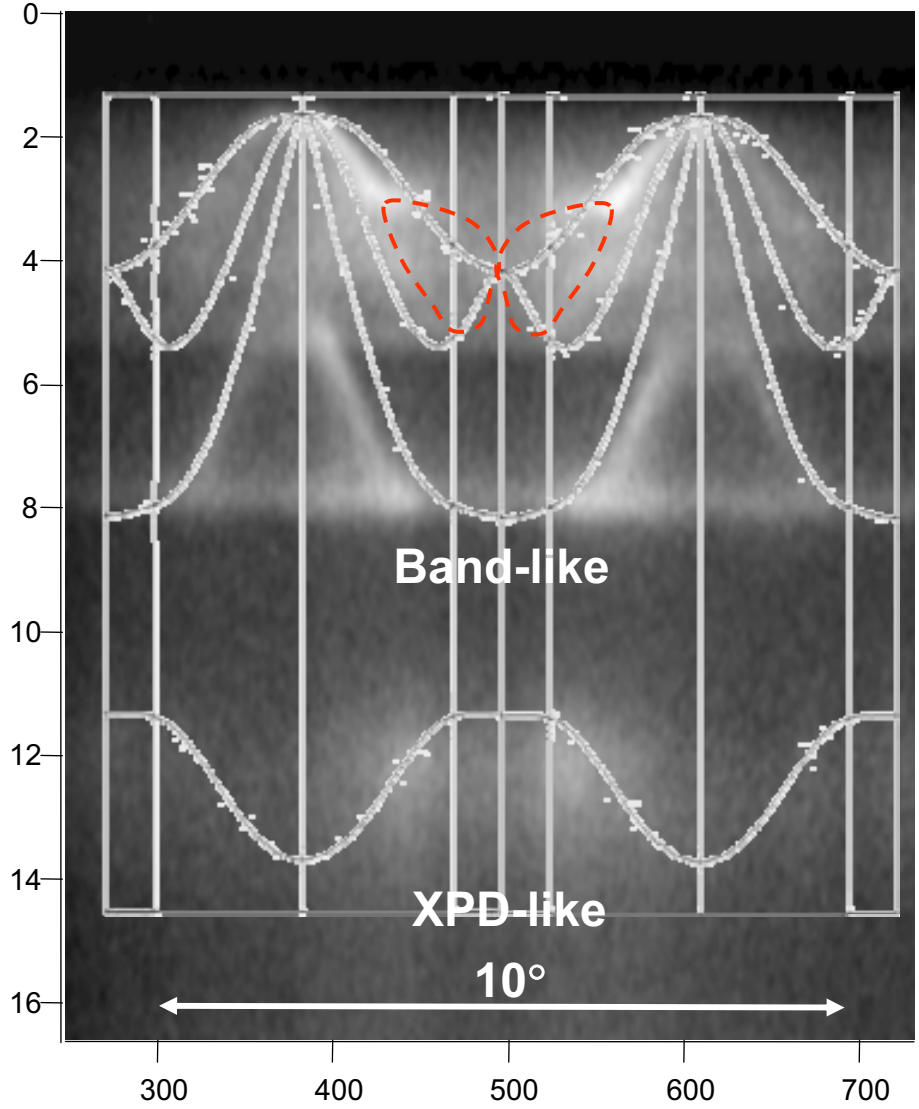

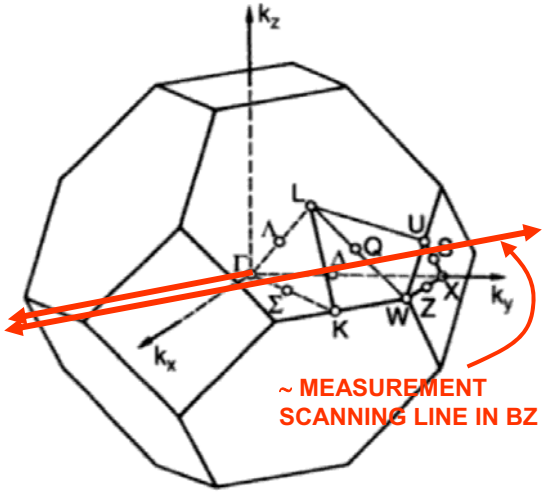

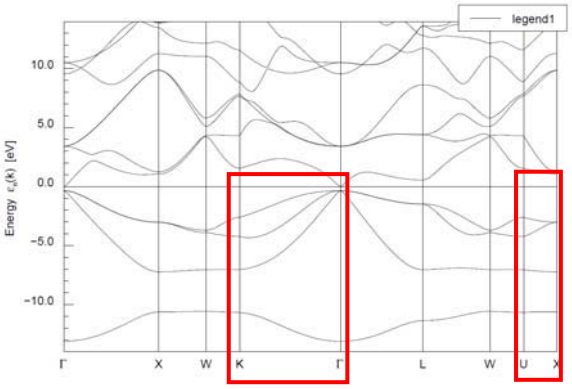

Expt.-Gray, Papp, Ueda, Yamashita, Kobayashi
Theory- Pickett, Ylvisaker

Comparing Experiment and One-Step KKR Theory

GaAs Valence Bands

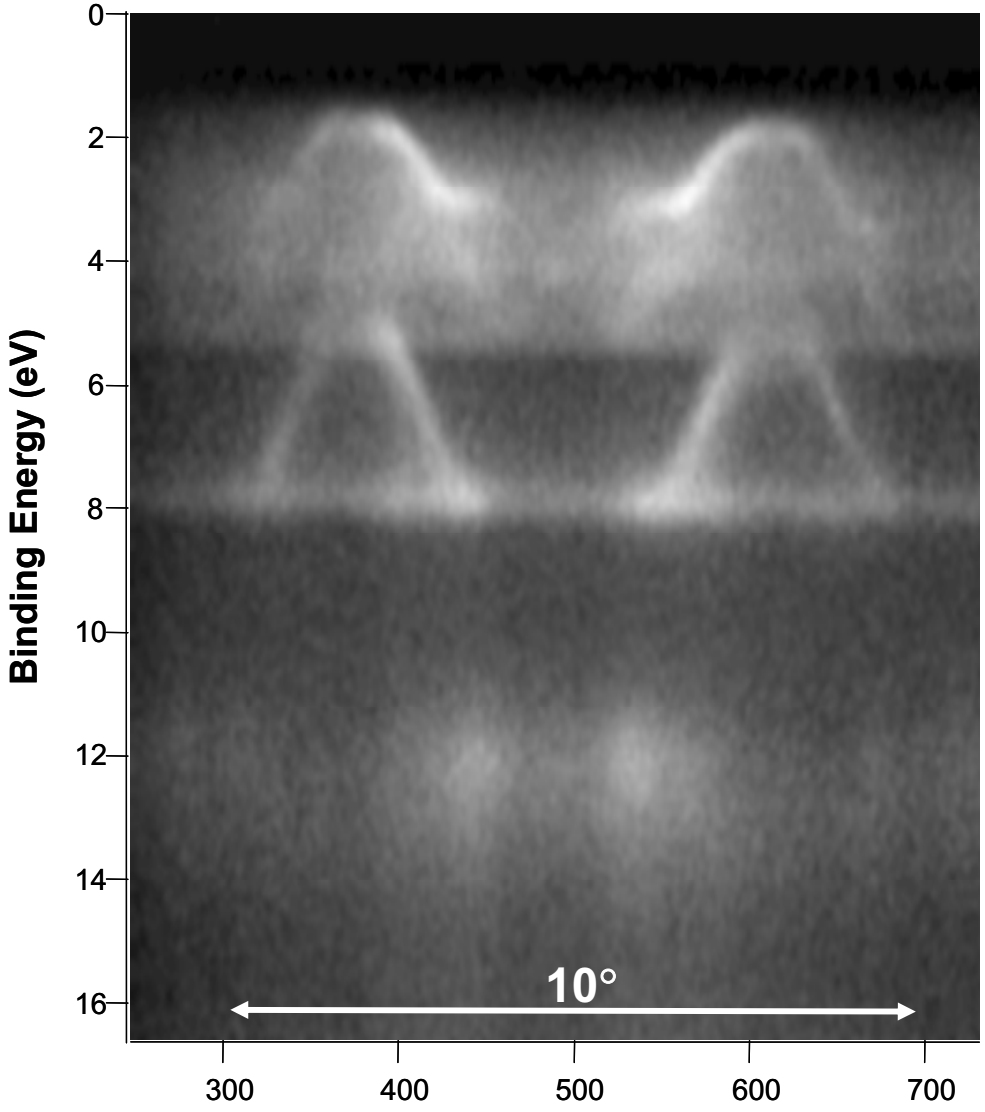

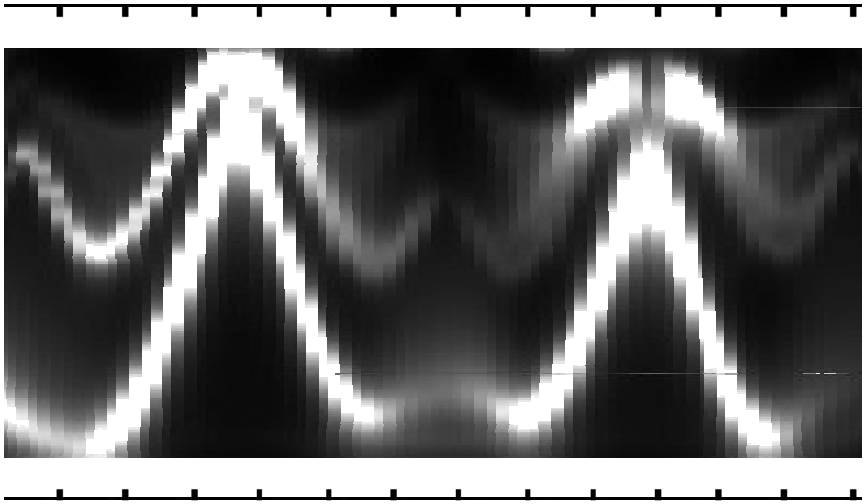

One-step theory-Minar, Braun, Ebert

Expt.-Gray, Papp, Ueda, Yamashita, Kobayashi

Looking ahead-conservatively
Photon energies yielding DW factors of 0.5 at 20 K

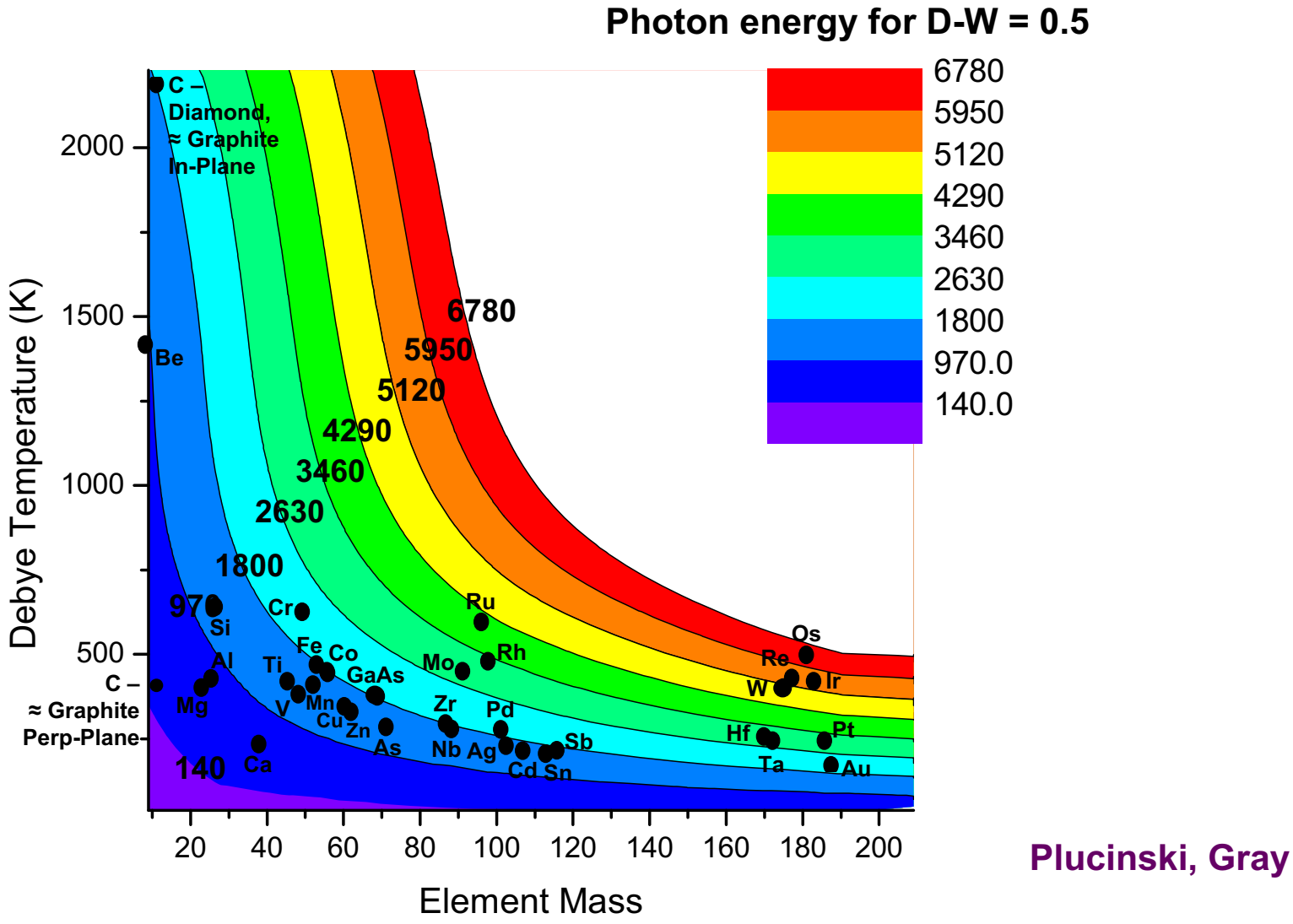

Plucinski, Gray

Outline

Surface, interface, and nanoscience—short introduction

Some surface concepts and techniques→photoemission

Synchrotron radiation: experimental aspects

Electronic structure—a brief review

The basic synchrotron radiation techniques:
more experimental and theoretical details

Valence-level photoemission

Core-level photoemission

Photoemission with high ambient pressure
around the sample

Outline

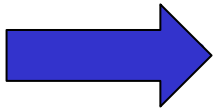

Core-level chemical shifts: the potential model

- Core-level chemical shifts: equivalent-core (Z+1) and thermochemical energies
- Multiplet splittings
- Spin-orbit splitting, the Fano effect, and spin-polarized outgoing electrons
- Magnetic circular dichroism (MCD) in core-level emission
- Non-magnetic circular dichroism in core-level emission: a.k.a. circular dichroism in angular distributions (CDAD)
- Various other final state effects providing information in core-level spectra

Looking into the silicon dioxide layer with photoelectron spectroscopy

Charge transfer, e^-- e^- coulomb integral:

$$Shift \approx q_{Si} J_{Si2p,Si3p} =$$

$$\int \varphi^*_{2p}(\vec{r}_1)\varphi^*_{3p}(\vec{r}_2)\frac{e^2}{r_{12}}\varphi_{2p}(\vec{r}_1)\varphi_{3p}(\vec{r}_2)dV_1dV_2$$

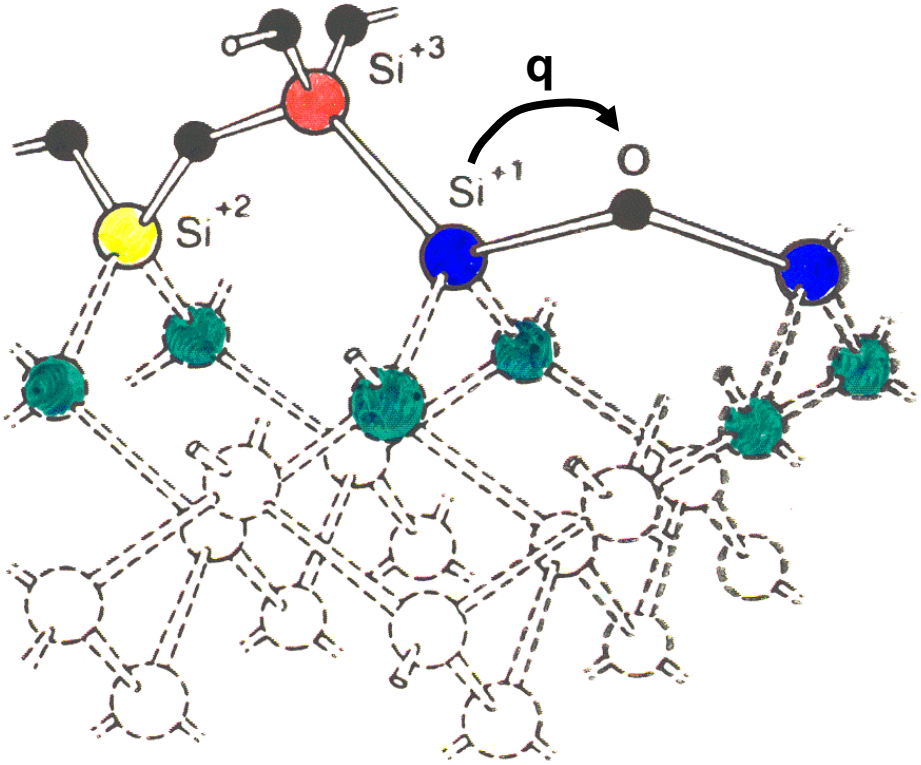

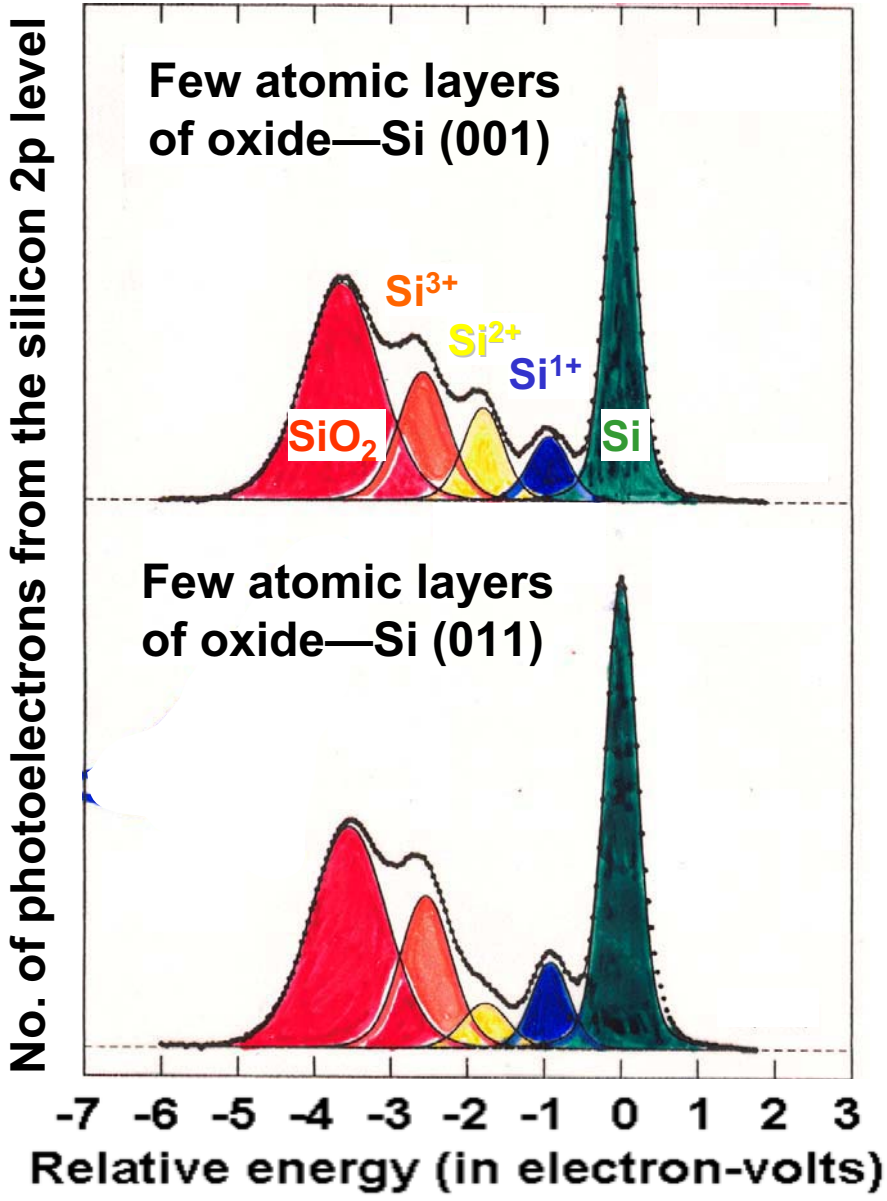

Himpsel et al., Phys. Rev. B 38, 6086 ('88)

CHEMICAL SHIFTS IN ADSORBATE & SUBSTRATE

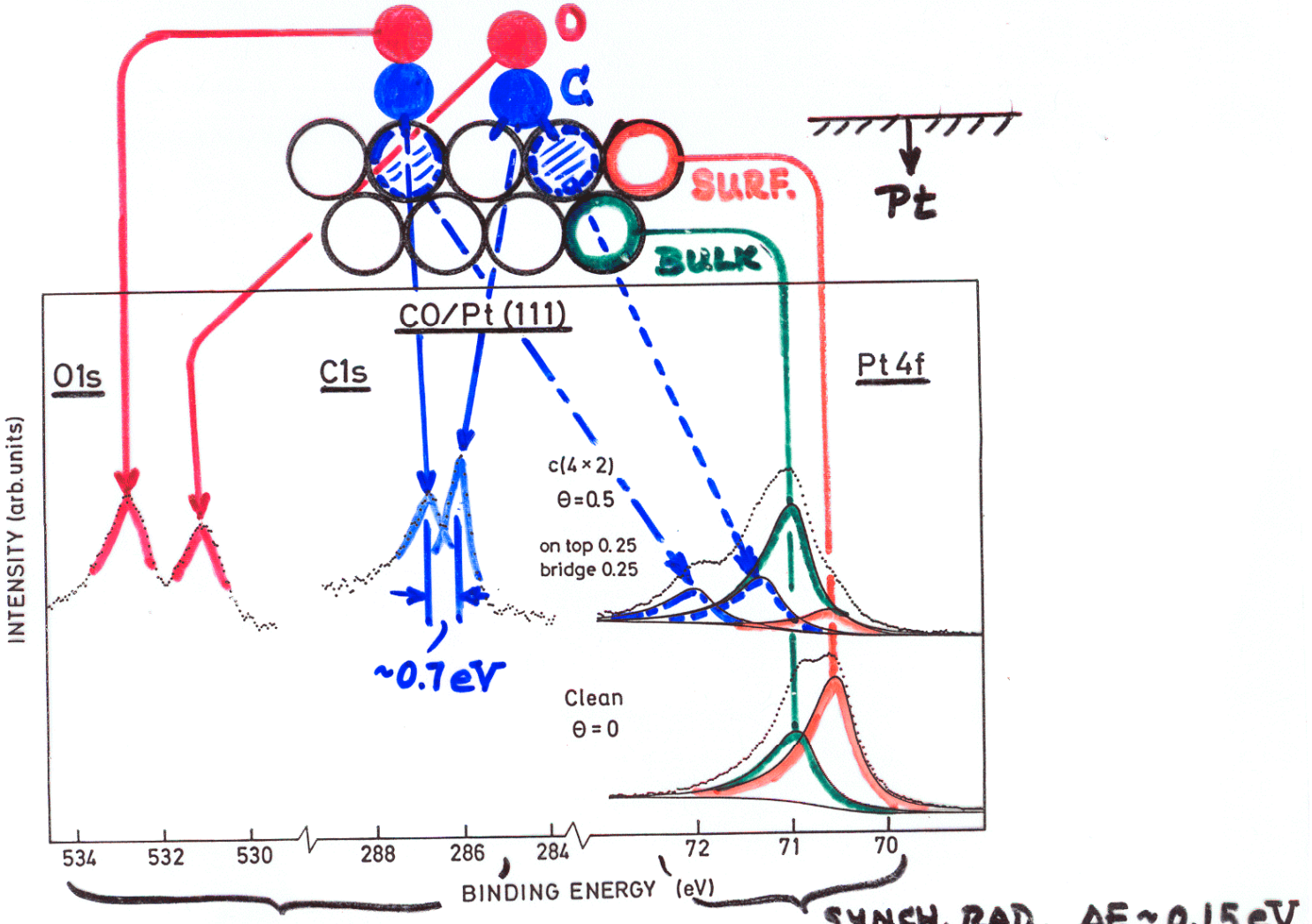

MONOCH. XPS, ΔE ~ 0.3 eV

SYNCH. RAD., ΔE ~ 0.15 eV

BJÖRNEHOLM ET AL. (NILSSON GRP., UPPSALA)

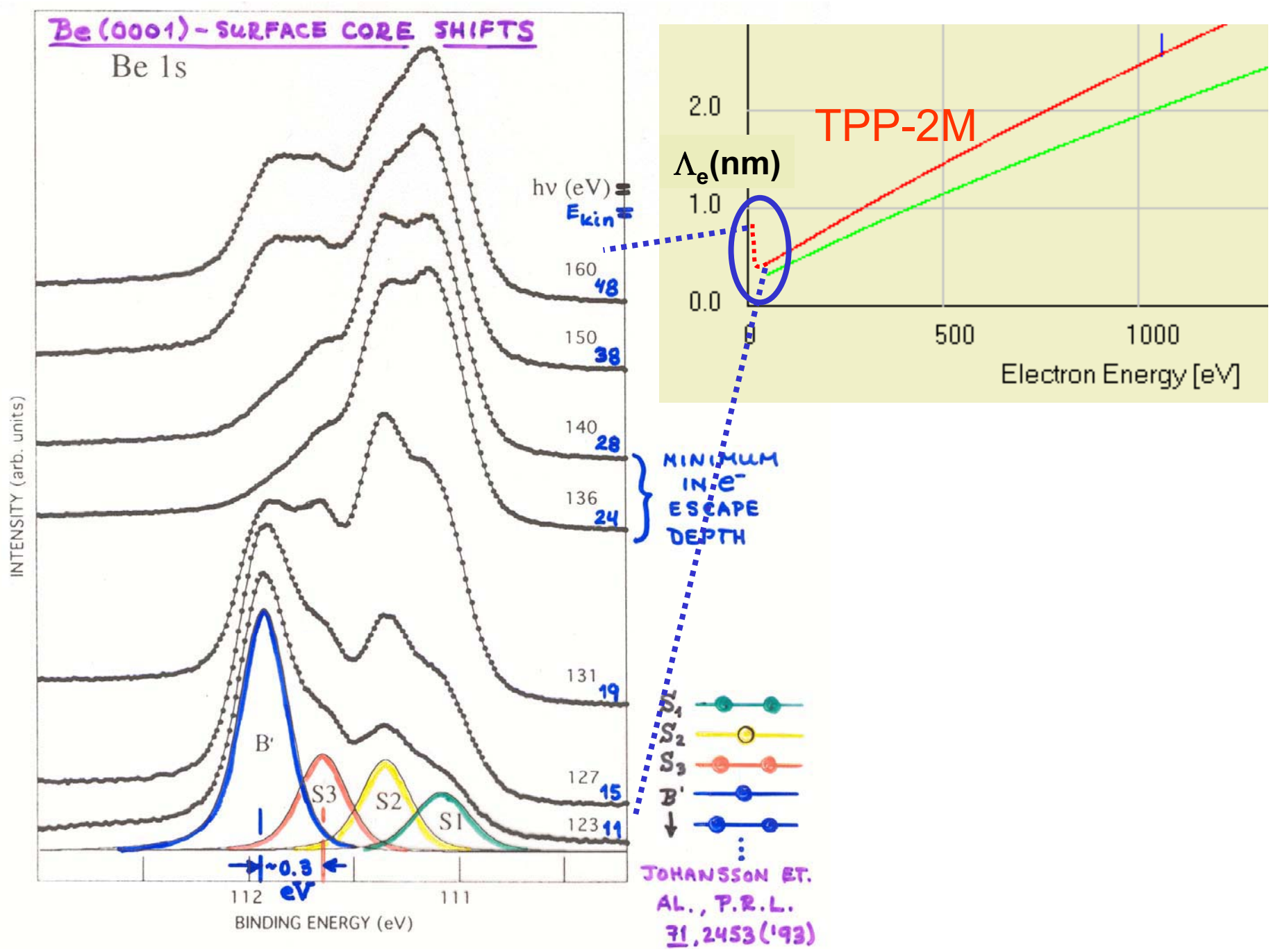
Be (0001) - SURFACE CORE SHIFTS
Be 1s
hν (eV) =
E_kin =
160
48
150
38
140
28
136
24
131
19
127
15
123
11
B'
S3
S2
S1
~0.3 eV
112
111
BINDING ENERGY (eV)
INTENSITY (arb. units)
MINIMUM IN e⁻ ESCAPE DEPTH
S1
S2
S3
B'
JOHANSSON ET. AL., P.R.L. 71, 2453 ('93)
TPP-2M
Λe(nm)
2.0
1.0
0.0
0
500
1000
Electron Energy [eV]

What does the hole do?

BINDING ENERGIES + KOOPMANS' THEOREM:

N-e^- SCH. EQN. — $\hat{H}(N)\Psi_j(N) = E_j(N)\Psi_j(N)$, $j = 1, 2 \ldots$

MINIMIZE $E_j(N)$ $\Big\{$ $\Psi_j \approx \Phi_j$ = SLATER DET.

N 1-e^- HARTREE-FOCK EQNS. — $\hat{h}(1)\varphi_k(1) = \varepsilon_k(1)\varphi_k(1)$

- COUPLED INTEGRO-DIFF.
- COULOMB + EXCHANGE

$E_b(k) = k^{th}$ BINDING ENERGY $= E_f(N-1, k\ \text{hole}) - E_i(N)$ (+) EXACT

or $E_b(k) = -\varepsilon_k$ IF $\varphi_{ki} = \varphi_{kf}$ (FROZEN ORBITAL)

KOOPMANS' THEOREM

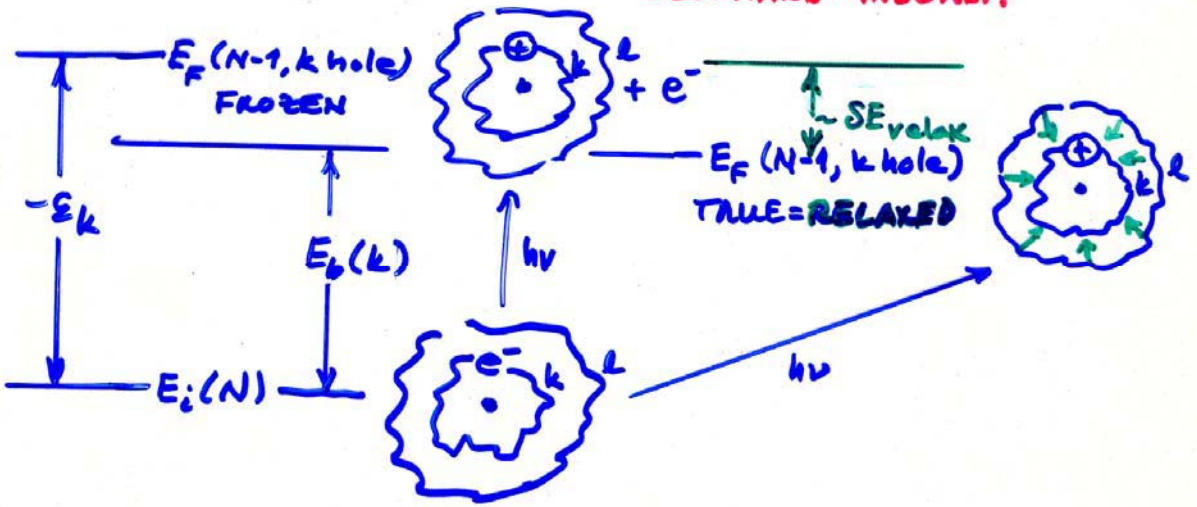

⇒ RELAXATION, SCREENING, CONFIGURATION INTERACTION, SELF-ENERGY EFFECTS ALWAYS PRESENT; ANDERSON IMPURITY MODEL ETC.

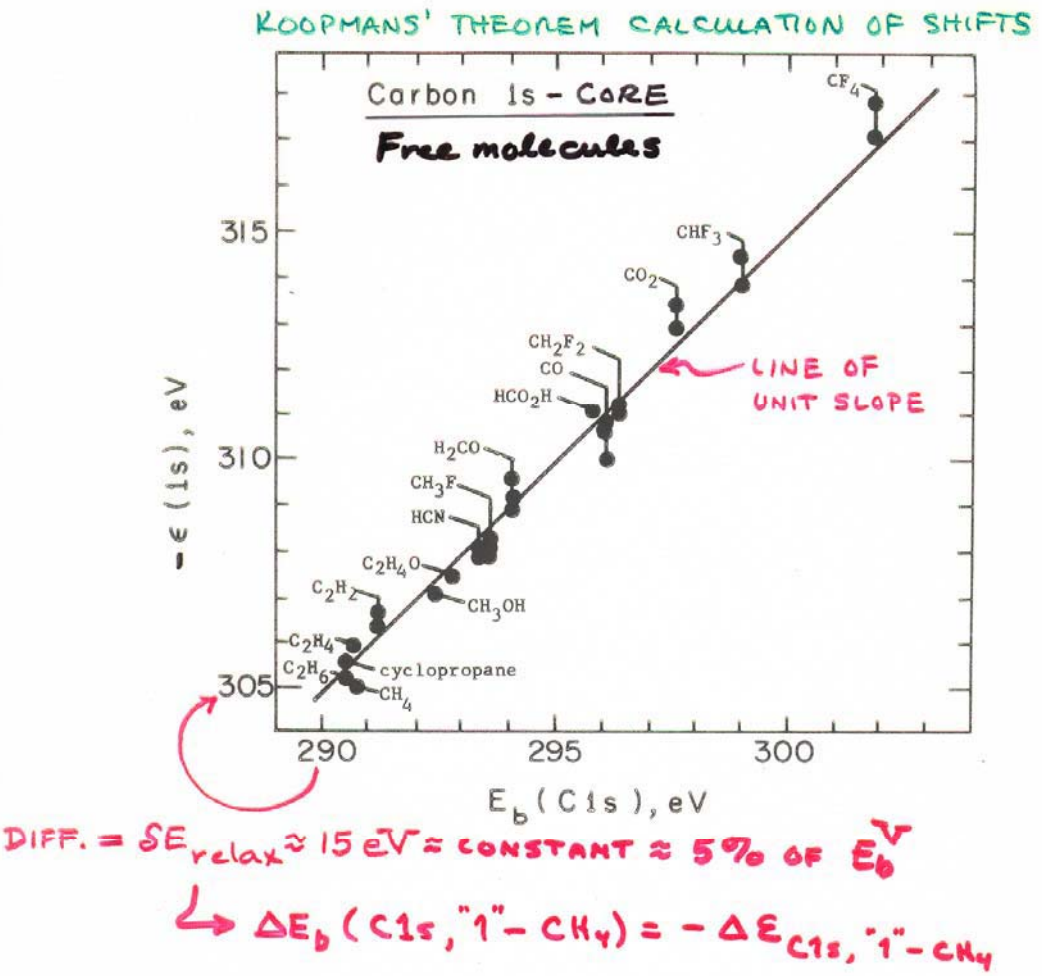

Figure 18 -- Plot of carbon 1s binding energies calculated via Koopmans' Theorem against experimental binding energies for several carbon-containing gaseous molecules. For some molecules, more than one calculated value is presented. The slope of the straight line is unity. The two scales are shifted with respect to one another by 15 eV, largely due to relaxation effects. All of the theoretical calculations were of roughly double-zeta accuracy or better. (From Shirley, reference 7.)

"Basic Concepts of XPS"
Figure 18

Outline

- Core-level chemical shifts: the potential model
- Core-level chemical shifts: equivalent-core (Z+1) and thermochemical energies
- Multiplet splittings
- Spin-orbit splitting, the Fano effect, and spin-polarized outgoing electrons
- Magnetic circular dichroism (MCD) in core-level emission
- Non-magnetic circular dichroism in core-level emission: a.k.a. circular dichroism in angular distributions (CDAD)
- Various other final state effects providing information in core-level spectra

POTENTIAL MODEL FOR CORE-LEVEL CHEMICAL SHIFTS

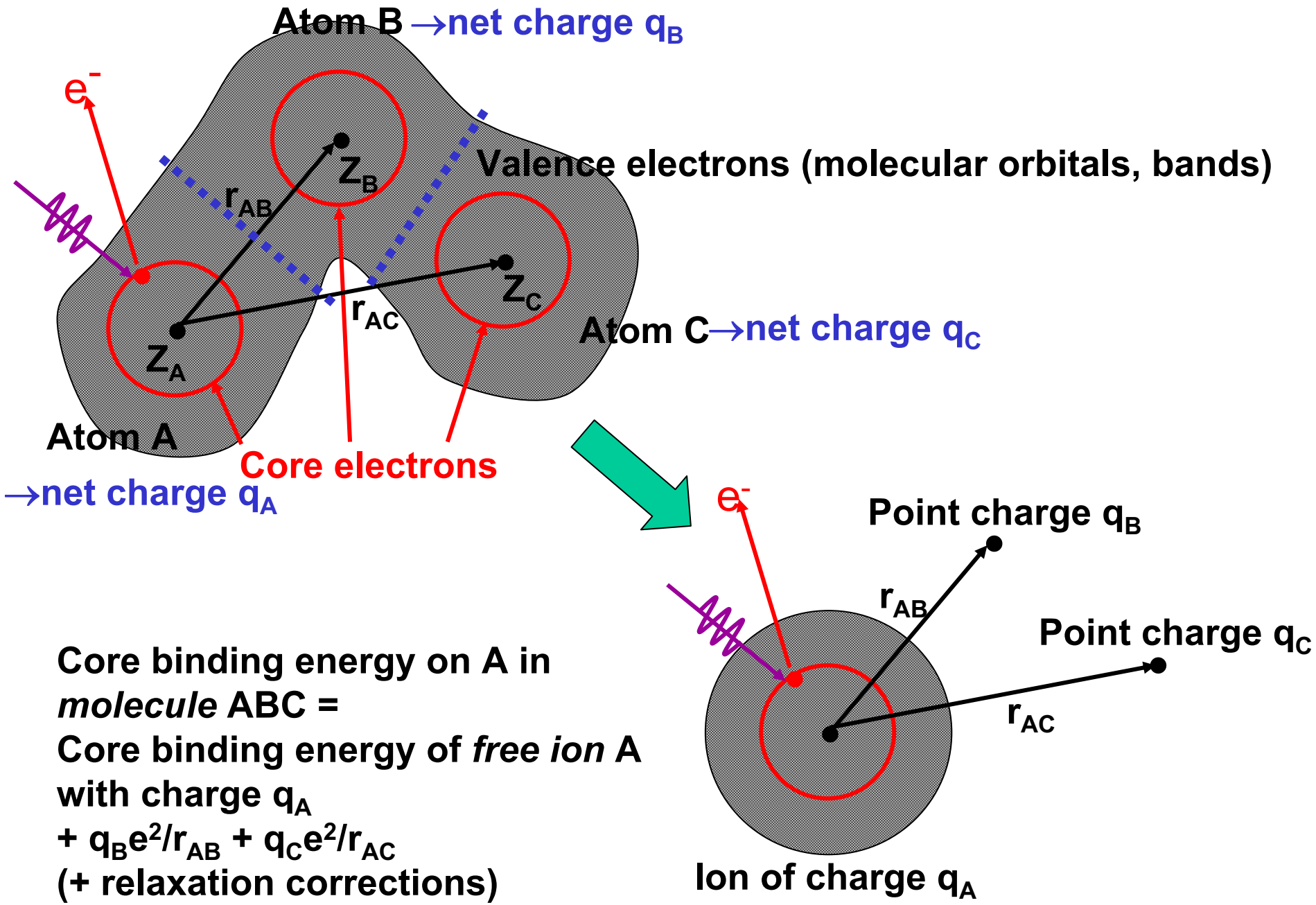

Core binding energy on A in *molecule* ABC =
Core binding energy of *free ion* A with charge q_A
+ $q_B e^2/r_{AB}$ + $q_C e^2/r_{AC}$
(+ relaxation corrections)

FREE-ION (INTRAATOMIC) ASPECTS OF SHIFTS: KOOPMANS' THEOREM & CLASSICAL CHARGED SHELL

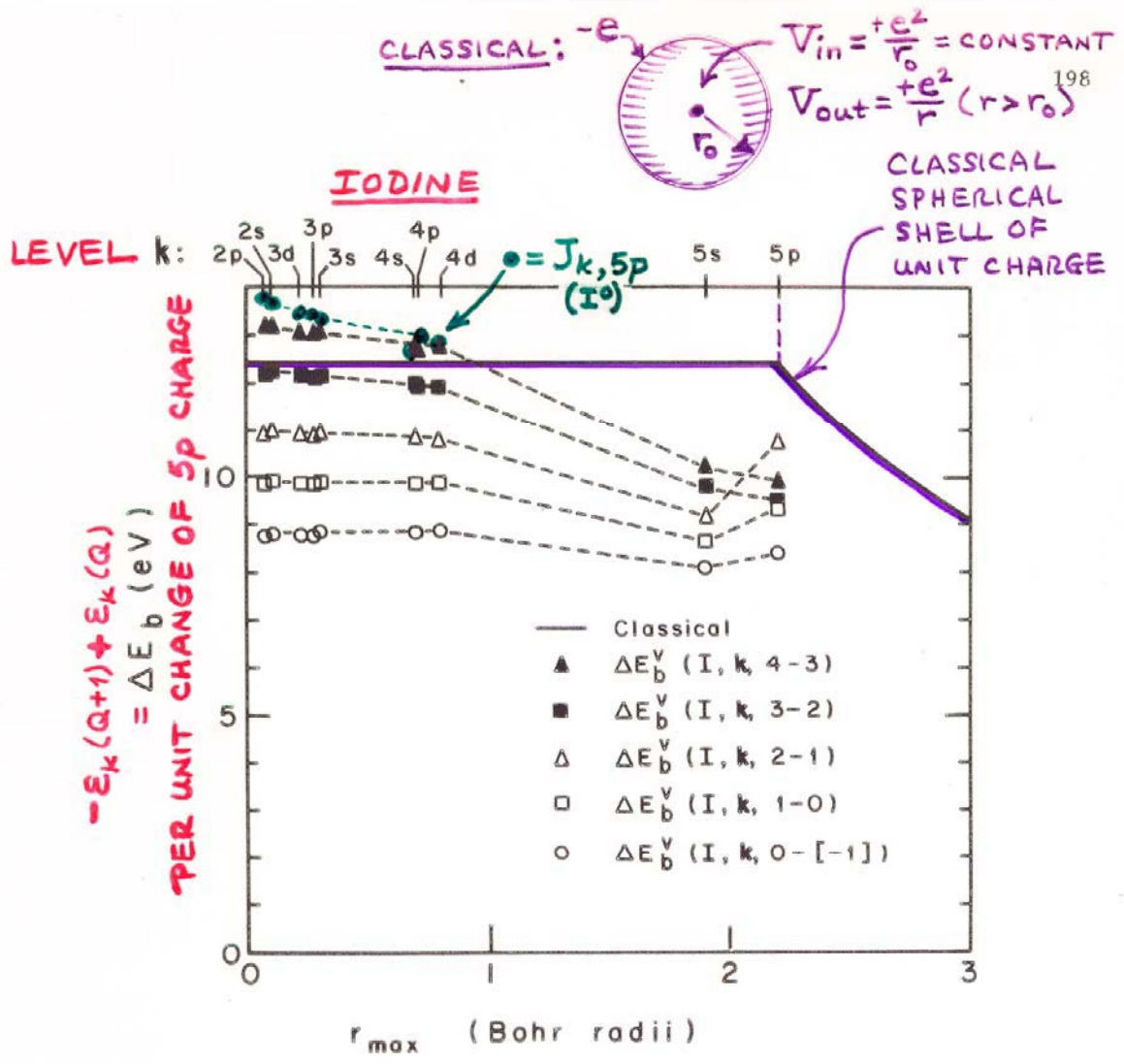

⇒ REMOVAL/ADDITION OF VALENCE e^- CHARGE IN BONDING SHIFTS ALL INNER e^- E_b's ≈ E_K's BY ~SAME AMOUNT

"Basic Concepts of XPS"
Figure 19

POTENTIAL MODEL CALCULATION OF CARBON CHEMICAL SHIFTS

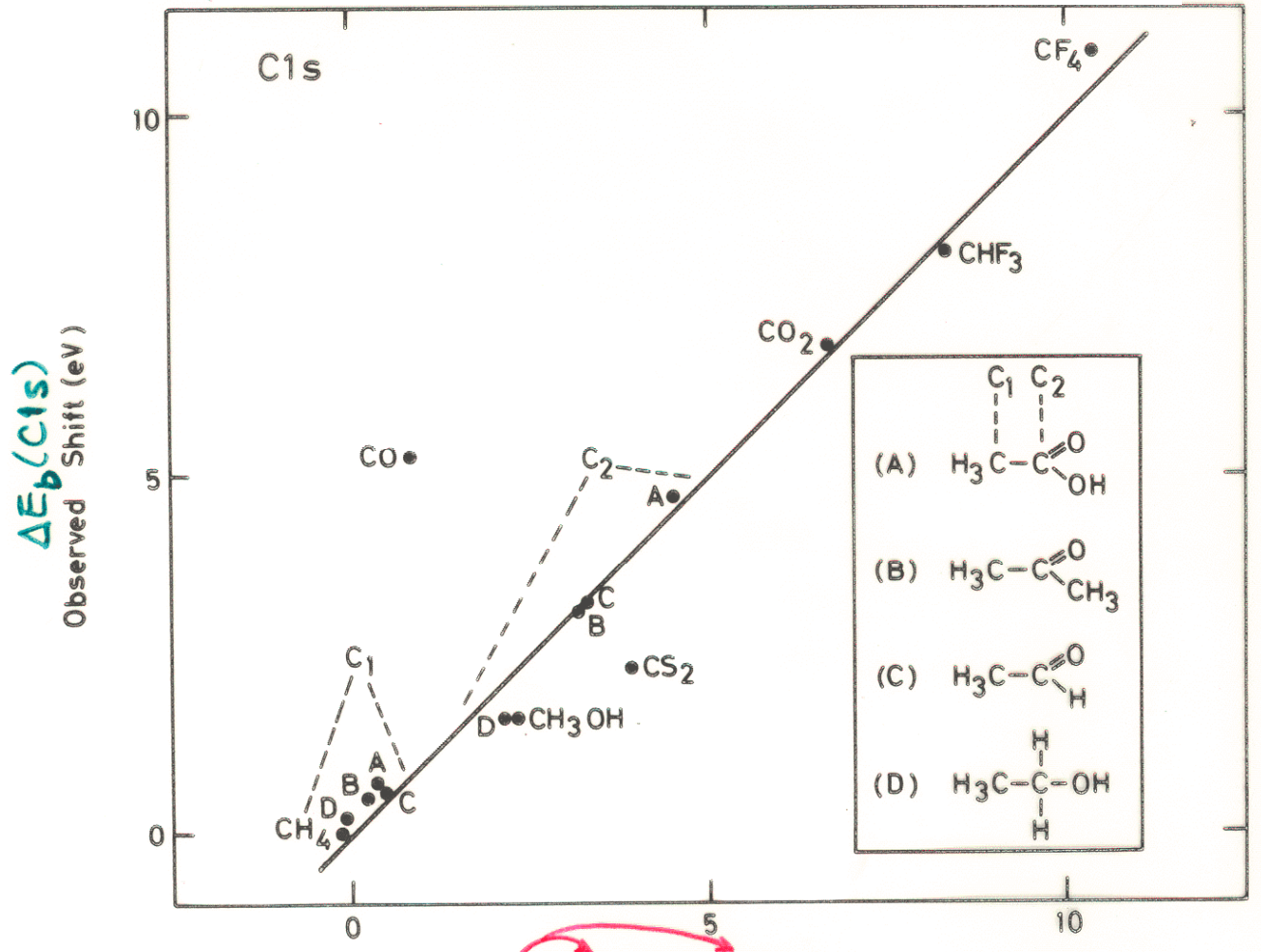

"Basic Concepts of XPS"
Figure 24

Outline

- Valence-band spectra: low-energy UPS limit and high-energy XPS limit
- Core-level chemical shifts: the potential model
- Core-level chemical shifts: equivalent-core (Z+1) and thermochemical energies
- Multiplet splittings
- Spin-orbit splitting, the Fano effect, and spin-polarized outgoing electrons
- Magnetic circular dichroism (MCD) in core-level emission
- Non-magnetic circular dichroism in core-level emission: a.k.a. circular dichroism in angular distributions (CDAD)
- Various other final state effects providing information in core-level spectra

CORRELATION OF THERMOCHEMICAL DATA WITH CHEMICAL SHIFTS: EQUIVALENT-CORE OR (Z+1) MODEL

N core = N $1s^2$ = N^{5+}

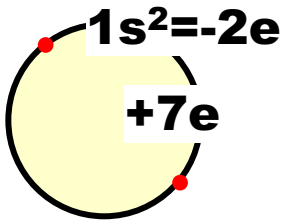

Assume:
N^{6+*} core with
1s hole = N^{6+*} =

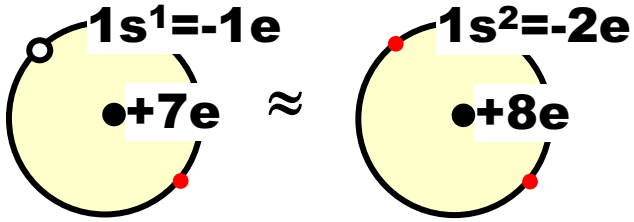

= O^{6+} core

Plus see pp. 92-93 in "Basic Concepts of XPS"

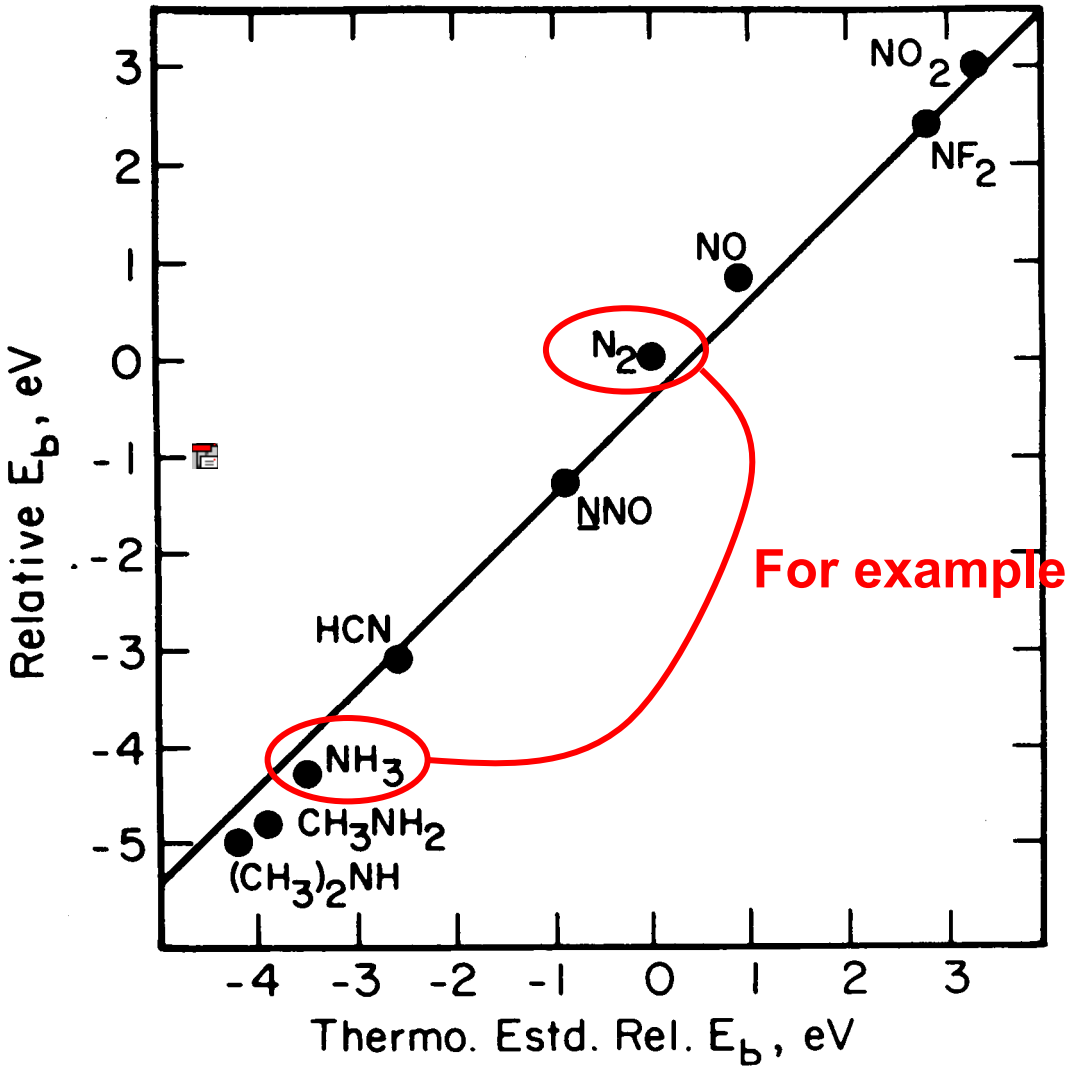

Jolly et al.

Binding energies: * = N 1s core hole present

$$NH_3 \rightarrow NH_3^{+*} + e^- : \Delta E_1 = E_b^V(N1s, NH_3)$$

$$N_2 \rightarrow N_2^{+*} + e^- : \Delta E_2 = E_b^V(N1s, N_2)$$

Adding and subtracting:

$$NH_3 + N_z^{+*} \rightarrow NH_3^{+*} + N_2 : \quad \Delta E = \Delta E_1 - \Delta E_2$$

$$= E_b^V(N1s, NH_3) - E_b^V(N1s, N_2)$$

$$= \Delta E_b^V(N1s, NH_3 - N_2)$$

The chemical shift

Replacing real N 1s core with equivalent O 1s core:

$$NH_3 + NO^+ \rightarrow OH_3^+ + N_2 : \quad \Delta E = \Delta E_b^V(N1s, NH_3 - N_2) + \cancel{\Delta E_{ce} - \Delta E_{ce}}$$

$$= \Delta E_b^V(N1s, NH_3 - N_2)$$

A thermochemical energy

DERIVATION OF HEAT OF SURFACE SEGREGATION FROM SURFACE CORE-LEVEL CHEMICAL SHIFTS

Fig. 4.30. The XPS surface core level shift approach to the heat of segregation of a binary alloy (Egelhoff, 1983). (Zangwill, p. 87)

$\Delta E_b = \Delta H_{surf.\ segregation}$

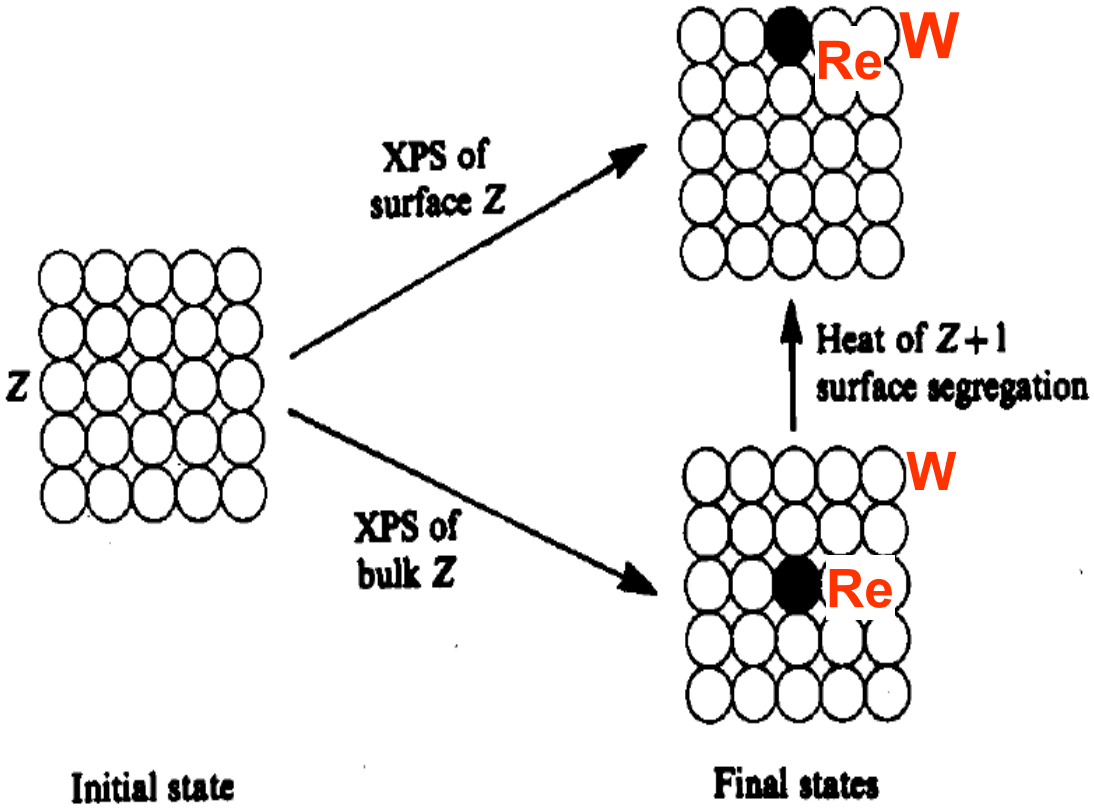

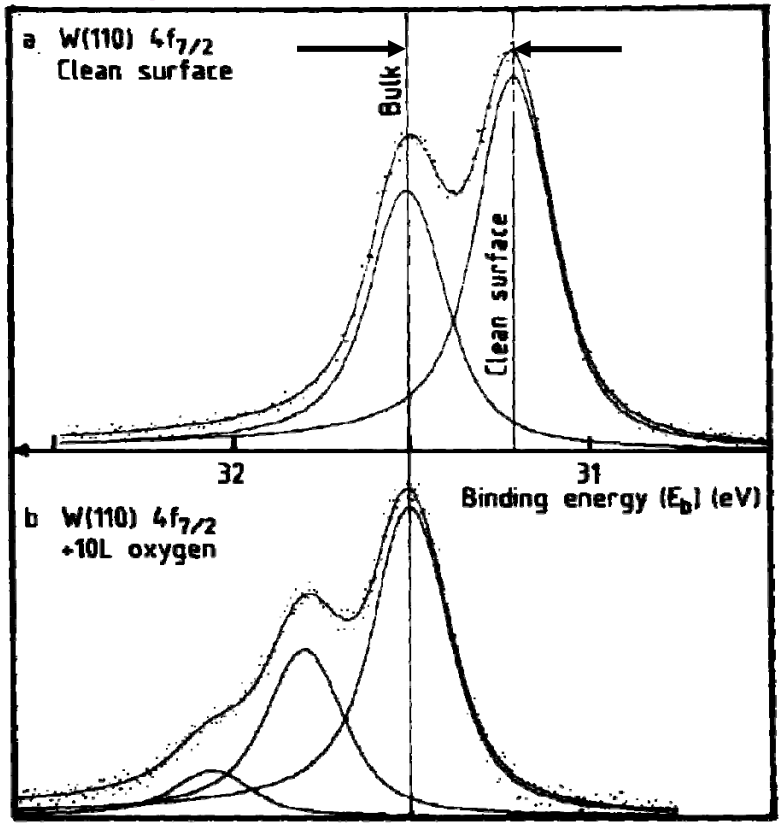

Spanjaard et al., Surf. Sci. Repts. 5, 1 (1985)

W(110)/O—W $4f_{7/2}$ Chemical Shifts

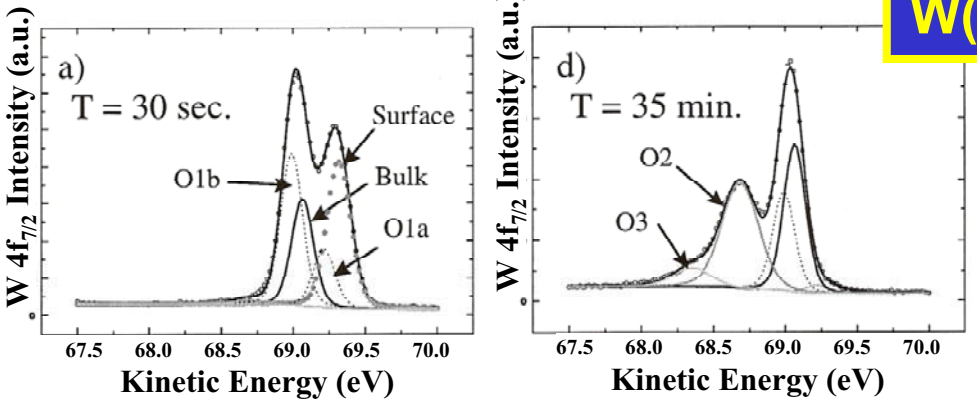

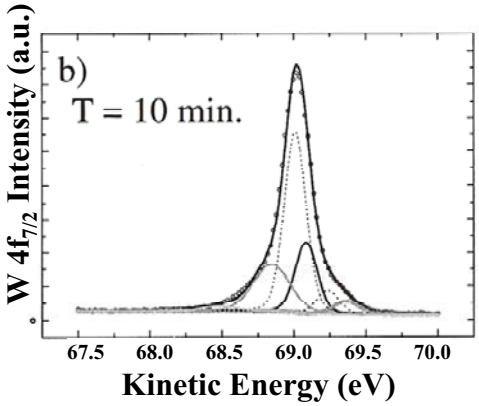

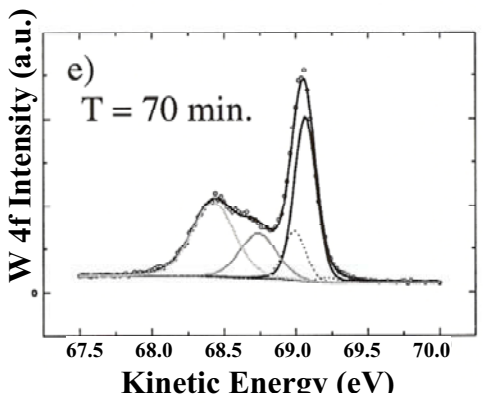

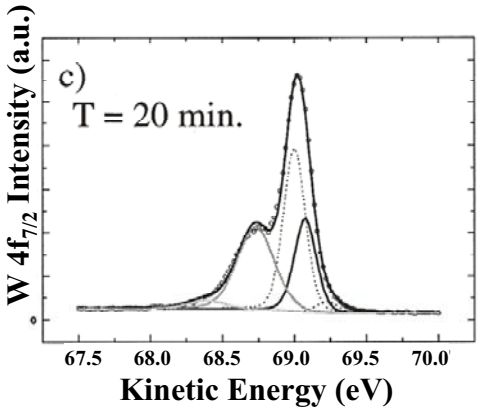

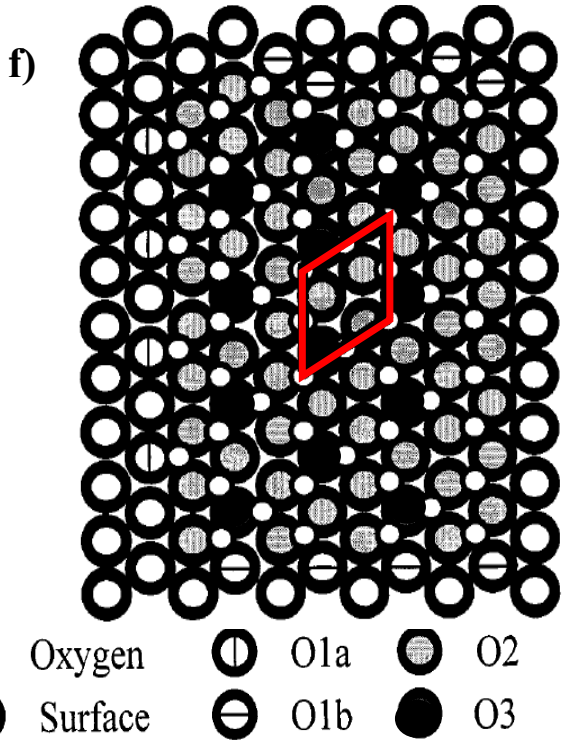

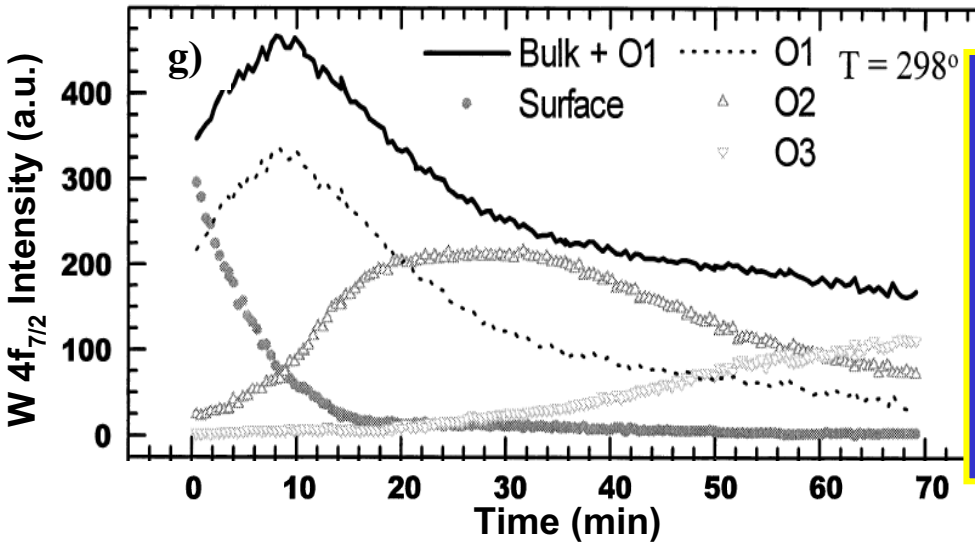

An early time-resolved reaction study (more later)

Ynzunza et al.,
Surf. Sci. 459 (2000) 69

Outline

- Valence-band spectra: low-energy UPS limit and high-energy XPS limit
- Core-level chemical shifts: the potential model
- Core-level chemical shifts: equivalent-core (Z+1) and thermochemical energies
- Multiplet splittings and magnetism
- Spin-orbit splitting, the Fano effect, and spin-polarized outgoing electrons
- Magnetic circular dichroism (MCD) in core-level emission
- Non-magnetic circular dichroism in core-level emission: a.k.a. circular dichroism in angular distributions (CDAD)
- Various other final state effects providing information in core-level spectra

Multiplet splitting in core levels of transition metal oxides

$$BE = h\nu - E_{kin} = \underbrace{E^*(N-1)}_{\text{Final state}} - \underbrace{E_0(N)}_{\text{Initial state}}$$

Open 3d shell, net spin S_{Mn}

$h\nu$

$|3s\rangle$

Upon photoemission, two possible final states

$|3s\rangle$

$J^{eff}_{3s,VB(3d)}$

$|3s\rangle$

$$K^{eff}_{3s,VB(3d)} \approx \int \varphi_{3s}(\vec{r}_1)\varphi_{3d}(\vec{r}_2)\frac{e^2}{r_{12}}\varphi_{3d}(\vec{r}_1)\varphi_{3s}(\vec{r}_2)dV_1dV_2$$

The splitting between the two peaks is given by

$$\Delta E_{3s} \approx (2S_{Mn} + 1)\, K^{eff}_{3s,VB(3d)}$$

(Van Vleck Theorem)

For the cubic manganites in simplest doping model,

$S_{Mn} = 1/2(4-x) \rightarrow$

$$\Delta E_{3s} \approx [5-x]\, K^{eff}_{3s,VB)3d)}$$

with $K^{eff}_{3s,VB} \approx 1.1$ eV

E.g., MnF_2

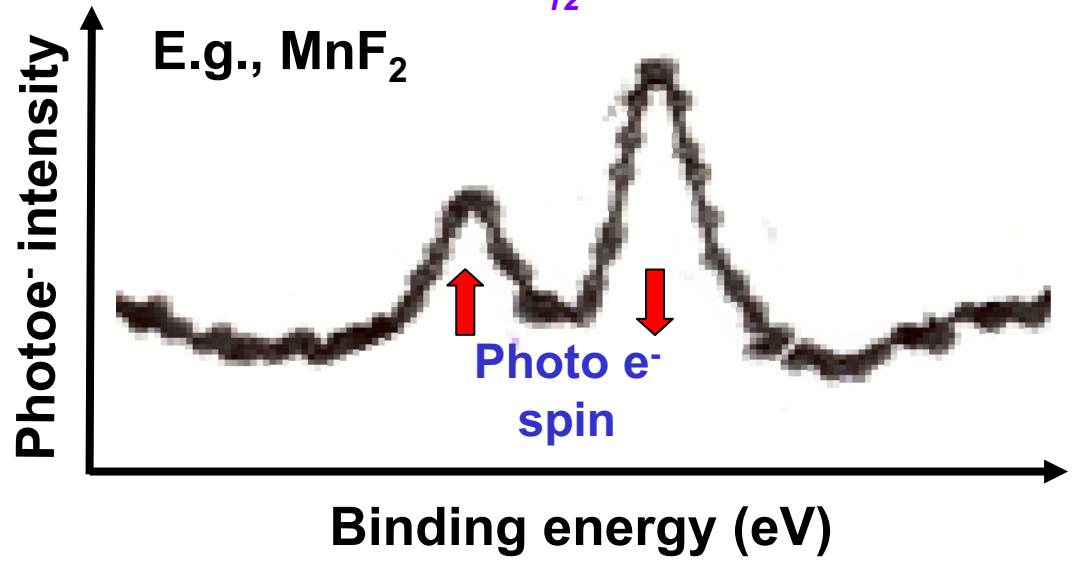

CORE-LEVEL MULTIPLET SPLITTINGS IN Mn COMPOUNDS

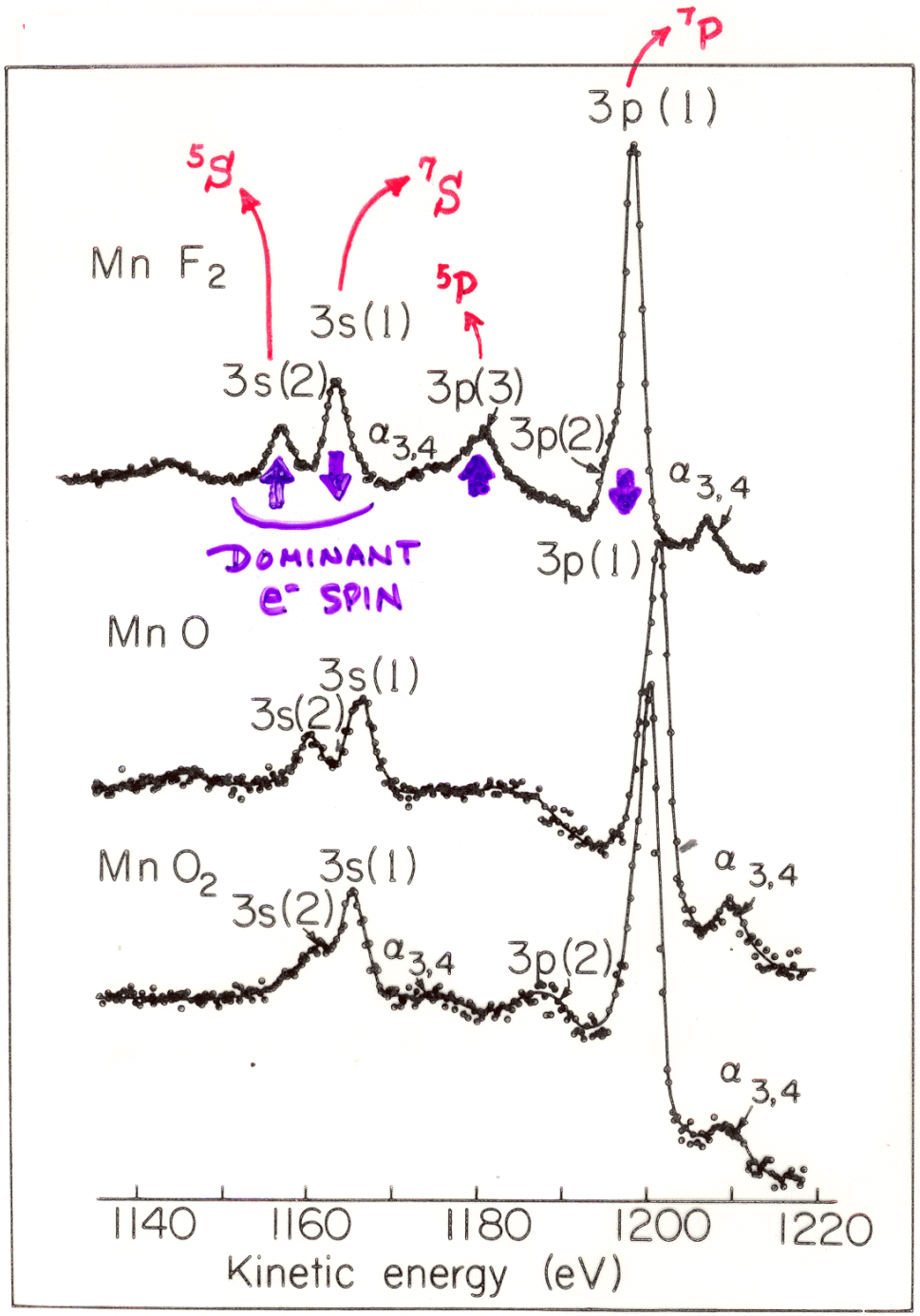

"Basic Concepts of XPS"
Figure 31

ORIGIN OF MULTIPLET SPLITTINGS IN Mn^{2+}: "ONE-ELECTRON" THEORY

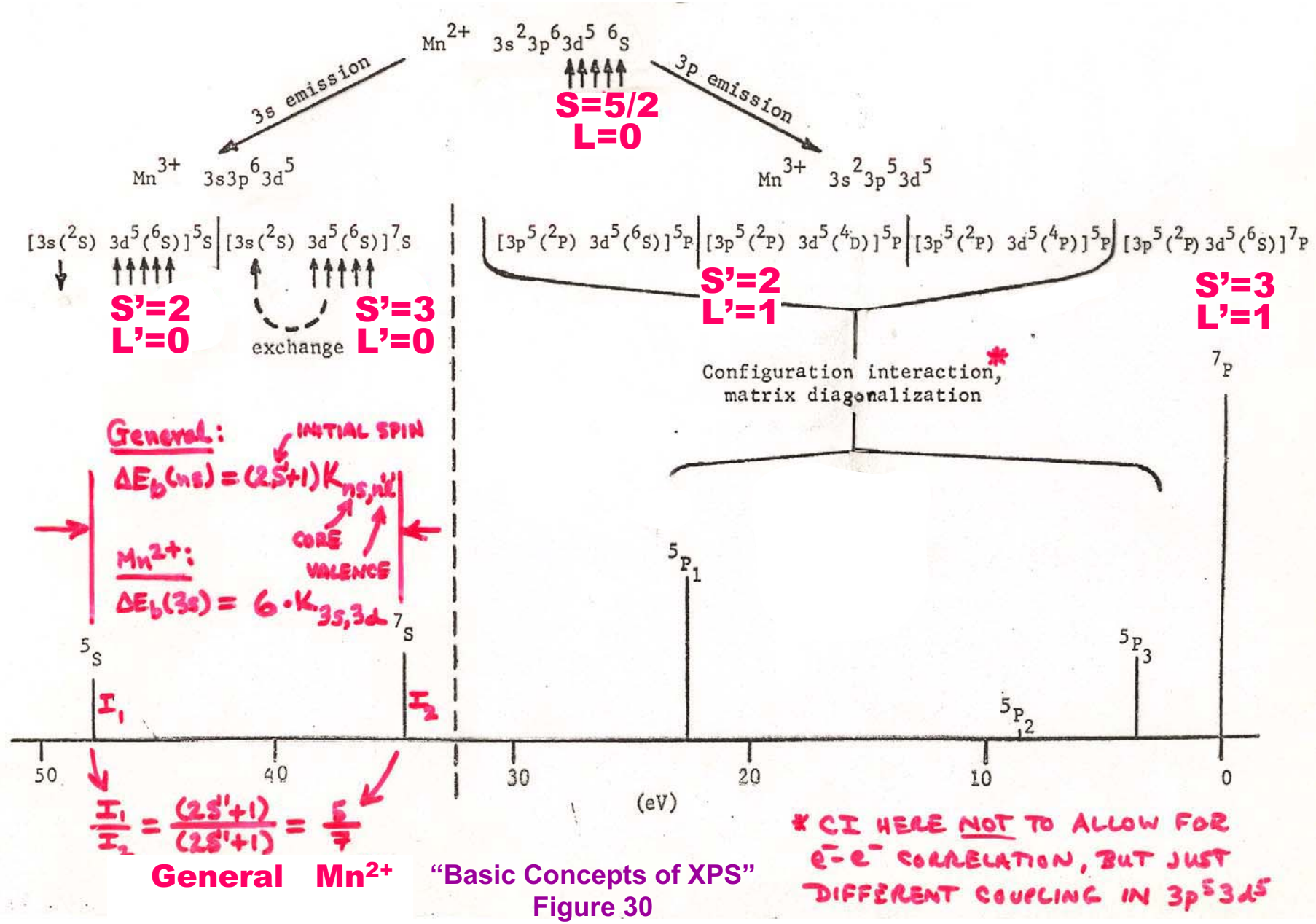

"Basic Concepts of XPS"
Figure 30

COMPARISON OF GAS-PHASE AND SOLID-STATE SPECTRA

EXPT.: (a), (b), (d), HERMSMEIER ET AL., PHYS. REV. LETT. 61, 2592 (1988) (OUR GROUP)

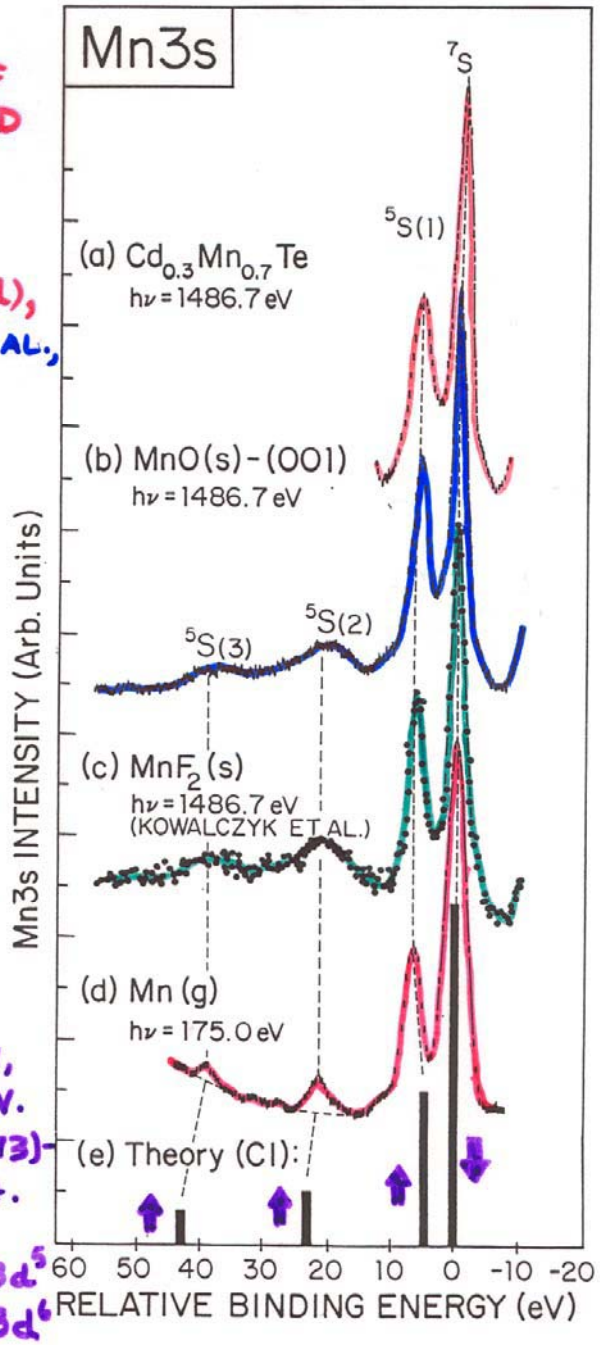

Correlation CI effects: anti-parallel electrons

THEORY: BAGUS, FREEMAN, SASAKI, PHYS. REV. LETT. 30, 850 (1973) - ATOMIC CONFIG. INT. IN

$Mn^{3+}\ldots 3s^1\ldots 3d^5$

+ $Mn^{3+}\ldots 3s^2 3p^4 3d^6$

"Basic Concepts of XPS"
Figure 33

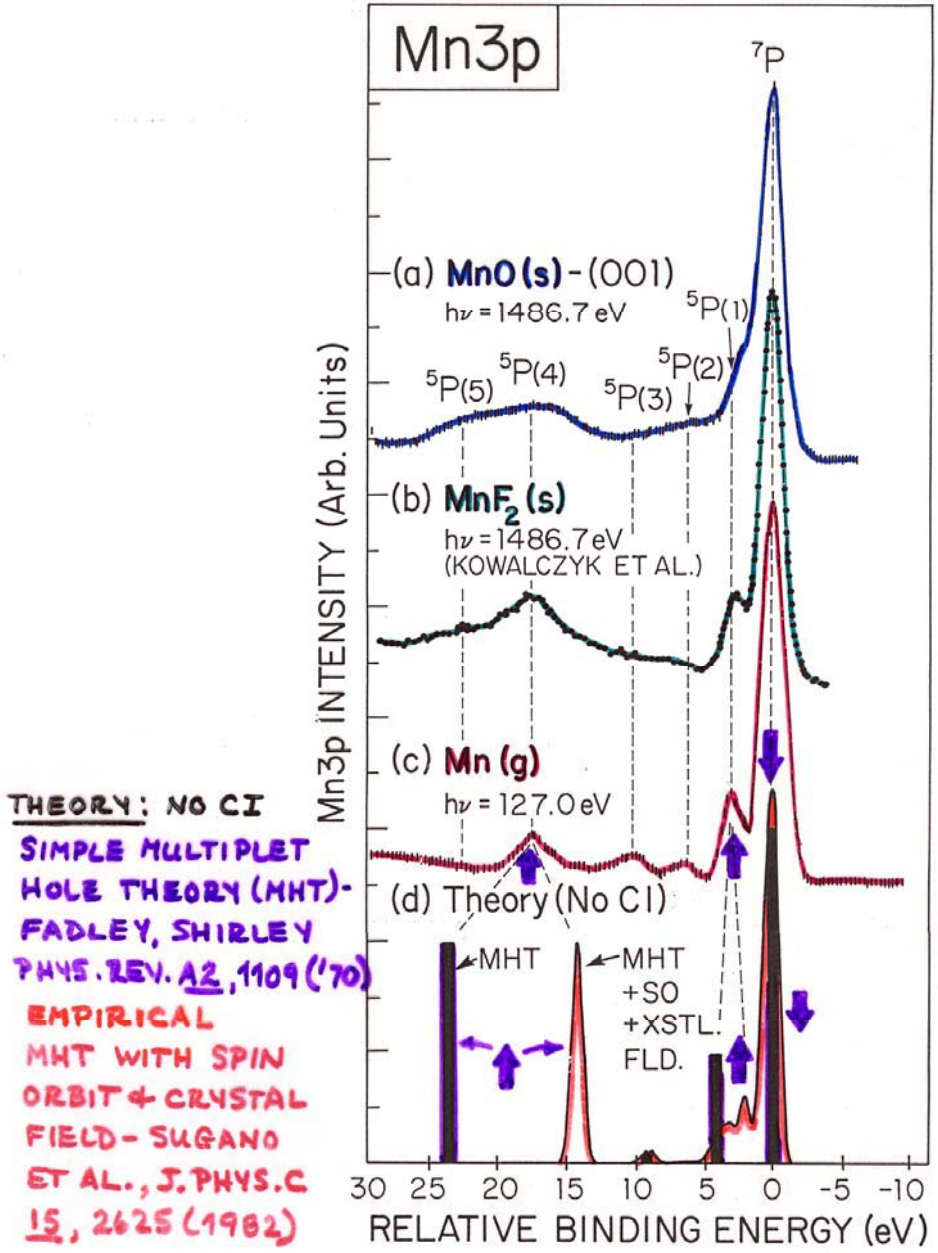

THEORY: NO CI

SIMPLE MULTIPLET HOLE THEORY (MHT) - FADLEY, SHIRLEY PHYS. REV. A2, 1109 ('70)

EMPIRICAL MHT WITH SPIN ORBIT & CRYSTAL FIELD - SUGANO ET AL., J. PHYS. C 15, 2625 (1982)

HERMSMEIER ET AL., P.R.L. 61, 2592 ('88)

Temperature dependence of Mn3s and O1s spectra in a colossal magnetorestive (CMR) oxide: $La_{0.7}Sr_{0.3}MnO_3$

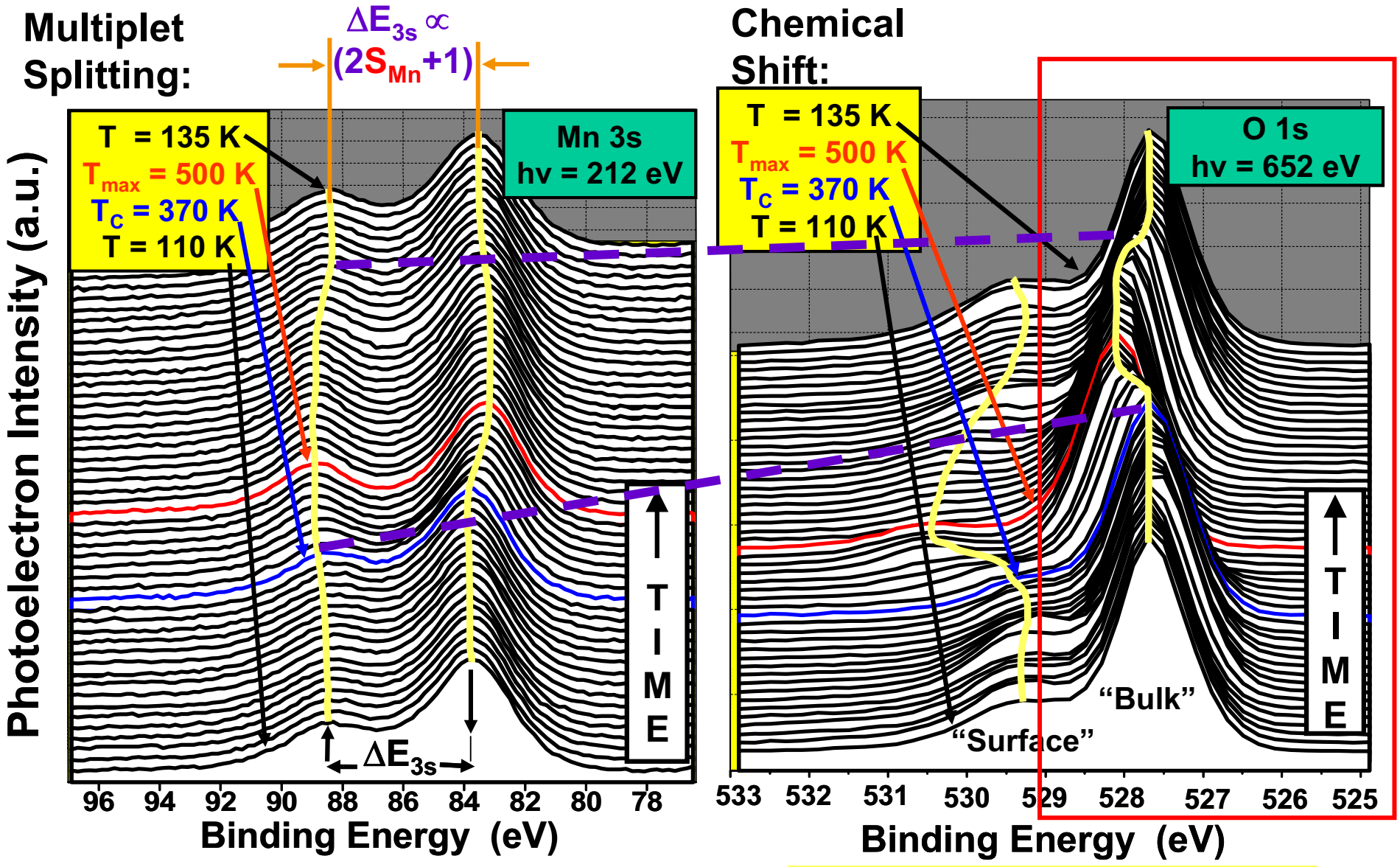

Increase of the Mn3s splitting-reversible

Increase of O1s BE-reversible

T dependence of Mn 3s binding energies

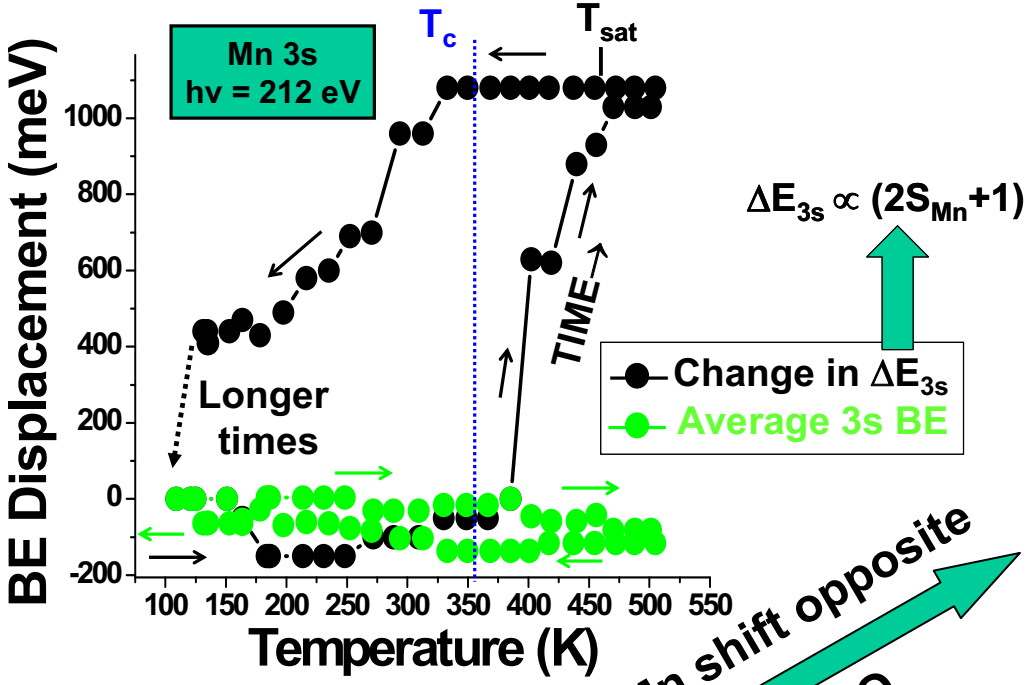

$\Delta E_{3s} \propto (2S_{Mn}+1)$

Change in ΔE_{3s}

Average 3s BE

T dependence of bulk O 1s binding energy

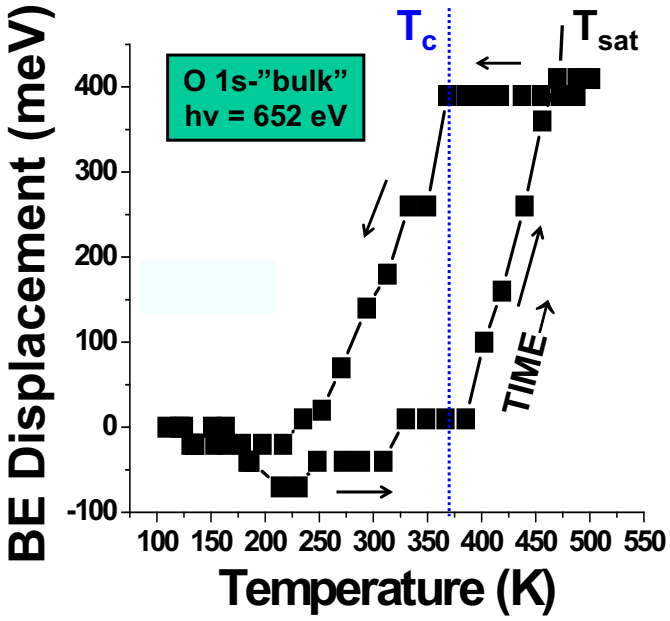

Mn shift opposite to O

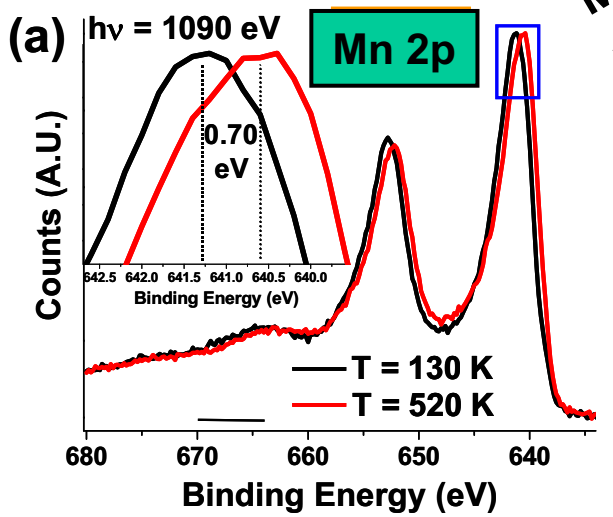

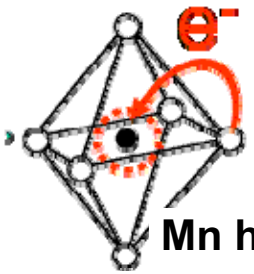

O more positive

Mn higher spin, more negative

Theory: self-interaction corrected local spin density results for LSMO → elongating octahedron makes Mn^{3+} more stable than Mn^{4+}

Banach, Temmerman, PRB 69, 054427 ('04)

Mannella et al., Phys. Rev. Lett. 92, 166401 (2004)

Suggested scenario—LSMO, x = 0.3, 0.4

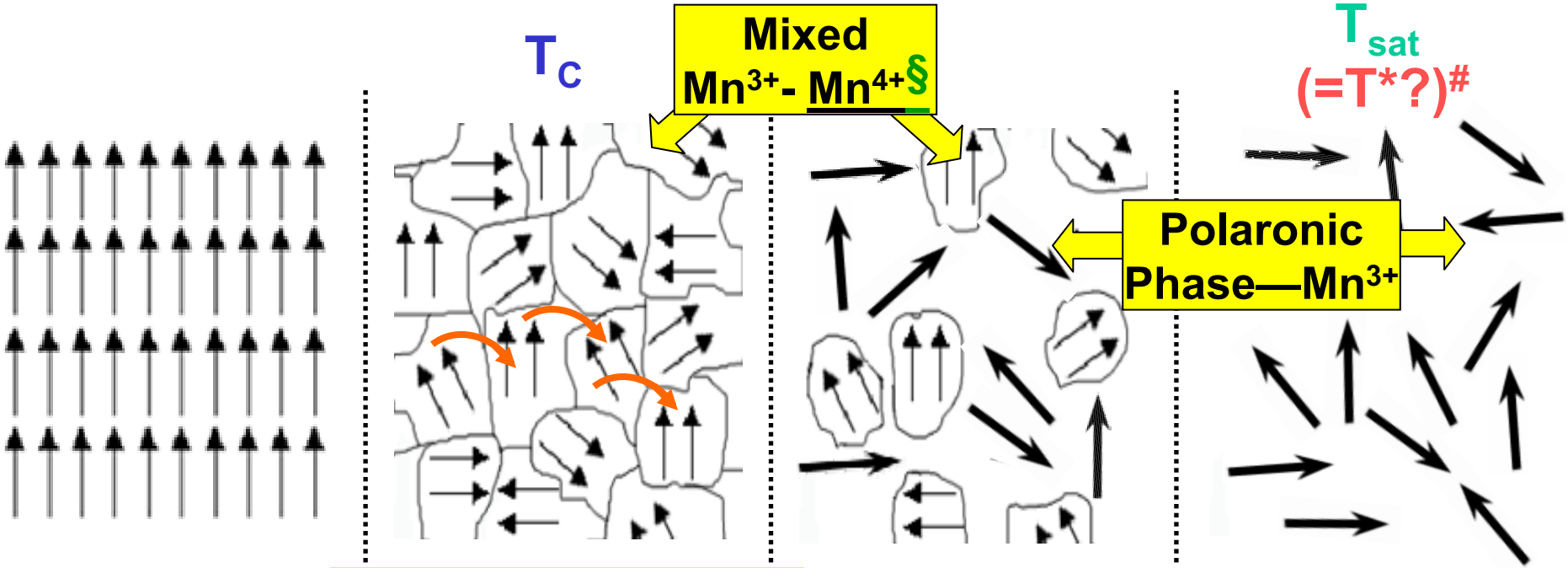

Long-range ferromagnetic order

Loss of long - range order at T_C: some percolation

Short - range order above T_C up to T_{sat} Jahn-Teller distortion

§Self-interaction corrected local spin density calcs. suggest Mn^{4+} dominant, but conversion to Mn^{3+} with JT distortion
Banach, Temmerman, PRB 69, 054427 ('04)

T* = new T scale suggested from theory
Dagotto et al.
PRL 87, 277202 (2001)

Mannella et al., PRL 92, 166401 ('04); PRB 70, 224433 ('04), and to be publ.

DIRECT OBSERVATION OF SPIN-SPLIT CORE LEVELS IN A FERROMAGNET

$$\frac{I_\uparrow - I_\downarrow}{I_\uparrow + I_\downarrow}$$

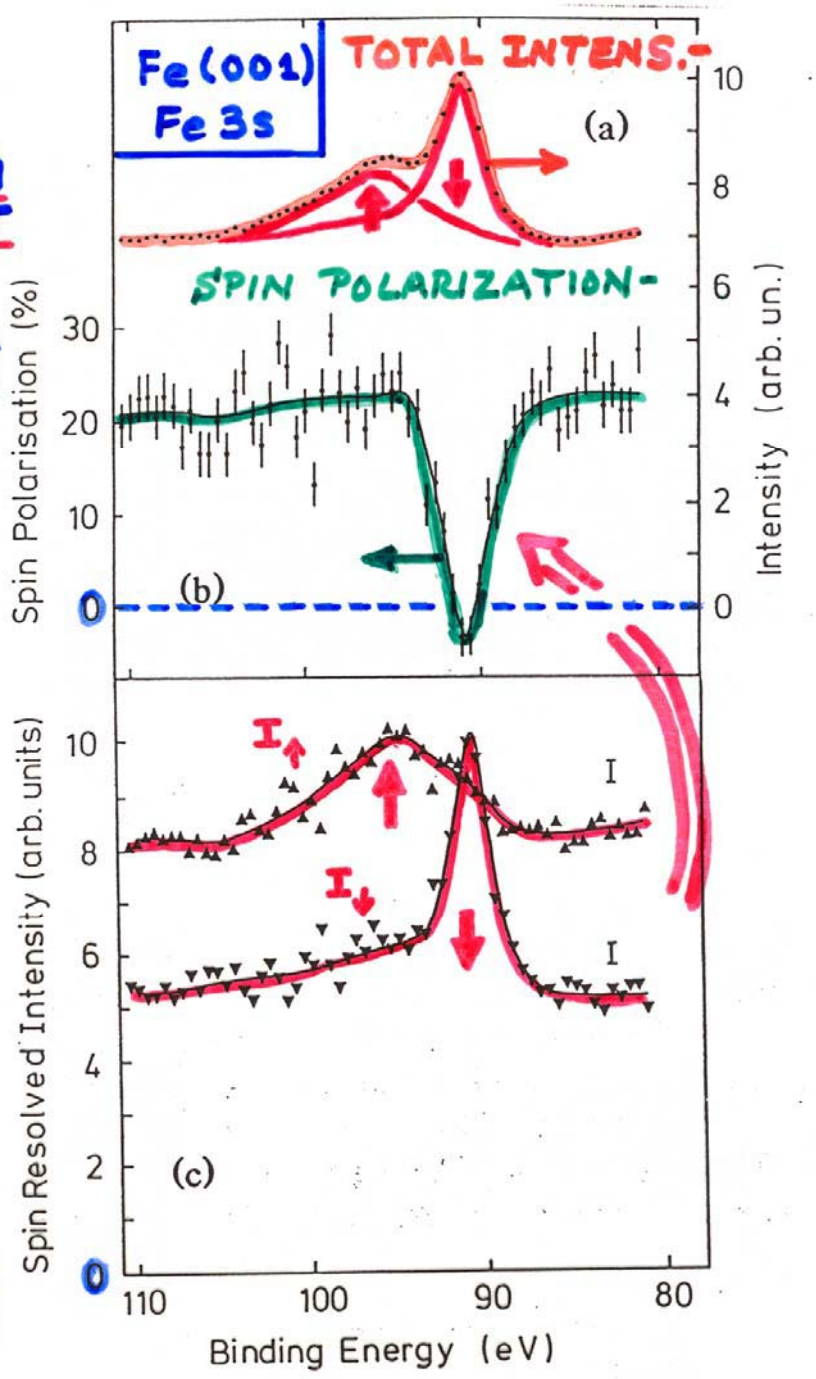

HILLEBRECHT ET AL., PHYS. REV. LETT. 65, 2450 (1990)

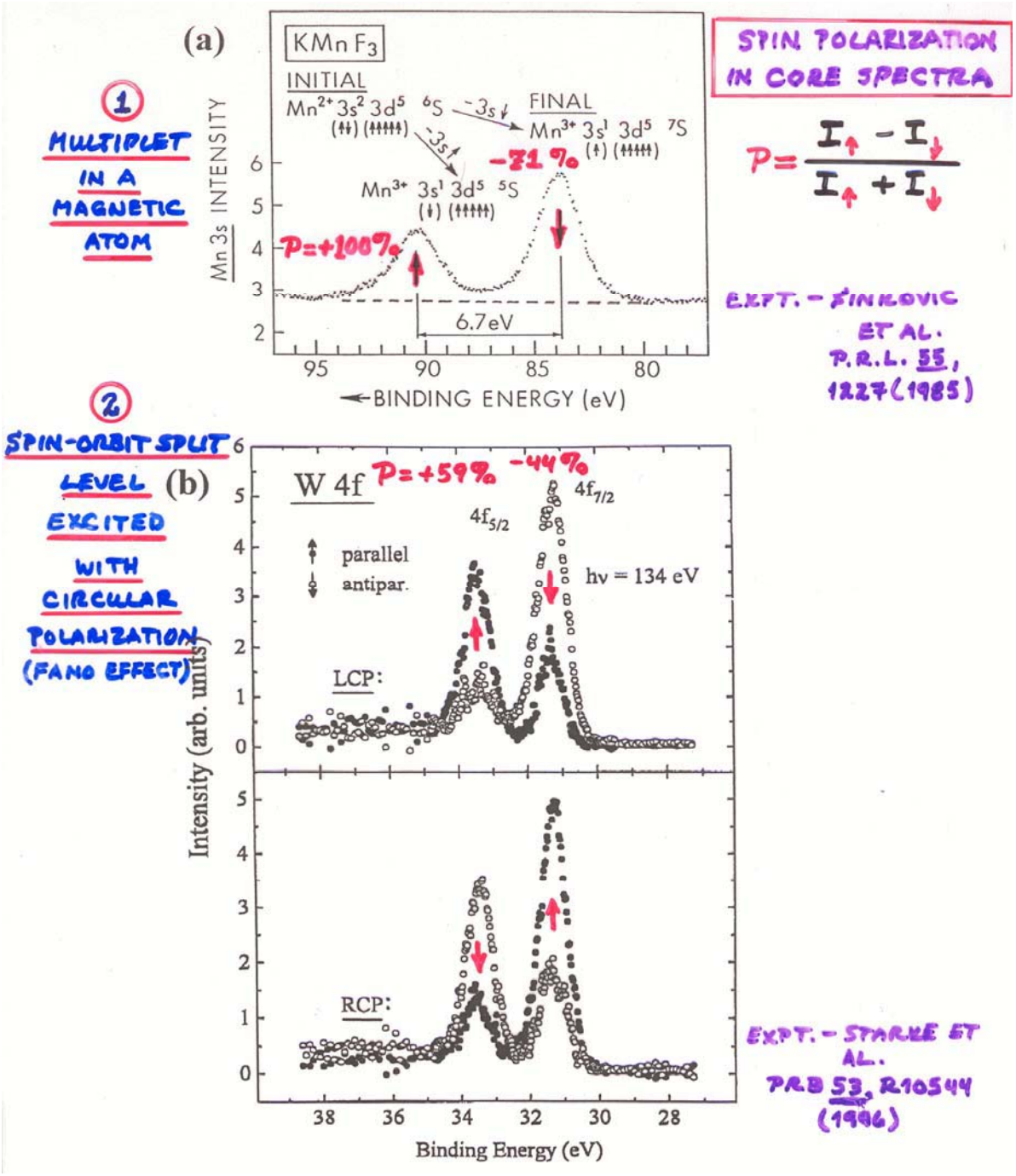

Spin <u>internally</u> referenced to spin of each ion

Spin <u>externally</u> referenced to $\vec{k}_{h\nu}$ and $\vec{M}$ of sample

✚ MORE COMPLEX MULTIPLETS FOR L > 0 WITH SPIN-ORBIT COUPLING:

Mn 2p emission from MnF_2:

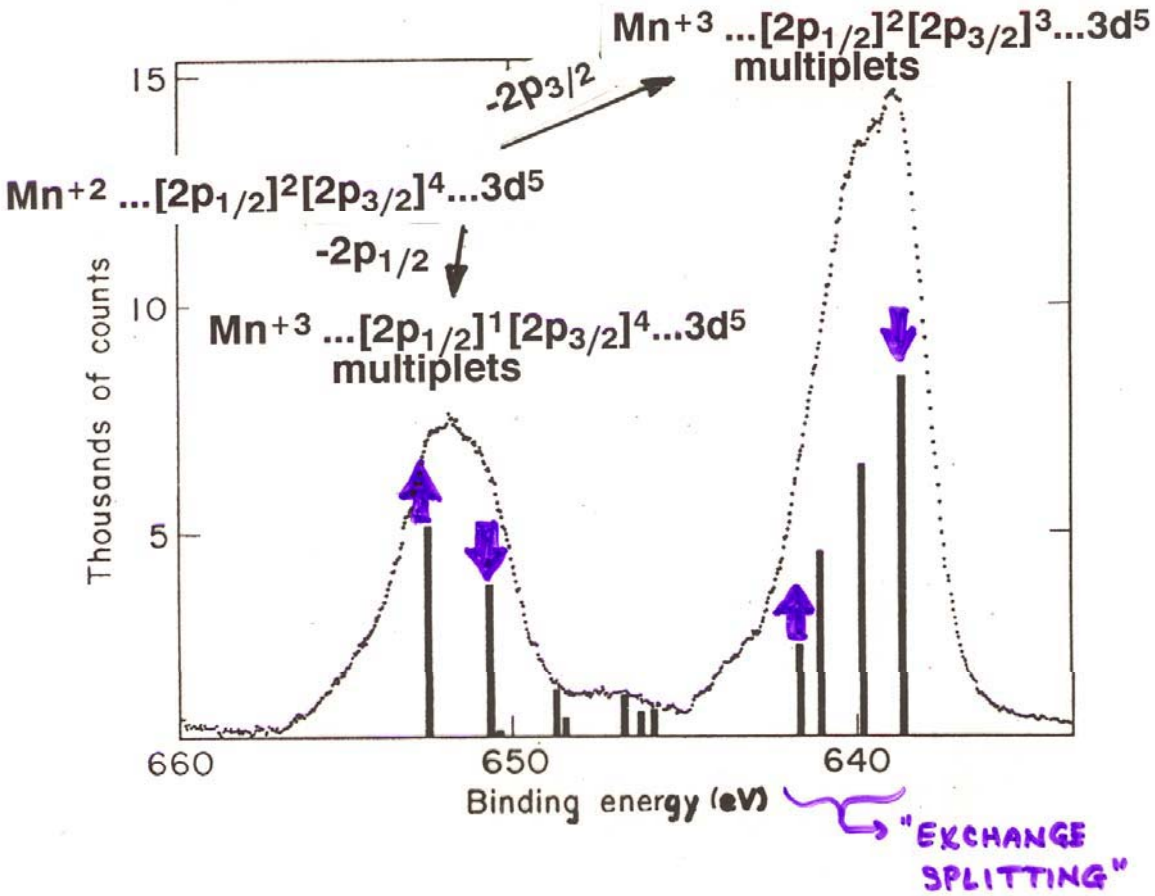

Expt.--Kowalczyk et al., Phys. Rev. B11, 1721 (1975)

Theory--Gupta and Sen, Phys. Rev. B10, 71 (1974)

Park et al., Phys. Rev. B37, 10867(1988)

MULTIPLETS IN FREE MOLECULES

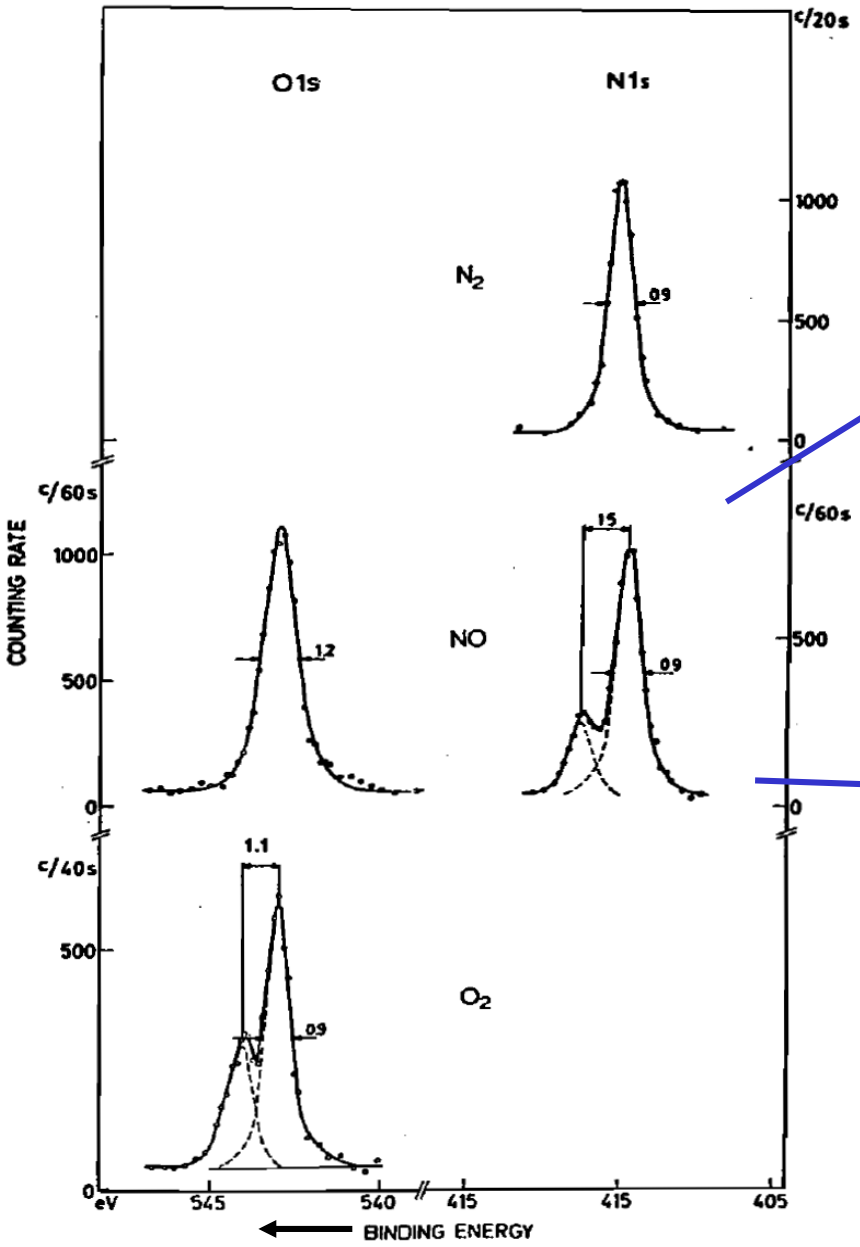

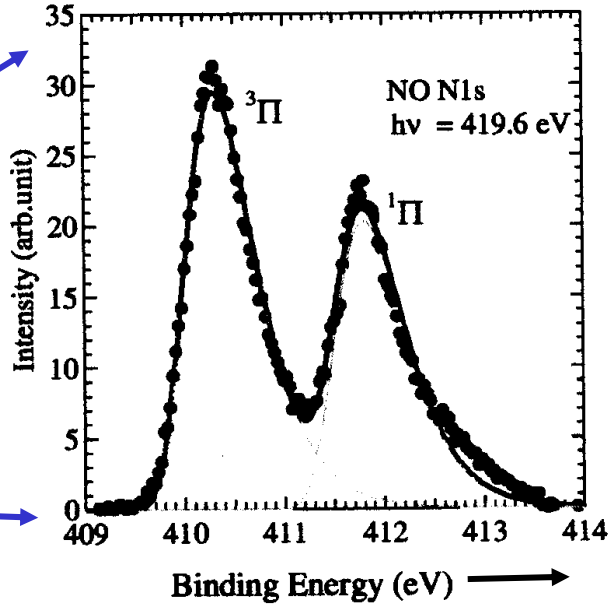

Hosaka et al., J. Phys. B 36, 4617 (2003), and earlier theory from Bagus and Schaefer, J. Chem. Phys. 55, 1474 (1971)

Fig. 34
Basic Concepts of XPS

Outline

- Valence-band spectra: low-energy UPS limit and high-energy XPS limit
- Core-level chemical shifts: the potential model
- Core-level chemical shifts: equivalent-core (Z+1) and thermochemical energies
- Multiplet splittings
- Spin-orbit splitting, the Fano effect, and spin-polarized outgoing electrons
- Magnetic circular dichroism (MCD) in core-level emission
- Non-magnetic circular dichroism in core-level emission: a.k.a. circular dichroism in angular distributions (CDAD)
- Various other final state effects providing information in core-level spectra

PHOTOELECTRON EMISSION - BASIC MATRIX ELEMENTS + SELECTION RULES:

- **ATOMIC-LIKE (LOCALIZED) STATES ⇒ CORE:**

$$\varphi_i(\vec{r}) = \varphi_{n_i \ell_i m_i}(r,\theta,\phi) = R_{n_i \ell_i}(r) Y_{\ell_i m_i}(\theta,\phi)$$

PLUS SPIN:

$$\begin{cases} \alpha(\sigma) = m_{si} = +\tfrac{1}{2} = \uparrow \\ \beta(\sigma) = m_{si} = -\tfrac{1}{2} = \downarrow \end{cases}$$

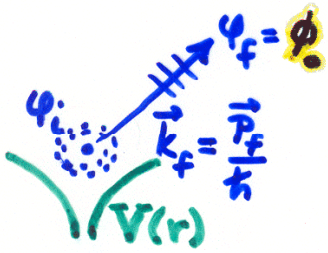

$$\varphi_f(\vec{r},\vec{k}_f) = \varphi_{E_f}(\vec{r},\vec{k}_f) \begin{cases} \alpha(\sigma) \\ \beta(\sigma) \end{cases}$$

$$= 4\pi \sum_{\ell_f, m_f} i^{\ell_f} e^{-i\delta_{\ell_f}} Y^*_{\ell_f m_f}(\theta_{k_f}, \phi_{k_f}) Y_{\ell_f m_f}(\theta,\phi) R_{E_f \ell_f}(r) \begin{cases} \alpha(\sigma) \\ \beta(\sigma) \end{cases}$$

(δ_{ℓ_f}: PHASE SHIFT OF ℓ_f WAVE IN $V(r)$)

DIPOLE APPROX.: INT. $\propto |\langle \varphi_f | \hat{\varepsilon} \cdot \vec{r} | \varphi_i \rangle|^2 = |\hat{\varepsilon} \langle \varphi_f | \vec{r} | \varphi_i \rangle|^2 \Rightarrow$

EQUIVALENT WITHIN CONSTANT FACTOR ($\vec{p} \leftrightarrow \vec{\nabla} V(r)$)

- $\Delta \ell = \ell_f - \ell_i = \pm 1$ TWO CHANNELS
- $\Delta m = m_f - m_i = 0, \pm 1$ LINEAR POLARIZ.
- $\Delta m = \pm 1$, CIRCULAR POLARIZATION

$\Delta m_s = m_{sf} - m_{si} = 0$!

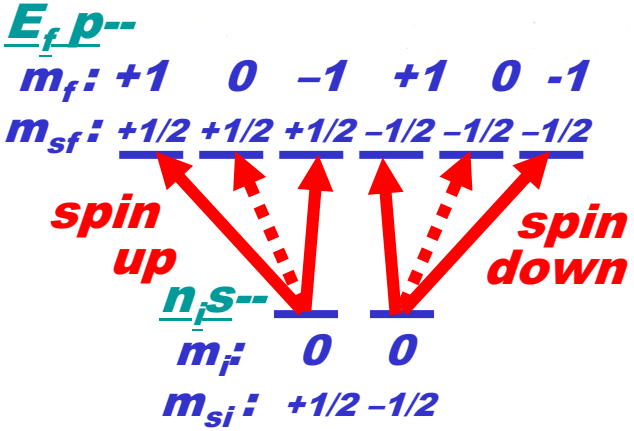

FOR A GIVEN $n_i \ell_i m_i m_{si}$: SUM OVER DEGENERATE INITIAL STATES $m_i m_{si}$ AND AVERAGE OVER FINAL STATES $E_f \ell_f m_f m_{sf}$ ACCESSED FROM EACH m_i TO YIELD DIFFERENTIAL SUBSHELL PHOTOELECTRIC CROSS SECTION :

$$d\sigma_{n_i \ell_i} / d\Omega$$

$\propto$ PROBABILITY PER UNIT SOLID ANGLE OF EXCITING ONE ELECTRON FROM SUBSHELL $n_i \ell_i$ INTO THE DIRECTION k_f

• SPIN-ORBIT SPLITTING OF LEVELS:

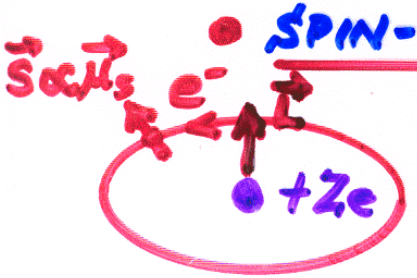

$\Rightarrow$ EFFECTIVE $\vec{B}$ (NUCLEUS AROUND e^-) $\propto \vec{L}$

$$\hat{H}_{s\text{-}o} = \xi(r)\,\vec{l}\cdot\vec{s}$$

• SPLITS ALL nl LEVELS $2(2l+1)$

- $nlj = l+1/2$ — $2l+2$
- $nlj = l-1/2$ — $2l$

• MIXES SPIN + ORBITAL ANGULAR MOM.:

$$\psi_{nljm_j} = C_1\psi_{nl,m_j-1/2}\begin{pmatrix}1\\0\end{pmatrix} + C_2\psi_{nl,m_j+1/2}\begin{pmatrix}0\\1\end{pmatrix}$$

$\begin{pmatrix}1\\0\end{pmatrix} = m_s = +1/2 = \uparrow$ $\qquad$ $\begin{pmatrix}0\\1\end{pmatrix} = m_s = -1/2 = \downarrow$

WITH C1 AND C2 TABULATED CLEBSCH-GORDAN OR WIGNER 3j SYMBOLS

PHOTOELECTRON SPIN POLARIZATION FROM CIRCULAR POLARIZATION AND SPIN–ORBIT SPLITTING

(THE FANO EFFECT)

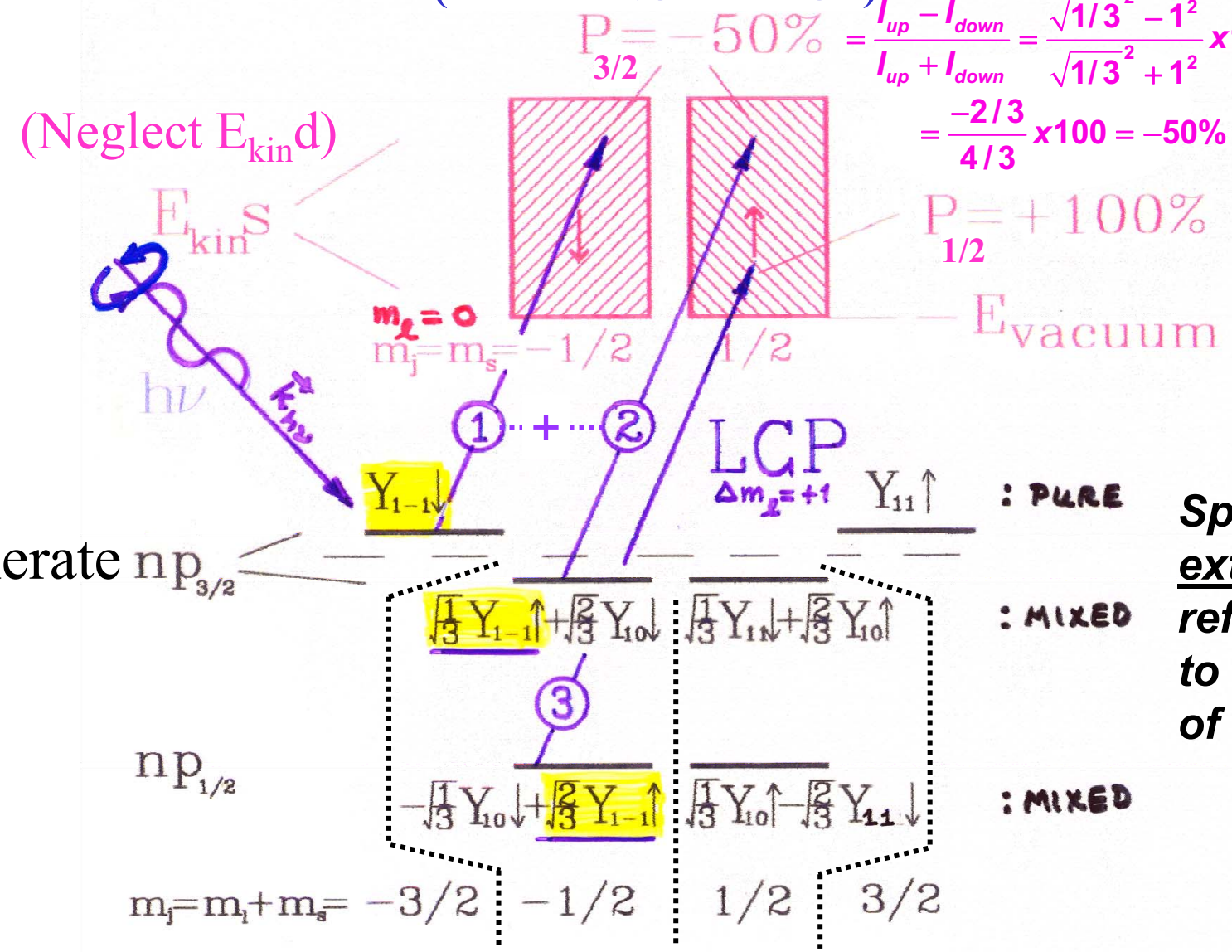

Spin <u>externally</u> referenced to $\vec{k}_{h\nu}$ and $\vec{M}$ of sample

Spin polarization in core photoelectron spectra—expt.

SPIN-ORBIT SPLIT LEVEL (b) EXCITED WITH CIRCULAR POLARIZATION (FANO EFFECT)

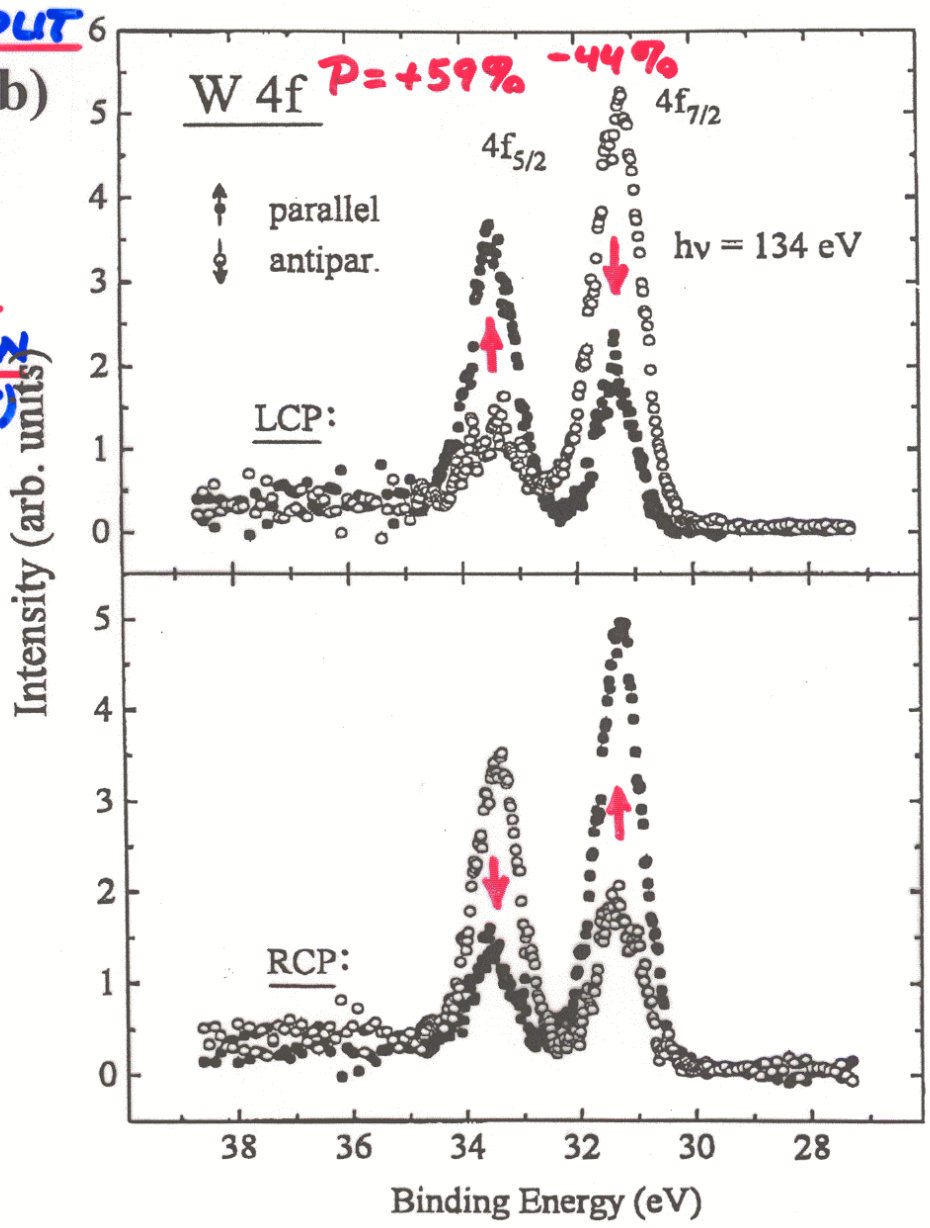

EXPT. - STARKE ET AL. PRB 53, R10544 (1996)

Outline

•Valence-band spectra: low-energy UPS limit and high-energy XPS limit

•Core-level chemical shifts: the potential model

•Core-level chemical shifts: equivalent-core (Z+1) and thermochemical energies

• Spin-orbit splitting, the Fano effect, and spin-polarized outgoing electrons

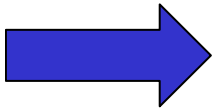

• Magnetic circular dichroism (MCD) in core-level emission

• Non-magnetic circular dichroism in core-level emission: a.k.a. circular dichroism in angular distributions (CDAD)

•Various other final state effects providing information in core-level spectra

Typical experimental geometry for energy- and angle-resolved photoemission measurements

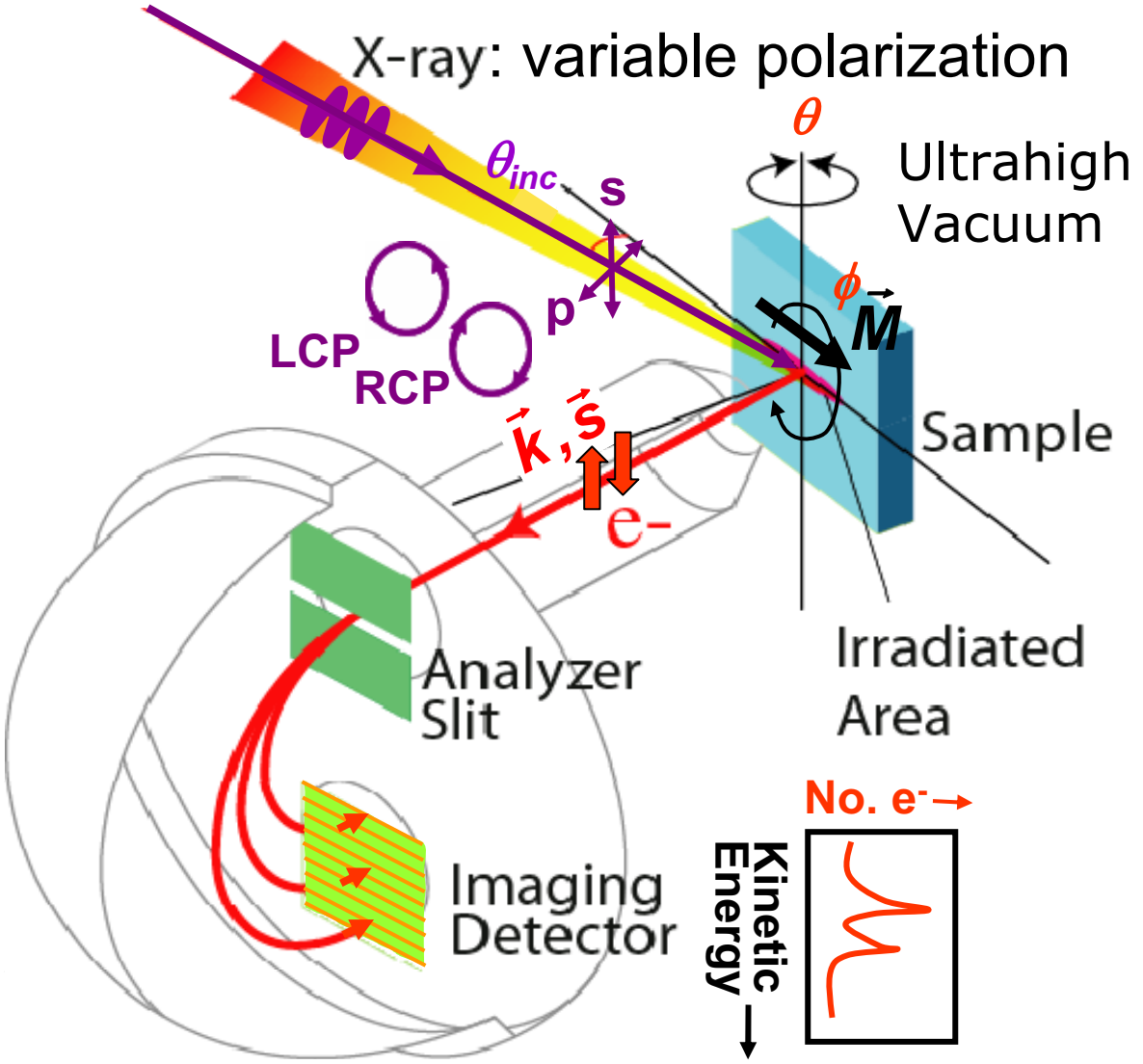

1st Expt. Magnetic Circular Dichroism 1-e- Theo.

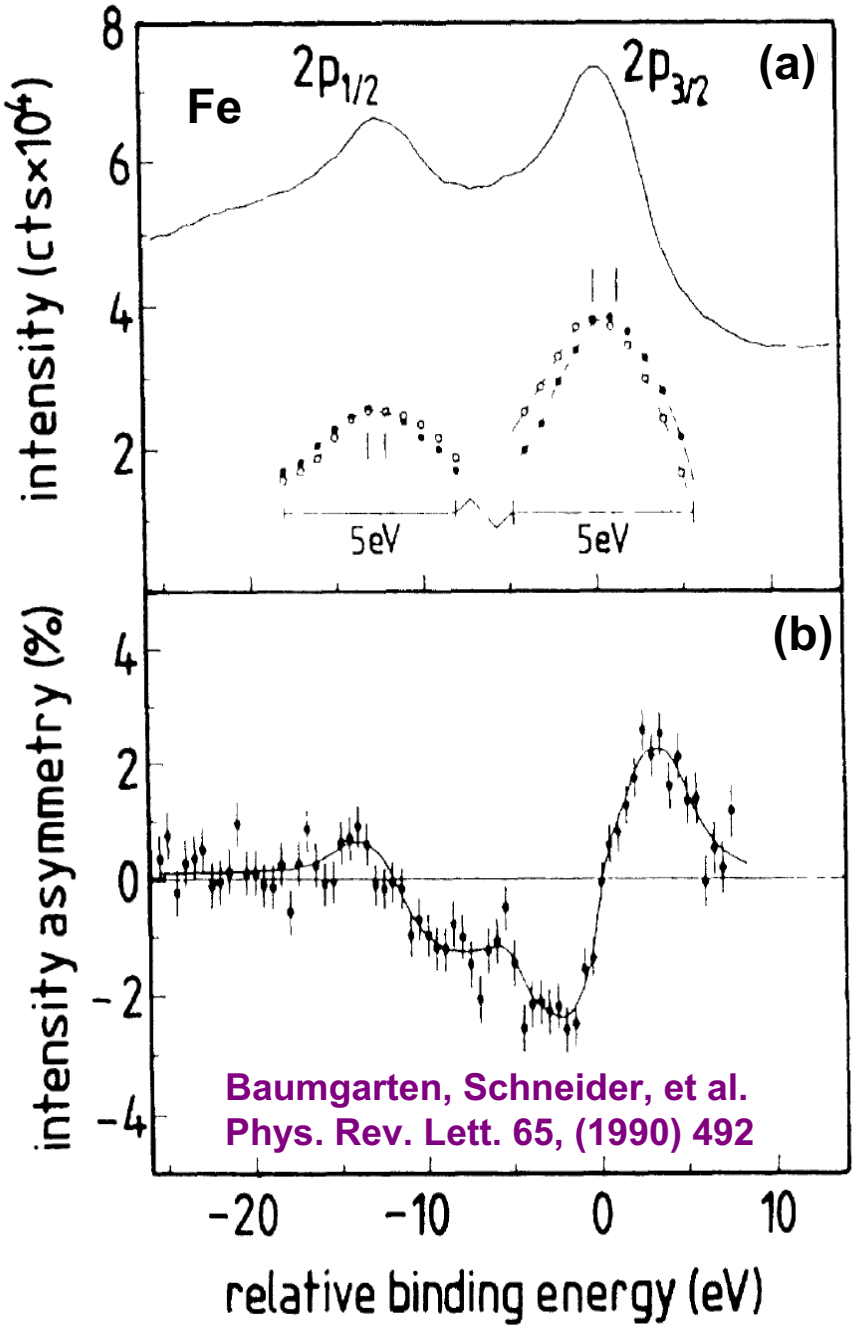

Baumgarten, Schneider, et al.
Phys. Rev. Lett. 65, (1990) 492

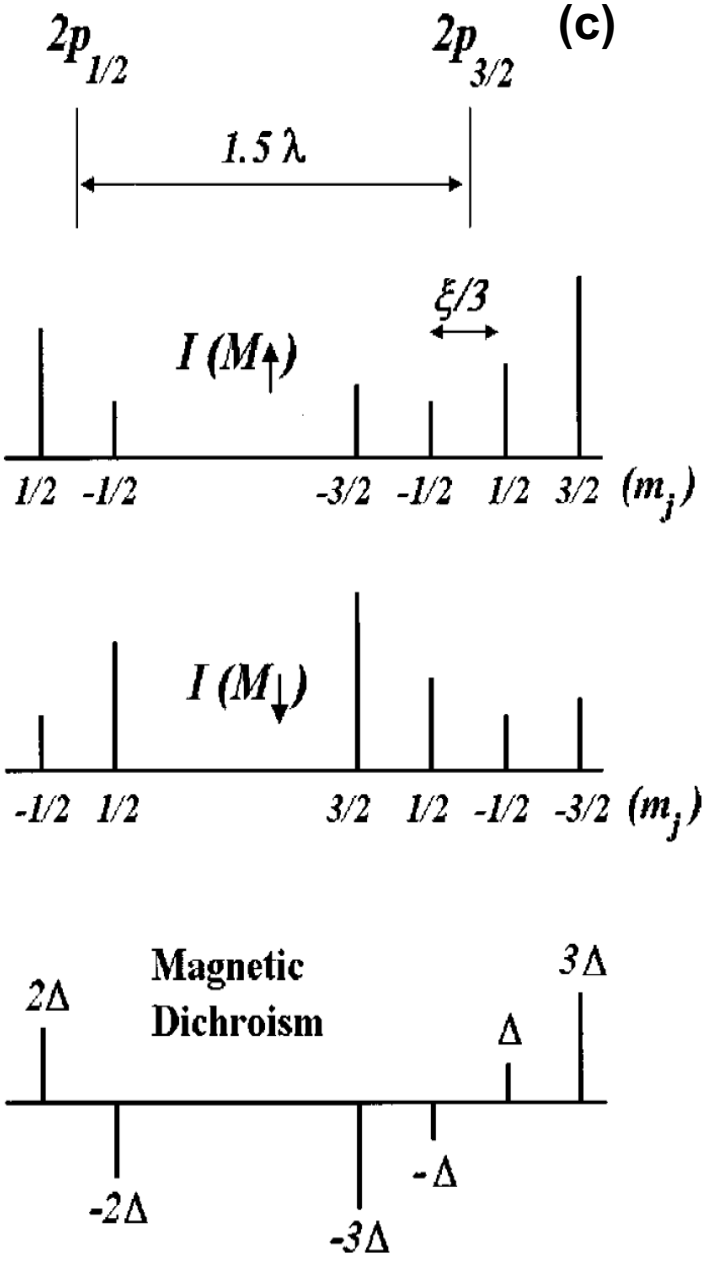

Menchero, Phys. Rev. B 57 (1998)993

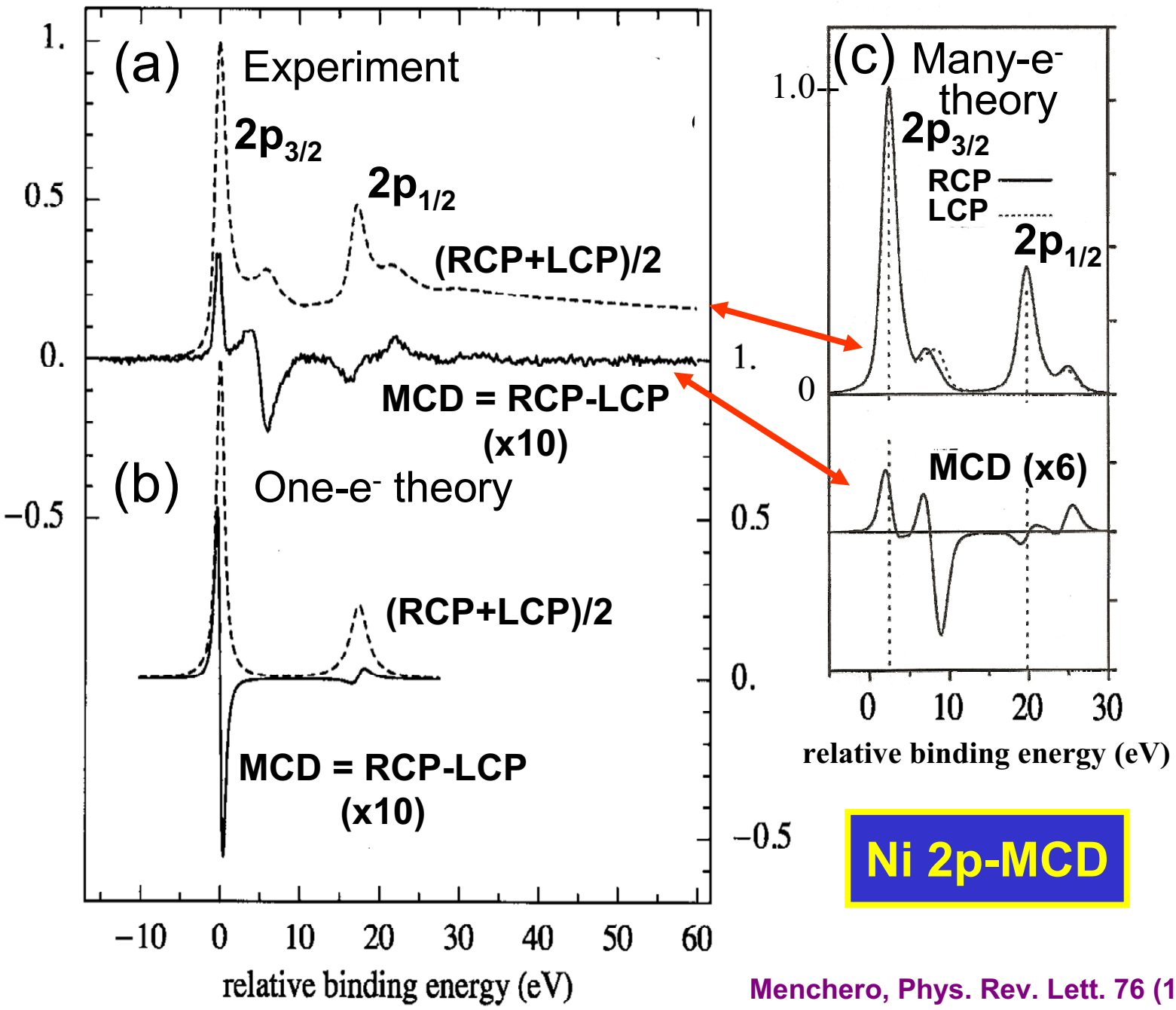

Van der Laan et al., J. Phys. Condens. Matter 12 (2000) L275

Menchero, Phys. Rev. Lett. 76 (1996) 3208

Application to a buried interface: with standing wave excitation

Cr magnetization Is antiparallel to Fe; systematic variation of MCD strengths vs d_{cr}

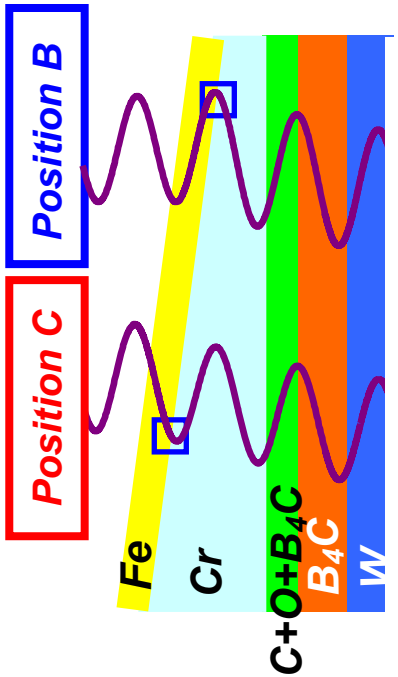

Fe & Cr 2p MCD Data from wedge (Fe/Cr)+SWG

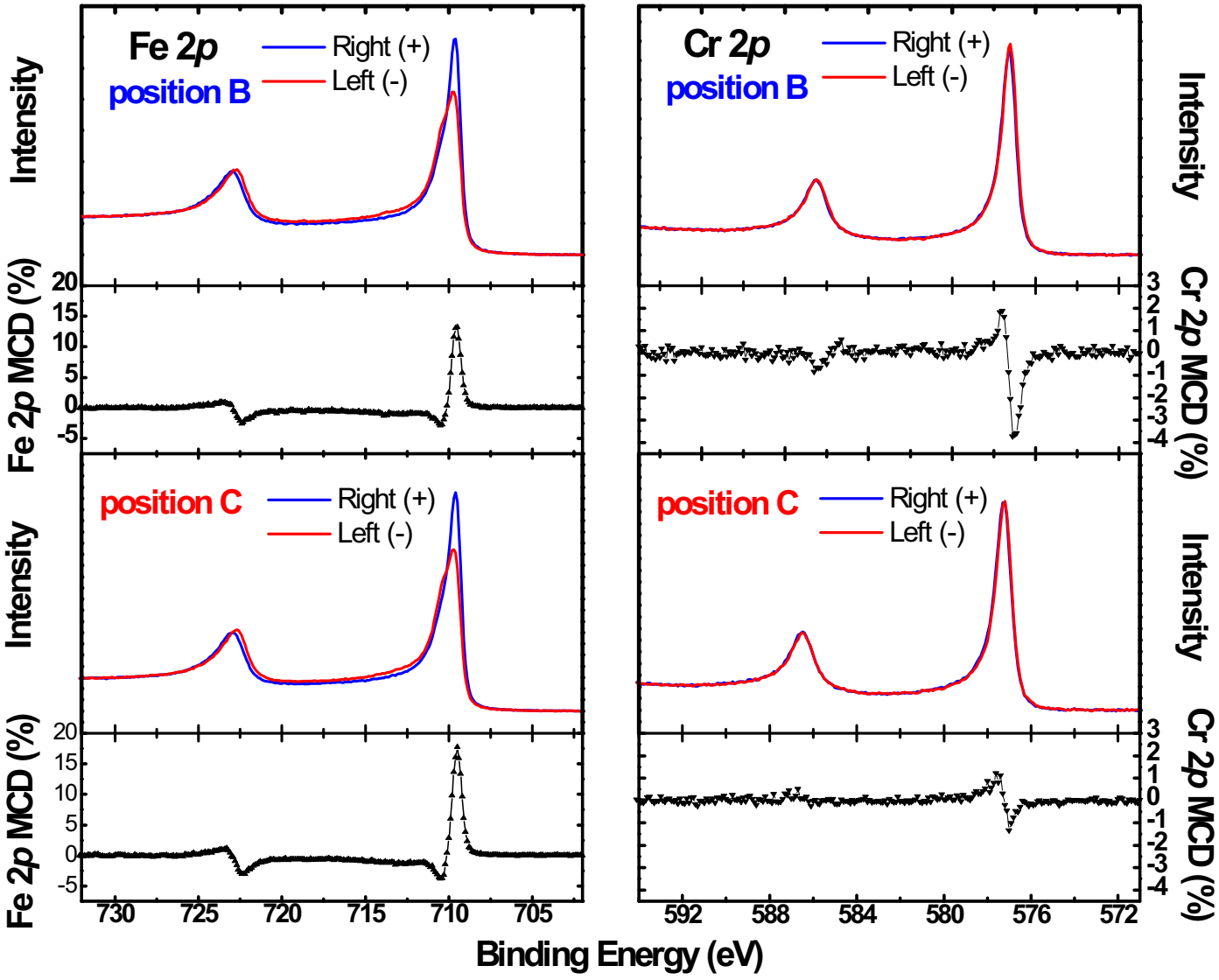

S.H. Yang , B.S. Mun et al., J. Phys. Cond. Matt. 14, L406 (2002)

Some first MCD data with hard x-ray excitation

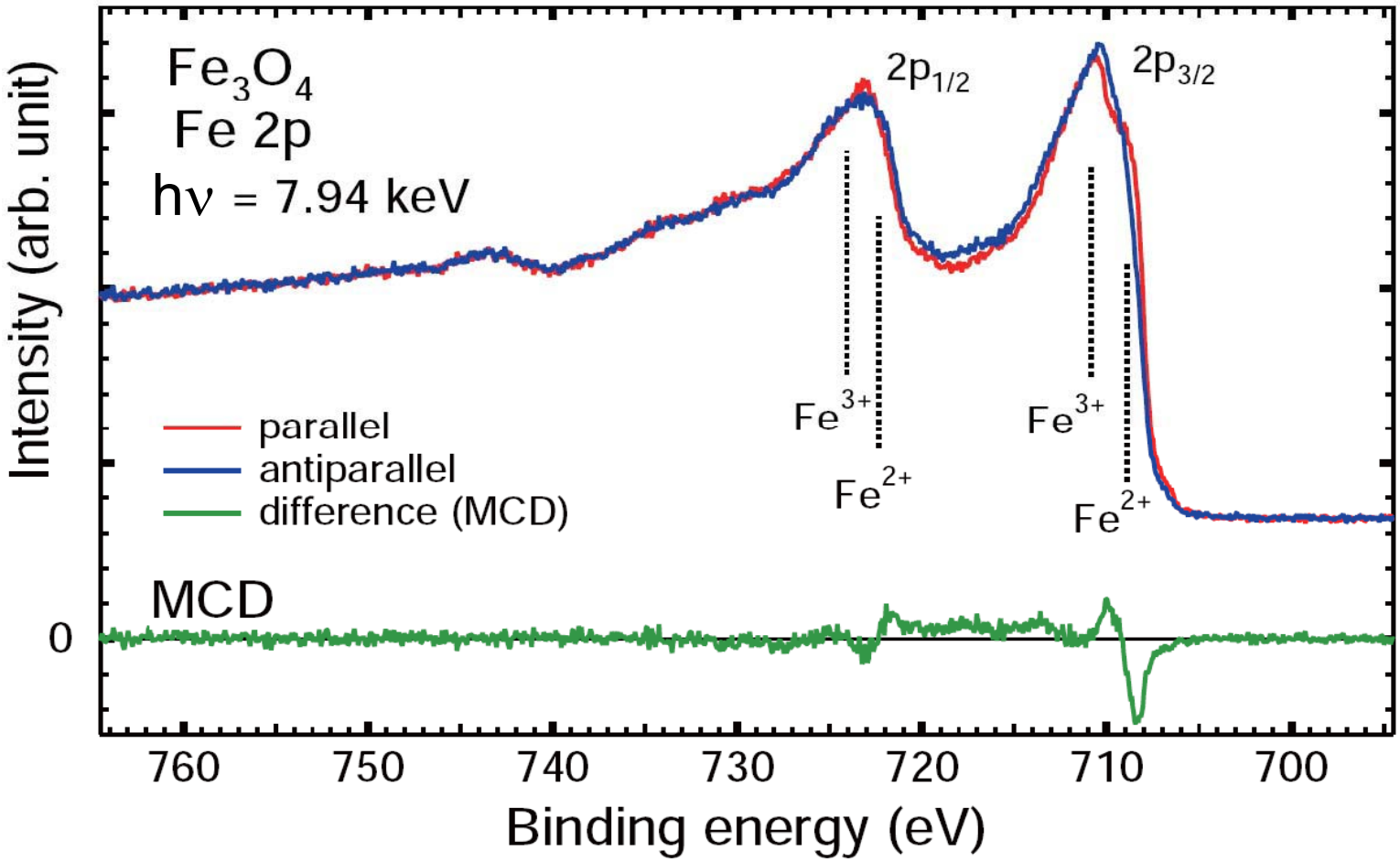

S. Ueda et al., Appl. Phys. Exp., in press
SPring8-BL15XU

Outline

- Valence-band spectra: low-energy UPS limit and high-energy XPS limit
- Core-level chemical shifts: the potential model
- Core-level chemical shifts: equivalent-core (Z+1) and thermochemical energies
- Multiplet splittings
- Spin-orbit splitting, the Fano effect, and spin-polarized outgoing electrons
- Magnetic circular dichroism (MCD) in core-level emission
- Non-magnetic circular dichroism in core-level emission: a.k.a. circular dichroism in angular distributions (CDAD)
- Various other final state effects providing information in core-level spectra

Circular dichroism in angular distributions:
C 1s emission from CO, E_{kin} = 200 eV

Linear p polarization:

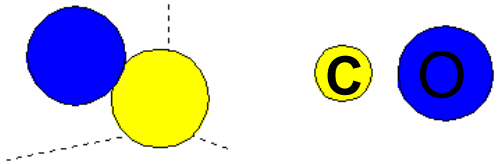

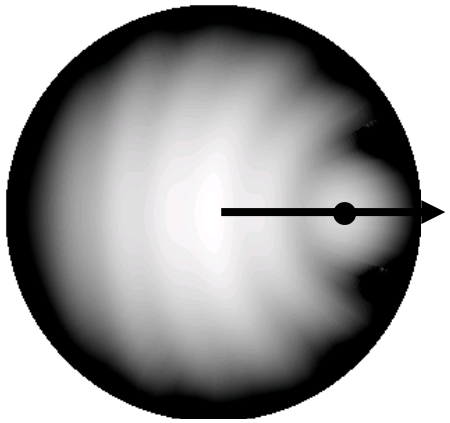

Oxygen forward scattering peak

Right circular polarization:

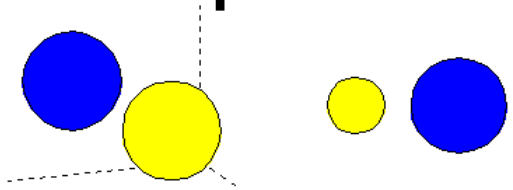

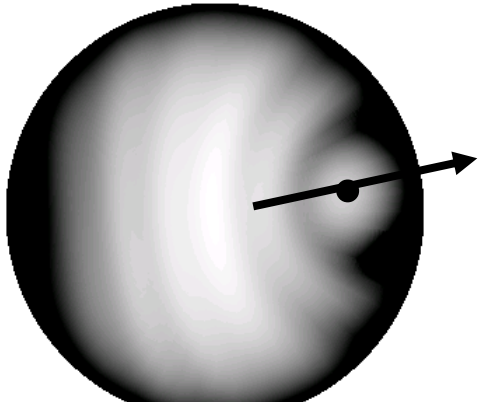

Circular dichroism! Why?

Left circular polarization:

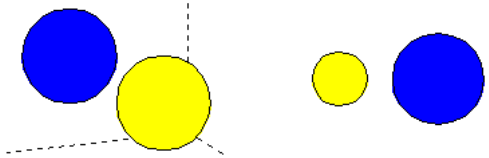

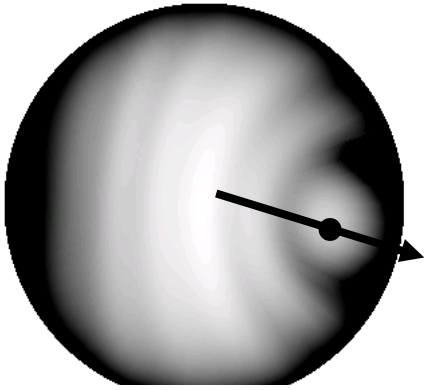

CIRCULAR DICHROISM IN PHOTOELECTRON ANGULAR DISTRIBUTIONS (CDAD)

Non-magnetic dichroism effects due to photoelectron diffraction

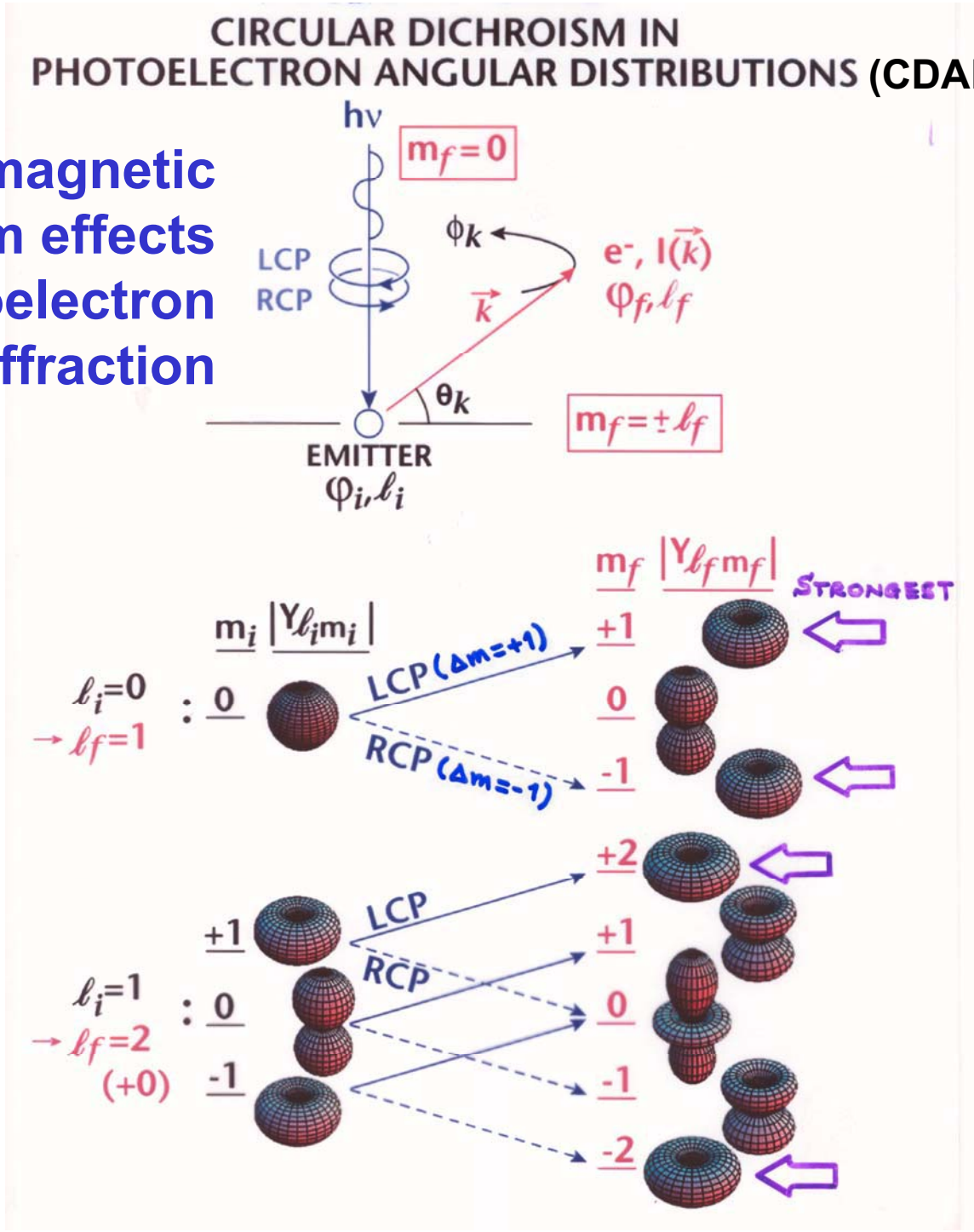

CIRCULAR DICHROISM IN PHOTOELECTRON DIFFRACTION

CONSTANT-PHASE SURFACE OF:

$$\psi_{\text{PHOTOE}^-}(r,\theta,\phi) \propto \frac{e^{ikr}}{r} \Theta_{lm} e^{i m_f \phi}$$

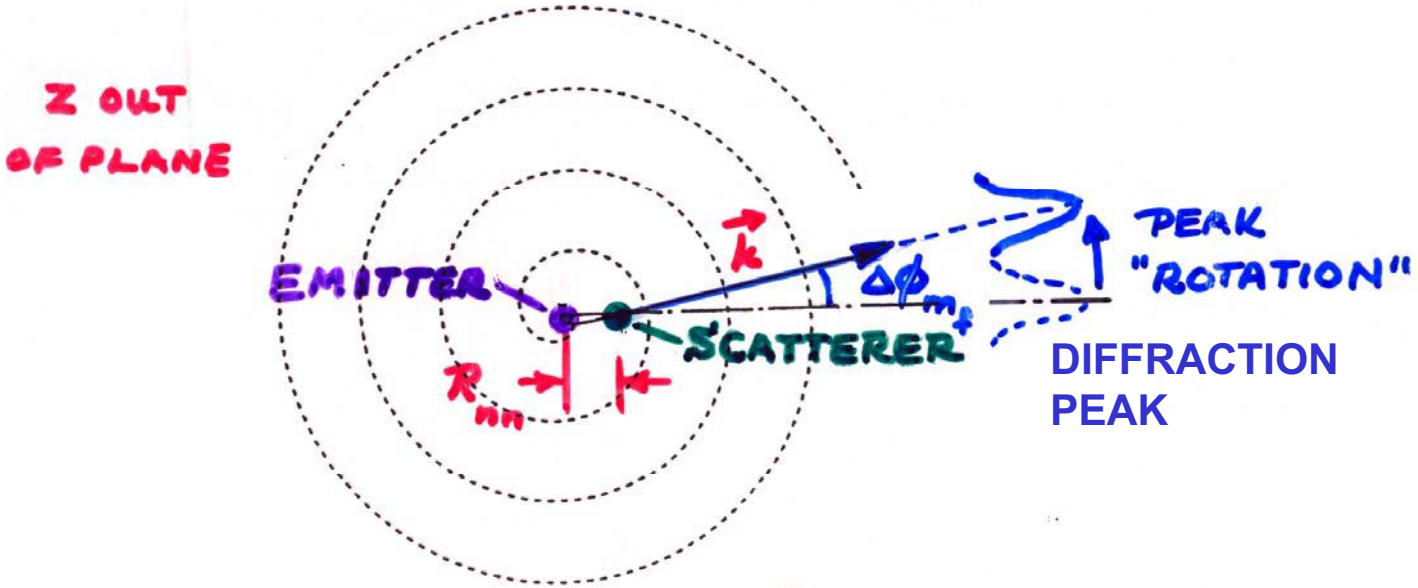

$$\left\| \Delta\phi_{m_f} = \frac{m_f}{R_{nn,\parallel} k_\parallel} \right\|$$

$$\overline{m_f} \approx m_{f,\max}$$

DAIMON ET AL.
JPN. J. APPL. PHYS.
32, L1480 ('93)

CIRCULAR DICHROISM - NON-MAGNETIC SYSTEMS

Si2p -- 250eV = E_{kin}

EXPERIMENT

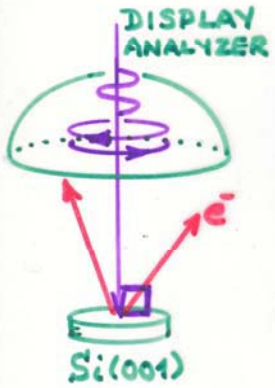

(a) LCP (b) RCP

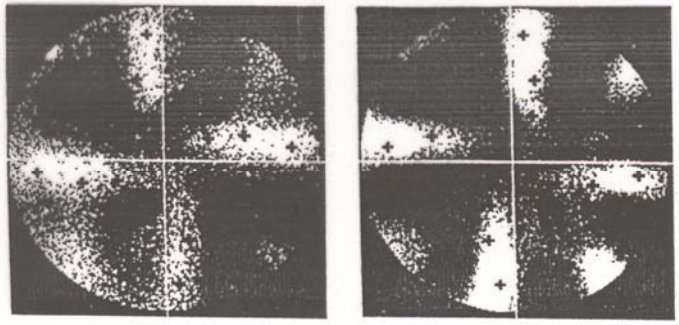

DAIMON ET AL.
JPN. J. APPL. PHYS.
32, L1480 ('93)

THEORY

(c) LCP (d) RCP

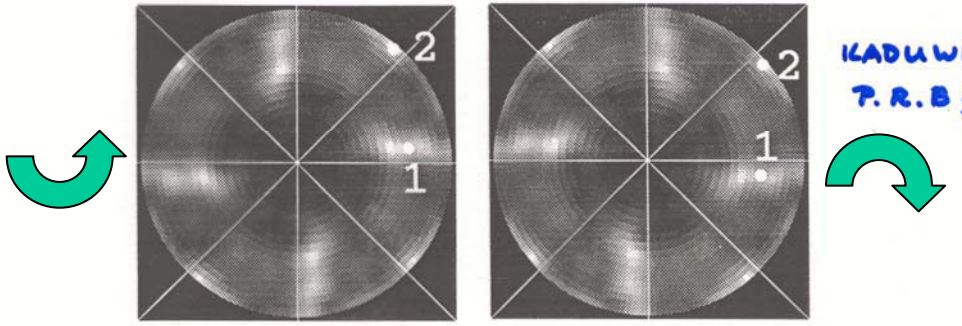

KADUWELA ET AL.
P. R. B 50, 6203 ('94)

(e) UNPOLARIZED

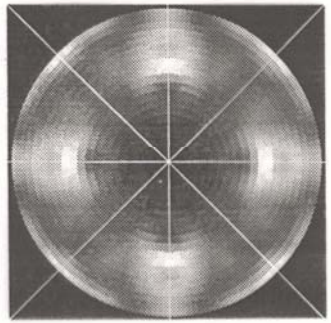

Outline

- Valence-band spectra: low-energy UPS limit and high-energy XPS limit
- Core-level chemical shifts: the potential model
- Core-level chemical shifts: equivalent-core (Z+1) and thermochemical energies
- Multiplet splittings
- Spin-orbit splitting, the Fano effect, and spin-polarized outgoing electrons
- Magnetic circular dichroism (MCD) in core-level emission
- Non-magnetic circular dichroism in core-level emission: a.k.a. circular dichroism in angular distributions (CDAD)
- Various other final state effects providing information in core-level spectra

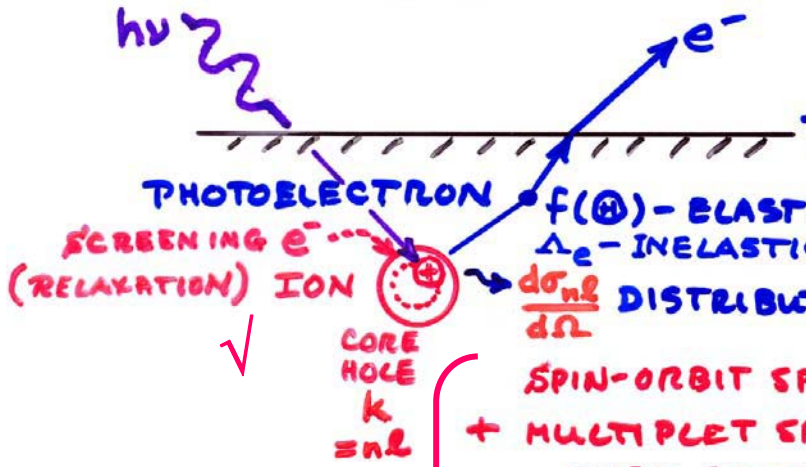

√ = covered so far

ADDITIONAL SOURCES OF STRUCTURE (AND INFORMATION!) IN SPECTRA BEYOND CHEMICAL SHIFTS

- SPIN-ORBIT SPLITTING (EASY) √
- \+ MULTIPLET SPLITTING (OPEN-SHELL SYSTEMS), XSTAL FIELD √
- \+ CORRELATION / CONFIGURATION INTERACTION √
- \+ SHAKE-UP / SHAKE-OFF / e⁻-HOLE
- \+ SCREENING / NON-SCREENING: CONFIGURATION INTERACTION
- \+ VIBRATIONAL EXCITATIONS √
- \+ RESONANT PHOTOEMISSION ($h\nu \approx E_{b,nl'}$) √

REALLY ALL AT ONCE, BUT SUM RULES + THEORY HELP

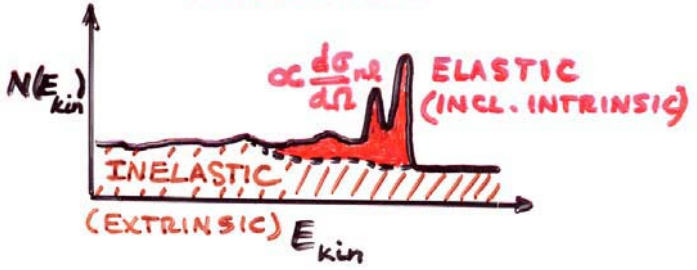

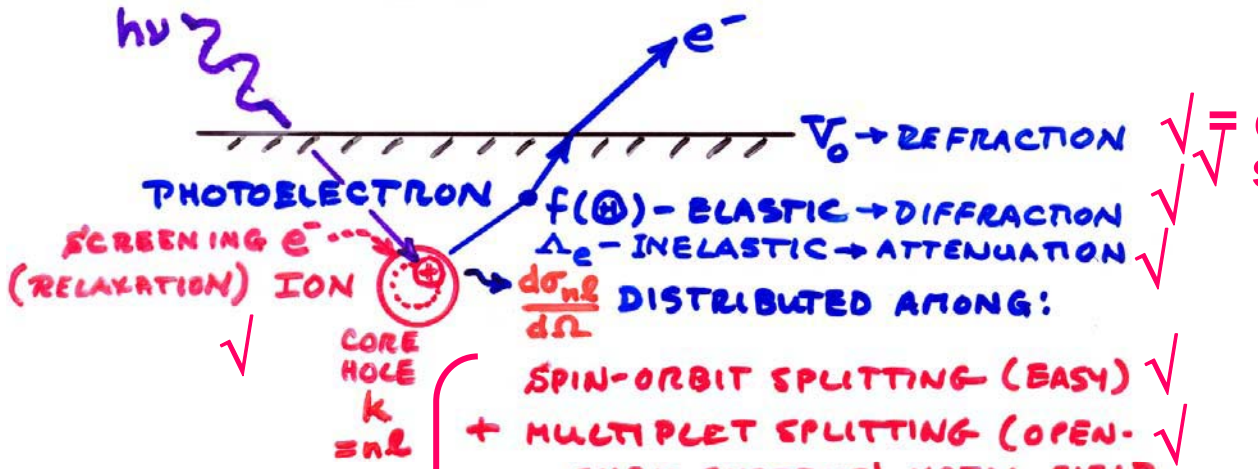

√ = covered so far

ADDITIONAL SOURCES OF STRUCTURE (AND INFORMATION!) IN SPECTRA BEYOND CHEMICAL SHIFTS

- SPIN-ORBIT SPLITTING (EASY) √
- \+ MULTIPLET SPLITTING (OPEN-SHELL SYSTEMS), XSTAL FIELD √
- \+ CORRELATION / CONFIGURATION INTERACTION √
- \+ SHAKE-UP / SHAKE-OFF / e⁻-HOLE
- \+ SCREENING / NON-SCREENING: CONFIGURATION INTERACTION
- \+ VIBRATIONAL EXCITATIONS
- \+ RESONANT PHOTOEMISSION ($h\nu \approx E_{b,nl'}$) √

REALLY ALL AT ONCE, BUT SUM RULES + THEORY HELP

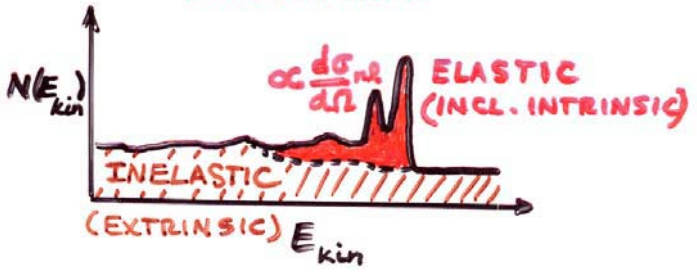

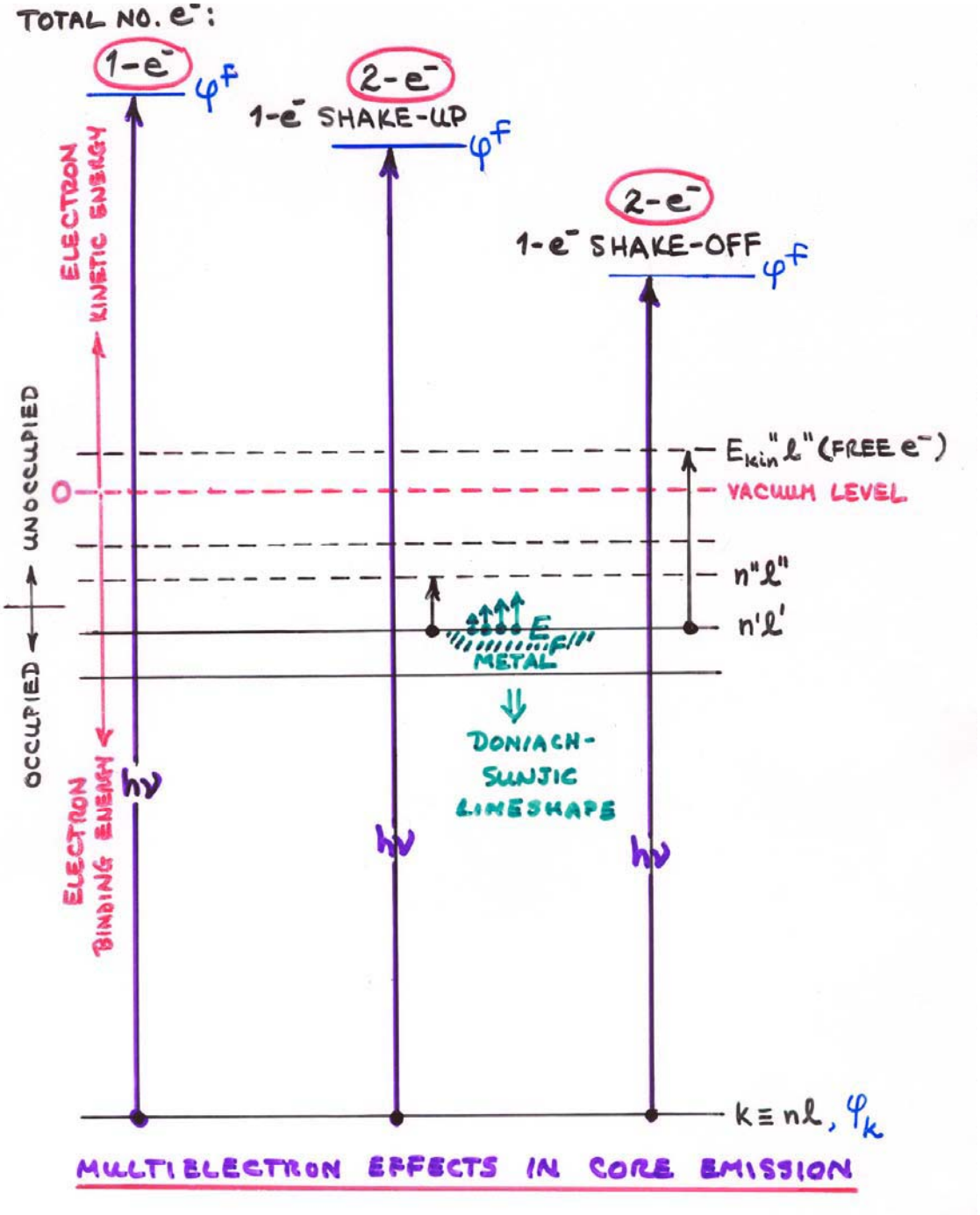

MULTIELECTRON EFFECTS IN CORE EMISSION

INTENSITIES IN PHOTOELECTRON SPECTRA:

- GENERAL: FINAL STATE K (k-SUBSHELL + ALL OTHER DESIG.)

$$\text{INT.}_K \propto \left| \hat{e} \cdot \langle \Psi^f_{tot}(N,K) | \sum_{i=1}^{N} \vec{r}_i | \Psi^i(N) \rangle \right|^2 \quad \text{(DIPOLE APPROX.)}$$

- BORN-OPPENHEIMER: e^-'s FAST, VIBRATIONS SLOW

$$\text{INT.}_K \propto \underbrace{|\langle \psi^f_{VIB,v'} | \psi^i_{VIB,v} \rangle|^2}_{\text{FRANCK-CONDON FACTOR}} \left| \hat{e} \cdot \langle \Psi^f_{e^-}(N,K) | \sum_{i=1}^{N} \vec{r}_i | \psi^i_{e^-}(N) \rangle \right|^2$$

- SUDDEN APPROXIMATION: $\varphi_k \rightarrow \varphi_f$ = PHOTOe^- (FAST)

$$\left.\begin{array}{l} \varphi_1 \rightarrow \varphi_1' \\ \vdots \\ \varphi_{k-1} \rightarrow \varphi_{k-1}' \\ \varphi_{k+1} \rightarrow \varphi_{k+1}' \\ \vdots \\ \varphi_N \rightarrow \varphi_N' \end{array}\right\} \text{(SLOW)}$$

k HOLE →

$$\text{INT.}_K \propto |\langle \psi^f_{VIB,v'} | \psi^i_{VIB,v} \rangle|^2 \left| \langle \underbrace{\Psi^f_{e^-}(N-1,K) | \Psi_K(N-1,K)}_{\text{k MISSING}} \rangle \right|^2$$

$$\left| \hat{e} \cdot \langle \varphi_f | \vec{r} | \varphi_k \rangle \right|^2$$

↳ NORMAL $\frac{d\sigma_K}{d\Omega}$

SAME SUBSHELL COUPLING + TOTAL L,S → "MONOPOLE"

- SLATER DETS. FOR $\Psi^f_{e^-} = \det(\varphi_1' \varphi_2' \cdots \varphi_{k-1}' \varphi_{k+1}' \cdots \varphi_N')$

$$\Psi_K = \det(\varphi_1 \varphi_2 \cdots \varphi_{k-1} \varphi_{k+1} \cdots \varphi_N)$$

$$\text{INT.}_K \propto |\langle \psi^f_{VIB,v'} | \psi^i_{VIB,v} \rangle|^2 |\langle \varphi_1' | \varphi_1 \rangle|^2 |\langle \varphi_2' | \varphi_2 \rangle|^2 \cdots$$

$$|\langle \varphi_{k-1}' | \varphi_{k-1} \rangle|^2 |\langle \varphi_{k+1}' | \varphi_{k+1} \rangle|^2 \cdots |\langle \varphi_N' | \varphi_N \rangle|^2 \cdot$$

$$\left| \hat{e} \cdot \langle \varphi_f | \vec{r} | \varphi_k \rangle \right|^2$$

1e- DIPOLE → $d\sigma/d\Omega$

(N-1)e^- SHAKE-UP/ SHAKE-OFF → "MONOPOLE"

- PLUS DIFFRACTION EFFECTS IN φ_f ESCAPE

NEON 1S SHAKE-UP / SHAKE-OFF:

$Ne\ 1s^2 2s^2 2p^6\ {}^1S \xrightarrow{-e^-} Ne^+\ 1s^1 2s^2 2p^6\ {}^2S$

1-e^- SHAKE-UP: ($Ne^+\ 1s^1 2s^2 2p^5 np^1\ (n=3,4,5,\cdots)\ {}^2S$
$Ne^+\ 1s^1 2s^1 2p^6 ns^1\ (n=3,\cdots)\ {}^2S$

2-e^- SHAKE-UP: $Ne^+\ 1s^1 2s^2 2p^4 3p^2\ {}^2S$

2p SHAKE-OFF: $Ne^+\ 1s^1 2s^2 2p^5, E_{kin}"p"\ {}^2S$

"Basic Concepts of XPS"
Figure 36

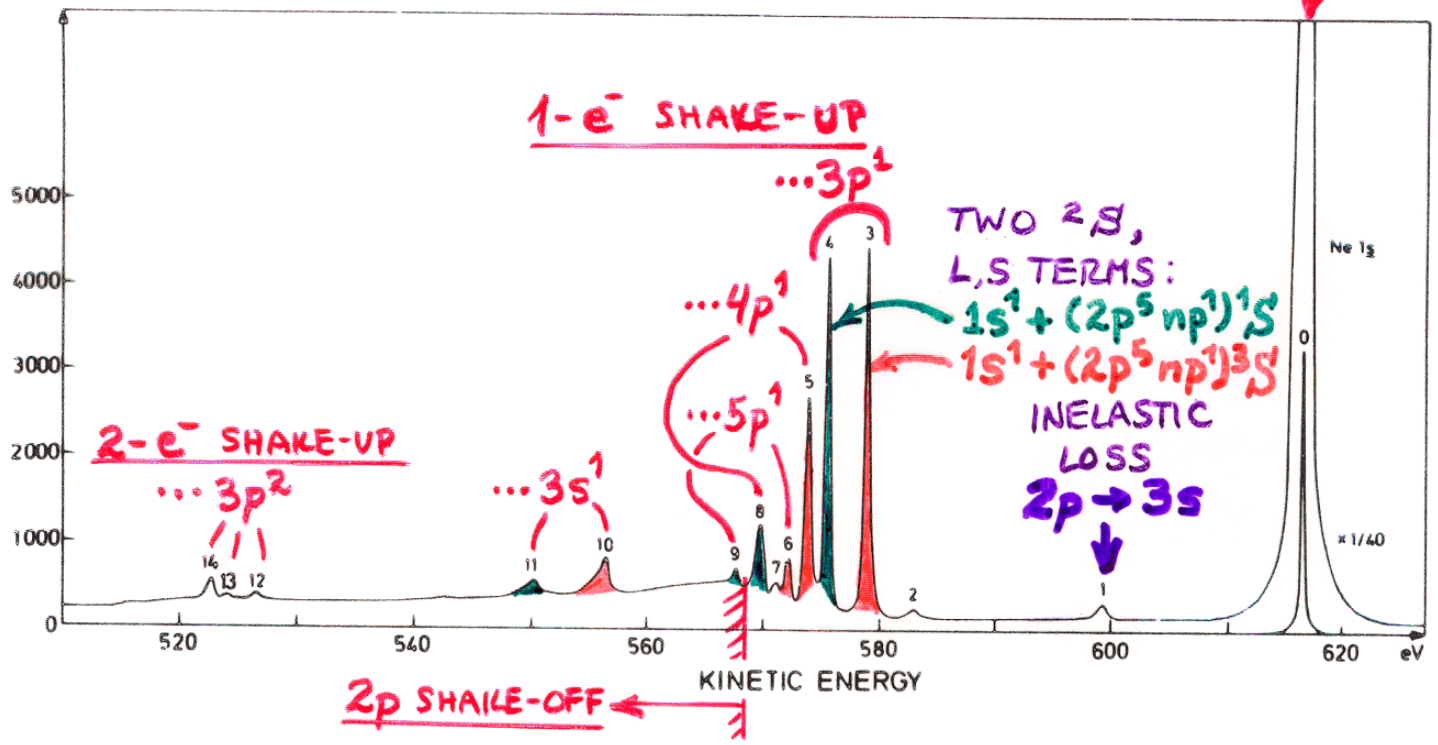

OVERALL: ~12% SHAKE-UP + 16% SHAKE-OFF ≈ 28% OF EVENTS

BAND THEORY—D.O.S:

ELECTRON-HOLE EXCITATIONS IN METALS:

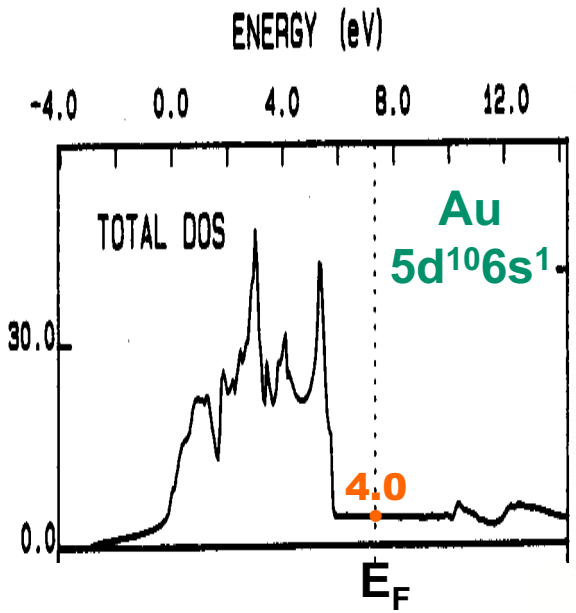

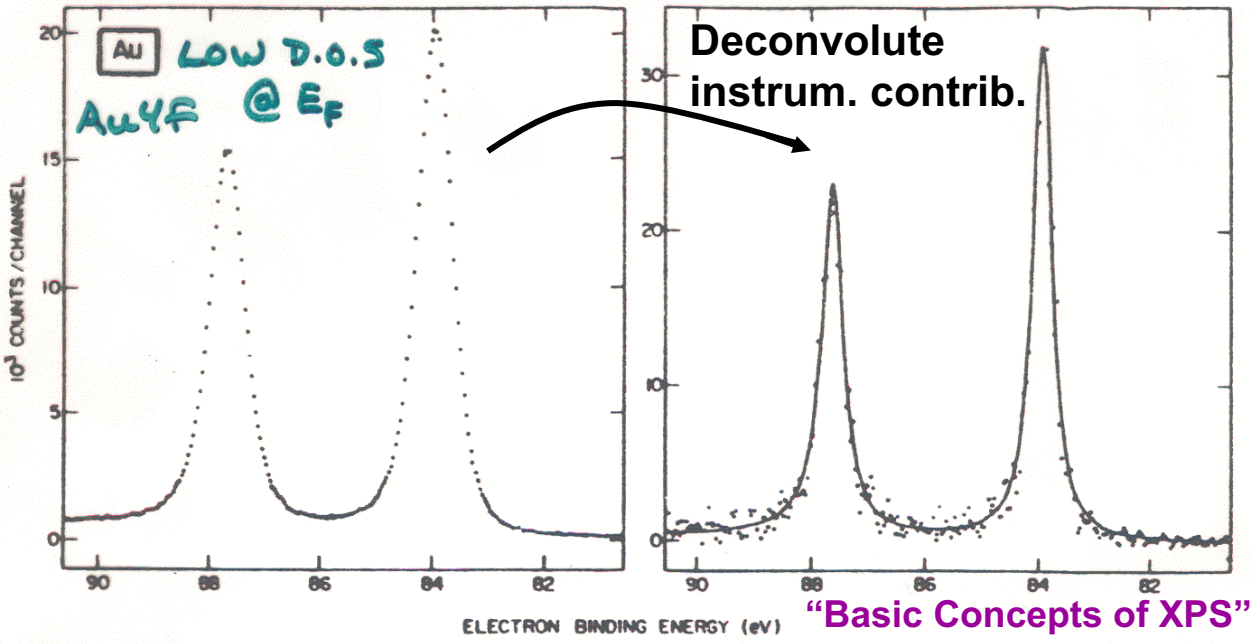

"Basic Concepts of XPS"
Figure 10

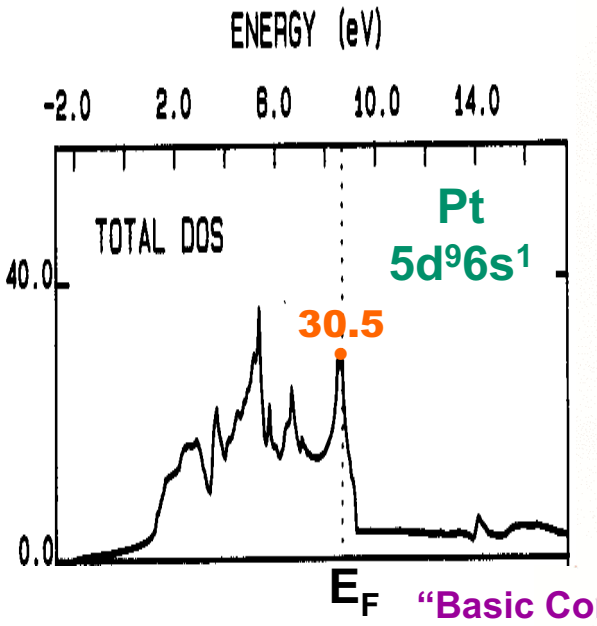

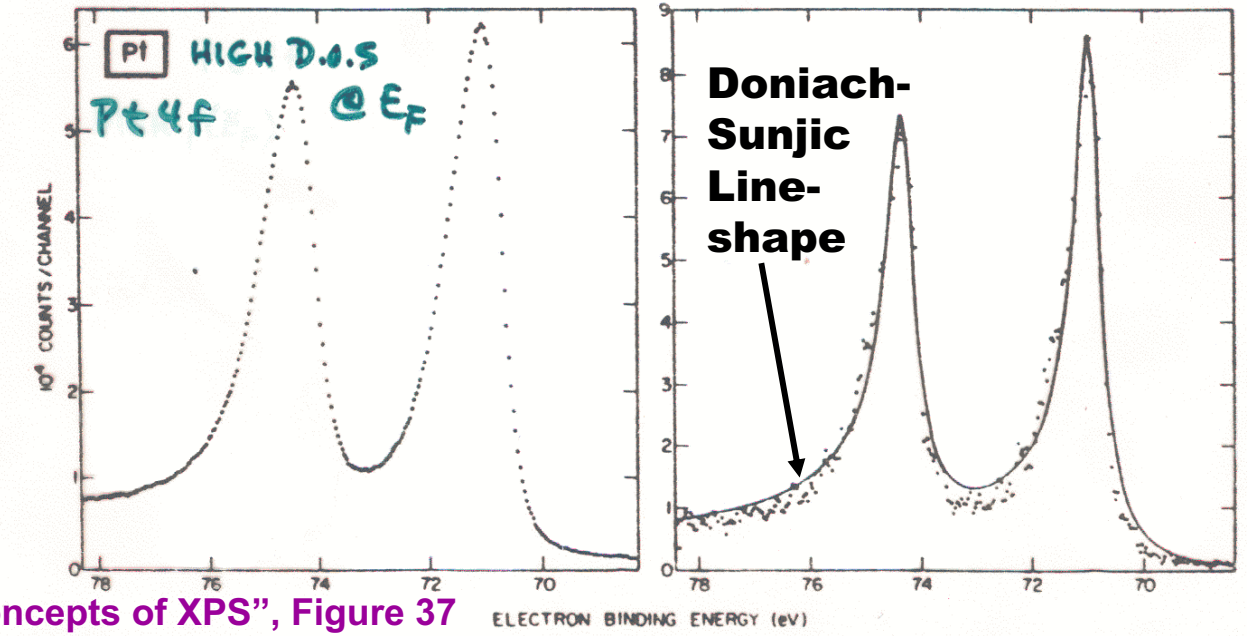

"Basic Concepts of XPS", Figure 37

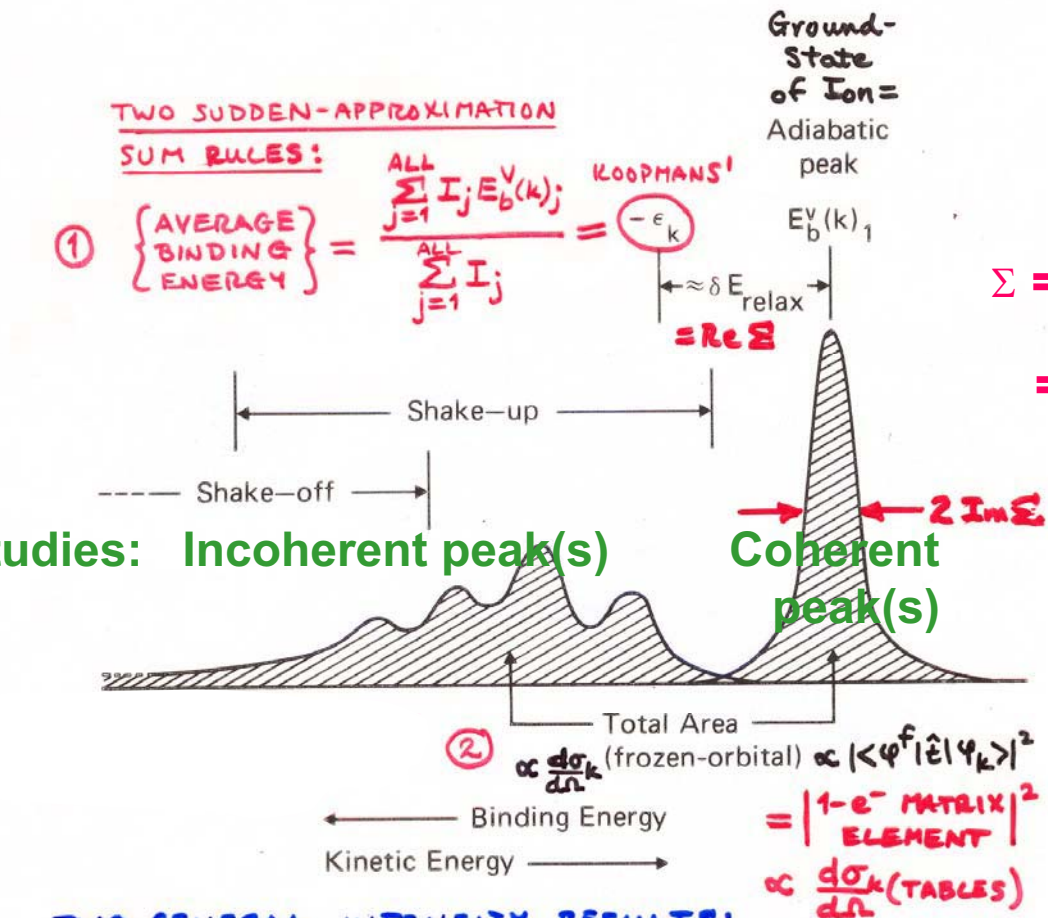

Σ = many-body "self energy"
= ReΣ + iImΣ

In valence-band studies: Incoherent peak(s) Coherent peak(s)

$2\,\mathrm{Im}\Sigma = \Delta E$

$\Delta E \tau_{\text{lifetime}} \approx \hbar/2$

Figure 8 -- Schematic illustration of a photoelectron spectrum involving shake-up and shake-off satellites. The weighted average of all binding energies yields the Koopmans' Theorem binding energy $-\epsilon_k$ (sum rule (77)), and the sum of all intensities is proportional to a frozen-orbital cross section σ_k (sum rule (78)). The adiabatic peak corresponds to formation of the ground-state of the ion $(E_b(k)_1 \equiv E_b(K=1))$.

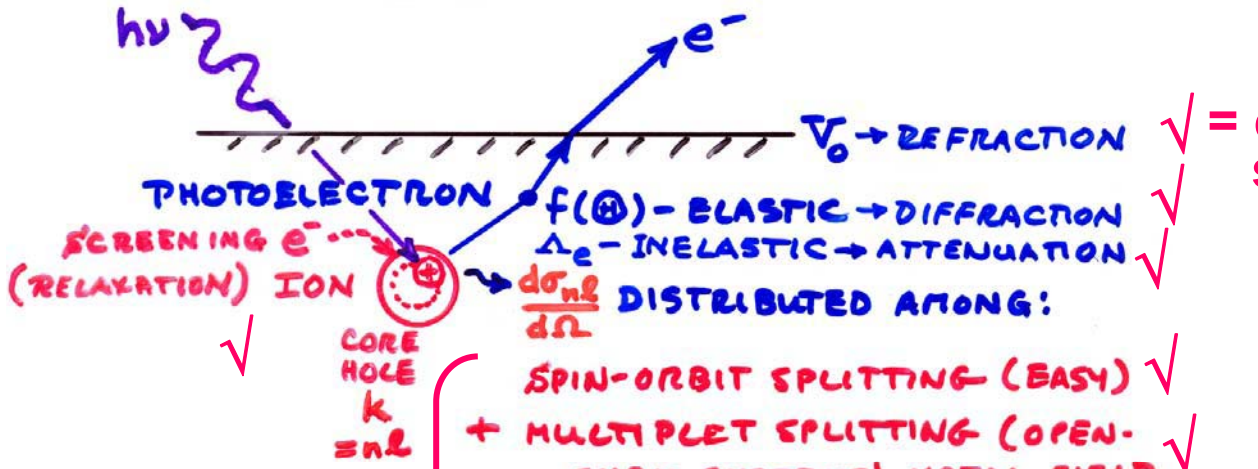

√ = covered so far

ADDITIONAL SOURCES OF STRUCTURE (AND INFORMATION!) IN SPECTRA BEYOND CHEMICAL SHIFTS

REALLY ALL AT ONCE, BUT SUM RULES + THEORY HELP

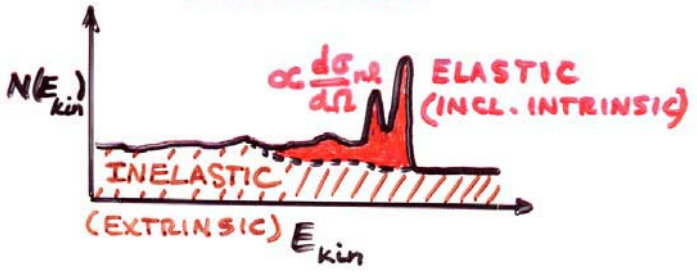

Basic energetics—Many e- & many atom picture

$$h\nu = E_{binding}^{Vacuum} + E_{kinetic} = E_{binding}^{Fermi} + \varphi_{spectrometer} + E_{kinetic}$$

$$E_{binding}^{Vacuum}(Qn\ell j, K) = E_{final}(N-1, Qn\ell j\ hole, K) - E_{initial}(N)$$

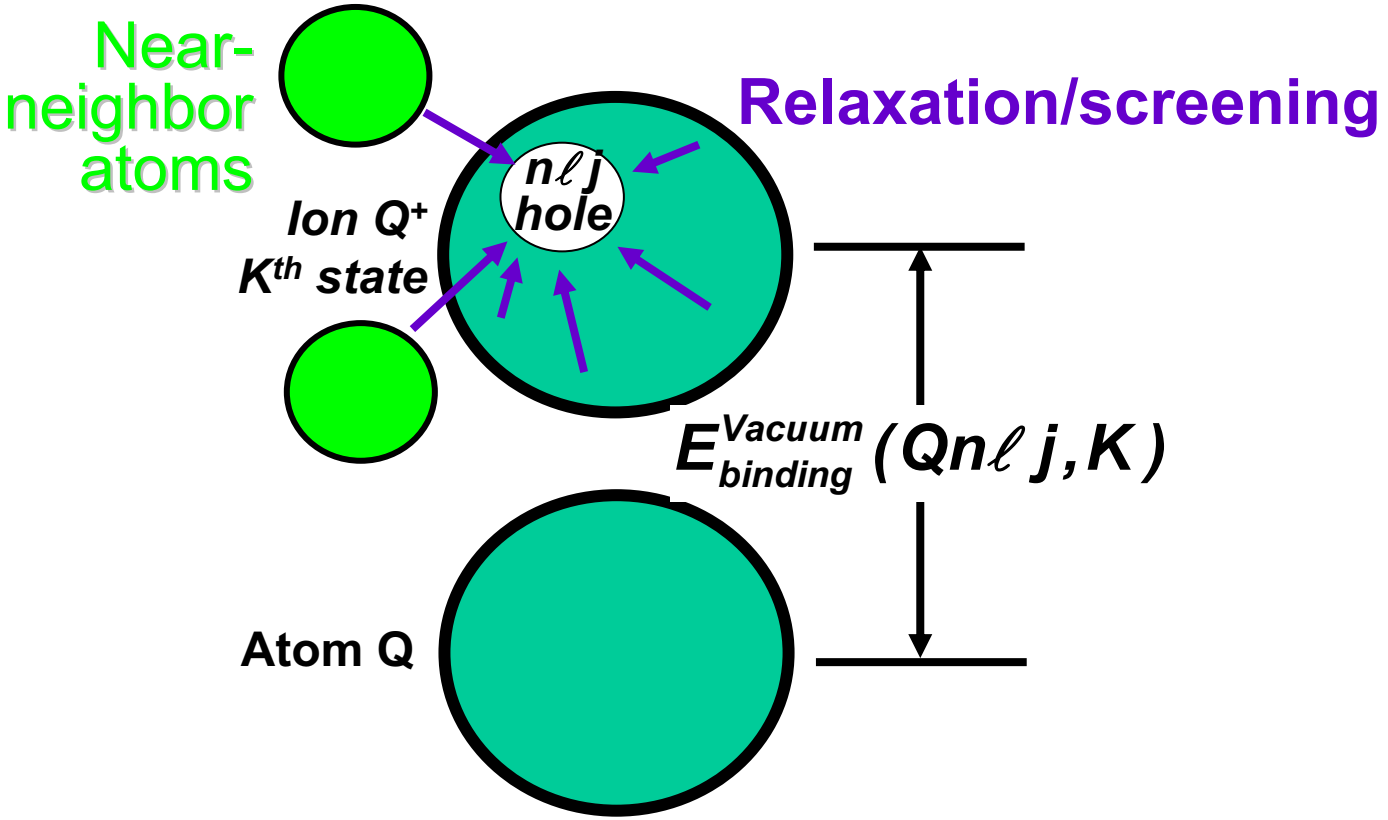

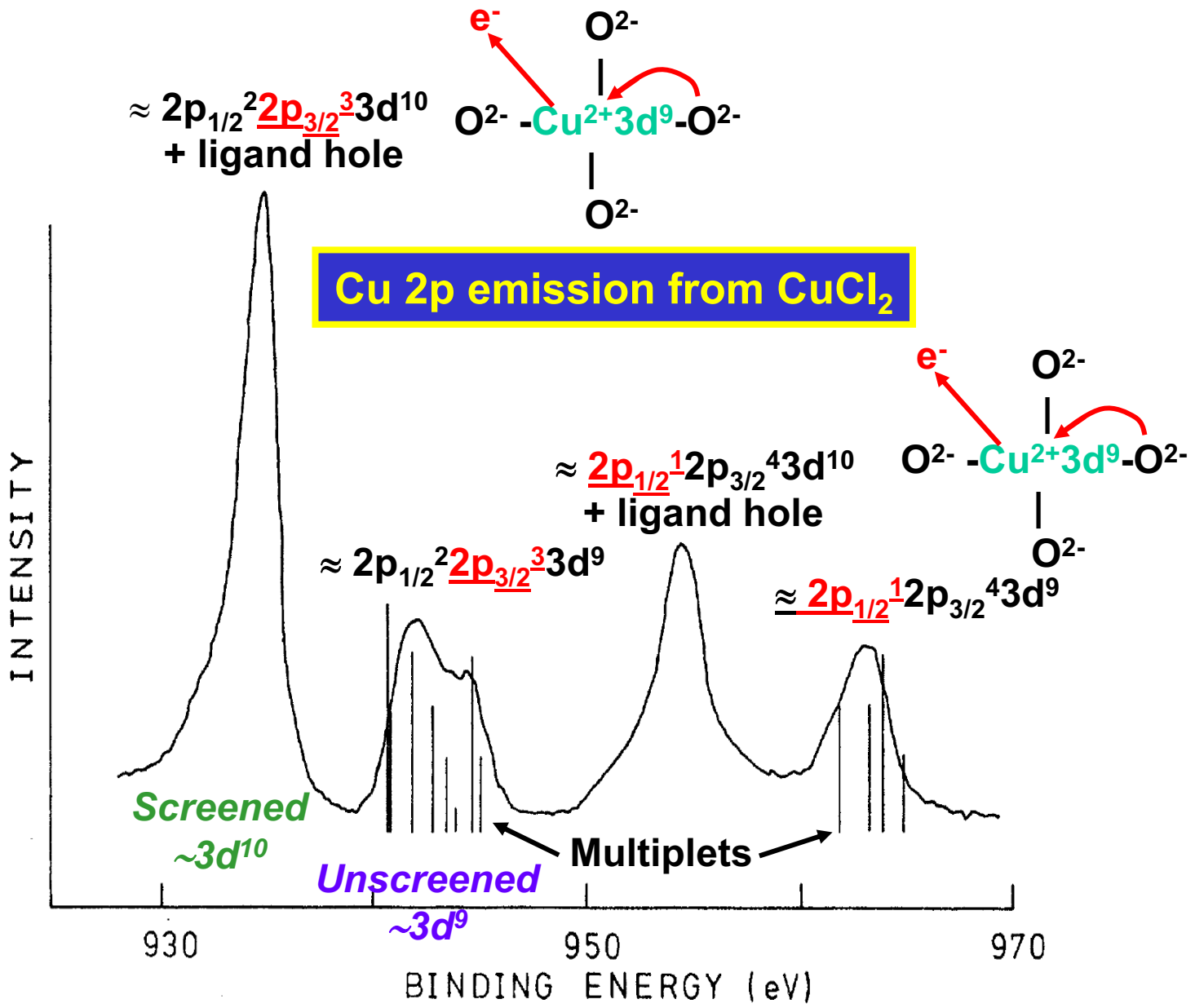

$$\Psi_{final,K}(N-1) = C_{1,K}(2p_{1/2}^2 2p_{3/2}^3 3d^{10} + C\ell\ hole) + C_{2,K}(2p_{1/2}^2 2p_{3/2}^3 3d^9)$$

Van der Laan et al., Phys. Rev. B 23 (1981) 4369

SATELLITES & CHARGE-TRANSFER SCREENING

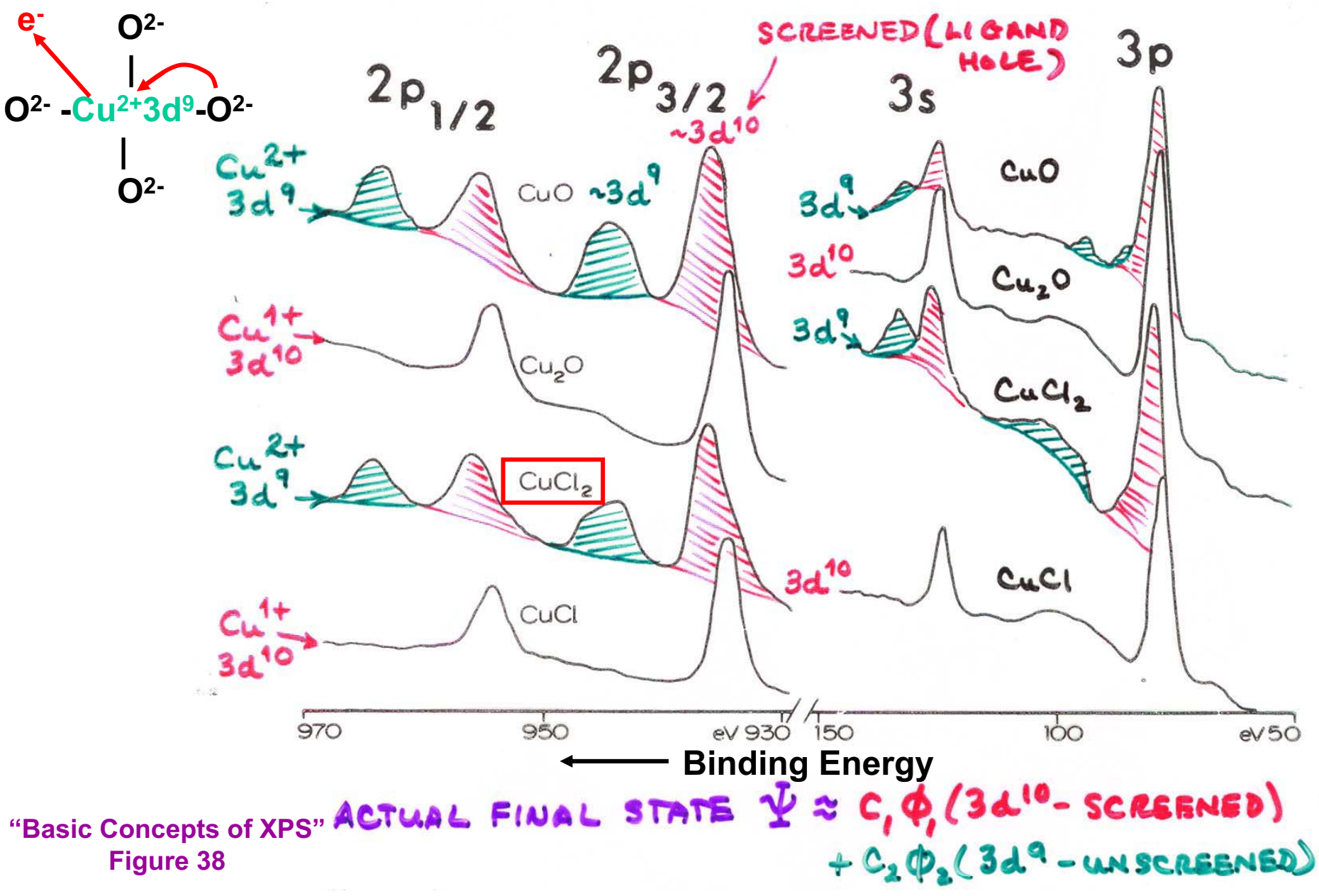

ACTUAL FINAL STATE $\Psi \approx C_1\Phi_1$ (3d10 - SCREENED)
$+ C_2\Phi_2$ (3d9 - UNSCREENED)

"Basic Concepts of XPS"
Figure 38

Screening depends on Ionicity/covalency→ satellite intensities can be used to measure interaction parameters

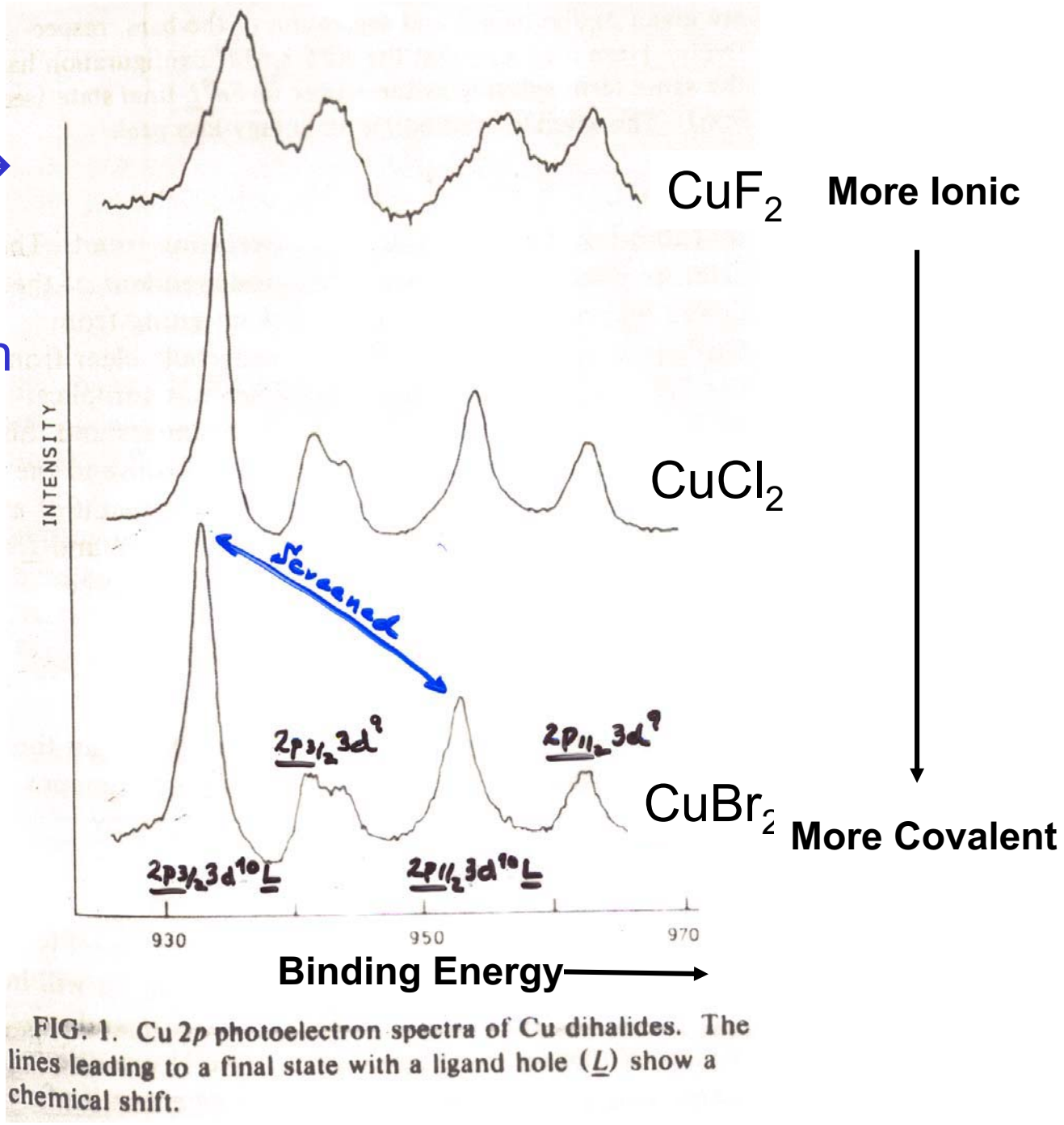

FIG. 1. Cu 2*p* photoelectron spectra of Cu dihalides. The lines leading to a final state with a ligand hole ($\underline{L}$) show a chemical shift.

Screening depends on Ionicity/covalency→ satellite intensities can be used to measure interaction parameters

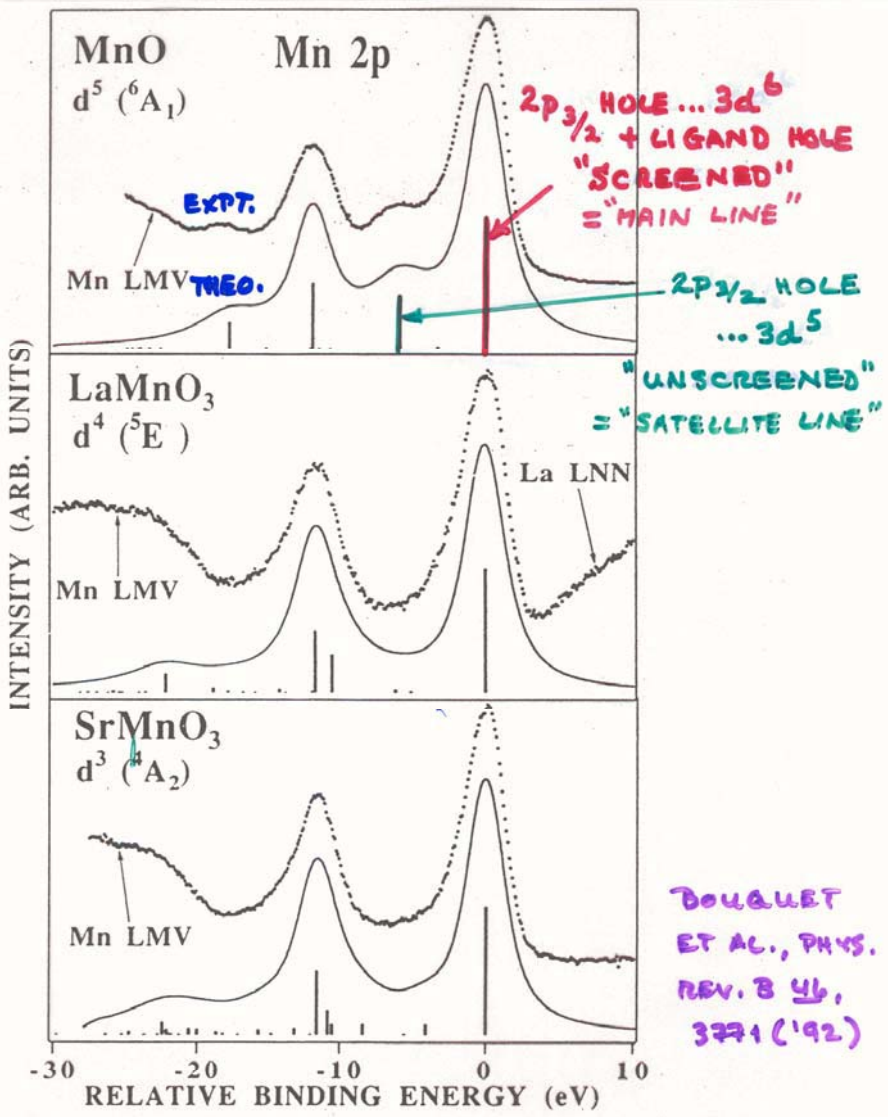

FIG. 1. Theoretical $2p$ core-level XPS spectra (solid line) compared with experimental data (dots) after background subtraction for Mn cations with varying valence. Emission due to the Mn *LMV* Auger peak is observed on the high-binding-energy side of the $2p_{1/2}$ spin-orbit peak, partially obscuring the $2p_{1/2}$ satellite structure.

Anderson Impurity Model Configuration Interaction Approach to Core-Hole Screening in Transition Metals and Rare Earths

(SUGANO, LARSSON ~> SAWATZKY, VAN DER LAAN, FUJIMORI, OH, ET AL.)

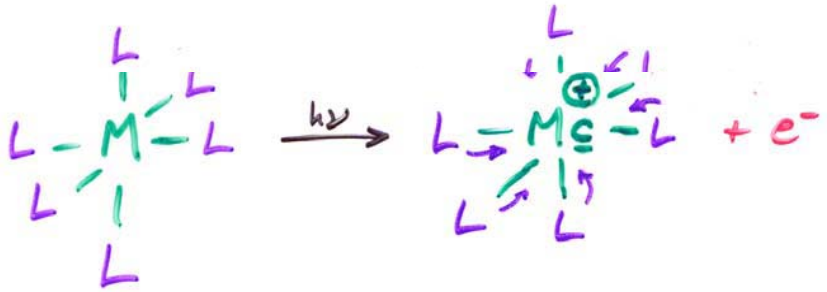

$\underline{c}$ = CORE HOLE ON METAL

$\underline{L}$ = VALENCE (p) HOLE ON LIGAND

de Groot computer program

$$\psi_i = a_0|d^n\rangle + \sum_m a_m|d^{(n+m)}\underline{L}^m\rangle$$

$$\psi_f = b_0|\underline{c}d^n\rangle + \sum_m b_m|\underline{c}d^{(n+m)}\underline{L}^m\rangle$$

WITH INTERACTIONS OF:

$10Dq$ = CRYSTAL FIELD (OFTEN NEGLECTED)

Δ = LIGAND-TO-METAL CHARGE TRANSF. ENERGY
$= E(d^{n+1}\underline{L}) - E(d^n)$

U = d-d COULOMB REPULSION ENERGY
$= E(d^{n-1}) + E(d^{n+1}) - 2E(d^n)$

T = LIGAND p-TO-METAL d HYBRIDIZATION
$= \langle d_\alpha|\hat{H}|p_\alpha\rangle$ (α = SAME SYMMETRY)

Q = CORE-HOLE-TO-d INTERACTION: $\langle \underline{c}|\hat{H}|d\rangle \approx J_{cd}$

WITH INTENSITIES FROM SUDDEN APPROX.

AS:

$$I(E_{kin}) \propto \sum_{f,k} |\langle \psi_f(N-1,k)|\psi_R(N-1,k)\rangle|^2 \cdot \delta(h\nu - E_f - E_{kin})$$

($\underline{c}$ = CORE HOLE)

WHERE: $\psi_R(N-1,k) = \psi_i(N \text{ WITH } k \text{ HOLE} = \underline{c})$

E.g.—Crystal field in Mn^{3+} with negative octahedral ligands

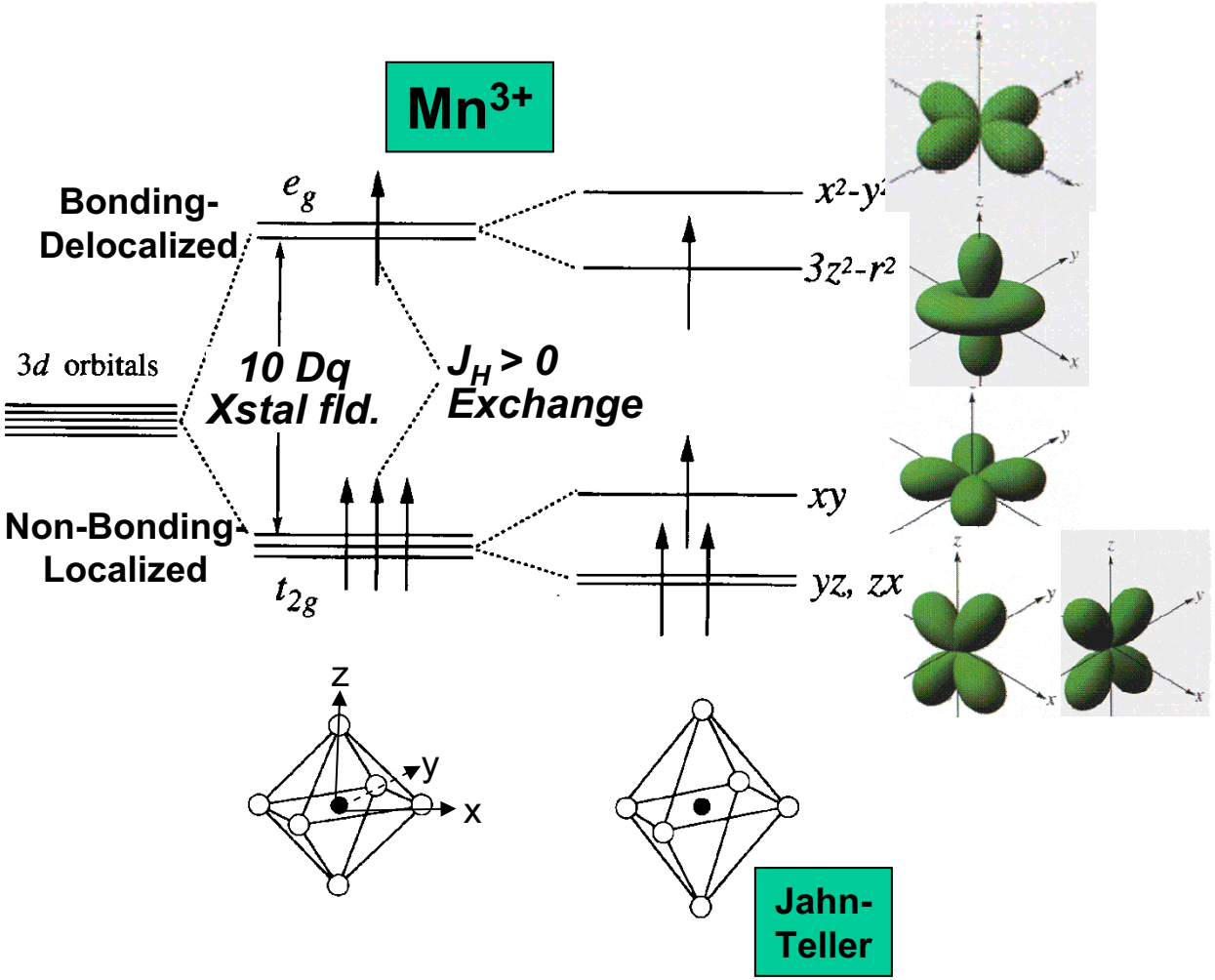

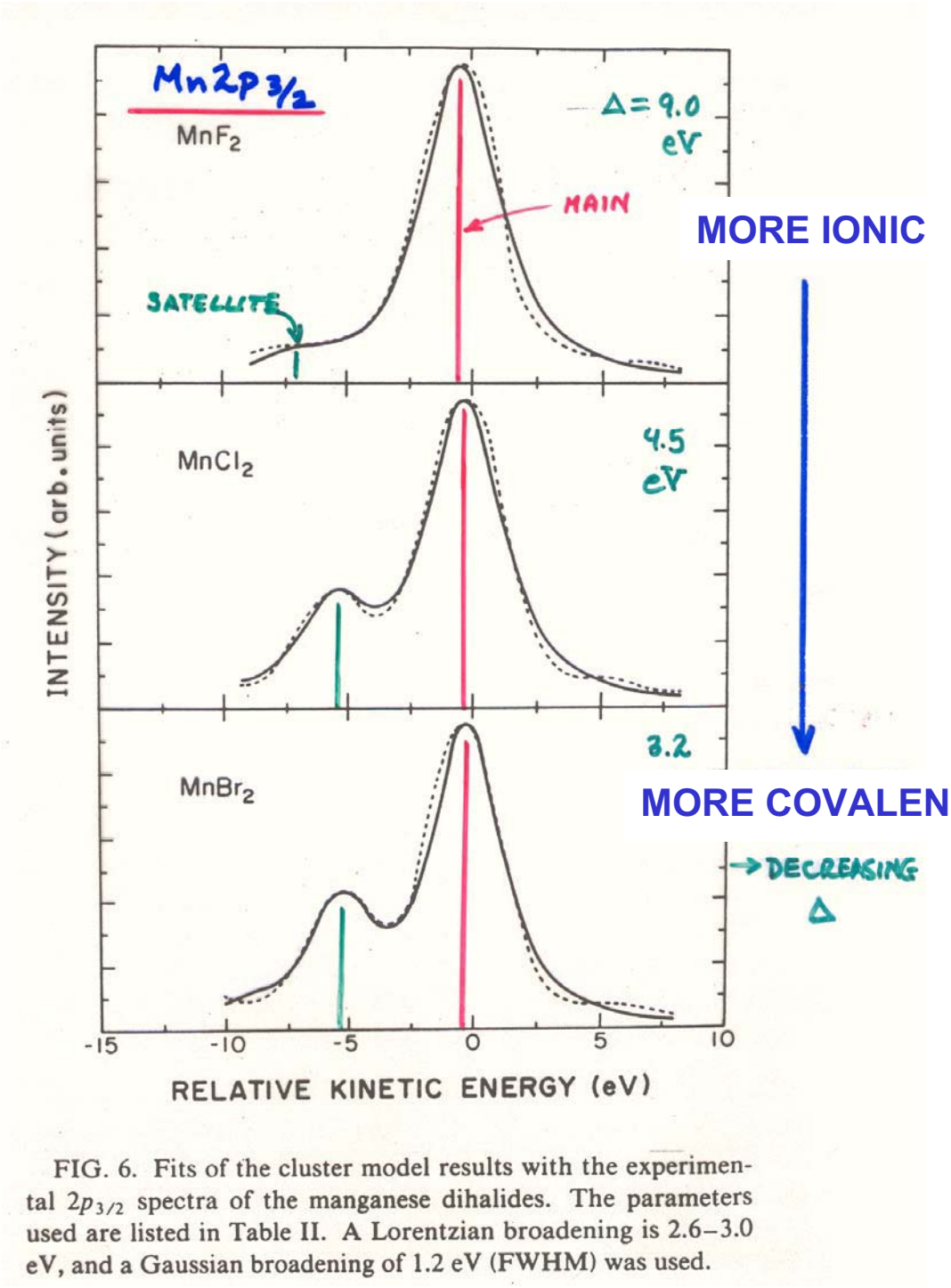

FIG. 6. Fits of the cluster model results with the experimental $2p_{3/2}$ spectra of the manganese dihalides. The parameters used are listed in Table II. A Lorentzian broadening is 2.6–3.0 eV, and a Gaussian broadening of 1.2 eV (FWHM) was used.

ANALYSIS VIA ANDERSON IMPURITY MODEL

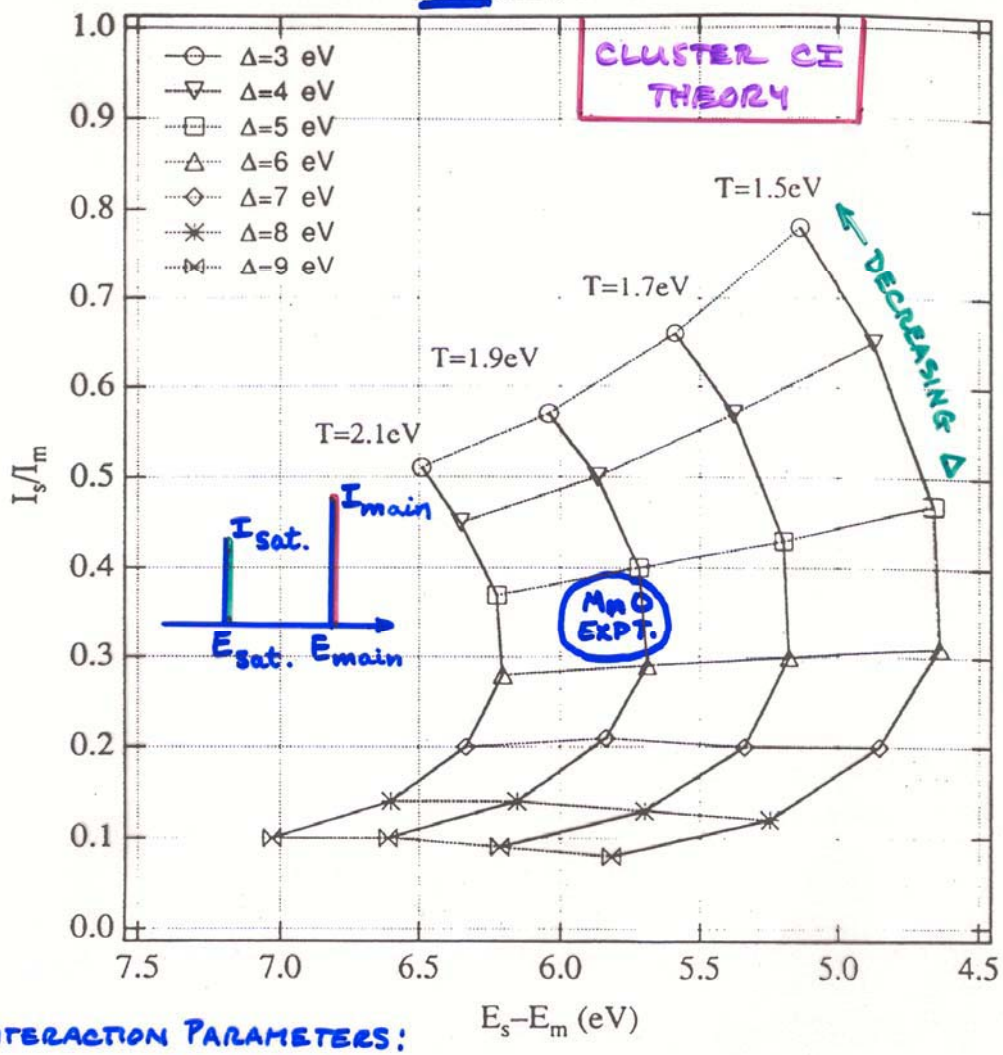

INTERACTION PARAMETERS:

U = 3d-3d COULOMB REPULSION ENERGY

Δ = LIGAND-TO-METAL CHARGE TRANSFER ENERGY

T = LIGAND p – METAL 3d HYBRIDIZATION ENERGY

Q = CORE HOLE-3d COULOMB

BOURQUET ET AL., J. EL. SP. 82, 87 (196)

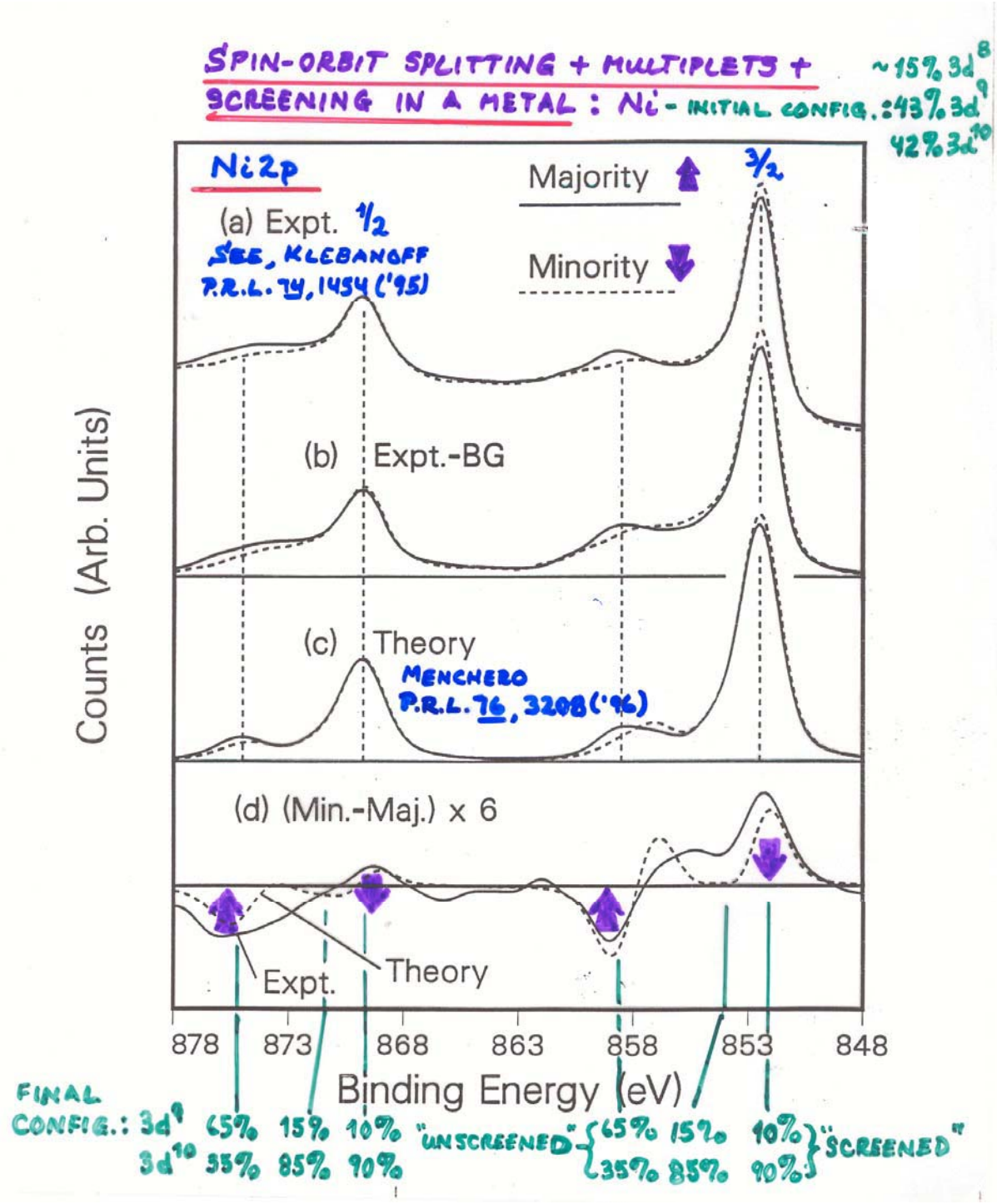
SPIN-ORBIT SPLITTING + MULTIPLETS + SCREENING IN A METAL : Ni - INITIAL CONFIG.: ~15% 3d^8, 43% 3d^9, 42% 3d^10
Ni 2p
Majority
Minority
3/2
1/2
(a) Expt.
SEE, KLEBANOFF P.R.L. 74, 1454 ('95)
(b) Expt.-BG
(c) Theory
MENCHERO P.R.L. 76, 3208 ('96)
(d) (Min.-Maj.) x 6
Expt.
Theory
Counts (Arb. Units)
878
873
868
863
858
853
848
Binding Energy (eV)
FINAL CONFIG.: 3d^9 65% 15% 10% "UNSCREENED" {65% 15% 10%} "SCREENED"
3d^10 35% 85% 90% {35% 85% 90%}

Many-electron and screening effects: $La_{0.7}Sr_{0.3}MnO_3$, $h\nu$ = 7700 eV

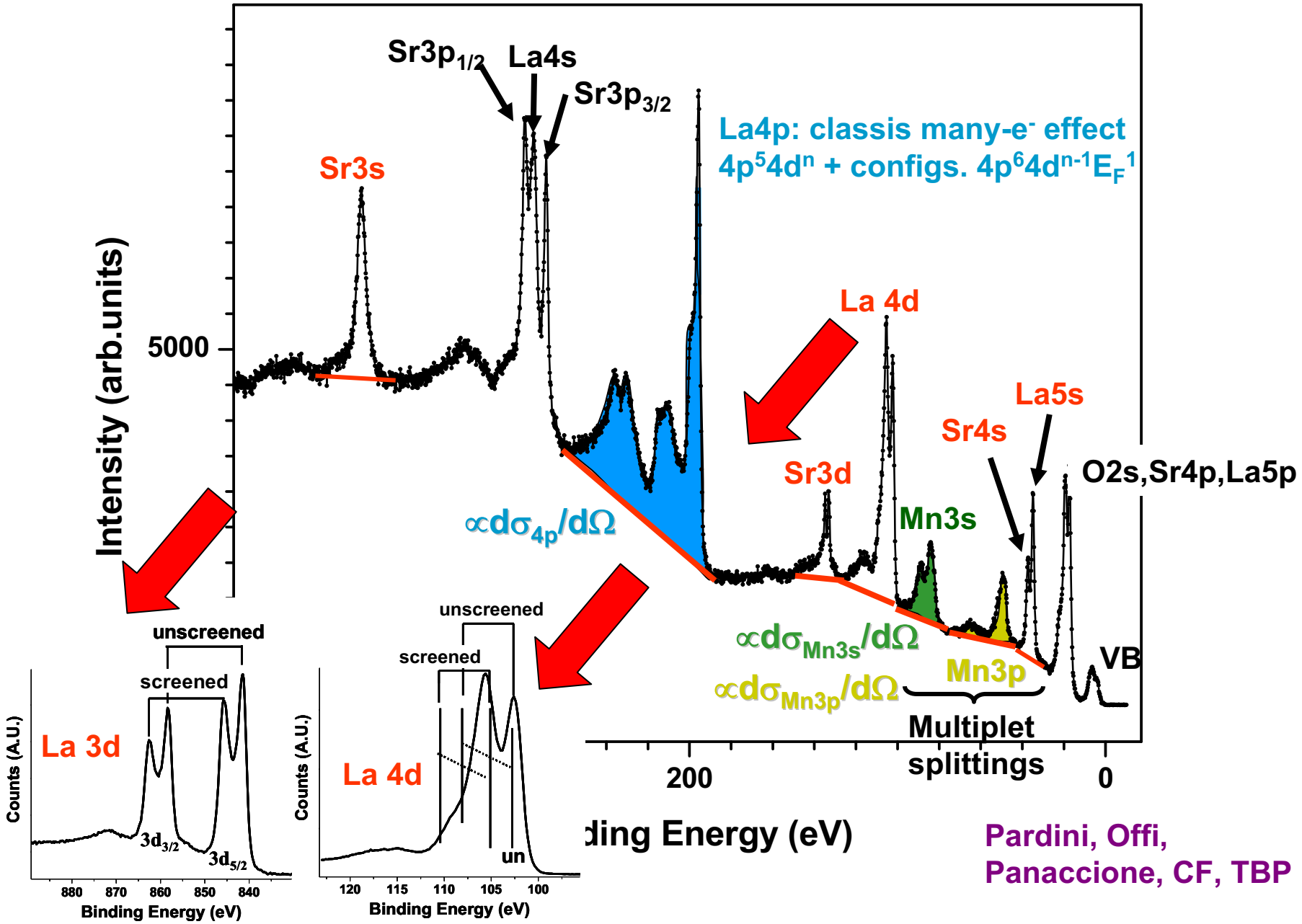

Pardini, Offi,
Panaccione, CF, TBP

Temperature dependence of Mn2p spectra: $La_{0.7}Sr_{0.3}MnO_3$
New satellite structures in hard x-ray core spectra

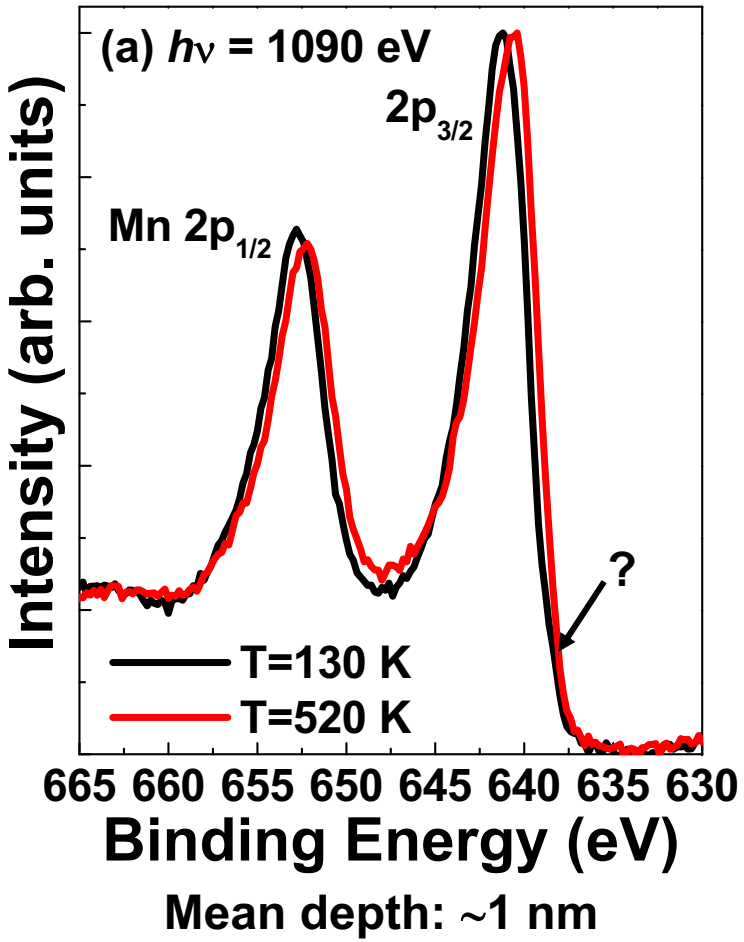

Mean depth: ~1 nm

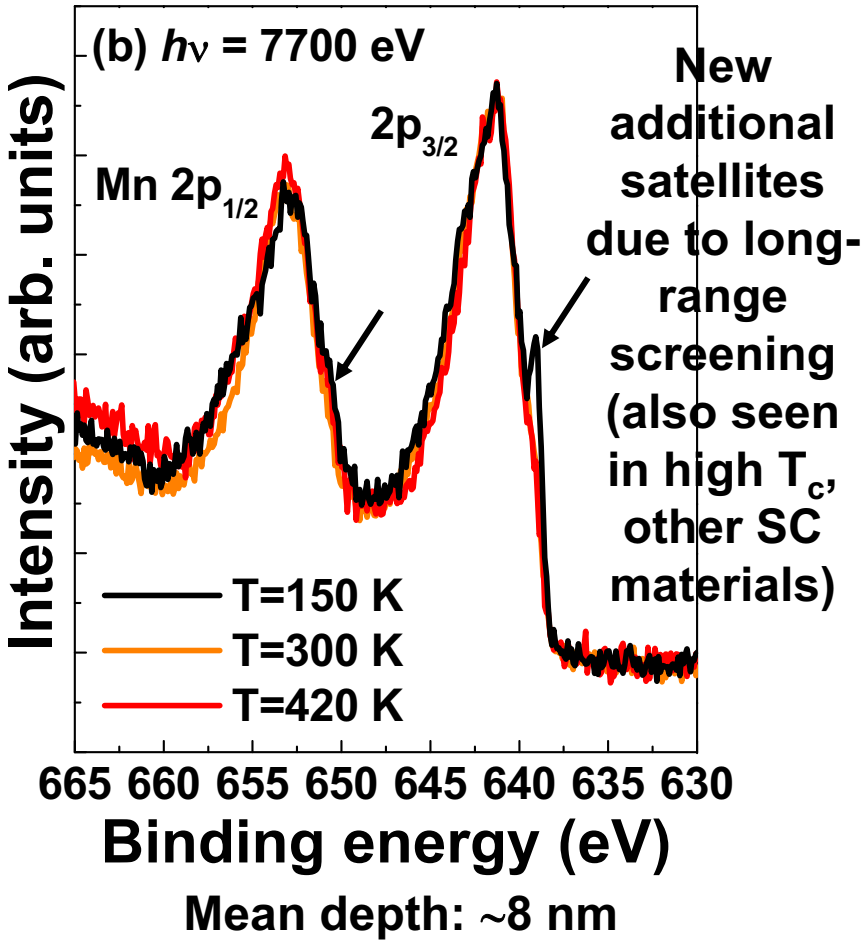

Mean depth: ~8 nm

→Suggests bulk electronic structure not reached until ca. 8 nm depth

Offi, Mannella, et al., Phys. Rev. B 2008, 77, 174422

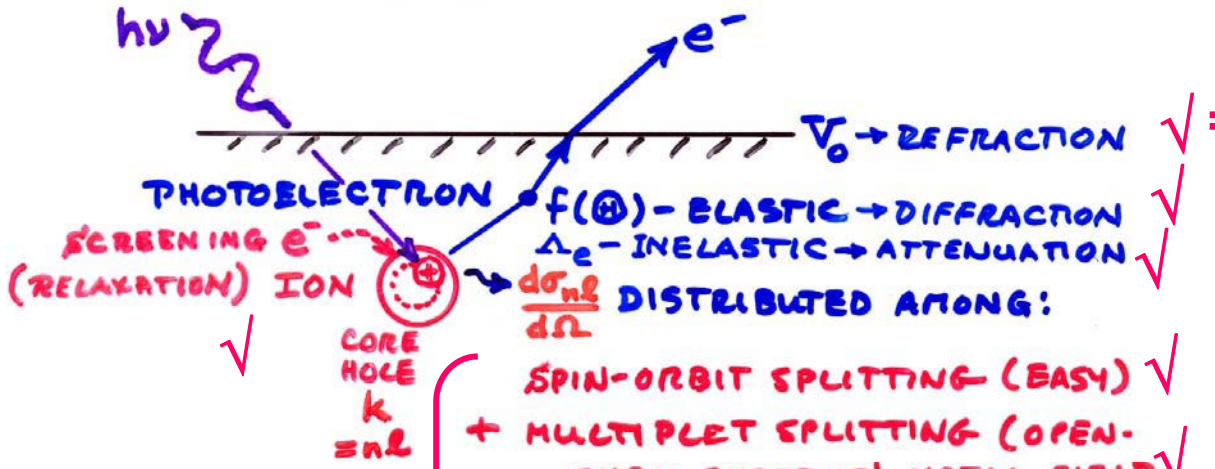

√ = covered so far

ADDITIONAL SOURCES OF STRUCTURE (AND INFORMATION!) IN SPECTRA BEYOND CHEMICAL SHIFTS

- SPIN-ORBIT SPLITTING (EASY) √
- \+ MULTIPLET SPLITTING (OPEN-SHELL SYSTEMS), XSTAL FIELD √
- \+ CORRELATION / CONFIGURATION INTERACTION √
- \+ SHAKE-UP / SHAKE-OFF / e⁻-HOLE √
- \+ SCREENING / NON-SCREENING: CONFIGURATION INTERACTION √
- \+ VIBRATIONAL EXCITATIONS ←
- \+ RESONANT PHOTOEMISSION ($h\nu \approx E_{b,n'l'}$) √

REALLY ALL AT ONCE, BUT SUM RULES + THEORY HELP

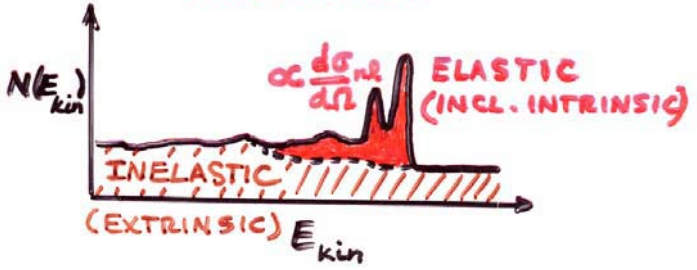

INTENSITIES IN PHOTOELECTRON SPECTRA:

- GENERAL: FINAL STATE K (k-SUBSHELL + ALL OTHER DESIG.)

$$\text{INT.}_K \propto \left| \hat{e} \cdot \langle \Psi^f_{tot}(N,K) | \sum_{i=1}^{N} \vec{r}_i | \Psi^i(N) \rangle \right|^2 \quad \text{(DIPOLE APPROX.)}$$

- BORN-OPPENHEIMER: e^-'s FAST, VIBRATIONS SLOW

$$\text{INT.}_K \propto \underbrace{|\langle \psi^f_{VIB,v'} | \psi^i_{VIB,v} \rangle|^2}_{\text{FRANCK-CONDON FACTOR}} \left| \hat{e} \cdot \langle \Psi^f_{e^-}(N,K) | \sum_{i=1}^{N} \vec{r}_i | \Psi^i_{e^-}(N) \rangle \right|^2$$

- SUDDEN APPROXIMATION: $\varphi_k \rightarrow \varphi_f$ = PHOTOe^- (FAST)

k HOLE $\rightarrow$ $\varphi_1 \rightarrow \varphi'_1, \ldots, \varphi_{k-1} \rightarrow \varphi'_{k-1}, \varphi_{k+1} \rightarrow \varphi'_{k+1}, \ldots, \varphi_N \rightarrow \varphi'_N$ (SLOW)

$$\text{INT.}_K \propto |\langle \psi^f_{VIB,v'} | \psi^i_{VIB,v} \rangle|^2 \underbrace{|\langle \Psi^f_{e^-}(N-1,K) | \Psi_K^{\dagger}(N-1,K) \rangle|^2}_{k \text{ MISSING}} \left| \hat{e} \cdot \langle \varphi_f | \vec{r} | \varphi_k \rangle \right|^2$$

SAME SUBSHELL COUPLING + TOTAL L,S → "MONOPOLE"

$\hookrightarrow$ NORMAL $\dfrac{d\sigma_K}{d\Omega}$

- SLATER DETS. FOR $\Psi^f_{e^-} = \det(\varphi'_1 \varphi'_2 \cdots \varphi'_{k-1} \varphi'_{k+1} \cdots \varphi'_N)$

$$\Psi_K = \det(\varphi_1 \varphi_2 \cdots \varphi_{k-1} \varphi_{k+1} \cdots \varphi_N)$$

$$\text{INT.}_K \propto |\langle \psi^f_{VIB,v'} | \psi^i_{VIB,v} \rangle|^2 |\langle \varphi'_1 | \varphi_1 \rangle|^2 |\langle \varphi'_2 | \varphi_2 \rangle|^2 \cdots$$
$$|\langle \varphi'_{k-1} | \varphi_{k-1} \rangle|^2 |\langle \varphi'_{k+1} | \varphi_{k+1} \rangle|^2 \cdots |\langle \varphi'_N | \varphi_N \rangle|^2 \cdot \left| \hat{e} \cdot \langle \varphi_f | \vec{r} | \varphi_k \rangle \right|^2$$

1e- DIPOLE → $d\sigma/d\Omega$

$(N-1)e^-$ SHAKE-UP/ SHAKE-OFF → "MONOPOLE"

- PLUS DIFFRACTION EFFECTS IN φ_f ESCAPE

VIBRATIONAL STRUCTURE IN VALENCE-LEVEL (MO) SPECTRA

Diatomic A-B example

(Also applies to core-level emission if equilibrium distance changes on forming core hole)

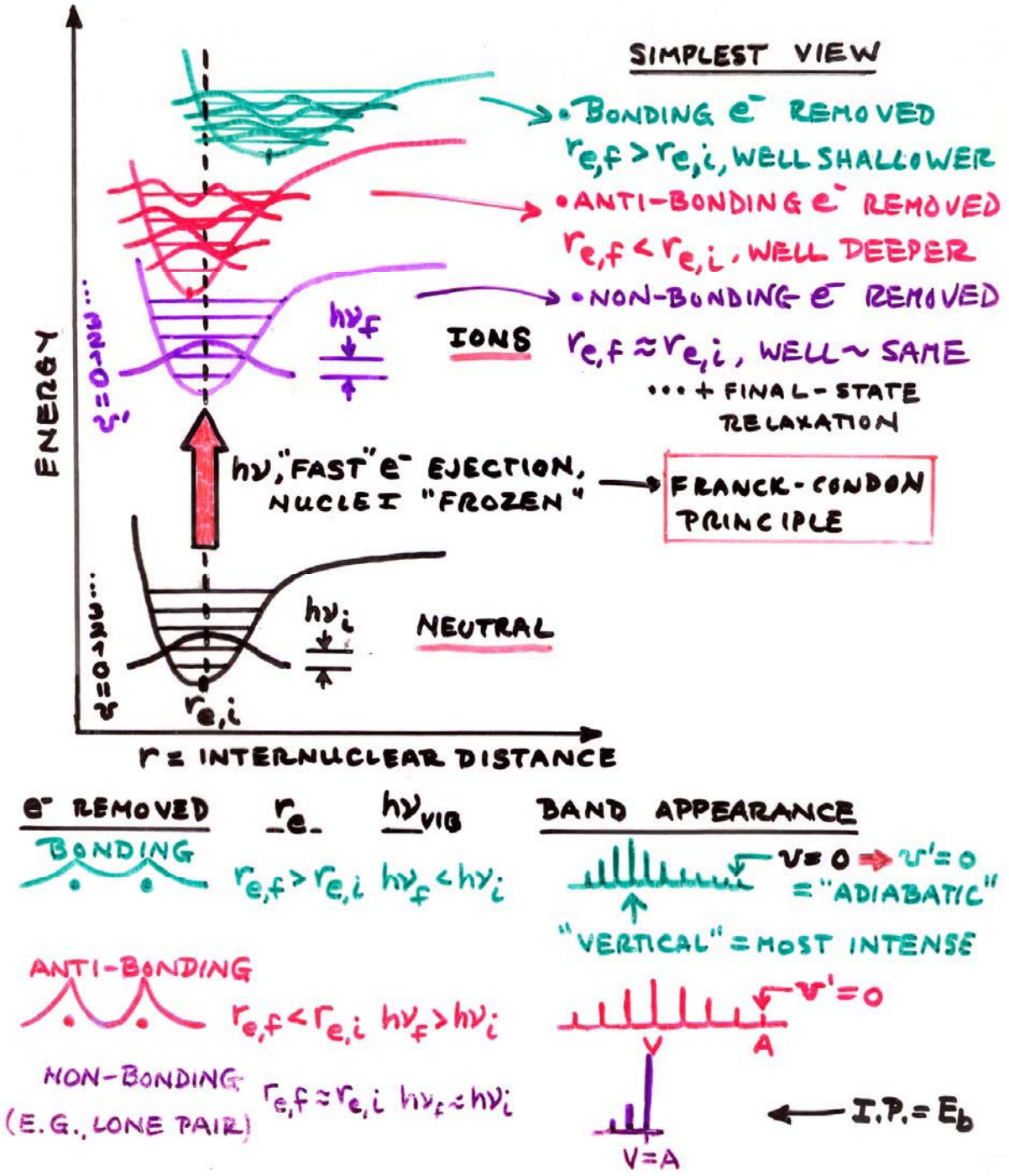

VIBRATIONAL STRUCTURE IN VALENCE-LEVEL (MO) SPECTRA

H_2 Hydrogen

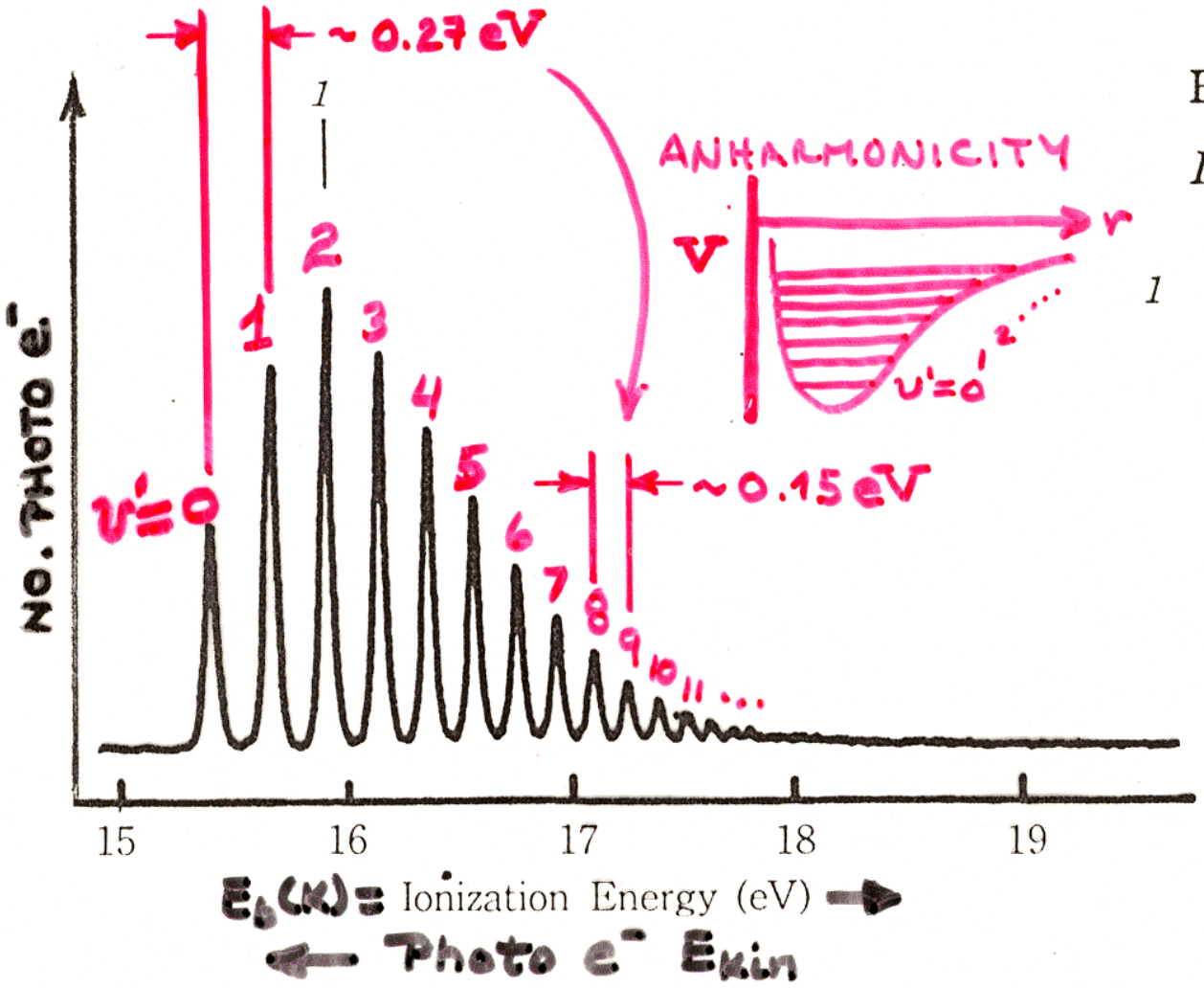

Exptl.[a] I_v (eV)
1 15.98

(9) **CO** Carbon Monoxide

UV PHOTOELECTRON SPECTRUM OF CO

Vibrational fine structure

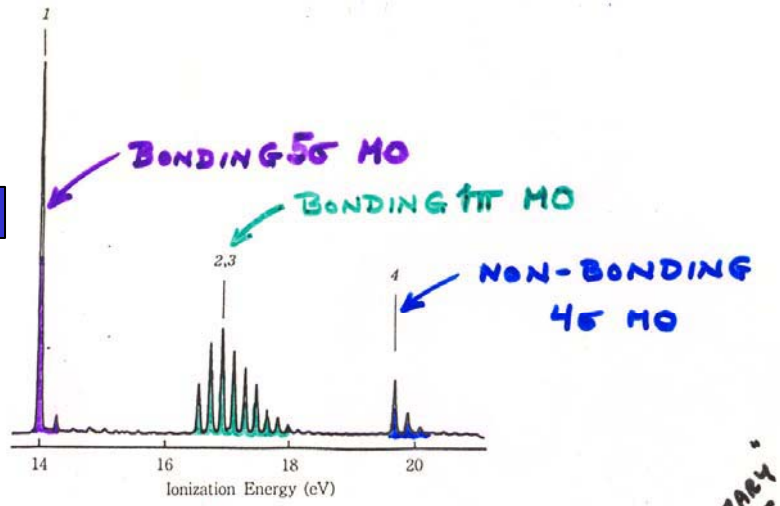

KOOPMANS' — CI FINAL STATE — "PRIMARY HOLES"

	Exptl.[a]	SCF MO [6-31 G][b]			CI (Ionic State) [6-31 G][c]		
	I_v(eV)	$-\varepsilon$(eV)	MO	Character	E(eV)	State	Configuration
1	14.01	14.99	5σ (7)	σ_{CO}	13.11	$1^2\Sigma^+$	$0.93(7^{-1})$ $-0.15(6^{-1},7^{-1},9^1)_a$ $-0.15(5^{-1},7^{-1},8^1)_a$
2	16.91	17.48	1π (6, 5)	π_{bond}	16.69	$1^2\Pi$	$0.95(6^{-1})$; $0.95(5^{-1})$
3	16.91	17.48					
4	19.72	21.69	4σ (4)	n_O	19.29	$2^2\Sigma^+$	$0.92(4^{-1})$ $+0.16(6^{-1},7^{-1},9^1)_a$ $+0.16(5^{-1},7^{-1},8^1)_a$

RELAX. + CORREL.

a) The spectrum : this work. The I_v's : Turner *et al.* (215). See also other works : Turner and May (215 a) ; Carlson and Jonas (54) ; Gardner and Samson (104) ; Edqvist *et al.* (90) ; Potts and Williams (182 a) ; and Natalis *et al.* (165).
b) We used the bond length reported (A 3) ; symmetry $C_{\infty h}$. $E_{SCF}=-112.6672$ hartree. In 4-31 G calculations, $E_{SCF}=-112.5524$ hartree and $-\varepsilon$(eV)=14.93, 17.41, 17.41, and 21.60.
c) CI-II. (9, 8)=1π. $|N\rangle=0.98$ (SCF). The results obtained in other CI levels are given in Appendix B.

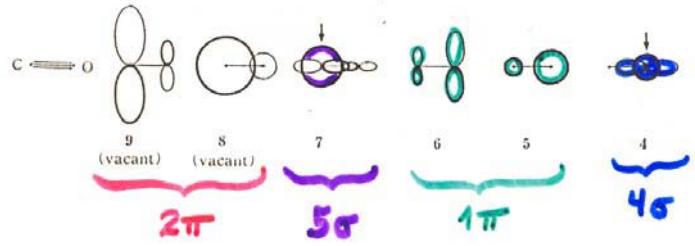

Kimura et al., "Handbook of Hel Photoelectron Spectra"

THE UV PHOTOELECTRON SPECTRUM OF HCl

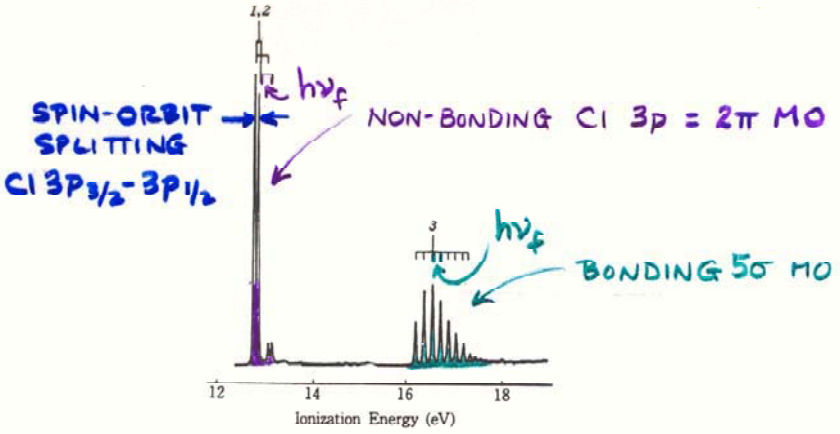

KOOPMANS' THEO. CONFIG. INT. ON FINAL STATE

	Exptl.[a]	SCF MO [4-31 G][b]			CI (Ionic State) [4-31 G][c]		
	I_v (eV)	$-\varepsilon$ (eV)	MO	Charactor	E (eV)	State	Configuration
1	12.75	12.77	2π (9, 8)	n_{Cl}	11.97	$1^2\Pi$	0.98(9⁻¹) ; 0.98(9⁻¹)
2	12.85	12.77					
3	16.28	16.50	5σ (7)	σ_{HCl}	16.10	$1^2\Sigma^+$	0.98(7⁻¹)

CI HOLE

WEIGHTING

a) The spectrum : this work. The I_v's : Frost *et al.* (102). See also other works : Lempka *et al.* (150) ; Turner *et al.* (215) ; and Weiss *et al.* (224).
b) We used the bond length reported in Ref. (A 5) ; symmetry $C_{\infty v}$. $E_{SCF} = -459.5631$ hartree.
c) CI-V. $|N\rangle = 0.99$ (SCF).
CI-V' : E(eV) = 12.01 and 16.11.
CI-III : E(eV) = 12.60 and 16.79.

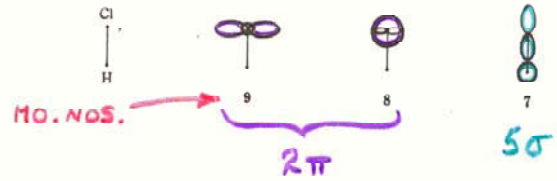

(FROM KIMURA ET AL., "HANDBOOK OF He I PHOTOELECTRON SPECTRA OF FUND. ORGANIC MOLECULES")

VIBRATIONAL FINE STRUCTURE IN CORE SPECTRA

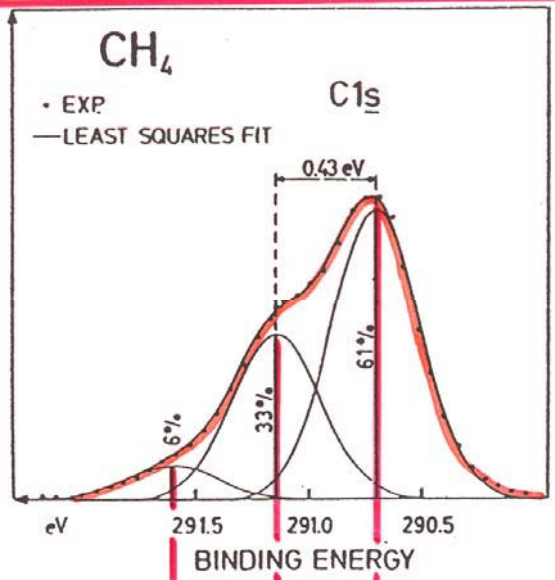

MONOCHROMATIZED LABORATORY X-RAY SOURCE

1970 SIEGBAHN, GELIUS, ET AL.

"Basic Concepts of XPS"
Figure 40

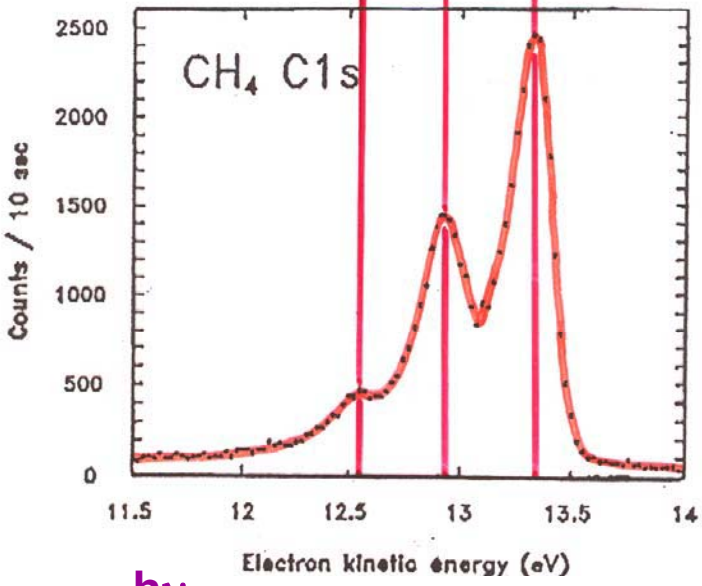

NEW SR BEAMLINE AT BROOK-HAVEN (~5-10X FASTER @ALS)

1991 BRADSHAW, KAINDL, ET AL.

CH distance = 1.10 Å
NH distance = 1.00 Å
Equivalent-core

$$CH_4 \xrightarrow{h\nu} [C(1s\ hole)H_4]^{+*} + e^- \approx [NH_4]^+ + e^-$$

Vibrational fine structure in C 1s photoemission from ethane: two progressions v_a at 0.407 eV and v_b at 0.176 eV and various excitations (v_a ,v_b)

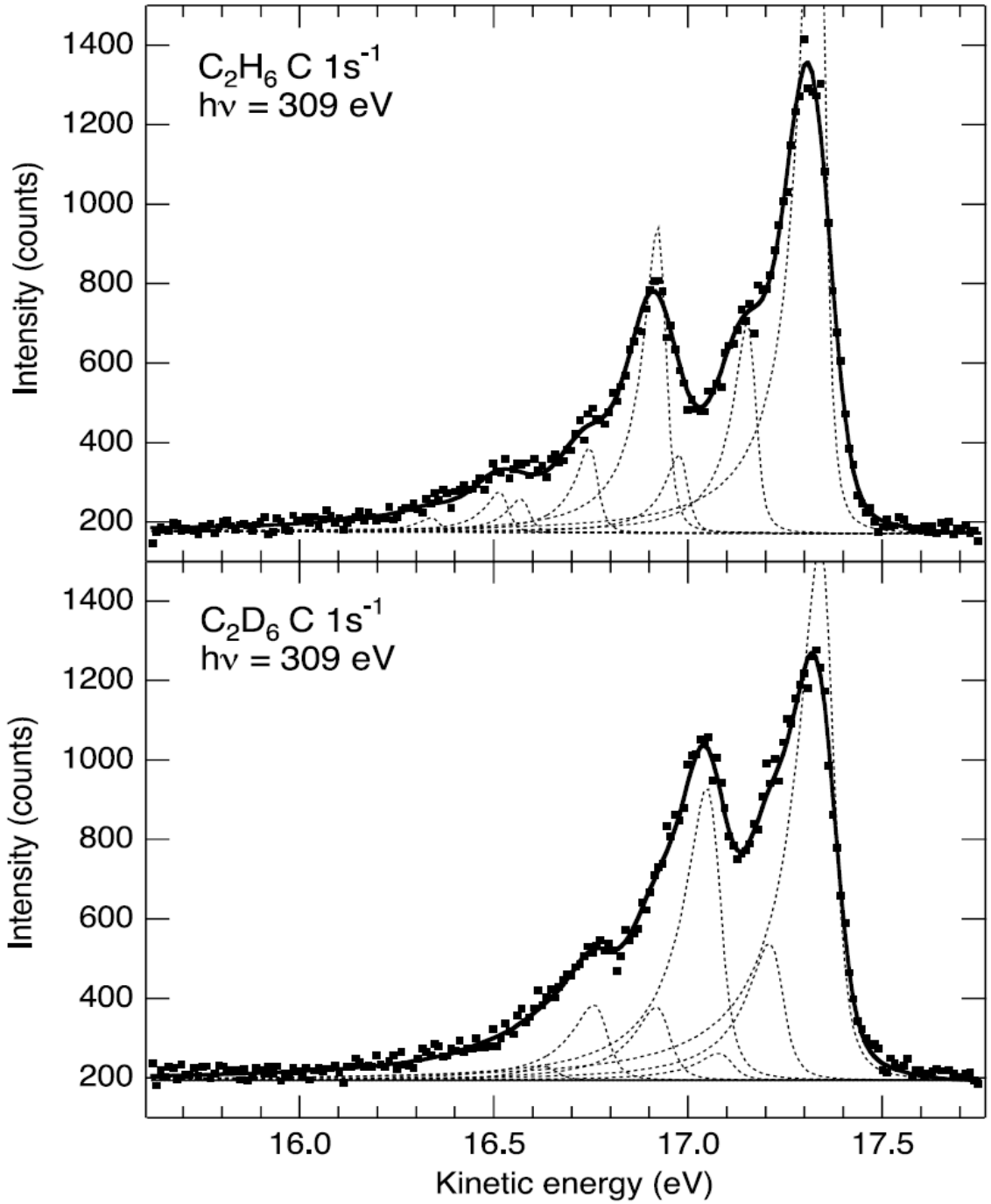

Rennie et al.,
J. Phys. At. Mol. Opt. Phys. 32, 2691 (1999)

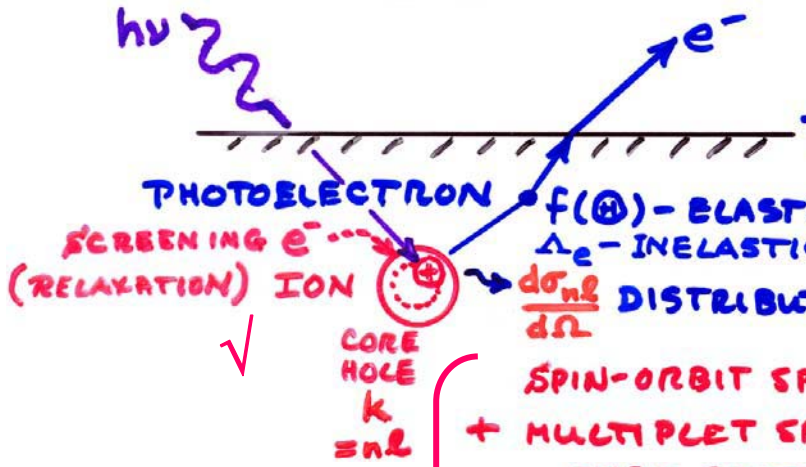

√ = covered so far

ADDITIONAL SOURCES OF STRUCTURE (AND INFORMATION!) IN SPECTRA BEYOND CHEMICAL SHIFTS

- SPIN-ORBIT SPLITTING (EASY) √
- + MULTIPLET SPLITTING (OPEN-SHELL SYSTEMS), XSTAL FIELD √
- + CORRELATION / CONFIGURATION INTERACTION √
- + SHAKE-UP / SHAKE-OFF / e⁻-HOLE √
- + SCREENING / NON-SCREENING: CONFIGURATION INTERACTION √
- + VIBRATIONAL EXCITATIONS √
- + RESONANT PHOTOEMISSION (hν ≈ $E_{b,nl'}$) √

REALLY ALL AT ONCE, BUT SUM RULES + THEORY HELP

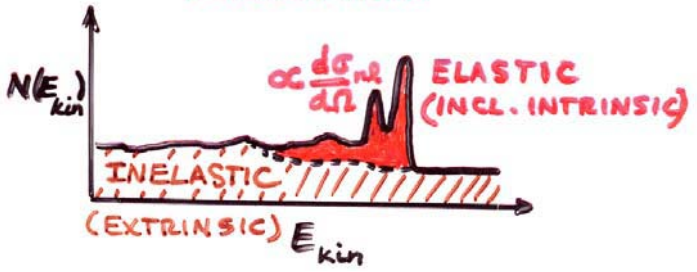

Outline

Surface, interface, and nanoscience—short introduction

Some surface concepts and techniques→photoemission

Synchrotron radiation: experimental aspects

Electronic structure—a brief review

The basic synchrotron radiation techniques:
more experimental and theoretical details

Valence-level photoemission

Core-level photoemission

Photoemission with high ambient pressure
around the sample

Bridging the Pressure Gap: Chemical-State- and Time- Resolved Oxidation of Si at Multi-Torr Pressures

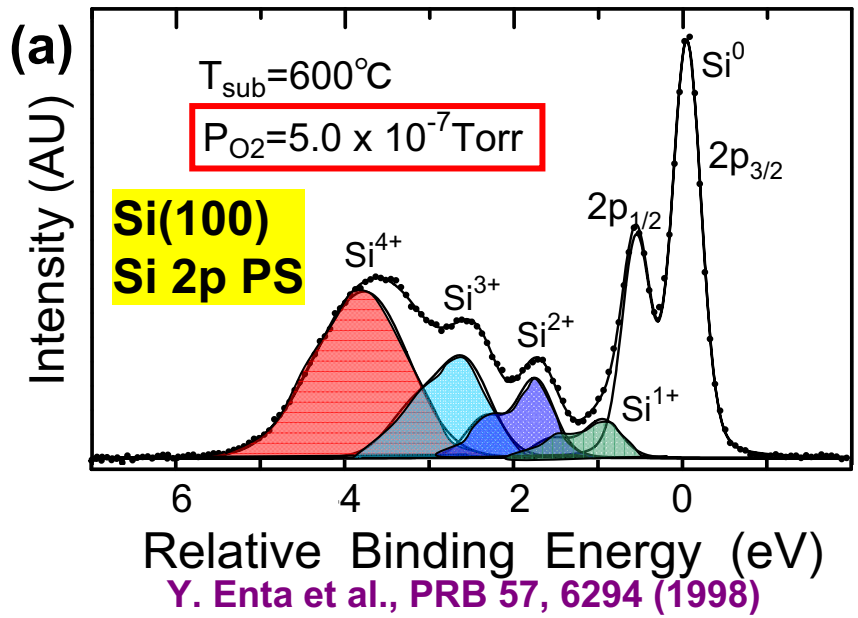

Y. Enta et al., PRB 57, 6294 (1998)

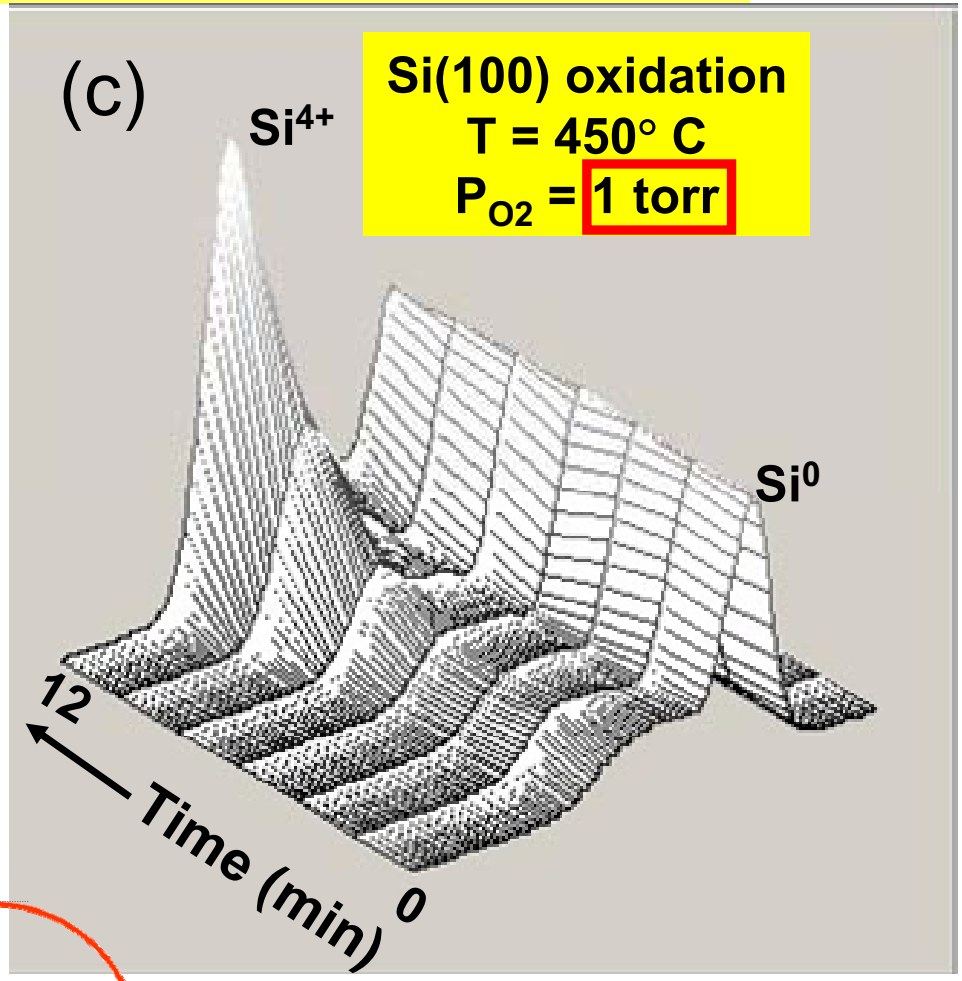

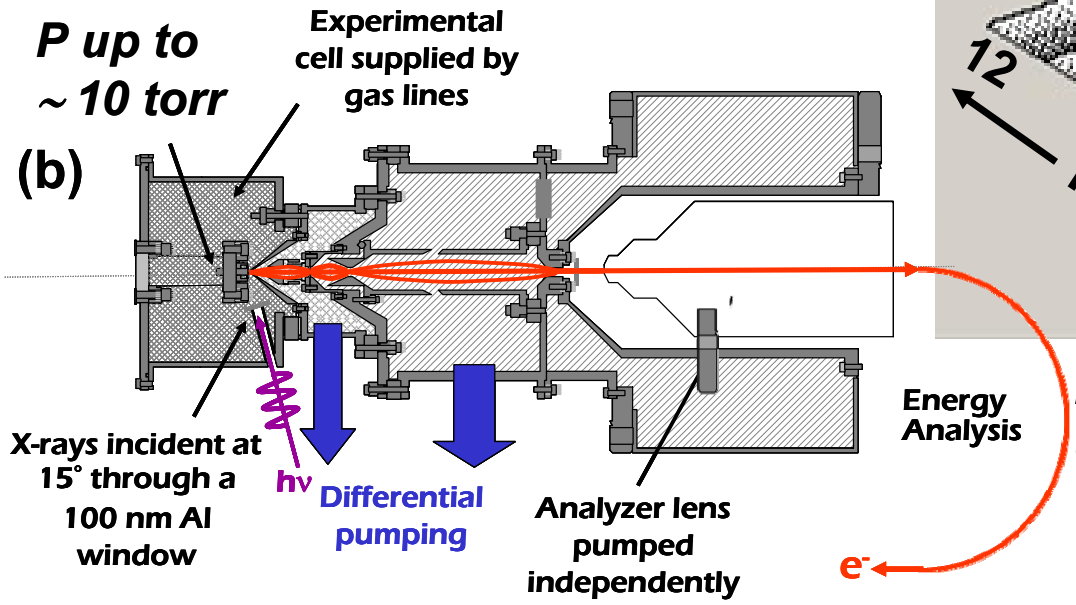

P ≈ 10^{-7} torr or better

Ogletree et al., Rev. Sci. Inst. 73, 3872 (2002)—SR, ALS
Bluhm, Salmeron, Schlögl—ALS, BESSY
Enta, Mun et al., Appl. Phys. Lett. 92, 012110 (2008); J. Appl. Phys. 103, 044104(2008)

Watching the oxide grow in real time: constant P, variable T

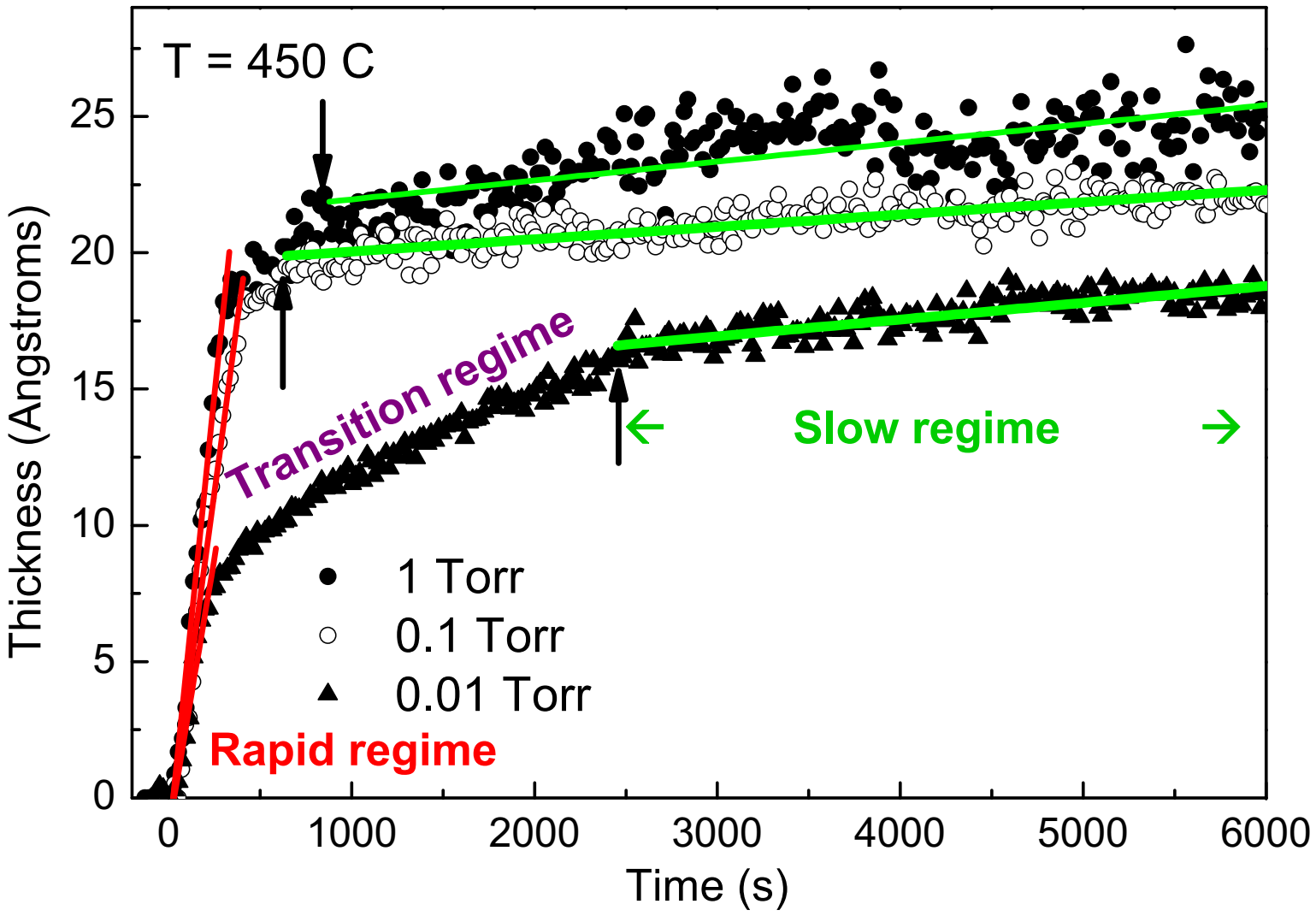

Typical experimental geometry for energy- and angle-resolved photoemission measurements

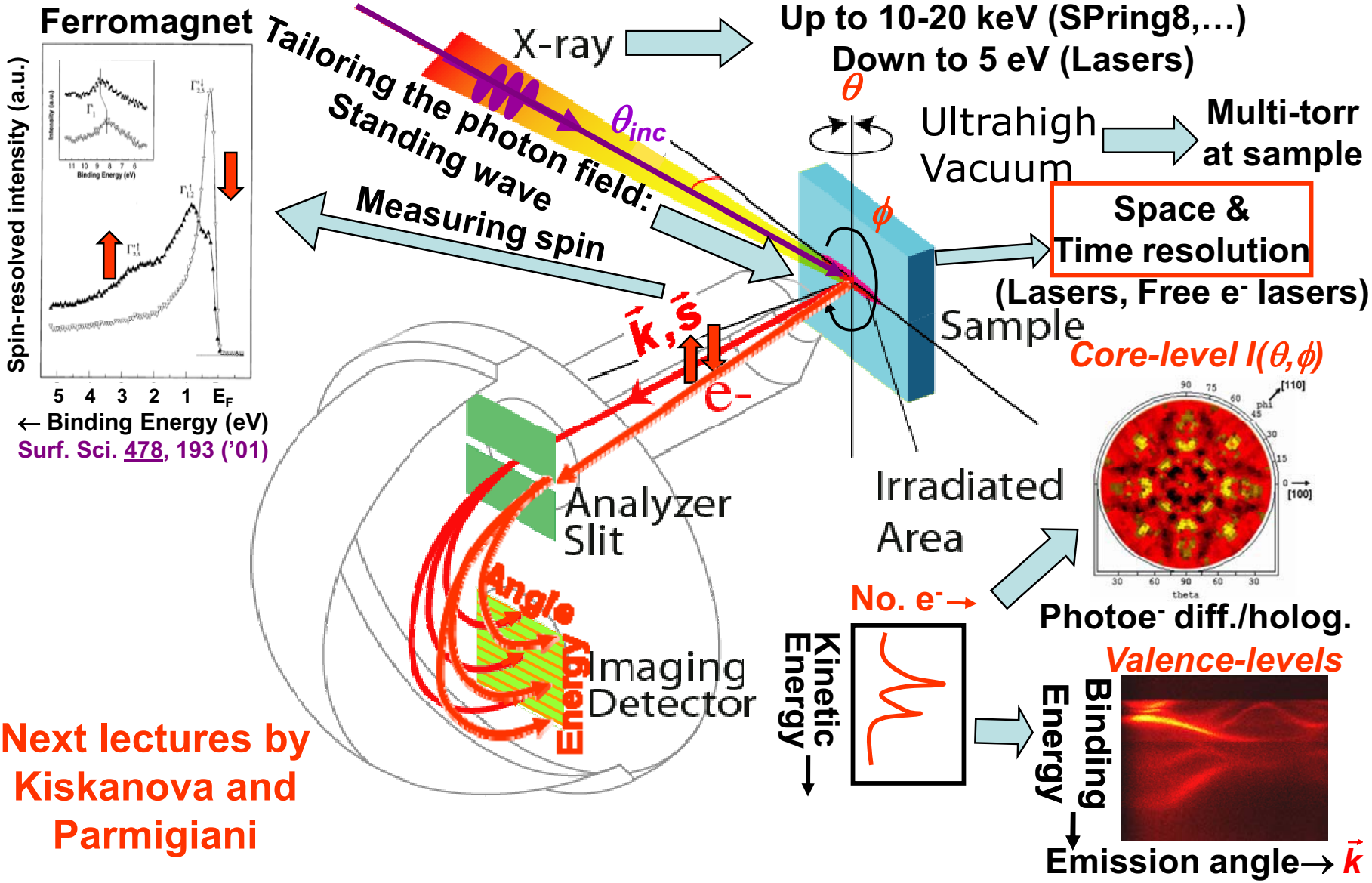

Thank your for your attention!